Investigating the Roles of the Cellular DEAD-box Protein DDX3 in the Hepatitis C Virus Lifecycle

Séamus Stack

A thesis presented for the degree of Doctor of Philosophy
College of Medical, Veterinary and Life Sciences
University of Glasgow

Centre for Virus Research
Institute of Infection Immunity and Inflammation
Church Street
Glasgow
G11 5JR

August 2013

Table of Contents

Abstract

Hepatitis C Virus (HCV) is a major cause of chronic hepatitis, with present estimates predicting that approximately 170 million people are currently infected with the virus worldwide. The majority of infections progress to chronicity, ultimately leading to fibrosis, cirrhosis and hepatocellular carcinoma. HCV, which belongs to the *Flaviviridae* virus family, has a single-stranded RNA genome of positive polarity that encodes a unique polyprotein approximately 3000 amino acids in length.

DDX3 is a member of the DEAD-box family of RNA helicases. It is a ubiquitous cellular protein possessing ATPase and helicase activities. The exact cellular function of DDX3 is as yet undefined, but there is evidence for its involvement in biological processes as diverse as splicing, translation initiation and repression, cell cycle regulation, nucleo-cytoplasmic RNA shuttling, RNA transport, interferon induction and apoptosis.

Recent studies have shown that DDX3 may be one of the primary host targets for manipulation by a number of different viruses, including HCV. The HCV core protein has been found to directly interact with DDX3. Previous studies conducted by our research group have shown that this interaction is dispensable for viral replication. Intriguingly, our group and others have shown that knockdown of endogenous DDX3 severely impairs HCV replication. However, the exact stage of the HCV lifecycle at which DDX3 functions is unknown. To investigate this, we used a number of *in vitro* cell systems available to us, comprising HCV psuedoparticles (HCVpp), subgenomic replicons (SGR) and the HCV cell culture system (HCVcc), to analyse how DDX3 depletion affected numerous cellular and molecular events vital to an efficient viral lifecycle.

The effect of DDX3 knockdown on these systems was determined by transducing Huh-7 cells with lentivirus encoding short hairpin RNA against the N-terminus of DDX3. Towards this end, we confirmed the important role DDX3 plays in the HCV lifecycle and deduced that DDX3 acts at a post-translation stage of the HCV lifecycle in Huh-7 cells, inhibiting an as yet undetermined aspect of RNA

replication. Results obtained also suggested that DDX3 is required for efficient HCV replication complex (RCs) function, as DDX3-deficient Huh-7 cells transiently transfected with SGR RNA exhibited diminished viral replication compared to control Huh-7 cells, yet no such reduction was observed in DDX3-depleted Huh-7 cells stably replicating SGR RNA. Although I did not observe the presence of DDX3 in RC during IF analysis, it is as yet unclear whether DDX3 is directly incorporated into these structures or influences their function in an indirect manner.

To determine if DDX3 knockdown had any specific effects on HCV assembly, we enlisted a subclone of Huh-7 cells with depleted CD81 levels called Huh7L-#4 cells for use in single-cycle infectious virus production experiments. DDX3 knockdown greatly altered infectious HCV production in these cells, to a far greater extent than that observed in Huh-7 cells, but HCV RNA replication was unperturbed in these cells. Subsequent analysis of infectious virus production and HCV RNA replication in DDX3-deficient shCD81 cells was performed to investigate if the phenotype observed in Huh7L-#4 cells was related to the absence of CD81. Our results confirmed that this was not the case.

In its totality, this study has uncovered important details regarding the importance of DDX3 in the HCV lifecycle, with data obtained suggesting that DDX3 plays a pleiotropic role in this lifecycle, with distinct responsibilities in undetermined aspects of HCV RNA replication and infectious virus production.

Figures and Appendices

Chapter 1 Figures

Chapter 2 Figures

Chapter 3 Figures

Chapter 4 Figures

Appendix Figures

Publication

Publications obtained from personal contribution to other studies

Angus, A. G., Loquet, A., Stack, S. J., Dalrymple, D., Gatherer, D., Penin, F. & Patel, A. H. (2012). Conserved glycine 33 residue in flexible domain I of hepatitis C virus core protein is critical for virus infectivity. *J Virol* **86**, 679-690.

Acknowledgements

Many thanks to –

My supervisor, Dr. Arvind Patel, for providing me with the opportunity to undertake my PhD at the Centre for Virus Research and his excellent guidance and support throughout the practical and writing stages of my PhD.

Dr. Allan Angus, for his outstanding experimental expertise, guidance, support, proof reading and friendship.

I would also like to thank all past and present members of lab 325A, particularly Fiona and Cat, for making my time in the lab so enjoyable.

All my friends at the CVR (including, but not limited to, Yongxu, Claire, James, Kathleen, Patricia, Pete, Becky, Anna, Sarah, Jolanda, Wan, Chris) for their support throughout my PhD.

Finally, I would like to thank my parents, Michael and Elizabeth, and my sisters, Bríd and Muireann, for their constant support, love, understanding and motivation during this time.

Author’s Declaration

This work was completed at the University of Glasgow between October 2009 and October 2012 and has not been submitted for another degree. All work presented in this thesis was obtained by the author’s own efforts, unless otherwise stated.

Abbreviations

°C	degrees celcius
%	percentage
m	micro (10^{-6})
aa	amino acid
ADRP	adipocyte differentiation-related protein
AIG	anchorage independent growth
ALT	alanine aminotransferase
Amp	ampicillin
ANXA2	annexin A2
Apo	apolipoprotein
APC	antigen presenting cell
APS	ammonium persulphate
ARF	ADP-ribosylation factor
ARFP	alternative reading frame protein
ATP	adenosine-5'-triphosphate
bDNA	branched DNA
BLAST	blasticidin
bp	base pair(s)
BPB	bromophenol blue
BSA	bovine serum albumin
C-	carboxy-terminus
CAP-Rf	core associated protein-RNA helicase full-length
cdk	cyclin-dependent kinase
cDNA	complementary DNA
CHO	chinese hamster ovary (cells)
CHV	canine hepacivirus
cIAP	cellular inhibitor of apoptosis protein-1
CK1ε	Casein kinase 1 subunit ε
CLDN	claudin
CPE	cytopathic effect

CRM1	chromosome maintainance region 1
DAA	direct acting antiviral
DAPI	4',6-diamidino-2-phenylindole
DC-SIGN	dendritic-cell specific ICAM-3 grabbing non-integrin
DGAT1	diacylglycerol acyl transferase 1
dH_2O	deionised molecular biology grade water
DHH	differentiated human hepatocye-like cells
DMEM	Dulbecco's modified eagles media
DMSO	dimethyl sulphoxide
DMV	double membrane vesicle
DNA	deoxyribonucleic acid
dNTPs	deoxynucleotides triphosphates
dsRNA	double-stranded RNA
E.coli	Escherichia coli
ECL	enhanced chemiluminescence
EDTA	ethylenediaminetetra-acetic acid
EGF	epidermal growth factor
EIA	enzyme immunoassay
ELISA	enzyme-linked immunosorbant assay
eIF	eukaryotic translation initiation factor
EM	electron microscopy
EMCV	encephalomyocarditis virus
ER	endoplasmic reticulum
FAH	fumaryl acetoacetate hydrolase
FCH	fibrosing cholestatic hepatitis
FCS	foetal calf serum
FFU	focus-forming unit(s)
FITC	fluorescein isothiocyanate
g	gram
GAG	glycosaminoglycan
GFP	green fluorescent protein
GSK3	glycogen synthase kinase-3
h	hour(s)

HAV	hepatitis A virus
HBV	hepatitis B virus
HCC	hepatocellular carcinoma
HCl	hydrochloric acid
HCMV	human cytomegalovirus
HCV	hepatitis C virus
HCVcc (virus)	HCV cell culture-derived virus
HCVpp	HCV pseudoparticles
HDL	high-density lipoprotein
HeBS	HEPES-Buffered Saline
HFLC	human fetal liver cells
HGG	hypogammaglobulinaemia
HIV	human immunodeficiency virus
HL	hydrophobic loop
HRP	horseradish peroxidise
HS	heparan sulfate
HSC70	heat shock cognate protein 70
HSV	herpes simplex virus
Huh-7	human hepatoma 7 (cells)
HVR	hypervariable region
IF	indirect immunofluorescence
IFN	interferon
IGF2BP1	Insulin-like growth factor-II mRNA-binding protein 1
IgG	immunoglobulin G
igVR	intergenotypic variable region
IL	interleukin
IRES	internal ribosome entry site
IRF-3	IFN regulatory factor 3
ISG	IFN-stimulated gene
JFH	japanese fulminant hepatitis
kb	kilobase pair(s)
kDa	kilodalton(s)
KSHV	kaposi's sarcoma-associated herpesvirus

l	litre(s)
L-SIGN	liver/lymph node-specific ICAM-3 grabbing non integrin
LB	L-Broth
LCS	low complexity sequence
LD	lipid droplet
LDL	low-density lipoprotein
LDLR	low-density lipoprotein receptor
LEL	large extracellular loop
LVP	lipoviroparticle
m	milli (10^{-3})
m	metre(s)
M	molar
mAb	monoclonal antibody
MAF	membrane-associated foci
MAPK	mitogen-activated protein kinase
min	minute
MNV	murine norovirus
m.o.i	multiplicity of infection
MPT	mitochondrial permeability transition
mRNA	messenger RNA
mRNPs	messenger ribonulceoprotein particles
MS	mass spectrometry
MTP	microsomal triglyceride transfer protein
MW	membranous web
N-	amino terminus
nAbs	neutralizing antibodies
NaCl	sodium chloride
NANBH	non-A, non-B hepatitis
NPC1L1	Niemann-Pick C1-like 1 cholesterol absorption receptor
neo/G418	neomycin phosphotransferase
ng	nanogram (10^{-9})
NGS	next-generation sequencing

NH_4OAc	ammonium acetate
NMR	nuclear magnetic resonance
NPHV	nonprimate hepacivirus
NS	non-structural
OCLN	occludin
OD	optical density
ORF	open reading frame
pAb	polyclonal antibody
PAGE	polyacrylamide gel electrophoresis
PAMP	pathogen-associated molecular patterns
PCBP2	poly (rC)-binding protein 2
PBS	phosphate-buffered saline
PBST	PBS–Tween
PCR	polymerase chain reaction
pH	potential of hydrogen
PI	protease inhibitor
PIC	pre-initiation complex
PKR	protein kinase R
PLA2G4C	cytosolic phospholipase A2 gamma
pol	polymerase
PRR	pattern recognition receptor
PTB	polypyrimidine tract binding protein
RC	replication complex
RdRp	RNA-dependent RNA polymerase
RIG-I	retinoic-acid-inducible gene I
RISC	RNA-induced silencing complex
RLU	relative light units
RNA	ribonucleic acid
RNAi	RNA interference
RNase	ribonuclease
r.p.m	revolutions per minute
RRE	Rev responsive element
RTK	receptor tyrosine kinase
s	second(s)

SAA	serum amyloid A
SCID	severe combined immunodeficiency
SDS	sodium dodecyl sulphate
sE2	soluble E2
SEAP	secreted alkaline phosphatase
SEL	small extracellular loop
SGR	subgenomic replicon
shRNA	short hairpin RNA
siRNA	small inhibitory RNA
SP	signal peptidase
SPP	signal peptide peptidase
SR-BI	scavenger receptor class B member I
ssRNA	single-stranded RNA
STAT-C	specifically targeted antiviral therapy for hepatitis C
SVR	sustained viral response
TAP	tip-associated protein
TBE	tick-borne encephalitis
TBSV	Tomato bushy stunt virus
TEM	tetraspanin-enriched microdomain
TEMED	N'N'N'N'-tetramethylethylene-diamine
TLR3	Toll-like receptor 3
TMA	transcription-mediated amplification
TMD	transmembrane domain
TNF-α	tumour necrosis factor-alpha
TRIF	Toll/interleukin-1 receptor/resistance domain-containing adaptor inducing IFN
TRIS	2-Amino-2-(hydroxymethyl)-1,3-propanediol
TRITC	tetramethyl rhodamine isothiocyanate
U	unit
µ	micro
uPA	urokinase plasminogen activator
UTR	untranslated region
UV	ultraviolet

V	volts
VLDL	very-low density lipoprotein
VSV	vesicular stomatitis virus
VSVpp	VSV pseudoparticles
WT	wild-type
w/v	weight/volume ratio
YFV	yellow fever virus

One and Three Letter Amino Acid Abbreviations

Amino acid	Three letter code	One letter code
Alanine	Ala	A
Arginine	Arg	R
Asparagine	Asn	N
Aspartic acid	Asp	D
Cysteine	Cys	C
Glutamine	Gln	Q
Glutamic acid	Glu	E
Glycine	Gly	G
Histidine	His	H
Isoleucine	Ile	I
Leucine	Leu	L
Lysine	Lys	K
Methionine	Met	M
Phenylalanine	Phe	F
Proline	Pro	P
Serine	Ser	S
Threonine	Thr	T
Tryptophan	Trp	W
Tyrosine	Tyr	Y
Valine	Val	V

1. Introduction

1.1. Discovery of Hepatitis C Virus

It did not become clear until the 1970s, following the development of specific serological tests that allowed the diagnosis of hepatitis A virus (HAV) and hepatitis B virus (HBV), that most cases of post-transfusion hepatitis were caused by another unknown agent, designated "non-A, non-B hepatitis" or NANBH (Feinstone *et al*., 1975; Prince *et al*., 1974). Chimpanzees infected with blood extracted from an NANBH infected patient established that the agent was transmissible and capable of causing chronic infection (Alter *et al*., 1978; Hollinger *et al*., 1978; Tabor *et al*., 1978). A small enveloped virus was suggested as the cause of NANBH after polycarbonate filtration analysis and chloroform inactivation studies were performed (Bradley *et al*., 1985; Feinstone *et al*., 1983). However, conventional immunological methods failed to identify the etiological agent because of the low concentration of NANBH serum in chimpanzees. Further molecular characterisation of NANBH was impeded for a long time by the lack of cell culture and small animal model systems needed for propagation of the virus.

The development of more sophisticated molecular biology techniques such as molecular cloning and phage display facilitated the discovery of the causative agent of NANBH in Michael Houghton's lab at Chiron Corporation in the late 1980s. Scientists there used a "blind immunoscreening approach" where they reverse transcribed nucleic acid extracted from NANBH infected material before generating a complementary DNA (cDNA) library in bacteriophage to express polypeptides encoded by the cDNA. Serum derived from a patient with documented NANBH was then used to screen the library. A single bacteriophage clone (termed 5-1-1) was identified that expressed a polypeptide derived from the NANBH viral genome (Choo *et al*., 1989). Further experimentation revealed that the infectious agent was a single-stranded RNA (ssRNA) molecule approximately 9.6kb in length which possessed one continuous open reading frame (ORF). The new virus, named hepatitis C virus (HCV), was classified in the genus *Hepacivirus* of the *Flaviviridae* family (Choo *et al*., 1989).

1.2. Virion Properties and Classification

HCV has a genetic organisation and virion morphology similar to that of flaviviruses and pestiviruses and has been classified within the *Flaviviridae* family as a member of the *Hepacivirus* genus (Choo *et al*., 1991; Robertson *et al*., 1998; Takamizawa *et al*., 1991). Other members of the *Hepacivirus* genus include canine hepacivirus (CHV), which infects dogs, and nonprimate hepacivirus (NPHV), which infects horses (Kapoor *et al*., 2011; Burbelo *et al*., 2012). The *Flaviviridae* family also includes the flaviviruses such as dengue, yellow fever virus (YFV) and tick-borne encephalitis virus (TBE), the pestiviruses such as bovine viral diarrhoea virus (BVDV) and classic swine fever virus (CSFV) and the pegiviruses such as GBV-A, -B, -C and -D (Choo *et al*., 1991; Linnen *et al*., 1996; Miller & Purcell, 1990; Stapleton *et al*., 2011). Members of the *Flaviviridae* family possess a positive ssRNA genome which encodes a long polyprotein composed of structural and non-structural proteins (Reed & Rice, 2000). The genomes of *Flaviviridae* family members are typically encapsidated by an icosahedral capsid, which is surrounded by an outer envelope (Clarke, 1997). Studies analysing HCV morphology clarified that it shared these family characteristics (Bradley *et al*., 1985; He *et al*., 1987; Kaito *et al*., 1994). Using electron microscopy (EM), Kaito *et al*. (1994) confirmed that HCV particles in serum were ~ 55-65 nm in diameter consisting of a spherical outer structure with spike-like projections and a ~ 30-35 nm inner capsid.

HCV exhibits high genetic variability. Comparison of HCV nucleotide sequences recovered from infected individuals has revealed the existence of seven different genotypes, which differ by 30-35 % at the nucleotide level. These genotypes can be further subdivided into more closely related subtypes, which differ in their nucleotide sequence by 20-25 % (Gottwein et al., 2009; Kuiken & Simmonds, 2009; Simmonds, 2004; Simmonds *et al*., 2005). Variation is not evenly spread throughout the genome, as the viral glycoproteins E1 and E2 and the non-structural protein NS5A display the greatest diversity, while the 5' untranslated region (5'UTR) and the capsid protein core are much more conserved in nature (Simmonds, 2004). Furthermore, within an infected individual, HCV does not exist as a single entity, rather a multitude of circulating mutant microvariants from a predominant "master sequence", a phenomenon referred to

as quasispecies (Gomez *et al*., 1999; Holland *et al*., 1992; Martell *et al*., 1992). This genetic variability is heavily influenced by the error-prone nature of the RNA dependent RNA polymerase (RdRp), the high viral production rate (10^{12} particles/day) and the selective pressure exerted by the host immune defences (Neumann *et al*., 1998; Troesch *et al*., 2006). HCV genotypes can differ in terms of severity of the resultant disease, ability to establish persistent infection and response to antiviral therapy (Simmonds, 2004).

In density gradients, HCV RNA-containing particles have been shown to associate with very low density lipoprotein (VLDL) and low density lipoprotein (LDL), forming complexes called lipoviroparticles (LVPs). HCV particles have also been found to form complexes with immunoglobulin (Nielsen *et al*., 2006; Thomssen et al., 1993). As a result of these interactions, HCV serum particles can exhibit a broad range of buoyant density and sedimentation, which varies depending on the method of analysis used (Andre *et al*., 2002; Choo *et al*., 1995; Thomssen *et al*., 1992). Infectious virions are found in the lowest density fractions (~ 1.06 g/ml), which are associated with LDL and VLDL, while those particles found at higher densities (1.17-1.21 g/ml) display far lower infectivity (Choo *et al*., 1995; Hijikata *et al*., 1993b; Thomssen *et al*., 1992).

The development of a robust HCV cell culture infectious system (HCVcc) has allowed the biophysical and biochemical nature of the HCV virion to be further characterised. As HCVcc virions are known to associate with VLDLs (Chang *et al*., 2007), are heterogenous, spherical particles (Wakita *et al*., 2005) and have been found after gradient analyses to sediment their most infectious material at densities in line with the peak of infectivity for HCV *in vivo* (1.09-1.10 g/ml) (Lindenbach *et al*., 2005), HCVcc particles were initially believed to be biophysically similar to those found *in vivo*. Electron cryomicroscopy studies of HCVcc particles revealed an electron-dense bilayer around certain particles, which allowed differentiation between two morphologically distinct particle classes (enveloped and nonenveloped) that had different diameters (~ 60 nm versus ~ 40 nm). The similar frequencies and size distributions of these different particle populations found in cell-culture derived virus compared very favourably to morphologies obtained with wild-type virus from infected patients (Gastaminza *et al*., 2010). However, while HCVcc is known to have a tight association with apoE and apoC1 (Chang *et al*., 2007; Meunier *et al*., 2008a), the interaction of HCVcc with apoB

is sporadic and inefficient, in contrast to LVPs, which have a strong association with this apolipoprotein (Merz *et al*., 2011). Due to the inability of HCVcc to capture apoB-specific antibodies with regularity, HCVcc particles likely resemble apoE-positive and primarily apoB-negative lipoproteins (Bartenschlager *et al*., 2011).

HCVcc RNA containing particles have been seen to sediment at a density of ~ 1.15 g/ml. The fact that the HCV structural proteins core, E1 and E2 were also observed in the same peak fraction of the density gradient confirmed that these proteins are components of the virion (Wakita *et al*., 2005). Indeed, while the E1 and E2 envelope glycoproteins assemble as noncovalent heterodimers intracellularly, virion-associated glycoproteins form large covalent complexes stabilized by disulfide bridges. Furthermore, these complexes were recognized by CD81, a HCV receptor, as well as heparin, a heparan sulphate homologue, indicating that the envelope glycoproteins are in a functional confirmation competent for HCV entry (Vieyres *et al*., 2010).

1.3. HCV Transmission and Epidemiology

Recent estimates predict that ~ 3 % of the world's population, equivalent to 170 million people, are infected with HCV (Thomson, 2009). HCV is the leading cause of liver transplantation in developed countries and is believed to account for 27 % of cirrhosis and 25 % of hepatocellular carcinoma (HCC) worldwide (Alter, 2007). While HCV is endemic in most parts of the world, there are significant geographical differences in HCV infection patterns. Developed countries such as those in North America and Western Europe have low prevalence rates for the virus (0.6 % UK, 2 % US). Many developing nations in Africa and Asia have far higher prevalence rates for HCV, although there is limited data available in some of these countries to determine specific levels of infection (Thomson, 2009). Egypt has the highest prevalence rate, with HCV antibodies detected in 22 % of the general population (Shepard *et al*., 2005), reflecting prophylactic schistosomiasis treatment campaigns conducted with contaminated glass syringes over a number of decades. These nationwide campaigns represent the world's largest iatrogenic transmission of a blood-borne pathogen (Frank *et al*., 2000).

HCV infection is most commonly transmitted by percutaneous exposure to blood or blood products. The principal modes of transmission have changed over time and differ between countries. In industrialised nations, HCV transmission by blood transfusion has been virtually eradicated thanks to the implementation of blood-screening tests for HCV (Kuo *et al*., 1989; Huber *et al*., 1996). Injection drug use is now the primary mode of HCV transmission in these countries. In the developing world, unhygienic medical procedures and contaminated blood products remain the major factors behind transmission rates (Lavanchy, 1999). Sexual transmission and perinatal transmission are other routes of infection but are not common, and studies on both routes have provided inconsistent results (Alter, 2007). Given that most HCV infections are asymptomatic and that the majority of countries do not routinely screen for HCV infection, the incidence of HCV is difficult to accurately determine.

Significant variation is observed in the geographical distribution of the seven HCV genotypes (Fig 1.1). Genotypes 1-3 have a worldwide distribution and account for a great majority of infections in the western world. Genotype 4, however, is predominantly found in Africa and the Middle East, genotype 5 is largely restricted to South Africa, genotype 6 is prominent in South-East Asia while genotype 7 is primarily observed in central Africa (Gottwein *et al*., 2009; Nguyen & Keeffe, 2005; Simmonds 2004).

1.4. Natural History of Infection

The predominant site for HCV infection and replication is the liver. As with all diseases, there is no single typical course, rather a broad clinical spectrum of disease presentations and outcomes (Hoofnagle, 1997). HCV frequently establishes a chronic infection following an acute infection. Both conditions are described in the following sections.

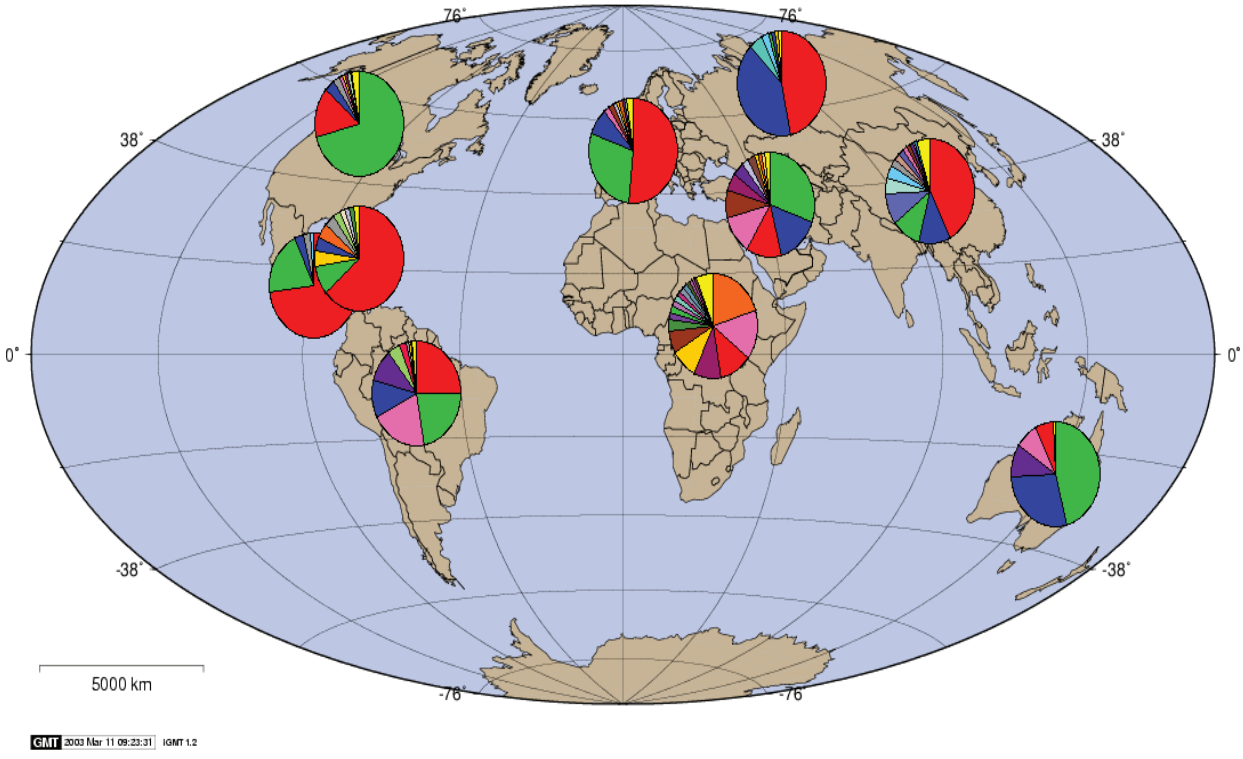

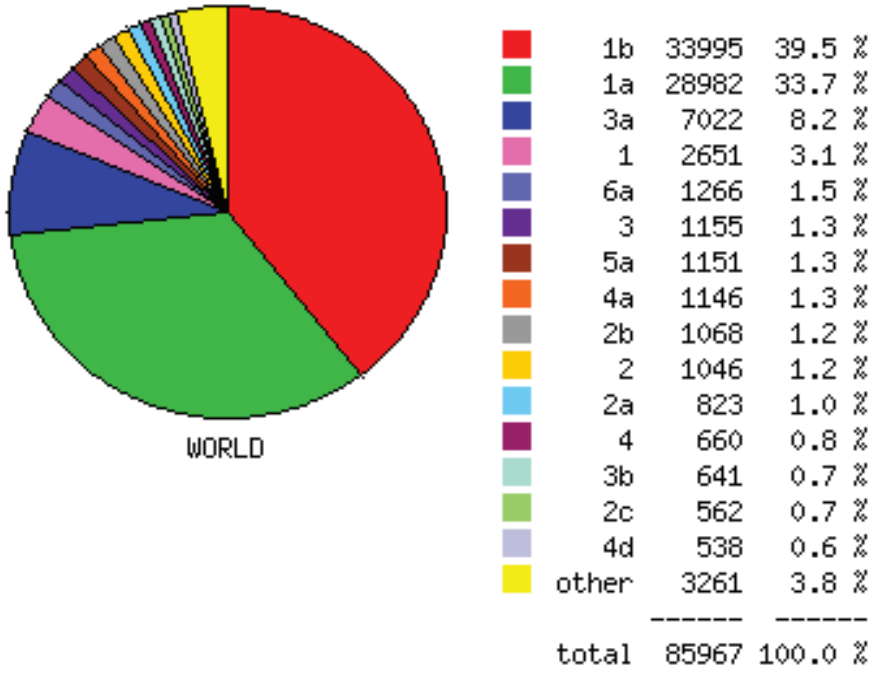

Figure 1.1. HCV subtype distribution worldwide.

The geographic and subtype distribution is shown for the 85, 967 sequences available online at http://hcv.lanl.gov (accessed February 27, 2013).

1.4.1. Acute Hepatitis C

Viremia is first detectable within 1 to 2 weeks post-HCV infection (Farci *et al*., 1991; Thimme *et al*., 2001) However, acute HCV infection is infrequently diagnosed because the majority of acutely infected individuals exhibit mild or no symptoms. Clinically acute HCV, which presents in ~ 20-30 % of cases, resembles other forms of acute viral hepatitis, with symptoms manifesting between 3-20 weeks post-infection (mean incubation period to onset of symptoms is 7 weeks) (Barrera *et al*., 1995; Hoofnagle, 1997; Thimme *et al*., 2001). Symptoms include malaise, nausea, dark urine, anorexia and jaundice. A number of weeks post-exposure, elevated alanine aminotransferase (ALT) activity is observed in the serum of the vast majority of patients with acute HCV. ALT levels, which signify hepatocyte necrosis, have been found to be greater than ten-fold higher than normal at their peak in 80 % of these patients (Farci *et al*., 1991; Hoofnagle, 1997; Thimme *et al*., 2001). Acute HCV infection resolves spontaneously in 15-40 % of infected individuals, although the exact mechanisms underlying this clearance are currently unknown. Rapid, fulminant hepatitis associated with acute HCV infection has been reported but is a rare occurrence (Farci *et al*., 1996). Fulminant hepatic failure is a dramatic clinical syndrome, characterised by massive necrosis of the liver, which arises shortly following infection in HCV-related cases (2-8 weeks). Monoclonality of a highly virulent viral population that circulates in the blood at high titres is thought to be important but not sufficient for the development of fulminant hepatitis, with changes to as yet undefined host factors also likely contributing to this hepatic failure (Farci *et al*., 1996; Kato *et al*., 2001).

1.4.2. Chronic Hepatitis C

The acute phase is considered the first 6 months after infection. HCV infection persisting for more than six months is defined as chronic infection. The majority (60-85 %) of individuals infected with HCV develop chronic infection. Chronic infection involves a continuing and constant viremia of ~ 10^{12} virions produced daily, although virion production is higher during the acute phase of infection (Neumann *et al*., 1998). Chronically infected patients can remain asymptomatic for more than three decades but can eventually develop serious liver conditions such as steatosis (fat accumulation in the

liver), hepatic fibrosis (structural liver damage) and compensated and decompensated cirrhosis (extensive tissue scarring). Serum ALT levels are usually continuously elevated during chronic infection, but this elevation correlates poorly with disease activity. Up to 20 % of patients develop cirrhosis within the first two decades of HCV infection (Yano *et al*., 1996). In patients with established cirrhosis, the risk of developing hepatocellular carcinoma (HCC), or cancer of the liver, is between 1-4 % each year (Hoofnagle, 2002).

It is not yet fully clear how HCV induces cirrhosis and HCC. As it has been shown that HCV is not significantly cytopathic in immunocompetent patients, hepatocellular damage in these individuals is likely brought about by the actions of cytotoxic $CD8^+$ T-cells on infected cells (McGuinness *et al*., 1996; Brillanti *et al*., 1993). While the time from infection to cirrhosis can be influenced by numerous host, viral and environmental factors such as age, sex, ethnicity, alcohol intake, underlying disease, viral genotype and viral quasispecies diversity (Bellentani & Tiribelli, 2001; Benhamou *et al*., 1999; Berenguer *et al*., 2000; Kenny-Walsh, 1999; Poynard *et al*., 1997, Villano *et al*., 1999), immunocompromised patients generally suffer a far more rapid and severe course of liver disease than those with healthy immune responses (Einav & Koziel, 2002), implying that liver cirrhosis induced by HCV infection is heavily mediated by the vigour of the infected individual's immune response. However, how HCV causes HCC is as yet unknown. The potential role of HCV in transcriptional regulation has long suggested an involvement in inducing phenotypic changes in hepatocytes. Adding weight to this theory, the incidence of HCC in transgenic mice expressing core protein has been found to be far greater than in control mice. Analysis of tumour cells in those mice with HCC also found higher levels of core expressed in these cells compared to surrounding normal hepatocytes (Moriya *et al*., 1997).

1.5. Immunological Response to HCV Infection

The immune system is divided into two major branches, the innate immune system and the adaptive immune system.

1.5.1. Innate Immunity

The innate immune system is nonspecific as to the type of pathogen it fights and is ready to be mobilized upon the first signs of infection (Pavio and Lai, 2003). This is achieved by cells responding to viral infection by rapidly inducing interferons (IFNs) upon recognition of viral pathogen-associated molecular patterns (PAMPs) by cellular proteins known as pattern recognition receptors (PRRs). Two specific PRRs, Toll-like receptor 3 (TLR3) and retinoic-acid inducible gene I (RIG-I), have been implicated in anti-HCV innate immunity (Saito *et al*., 2008; Wang *et al*., 2009b). These receptors sense double-stranded RNA (dsRNA), an important intermediate in the HCV replication cycle, before unleashing a signalling cascade that subsequently leads to the synthesis of the type I IFN IFN-β. Secreted IFN-β binds type 1 IFN-α/β receptors, causing autocrine/paracrine activation of the JAK-STAT signalling pathway, which results in the expression of IFN-α and numerous IFN-stimulated genes (ISGs), the genetic effectors of the host response to viral infection (Gale & Foy, 2005). Several ISGs have been shown to exhibit potent anti-HCV activity. 2′–5′ oligoadenylate synthetase (2-5 OAS) induces its antiviral effect by producing 2′,5′-linked oligoadenylate, which is the ligand and activator of RNase L, a ubiquitous enzyme in mammalian cells that can cleave viral and host RNAs to generate small RNA cleavage products that signal through the RIG-I/MDA5 pathway (Malathi *et al*., 2007). ADAR1 is an RNA-editing enzyme that deaminates adenosines in dsRNA, resulting in destabilization of RNA and accumulation of mutations (Taylor *et al*., 2005). Protein kinase R and P56 are two ISGs capable of inhibiting viral translation, the former by phosphorylating the α-subunit of the canonical eukaryotic initiation factor (eIF) 2, the latter by binding to eIF3 (Horner & Gale, 2009).. The expression of ISGs can also result in further amplification of the host IFN response through upregulation of IFN-β production (Sumpter *et al*., 2005). Type III IFNs have also been found to be induced directly upon viral infection, similar to IFN-β (Osterlund *et al*., 2007). The type III IFN IFNλ3 (IL28B) has been recently shown to play a pivotal role in HCV clinical outcome during the acute stage of infection (Kelly *et al*., 2011).

Despite the fact ISGs are stimulated by HCV, chronic infection is established in 80 % of exposed individuals. It is clear that HCV is able to subvert the host's innate immune

response, with numerous reports giving evidence that HCV can attenuate the IFN response at various different stages. The HCV NS3/4A protease is thought to target and cleave components of the RIG-I pathway necessary for an efficient interferon activation cascade (Foy *et al*., 2005). The capsid protein core can impair induction of ISGs by interfering with several aspects of JAK-STAT signalling (Melen *et al*., 2004; de Lucas *et al*., 2005). It has also been suggested that core removes the host DEAD-box protein DDX3 from the IFN-β-inducing complex, impairing IFN-β activation (Oshiumi *et al*., 2010a). NS5A is known to bind to downstream anti-HCV ISGs such as protein kinase R (PKR) and 2-5 OAS and disrupt their function. The envelope E2 protein is also believed to act as a decoy target to PKR (Horner & Gale, 2009; Rehermann, 2009, Taylor *et al*., 1999). These viral manipulations help HCV successfully avoid activating the innate immune response, which subsequently contributes to impairment of the adaptive immune response as cytokines produced during the innate immune response are essential for activation of adaptive immunity. While cellular innate immunity has been well-researched, less data is established about the humoral innate immune response. The humoral arm consists of PRRs such as complement C1q, collectins and ficolins, which can activate the complement cascade, leading to specific lysis of virions, opsonization of viruses and increased phagocytosis, and direct neutralization of virus particles (Tarr *et al*., 2012). However, as with cellular effectors, HCV has developed numerous sophisticated mechanisms of escape from these humoral processes, such as the ability of core and NS5A to disrupt transcription of complement C4 protein, a vital factor in opsonization and lysis of virions (Banerjee *et al*., 2011).

1.5.2. Adaptive Immunity

Like the innate immune response, the adaptive immune response can be divided into two categories, the cellular immune response, governed by T-lymphocytes, and the humoral immune response, governed by B-lymphocytes (Pavio & Lai, 2003).

1.5.2.1. Adaptive Cellular Immune Response

T-lymphocytes such as helper T-cells ($CD4^+$) and cytotoxic T-cells ($CD8^+$) are critical for HCV clearance, with strong, sustained and multispecific T-lymphocyte responses

associated with attenuated HCV infection (Thimme *et al*., 2001; Diepolder *et al*., 1996). In contrast, HCV chronic infection typically occurs in patients with weak, oligo/mono-specific or no virus-specific $CD4^+$ or $CD8^+$ T-cell responses during the acute phase of infection (Neumann-Haefelin *et al*, 2005). $CD4^+$ T-cells recognize viral peptides bound to major histocompatiblity complex (MHC) class II molecules present on the surface of professional antigen presenting cells (APCs). These responses are directed mainly against HCV non-structural proteins, often targeting the same immunodominant epitopes within NS3 (Diepolder *et al*., 1997; Hoffman *et al*., 1995). $CD4^+$ T-cells secrete cytokines such as tumour necrosis factor-α (TNF-α) that stimulate development of $CD8^+$ T-cells. Specific $CD8^+$ T-cells bind to MHC class I molecules on the surface of infected hepatocytes, leading to the elimination of these cells. $CD8^+$ T-cells can stop viral infection either by direct cytotoxicity or by non-cytolytic cytokine-mediated inhibition of replication (Guidotti & Chisari, 2001).

While depletion studies have confirmed that $CD8^+$ T-cells are the most important effector cells in controlling HCV infection (Grakoui *et al*., 2003; Shoukry *et al*., 2003), $CD4^+$ T-cells seem to play a central role in the antiviral immune response, either by inducing or maintaining cytotoxic activity or by directly secreting antiviral cytokines. $CD8^+$ T-cells are able to develop in the absence of $CD4^+$ T-cells, but cannot control viremia (Kaplan *et al*., 2007). In chronic HCV infection, two major factors contribute to $CD8^+$ T-cell failure, T-cell exhaustion and viral escape mutants (Klenerman & Thimme, 2012). $CD4^+$ T-cells and $CD8^+$ memory T-cells are present at low frequencies in individuals with resolved acute HCV infection. While evidence has shown that immunity against viral persistence can be acquired (Mehta *et al*., 2002), protective immunity to HCV is strain-specific and readily evaded by heterologous viruses (Sugimoto *et al*., 2005).

1.5.2.2. Adaptive Humoral Immune Response

B-lymphocytes are responsible for producing antibodies involved in the adaptive humoral immune response, with HCV specific antibodies detectable just 7 weeks post-infection (Pawlotsky, 2004). Antibodies are able to neutralize HCV infection, with serum from HCV-infected individuals capable of neutralizing virus infectivity *in vitro* and subsequently able to protect chimpanzees against infection (Farci *et al*., 1994).

Antibodies against all HCV antigens have been reported, but anti-envelope antibodies have been the most thoroughly studied, as these antibodies have been shown to partially protect chimpanzees against infection (Choo *et al*., 1994). The hypervariable region 1 (HVR1) of E2, a 27 aa stretch located at the N-terminus of the glycoprotein, is believed to be a major target for antibody production. This may be due to the fact that the HVR1 region is necessary for the binding of E2 to the scavenger receptor class B type I (SR-BI), a lipoprotein receptor molecule essential for viral entry (Scarselli *et al*., 2002). While antibodies against HVR1 have been found *in vivo*, they tend to be highly strain-specific, indicating that HVR1 harbours a neutralization epitope that is the site of escape mutations from the humoral immune response (Kato *et al*., 1993; Vieyres *et al*., 2011; Weiner *et al*., 1992). Also, HVR1 is necessary for the interaction between SR-BI and LDL, which is known to augment viral entry (Bartosch *et al*., 2005). This contradictory role for HVR1 suggests it may function as an immunological decoy for the virus, driving a strong antibody response against HVR1 but allowing the selection of antibody-escape mutants (Ray *et al*., 1999).

The lack of broadly neutralizing antibodies targeting HVR1 led to the search for other, well conserved, antibody targets. To date, there have been numerous monoclonal antibodies generated that target linear or conformational epitopes in E2 and inhibit HCV infection. The linear epitope spanning E2 residues 412-424, located just downstream of HVR1, is seen as a major neutralization target (Owsianka *et al*., 2005; Perotti *et al*., 2008; Tarr *et al*., 2006). This region is recognized by at least nine broadly neutralizing monoclonal antibodies. One of the best characterized is the mouse mAb AP33, which has been shown to potently neutralize HCV pseudoparticles (HCVpp) bearing glycoproteins representative of the major HCV genotypes and subtypes (Owsianka *et al*., 2005), as well as inhibiting JFH1 infectivity (Tarr *et al*., 2006). AP33 is proposed to neutralize HCV infection through inhibiting the interaction of E2 with the viral entry receptor CD81, a tetraspanin found on most cell types. This epitope recognized by AP33 is highly conserved, spanning residues 412-423, with single amino acid substitutions in the epitope shown to decrease viral fitness (Owsianka *et al.*, 2006; Tarr *et al.*, 2006) or increase particle vulnerability to nAbs (Dhillon *et al.*, 2010; Tao *et al.*, 2009). The high conservation of the AP33 epitope either suggests that the structural integrity of the epitope may be vitally important in maintaining the functional conformation of E2 or that the region is poorly immunogenic *in vivo*. While the

prevalence of antibodies reactive to this conserved E2 region *in vivo* varies from <2.5 % (Tarr *et al.*, 2007) to 15 % (Keck *et al*., 2013), this low level of reactivity may be due to a shielding effect exerted by HVR1, which is located immediately upstream of the AP33 epitope. It has also been suggested that virion-associated lipoproteins or E2 glycans shield this region of E2 from the host immune system (Tao *et al*., 2009; Helle *et al*., 2010). Other targets for neutralizing antibodies include the binding sites of cell surface receptors SR-BI and occludin (OCLN), known to interact with E2, and claudin-1 (CLDN-1), necessary for the formation of an E2-CD81-claudin-1 co-receptor complex (Edwards *et al*., 2012). While E1 appears to be less immunogenic than E2, a conserved epitope has been identified between residues 313-327 of the protein. mAbs targeting this E1 epitope have been found to strongly neutralize various HCV genotypes as well as inhibit JFH1 infectivity (Meunier et al., 2008b).

The heterogenous nature of patient cohorts, amplified by the differences in HCV strains, has hampered analysis on the association between antibody-mediated neutralization and viral clearance. However, these problems were absent from one study involving a cohort of 49 healthy women infected with the same genotype 1b strain by intravenous transmission (Pestka *et al*., 2007). In these patients, viral clearance was associated with the rapid induction of neutralizing antibodies in the early stage of infection and loss of these antibodies after recovery from infection. Those who developed chronic infection displayed either a greatly reduced or completely attenuated capacity to neutralize the virus in the early stages of infection, with induction of neutralizing antibodies delayed until the late stage of infection. Thus, it appears neutralizing antibodies can control HCV infection if induced in the early phase of infection, but HCV can persist despite the presence of neutralizing antibodies during the chronic phase of infection. Hence, it appears that antibodies do play a role in the neutralization of HCV but it is probable that other immune mechanisms contribute to viral clearance.

Antibodies may mediate neutralization by causing aggregation of virus particles, inhibiting virus-host interactions or preventing viral envelope fusion with cellular membranes. However, HCV utilizes numerous diverse mechanisms of escape from neutralizing antibodies. While the innate heterogeneity of HCV is a crucial factor in immune escape, preventing nAbs from binding to various viral epitopes, another prominent means of HCV survival is the use of virion-associated lipoproteins or glycans

present on the surface of E2 (the "glycan shield") to mask the HCV envelope glycoproteins from nABs (Helle *et al*., 2010; Tao *et al*., 2009). HCV has also been found to induce non-neutralizing antibodies (also referred to as "interfering antibodies) that can compete with nAbs for the same epitopes and allow establishment of a persistent infection despite a strong immune response (Zhang *et al*., 2007b; Zhang *et al*., 2009). HCV can also spread via cell-to-cell transmission without being secreted into the extracellular environment, thus avoiding the anti-viral effects of nAbs (Timpe *et al*., 2008; Witteveldt *et al*., 2009). The cellular receptors CD81, CLDN-1, OCLN and SR-BI are all essential for this process (Brimacombe *et al*., 2011).

1.6. Disease Progression

HCV is not considered to be an inherently cytopathic virus. The lack of a cytopathic effect is evident from analysis of numerous individuals with persistent infections who display HCV viraemia, yet continually express normal ALT levels and have no apparent liver cell damage (Koziel, 1997; Pawlotsky, 1998). Other arguments against a direct viral cytopathic effect (CPE) include the fact that transgenic mice expressing HCV structural proteins show no evidence of damage to liver cells (Koziel, 1997), and the observation that low levels of HCV RNA are found in sera from patients with HCV-associated fulminant hepatitis (Farci *et al*., 1996). It has long been assumed that liver injury and disease progression in HCV infection is immune-mediated. Indeed, the majority of the liver damage experienced in patients who fail to clear the virus is most likely due to compartmentalisation of HCV-specific $CD4^+$ or $CD8^+$ T-cells in the liver, which cause cell death through apoptosis, either directly using cytotoxic T cells or by abundant local cytokine secretion (Rehermann, 2009).

Despite the prominent role of the host immune response in the onset and progression of inflammatory hepatic lesions, there is abundant evidence in the literature supporting the theory that liver damage induced by HCV infection can be due to both the immune response and direct viral CPE. Steatosis, the accumulation of lipids in hepatocytes, is predominantly found in patients infected with HCV genotype 3 and is thought to be induced by this strain of the virus. Interestingly, this theory was confirmed after the outcome of steatosis was found to match the virological response to treatment in

genotype 3 infected patients with purely virus-induced steatosis. Furthermore, no such correlation was observed in patients with metabolic causes of steatosis who were infected with other HCV genotypes (Castera *et al*., 2005). The rapid disease progression seen in immunocompromised patients has also implicated viral factors in HCV pathogenesis. HCV-induced CPEs leading to liver injury can be found in patients suffering from fibrosing cholestatic hepatitis (FCH), a severe and progressive form of liver dysfunction seen in organ transplant recipients. The pathogenesis of this disease has been attributed to uninhibited viral replication within hepatocytes in the absence of an adequate cellular immune response, culminating in a direct CPE (Rosenberg *et al*., 2002). Other immunodeficient groups, such as individuals suffering from hypogammaglobulinaemia (HGG) or those co-infected with HIV/HCV, also exhibit extremely rapid cirrhosis progression rates compared to immunocompetent patients. As in FCH patients, the lack of an efficient immune response in such patients allows widespread viral replication to occur and thus, possibly, a direct HCV-induced CPE (Bjoro *et al*., 1999; Christie *et al*., 1997; Martinez-Sierra *et al*., 2003).

It is also widely recognized that chronic hepatitis C is associated with insulin resistance (IR) and type 2 diabetes. Apart from the well-characterised complications of diabetes, IR in chronic HCV patients predicts faster progression to fibrosis and cirrhosis that may culminate in liver failure and HCC and is also linked with a reduced level of SVR (see section 1.8.1) to pegylated IFN-α and ribavirin treatment (Douglas & George, 2009; Kawaguchi *et al*., 2011). Indeed, pathogenesis, cause of death, assessment and therapeutic strategy for hepatogenous insulin/diabetes differ from those for lifestyle-related type 2 diabetes. Furthermore, serum insulin levels are higher in diabetic patients with chronic liver disease than in patients with lifestyle-related diabetes. These results indicate that distinctive factors underlie the pathophysiology of hyperinsulinemia in these HCV-positive patients. IR is most strongly associated with HCV genotype 1 but severe IR has also been observed in patients with genotypes 3 or 4 (Cua *et al*., 2008; Moucari *et al*., 2008; Duseja *et al*., 2009).

1.7. Diagnosis of HCV Infection

HCV infection can be diagnosed utilising both serological and virological assays. Serological tests are performed using an enzyme immunoassay (EIA) to detect the presence of antibodies against various HCV epitopes. Once serum or plasma antibodies have been captured on the wells of microtitre plates using corresponding antigens, antigen-antibody complexes are then specifically revealed in a colorimetric enzymatic reaction. The degree of colour change is proportional to the level of antibody present in the sample. The HCV genotype of individual samples can be determined by looking for antibodies directed to genotype-specific HCV epitopes (Pawlotsky, 2002; Chevaliez & Pawlotsky, 2007).

Virological assays rely on HCV nucleic acid amplification and give both a qualitative and quantitative analysis of viral load. These tests are more sophisticated and thus, more useful, than serological assays as they can detect virus before antibodies are produced. HCV RNA is extracted and reverse transcribed into a single-stranded complementary DNA (cDNA), which is subsequently processed into a cyclic enzymatic reaction leading to the production of a large numbers of detectable copies. Polymerase chain reaction (PCR)-based assays are used to synthesize double-stranded copies of the HCV genome, whereas single-stranded copies can be generated by transcription-mediated amplification (TMA) (Chevaliez & Pawlotsky, 2007). While these methods give a qualitative measure of HCV RNA, quantitative analysis of HCV load can be determined by means of target amplification techniques such as competitive PCR or real-time PCR, or by signal amplification techniques such as the branched DNA (bDNA) assay. bDNA is a signal enhancement procedure involving hybridization of virus RNA after binding to specific ssDNA probes. However, real-time PCR has become the technique of choice to detect and quantify HCV RNA in clinical practice. Virological assays can determine HCV genotypes by using specific primers that bind signature sequences of each particular strain of virus (Chevaliez & Pawlotsky, 2007; Chevaliez & Pawlotsky, 2009). Developments in sequencing, particularly next-generation sequencing (NGS), now allow detection of all components of the complex mixture of genetically related yet distinct viral populations that exist in equilibrium in an infected individual, but this

approach is still too cumbersome and time-consuming to exist outside a research setting (Chevaliez *et al*., 2012).

1.8. Treatment of HCV Infection

Of those infected with HCV, 60-85 % proceed to a chronic state, in which there is very little chance of the infection spontaneously resolving. Of these chronically infected individuals, 15-30 % will develop cirrhosis over the course of the next three decades (Rosen, 2011). There is currently no vaccine against HCV, development of which is often thwarted by the heterogeneity of the virus. The current standard treatment for patients with HCV is a combination of pegylated IFN-α and ribavirin. In recent years, however, the development of several antiviral drugs, designed to interfere directly at specific stages of the HCV lifecycle, has resulted in the emergence of triple therapies for specific patient cohorts, with these antiviral drugs used alongside pegylated IFN-α and ribavirin in treatment (Pawlotsky, 2011). If these IFN-based treatments fail and patients subsequently develop decompensated liver cirrhosis or HCC, liver transplantation is the only available treatment option for individuals. However, even after successful transplantation, reinfection typically occurs due to circulating HCV in the blood. Reinfection of the graft is also associated with a more rapid disease progression, with a median time to cirrhosis of 8 to 10 years (Terrault & Berenguer, 2006)

1.8.1. Treatment of Infection with IFN-α and Ribavirin Combination Therapy

Initially, HCV infection was treated with IFN-α, but this monotherapy eliminated virus in <20 % of patients (Di Bisceglie & Hoofnagle, 2002). The conjugation of polyethylene glycol to recombinant IFN-α, resulting in pegylated IFN-α, was a major step in HCV treatment as the molecule had a longer half-life, a better pharmacokinetic profile and a better rate of virological response compared to IFN-α (Glue *et al*., 2000; Zeuzem *et al*., 2000). Administering the guanosine analogue ribavirin in combination with pegylated IFN-α further improved viral clearance rates (despite the fact ribavirin monotherapy is ineffective) and has become the "standard-of-care" therapy for HCV

treatment (Di Bisceglie *et al*., 1992; Feld & Hoofnagle, 2005). In spite of this, a sustained virological response (SVR) – defined by undetectable HCV RNA 24 weeks after treatment completion, associated with permanent cure in 99 % of cases – is achieved in only 40-50 % of patients infected with genotypes 1 or 4, improving to ~ 80 % of patients infected with genotypes 2 or 3 (Soriano *et al*., 2009). Several pretreatment factors can adversely influence the SVR rate, including older age, male sex, African American race, obesity, presence of cirrhosis or advanced fibrosis and absence of significant co-morbidities (Feld & Hoofnagle, 2005; Tsubota *et al*., 2011). This therapy is also extremely expensive and can cause side effects including headaches, fever, myalgia, haemolytic anaemia and severe depression (Fried, 2002).

The mechanism by which pegylated IFN-α and ribavirin exert a therapeutic effect against HCV infection is unknown. IFN-α is a member of the type-1 IFNs, which have all been implicated to play crucial roles in the innate immune response and exhibit antiviral, antiproliferative and immunomodulatory activities. IFN-α has potent antiviral activity, not by acting directly on the virus or replication cycle, but by inducing ISGs, which in turn promote a non-virus-specific antiviral state within the infected cell (Feld & Hoofnagle, 2005; Sen, 2001). However, it is not yet understood which of the numerous ISGs activated by IFN-α is responsible for inhibiting HCV. Ribavirin is a guanosine analogue and is phosphorylated intracellularly to produce mono-, di- and tri-phosphate forms. Misincorporation of ribavirin triphosphate by the HCV polymerase has been shown to lead to premature chain termination and inhibition of viral replication (Maag *et al*., 2001), while ribavirin monophosphate is known to be a competitive inhibitor of a cellular enzyme (inosine monophosphate dehydrogenase- IMPDH) vital for viral RNA synthesis (Feld & Hoofnagle, 2005; Lau *et al*., 2002). However, the minimal antiviral effects of ribavirin monotherapy indicate that neither of these processes are likely to be the major mechanism of action against HCV. Ribavirin has also been found to act as a viral mutagen, causing an accumulation of errors that may cause a collapse in viral fitness or remove a quasispecies population from an infected individual, termed “error catastophe” (Crotty *et al*., 2001). It is possible that ribavirin might reduce the ability of HCV to escape immune and antiviral responses, thus increasing the effectiveness of pegylated IFN-α.

1.8.2. Novel Antivirals

The development of HCV replicons and cell culture infectious systems has enabled the design of STAT-C (specifically targeted antiviral therapy for hepatitis C) compounds, also referred to as direct acting antiviral (DAA) molecules, which can specifically and directly target the HCV lifecycle (Rosen, 2011; Soriano *et al*., 2009). Indeed, two NS3/4A protease inhibitors (PIs), boceprivir and telaprevir, were approved by the US Food and Drug Administration (FDA) for clinical use in May 2011, the first new drugs approved for HCV treatment in over a decade. These PIs exert their effect by blocking the NS3/4A serine protease from cleaving the viral polyprotein and the interferon-β promoter stimulator 1 (Jacobson *et al*., 2012; Rosen, 2011). This first generation of PIs have been shown to reduce duration of therapy and increase SVR rates in genotype 1 patients from 40 to > 60 % when used in combination with pegylated IFN-α and ribavirin compared to standard pegylated IFN-α/ribavirin therapy. While this triple therapy represents a huge step forward, this treatment is still unsuitable for patients either intolerant of or with contraindications to pegylated IFN-α or ribavirin and is ineffective in patients with non-1 genotype HCV, previous null responders to pegylated IFN-α/ ribavirin therapy and those with advanced fibrosis (Gane, 2012; Jazwinski & Muir, 2011). Numerous unpleasant side-effects, including skin rash, nausea and anaemia, are regularly observed during treatment with telaprevir and boceprevir. Clinical trials have also discovered that the use of protease inhibitors in isolation leads to the rapid generation of viral mutations and resistance, but the presence of ribavirin in triple therapy prevents the risk of emerging PI-resistant HCV strains (Pawlotsky, 2011; Soriano *et al*., 2009).

Other drug classes entering the HCV treatment landscape include nucleoside analogue and non-nucleoside polymerase inhibitors, NS5A inhibitors and cyclophilin inhibitors. Inhibition of the cellular-encoded cyclophilins, notably cyclophilin A (CypA), is believed to account for the anti-HCV activity of cyclosporine A (CsA) and its analogues, which target the isomerase activity of these proteins (Chatterji *et al*., 2009; Kaul *et al*., 2009). As a direct interaction of CypA with viral replicase components NS5A and NS5B has been reported (see sections 1.9.8 and 1.9.9), and HCV resistance to CsA is linked to the emergence of resistance mutations that map to NS5A and NS5B

(Fernandes et al., 2007; Robida et al., 2007), it has been suggested that NS5A and NS5B may govern the dependence of the virus on CypA-mediated isomerase activity, although the molecular mechanisms involved in this process are as yet unclear. While none of these compounds have completed the range of clinical trials needed for full FDA approval, results from early clinical development studies are very encouraging in some cases. For instance, the NS5A inhibitor BMS-824 potently inhibits HCV replication and demonstrated promising efficacy during phase I clinical trials (Gao *et al*., 2010), while preliminary trials of the NS5B nucleoside analogue R7128 have shown the compound to be safe and well tolerated when administered together with pegylated IFN-α and ribavirin (Ali *et al*., 2008). A long-term goal for HCV treatment is to develop an IFN-free regimen that targets all HCV genotypes, giving therapeutic options to a far greater proportion of the HCV-infected community. Combining two different classes of STAT-C agents such as a PI and a polymerase or NS5A inhibitor is seen as the most effective and broad HCV therapy that avoids the use of interferon. Whether ribavirin will be needed for this therapy to combat drug resistance depends on the advances in characterisation of STAT-C compounds in the near future (Jacobsen *et al*, 2012; Pawlotsky, 2012).

1.9. HCV Genome Organisation and Function

The genome of HCV is a positive-sense, single stranded RNA molecule ~ 9.6 kb in length. The genome consists of a single open reading frame (ORF) encoding a polyprotein of ~ 3000 amino acids, flanked by two untranslated regions at the 5' and 3' ends (5'UTR and 3'UTR) (Fig 1.2). The polyprotein is cleaved by cellular and viral proteases to yield the HCV structural proteins core, E1 and E2 and the non-structural proteins NS2, NS3, NS4A, NS4B, NS5A and NS5B. Until recently, the ion channel p7 protein, which is located between the confirmed structural and non-structural proteins, was unassigned to either category. However, a stable interaction has been observed between p7 and NS2, while a similar association is not seen between p7 and any of the structural proteins, suggesting that p7 is a non-structural protein (Vieyres *et al*., 2013).

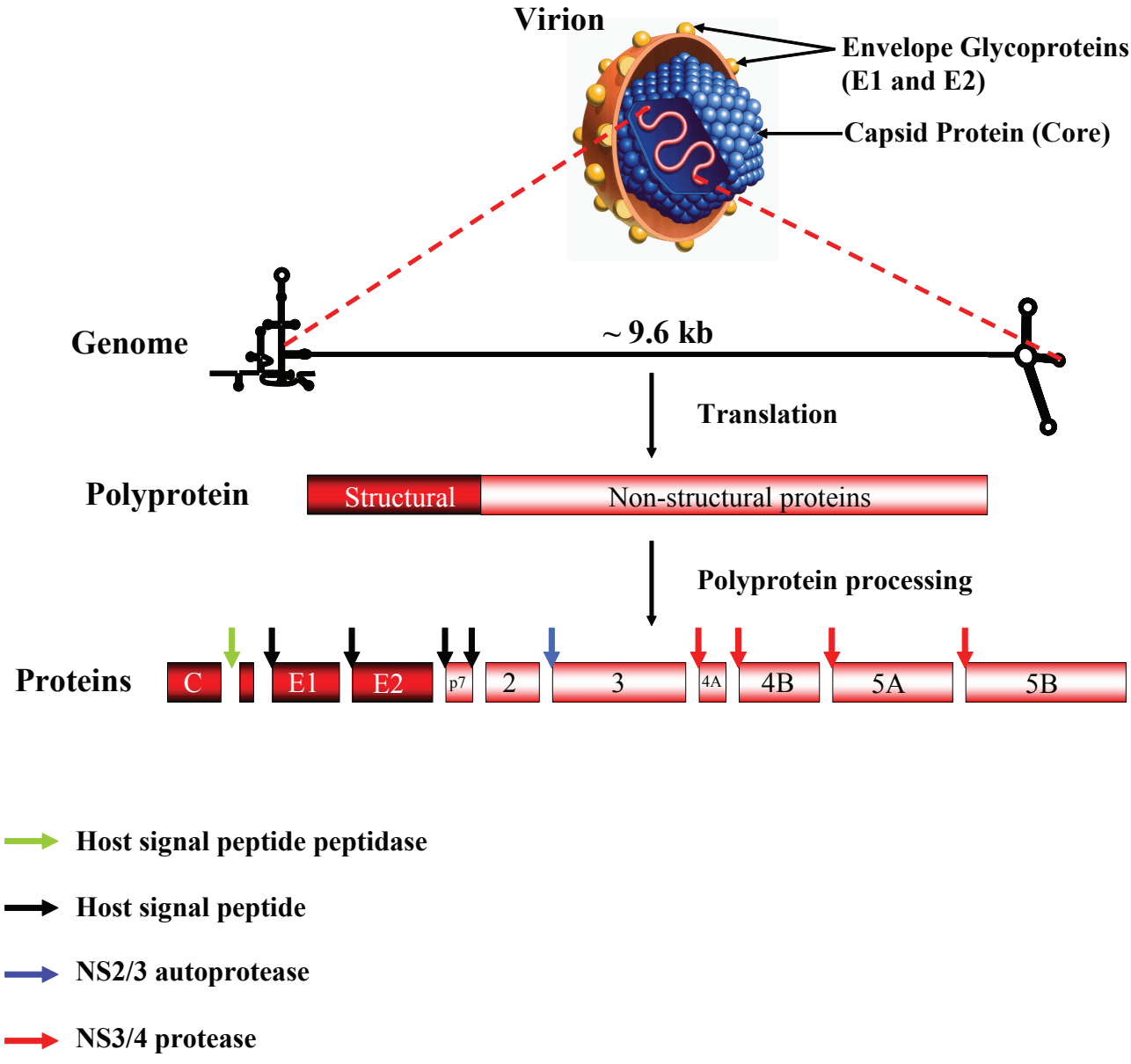

Figure 1.2. General features of the HCV genome and polyprotein processing.

5' and 3' UTRs flank the HCV ORF, which generates a single polyprotein with structural proteins (nucleocapsid protein or core, envelope glycoproteins E1 and E2, and probably p7) grouped at the N-terminus followed by the nonstructural proteins (NS2-5B). The polyprotein is cleaved into the 10 individual HCV proteins by both host and viral proteases through complex co- and posttranslational events. Adapted from Tellinghuisen *et al.* (2007).

1.9.1. The 5'UTR

The 5'UTR is a highly conserved sequence consisting of 341 nucleotides that contributes towards translation and replication of the viral genome (Bukh *et al*., 1992; Friebe *et al*., 2001; Honda *et al*., 1999). A combination of computational, phylogenetic and mutational analyses of the region identified four highly structured domains (domains I to IV) (Brown *et al*., 1992; Honda *et al*., 1996a; Honda *et al*., 1999; Smith *et al*., 1995). Translation of the HCV ORF occurs via an internal ribosome entry site (IRES) in a cap-independent manner. The HCV IRES, which incorporates domains II, III and IV of the 5'UTR together with the first 24-40 nucleotides of the core-coding sequence, directly recruits the 40S ribosomal subunit to the AUG codon and initiates protein translation (Honda *et al*., 1996b, Reynolds *et al*., 1996; Penin *et al*., 2004). Given that no ribosome scanning is necessary for translation to begin, eIF2, eIF3, eIF5 and eIF5B are the only eukaryotic translation factors that have been implicated in HCV translation (Pestova *et al*., 2008; Terenin *et al*., 2008). Domains II and III of the 5'UTR are vital for genome translation as they directly contact and position the 40S subunit to the AUG codon. Domain IV is not required for ribosome binding but it has been suggested that it might provide a mechanism for feedback regulation of HCV translation as the structural stability of domain IV negatively correlates with translation efficiency (Honda *et al*., 1996a). In addition to its role in ribosome binding, the 5'UTR is essential for genome replication. Domains I and II have been found to be sufficient for viral RNA synthesis, although replication efficiency is enhanced if the complete 5'UTR is available (Friebe *et al*., 2001; Kim *et al*., 2002).

As well as canonical translation factors such as eIF3, the 5'UTR is known to interact with a number of other cellular factors. These include the polypyrimidine tract binding protein (PTB) and the La autoantigen, which are thought to regulate HCV translation and replication through their interaction with the 5'UTR (Ali & Siddiqui, 1995; Ali & Siddiqui, 1997), although there is controversy about the necessity of PTB's role in translation (Brocard *et al*., 2007). The interaction between the 5'UTR and the poly (rC)-binding protein 2 (PCBP2) is involved in HCV replication, but has no effect on viral translation (Fukushi *et al*., 2001). Additionally, a liver-specific cellular microRNA, miR-122, binds to two adjacent sites in the 5'UTR (Jopling *et al*., 2005; Jopling *et al*.,

2008). Binding at both sites is needed for efficient viral translation (Henke *et al*., 2008). However, analysis of double-binding-site mutants indicate that the subsequent defects observed in HCV translation are not sufficient to explain the profound reductions also seen in viral replication and infectious virus production (Jangra *et al*., 2010), suggesting that miR-122 acts at additional steps in the virus life cycle. In line with this, it has been suggested that miR-122 can also protect the 5'UTR from nucleolytic degradation and prevent the induction of innate immune responses (Li *et al*., 2013a; Machlin *et al*., 2011).

1.9.2. Core

HCV core protein, at the very N-terminus of the HCV polyprotein, is presumed to form the viral nucleocapsid, which houses and protects the viral genome (McLauchlan, 2000). During the processing of core in the cell, a signal peptide between core and E1 undergoes an initial cleavage by the cellular enzyme signal peptidase (SP), releasing the N-terminal end of E1 and leaving an immature precursor of core, 191 aa in length, anchored in the ER membrane (Hussy *et al*., 1996; Moradpour *et al*., 1996; Santolini *et al*., 1994; Yasui *et al*., 1998). The signal peptide present at the C-terminus of core undergoes a second proteolytic event, this one mediated by the intramembrane protease signal peptide peptidase (SPP), which releases mature core from the ER membrane (McLauchlan *et al*., 2002; Pene *et al*., 2009). This SPP-mediated cleavage event and the subsequent trafficking of the mature core protein to lipid droplets (LDs) have been identified as crucial steps in virus production (Boulant *et al*., 2006; McLauchlan *et al*., 2002; Miyanari *et al*., 2007; Shavinskaya *et al*., 2007, Targett-Adams *et al*., 2008b).

Mature core is a 21 kDa protein that can be separated into two distinct domains, termed D1 and D2. D1, consisting of residues 1-117, is highly hydrophilic and is involved in RNA binding (Boulant *et al*., 2005) and multimerisation of the protein through homotypic interactions (Matsumoto *et al*., 1996). D2, spanning residues 118 to ~ 169, is more hydrophobic, containing two amphipathic α-helices connected by an unstructured region called the hydrophobic loop (HL) (Boulant *et al*., 2006). D2 is essential for core's association with LDs and ER membranes (Boulant *et al*., 2006; Hope & McLauchlan, 2000, Moradpour *et al*., 1996) and is also required for the accurate folding

of D1, which is unstructured when isolated (Boulant *et al*., 2005). Following its interaction with LDs, core directs the distribution of LDs into the vicinity of membranes bearing viral replication complexes, a process essential for the assembly of infectious HCV particles (Boulant *et al*., 2007; Miyanari *et al*., 2007).

The role of core in virion morphogenesis was first investigated by performing extensive mutagenesis across a large section (residues 57-191) of the protein, creating a total of 34 mutant viruses (Murray *et al*., 2007). This project revealed numerous residues critical for infectious virus production but not for viral RNA replication. Another mutagenesis study focusing on two highly conserved clusters of basic amino acids (residues 6-23 and 39-62) in core soon followed, identifying four residues (R50, K51, R59 and R62) that, when mutated to alanine in tandem, completely abrogated viral assembly (Alsaleh *et al*., 2010). Further work conducted by our group recently revealed that the alanine substitution of core residue G33 greatly reduces virus infectivity in the context of HCVcc (Angus *et al*., 2012). This mutation is thought to alter the conformation of a helix-loop-helix motif involving core residues 15-41. The passage of this assembly-defective virus identified compensatory mutations in close proximity to the original alanine substitution, suggesting that domain 1 of core has important functions in virion morphogenesis (Angus *et al*., 2012). In line with this, an adaptive cell-culture mutation in domain 1 of core (K74T) has recently been found to enhance viral protein-protein interactions and morphogenesis of infectious HCV (Jiang & Luo, 2012).

A recent study highlighted that the nucleocapsid-like particle of HCV most likely contains a dimer of core that is stabilized by a disulfide bond (Kushima *et al*., 2010). Mutational analysis revealed that the core C128 residue was responsible for this disulfide bond, without which virus particle assembly and viral capsid stability were adversely affected (Kushima *et al*., 2010). The translation of an alternative reading frame in the core coding sequence can also yield a 17 kDa protein called ARFP or F protein. This protein is expressed during natural HCV infection but has been found to be dispensable for virus replication *in vitro* and *in vivo* (McMullan *et al*., 2007; Vassilaki *et al*., 2008) However, chronic HCV patients have displayed specific immune responses to F protein (Xu *et al*., 2001), suggesting a role for the protein in the viral life cycle, as yet undetermined.

Amino acid sequence analysis indicates that core is the most conserved of all HCV proteins across all genotypes (Bukh *et al*., 1994), reflecting its essential role in the HCV lifecycle. With its extremely high level of conservation, it is hardly surprising that core has been reported to influence numerous diverse host cell functions including apoptosis, gene transcription, cell proliferation, immune response modulation, lipid metabolism and HCV related steatosis and carcinogenesis (see section 1.4.2) (Giannini & Brechot, 2003; Mclauchlan, 2000; Mclauchlan, 2009; Ray & Ray, 2001; Roingeard & Hourioux, 2008). As these observations were derived mainly from heterologous overexpression experiments, the relevance of these results are as yet unconfirmed. Despite this, core is known to engage in a wide range of interactions with viral and cellular proteins, with many of these associations mapped to residues within D1 of core (McLauchlan, 2000). The interaction of core with the cellular DEAD-box RNA helicase DDX3 has been a focus of study in our research group for many years. The importance and characteristics of this interaction will be explained in greater depth in section 1.12.3.4.

1.9.3. E1 and E2

Following genome translation, the viral envelope glycoproteins E1 and E2 are liberated from the viral polyprotein following proteolytic cleavage by host cell signal peptidases (Miyamura & Matsuura, 1993). These glycoproteins are located on the surface of the virion and are involved in host-cell entry by binding to cell surface receptors and fusing with host-cell membranes (Penin *et al*., 2004). E1 and E2 are type I transmembrane proteins with an N-terminal ectodomain translocated into the ER lumen and a short C-terminal transmembrane domain (TMD) inserted into the ER membrane (Op De Beeck *et al*., 2001). After their synthesis, E1 and E2 associate to form noncovalent heterodimers intracellularly (Lavie *et al*., 2007), but virion-associated glycoproteins form large covalent complexes stabilized by disulfide bridges in a HCVcc background (Vieyres *et al*., 2010). As functional E1 and E2 has been shown to form noncovalent heterodimers on the surface of HCVpp (Op De Beeck *et al*., 2004), the differences in glycoprotein maturation between HCVpp and HCVcc may account for the differences observed in HCV envelope protein function when these two systems are compared (Russell *et al*., 2008). Accurate folding of these proteins is highly influenced by modifications mediated by asparagine (N)-linked glycans. E1 and E2 contain up to 6

and 11 conserved glycosylation sites, respectively. These modifications not only aid glycoprotein folding but also facilitate HCV entry (Goffard *et al*., 2005, Lavie *et al*., 2007).

Hypervariable regions (HVR) have been identified within E2. The first 27 aa's of the E2 ectodomain form HVR1, a region highly implicated in cellular attachment. This region evolves rapidly in HCV-infected individuals, driven by antibody selection of immune-escape variants, indicating that HVR1 is under strong immune pressure (Mondelli *et al*., 2003). An HCV clone lacking HVR1 was shown to be infectious in chimpanzees, but this mutant virus was attenuated, suggesting a functional role for HVR1 in HCV entry (Forns *et al*., 2000). Despite the strong aa variability, the physico-chemical properties and confirmation of HVR1 are well conserved among the various genotypes and the region is globally basic (Penin *et al*., 2001). Mutation of basic residues at specific locations in HVR1 has been shown to greatly reduce virus entry, although this has no apparent effect on glycoprotein-receptor binding (Callens *et al*., 2005). While deletion of HVR1 reduces HCVcc infectivity by 5- to 10-fold, deletion of either of the other highly variable regions found in E2, HVR2 and the intergenotypic variable region (igVR), eliminates formation of glycoprotein heterodimers, reduces CD81 binding and abolishes virus entry, consistent with a global folding defect (McCaffrey *et al*., 2011).

Mutation of specific residues in the transmembrane domains of E1 and E2 are known to alter the fusion properties of the envelope glycoproteins, indicating that these proteins play an important part in the fusion process (Ciczora *et al*., 2007). While E1 may contain a putative fusion peptide in its ectodomain (Flint & McKeating, 1999; Garry & Dash, 2003), it is believed that E2 is a class II fusion protein with a β-sheet organisation and an internal fusion peptide (Penin *et al*., 2004). No high-resolution structural data currently exists for the HCV glycoproteins, but one group have constructed a homology model for E2 based on related class II fusion proteins using the positions of the protein's disulfide bridges together with functional data and secondary structure predictions (Krey *et al*., 2010). This model divides E2 into three domains arranged linearly, forming a rod-like molecule. The central domain (domain I) consists of an eight-stranded β-sandwich structure with an up-and-down topology that is present in all class II fusion proteins. A candidate fusion loop has been found at aa residues 502–520 in domain II, while the residues responsible for interaction with the tetraspanin CD81 can be found at

the interface of domains I and III, with the majority of residues present on domain I. Domain III separates Domain I from the stem region but is linked to Domain I via the igVR. This model also suggested that several glycans appear to frame the CD81 binding surface, partially shielding it from recognition by circulating antibodies (Krey *et al*., 2010).

E1 and E2 contain numerous conserved cysteine residues that form intramolecular disulfide bonds in the oxidizing environment of the ER. The overall conformation of the envelope glycoproteins depends on these bonds. Krey *et al*. (2010) determined the identity of the nine disulfide pairs formed by 18 conserved cysteine residues within the E2 ectodomain. Alanine scanning mutagenesis of each of these 18 residues confirmed that all nine disulfide bonds and their corresponding cysteine residues in E2 are essential for viral entry (McCaffrey *et al*., 2012). However, the contributions of each cysteine residue and the nine disulfide pairs to E2 structure varied, illustrating a complex pattern of intermolecular bonding. Recent studies have found that E2 can tolerate the presence of four cysteines existing at free thiols, leaving their predicted disulfide-bonding partners to participate in labile inter- and intramolecular disulfide-bonding arrangements that are critical for viral entry competence (Fraser *et al*., 2011; McCaffrey *et al*., 2012). Conserved histidine residues in E1 and E2 have also been found to play important roles in protein folding, CD81 receptor binding and viral entry (Boo *et al*., 2012). This is unsurprising, given that histidine plays a variety of structural and functional roles in protein folding and stability in general through its numerous diverse interactions with other amino acids. Residue H445 of E2 was also found to be a pH sensor that can trigger conformational changes associated with membrane fusion (Boo *et al*., 2012).

As well as CD81, several other cellular HCV receptors have been identified through their interaction with E2, including SR-BI and occludin (Liu *et al*., 2009, Pileri *et al*., 1998; Scarselli *et al*., 2002). While E2 is the best characterised subunit and is considered the major target of neutralizing antibodies and the main receptor-binding protein, E1 has recently been found to modulate E2 recognition by the cellular co-receptor CD81 (Wahid *et al*., 2013). This result strengthens the validity of earlier reports postulating that the correct conformational folding of each glycoprotein is dependent on the expression of the other (Deleersnyder *et al*., 1997; Lavie *et al*., 2007;

Michalak *et al*., 1997; Op De Beeck *et al*., 2001). Additionally, several host ER chaperones such as calnexin, calreticulin and BiP have been shown to interact with E1 and E2, suggesting that HCV exploits cellular factors during protein maturation (Dubuisson & Rice, 1996).

1.9.4. p7

p7 is a small (7 kDa) hydrophobic membrane protein located between the structural and non-structural regions of the HCV polyprotein. Cleavage of p7 from the viral polyprotein is mediated by a host signal peptidase, which, due to the presence of an E2-p7-NS2 precursor and stable E2-p7 form, is likely to occur post-translationally (Lin *et al*., 1994a). *In vitro*, p7 forms oligomers and is capable of conducting ions across artificial membranes in a cation-selective manner (Griffin *et al*., 2003; Montserret *et al*., 2010; Steinmann & Pietschmann, 2010). The precise oligomeric state of p7 is as yet unknown, with conflicting reports highlighting hexameric (Griffin *et al*., 2003; Luik *et al*., 2009) and heptameric species (Chandler *et al*., 2012; Clarke *et al*., 2006). p7 ion channel function can be inhibited by amantadine, a compound that inhibits the influenza A encoded M2 ion channel activity (Griffin *et al*., 2003). Due to this ability to oligomerize and sustain ion fluxes, p7 has been included into the viral protein family known as viroporins. Viroporins are small, virus encoded polypeptides that interact with membranes, comprising at least one transmembrane segment (Gonzalez & Carrasco, 2003). In line with this, each p7 monomer is composed of two transmembrane domains with both its N-and C- termini orientated towards the ER lumen. These transmembrane segments are connected by a hydrophilic loop orientated towards the cytosol (Carrere-Kremer *et al*., 2002).

The ion channel activity of p7 relies on its cytoplasmic loop. The topology of this hairpin-like structure is stabilized by two conserved basic residues at positions 33 and 35 of p7. These residues have been found to be essential for ion channel activity *in vitro* (Griffin *et al*., 2004), as well as production of infectious progeny in cell culture (Jones *et al*., 2007; Steinmann *et al*., 2007) and infectivity *in vivo* (Sakai *et al*., 2003). As well as these basic loop mutations, a conserved histidine at position 17 has also been found to be essential for genotype 1b p7 ion channel activity, a residue located within the

amino-terminal transmembrane domain that has been shown to line the channel lumen (Chew *et al*., 2009; StGelais *et al*., 2009).

Adaptive mutations in p7 have been found to enhance infectious virus production (Russell *et al*., 2008). Although p7 is not thought to play a role in viral RNA replication (Lohmann *et al*., 1999), there is evidence that p7 has numerous different functions in HCV production including roles in viral assembly and release (Jones *et al*., 2007; Steinmann *et al*., 2007; Wozniak *et al*., 2010). Wozniak *et al*. (2010) demonstrated that p7 controls proton (H^+) equilibration, resulting in a loss of intracellular compartment acidification. While mature virions are acid stable, intracellular virus can be inactivated by acidic pH, indicating that the reduction in acidification mediated by p7 is essential for the production of infectious virus. While this result indicates that p7 is involved at a late stage of virus production, it has been suggested that p7 acts at an earlier stage of virion morphogenesis as well. Jones *et al*. (2007) postulated that if p7 was functioning solely to protect glycoproteins from inactivation late in egress, infectious intracellular virus that had not yet been inactivated would be released by subjecting cells to freeze-thawing. No such virus was detectable, suggesting that p7 also likely acts early in viral morphogenesis prior to particle production and supports a post-assembly role for p7 proton channel function (Jones *et al*., 2007). Furthermore, mutation complementation analysis suggested that p7 interacts directly with other viral proteins as well as host proteins essential for virus production (Yi *et al*., 2007). The findings reported by Yi *et al*. (2007) were reinforced by a recent report focusing on the generation of a functional HA-tagged p7 variant, which confirmed the stable interaction between p7 and NS2 and the crucial nature of this association for the production of infectious HCV particles (Vieyres *et al*., 2013). The lack of a similar interaction between p7 and any of the HCV structural proteins implied that p7 is a non-structural protein. Furthermore, an anti-HA antibody could not neutralize virus produced from the HA-p7-tagged genome, whereas the same anti-HA antibody was able to neutralize virus particle infectivity from a control virus incorporating a HA-tagged ApoE. They also published data highlighting how a double-tagged virus they generated, incorporating a Flag epitope at the N-terminus of E2 and a double HA epitope at the terminus of p7, could be neutralized by an anti-Flag antibody but not by an anti-HA antibody (Vieyres *et al*., 2013). Despite these results, and the fact that there are many examples in nature of viroporins that are not incorporated into their respective virions (i.e., HIV Vpu and alphavirus 6K)

(Gonzalez & Carrasco, 2003), the authors stated that the incorporation of p7 into the HCV virus particle cannot be ruled out as a possibility. Indeed, p7 could be part of the virion but simply have no role in entry or its role in entry is unaffected by the anti-HA antibody used in these experiments. More sensitive detection methods may be required to determine if p7 is incorporated into the HCV virion, given that the M2 viroporin, a crucial factor in influenza entry, is present at extremely low levels on the influenza virion (14 to 68 copies per virion) (Zebedee & Lamb, 1988).

1.9.5. NS2

The 23 kDa NS2 protein is a nonglycosylated integral membrane protein. This non-structural protein has a hydrophobic amino-terminal subdomain containing three TMDs that localise NS2 to the ER membrane (Lorenz, 2010). NS2 also contains a carboxy-terminal cytoplasmic domain which, together with the first 181 residues of NS3, form a zinc-dependent cysteine autoprotease that cleaves the NS2/NS3 junction (Grakoui *et al*., 1993; Hijikata *et al*., 1993a). Crystallography of the NS2 C-terminal region revealed a dimeric protease (Lorenz *et al*., 2006; Gouttenoire *et al*., 2006). Each monomer encompasses two α-helices extended by a linker to six β-strands, with the α-helices of one subunit interacting with the β-strands of the other subunit and *vice versa* (Gorzin *et al*., 2012). The crystal structure of the NS2 C-terminus also identified a catalytic triad: His 143, Glu 163 and Cys 184 are entirely conserved in all HCV isolates, with mutagenesis of any of these residues to alanine abrogating proteolytic activity (Lorenz *et al*., 2006).

While NS2 has to be cleaved off the N-terminus of NS3 to allow formation of an active replicase, NS2 is not directly required for viral RNA replication (Lohmann *et al*., 1999). Full length NS2 is known to be essential for the production of infectious virus particles in HCVcc, although the proteolytic function of the protein is not needed for efficient viral production (Jirasko *et al*., 2008; Jones *et al*., 2007). It has also been observed that a number of cell culture adaptive mutations generated within the NS2 coding region greatly enhance virus production (Russell *et al*., 2008, Yi *et al*., 2007). The N-terminal transmembrane segment of NS2 seems to play a prominent role in HCV particle production. Indeed, studies of chimeric viral genomes derived from two different

genotypes or two strains of the same genotype have shown that virus production is most efficient when the transition point between the two genomes is after the first transmembrane segment of NS2 (Pietschmann *et al*., 2006). Additionally, there is increasing evidence to suggest that NS2 plays a central organizing role in viral particle assembly through physical interactions with various HCV structural and non-structural proteins, including E1, E2, p7, NS2, NS3 and NS5A (Jiang & Luo, 2012; Jirasko *et al*., 2010; Ma *et al*., 2011; Popescu *et al*., 2011a; Stapleford & Lindenbach, 2011). An ion channel-independent function of p7 is hypothesised to target NS2 to sites adjacent to replication complexes (Tedbury *et al*., 2011). A serine residue (S168) within NS2 has also been found to be vital for the efficiency of this process (Tedbury *et al*., 2011). At these subcellular sites, NS2 interacts with NS5A (and potentially other replication complex components), possibly mediating the interface between genome replication and particle assembly (Tedbury *et al*., 2011).

While numerous mutagenesis studies have implicated select residues within the NS2 N-terminal domain in the early steps of the assembly process (Jirasko *et al*., 2008; Jirasko *et al*., 2010; Phan *et al*., 2009; Pokrovskii *et al*., 2011; Stapleford & Lindenbach, 2011), a detailed mutational analysis spanning the first 92 residues of NS2 generated viral mutants that debilitated later steps of virus production also, most notably egress (De al Fuente *et al*., 2013).

1.9.6. NS3 & NS4A

NS3 is a 70 kDa multifunctional protein that features a serine protease domain located in the N-terminal one third and an NTPase/RNA helicase domain in the C-terminal two-thirds. NS4A, the smallest HCV-encoded protein at 6 kDa, serves as a co-factor for NS3's enzymatic activities (Bartenschlager *et al*., 1995; Lin *et al*., 1995; Tai *et al*., 1996). NS4A consists of an N-terminal hydrophobic domain, a central domain and a C-terminal acidic region and forms a non-covalent, heterodimeric complex with NS3. The central portion of NS4A contributes one β-strand to the NS3 N-terminal protease domain, allowing accurate folding of NS3 (Kim *et al*., 1996). The N-terminal region of NS4A forms a transmembrane α-helix required for the integral membrane association of the NS3/4A complex (NS3 is normally diffusely distributed in the cytoplasm in the

absence of NS4A) (Wolk *et al*., 2000), while the C-terminal region of NS4A interacts with other replicase components to contribute to HCV RNA replication and virus particle assembly (Lindenbach *et al*., 2007; Phan *et al*., 2011). Alanine-scanning mutagenesis of this C-terminal region in the context of a chimeric genotype 2a reporter virus found two mutants that inhibit RNA replication, as well as unearthing seven mutants which can effectively replicate but have severe viral assembly defects. Generation and analysis of second-site mutations that suppressed these NS4A defects revealed interactions that contribute to RNA replication and viral assembly, with an association between NS4A and NS4B implicated in the control of viral genome replication and an interaction between NS3 and NS4A linked to efficient viral assembly (Phan *et al*., 2011).

The C-terminus of NS4A has other roles that may be vital for the HCV lifecycle. This region is required for NS5A hyperphosphorylation (Lindenbach *et al*., 2007), which plays an important but as yet unknown role in HCV genome replication. While the NS4A replication mutants determined by Phan *et al*. (2011) did not display detectable differences in NS5A hyperphosphorylation, replication deficiency in genotype 1b replicons caused by NS4A mutations exhibited a greatly reduced hyperphosphorylation status. Furthermore, RNA replication and NS5A hyperphosphorylation were co-ordinately restored in these mutants by second-site suppressor mutations in NS3 (Lindenbach *et al*., 2007). This study also reported that the α-helical folding of this C-terminal NS4A region depends on local electrostatic interactions and could behave as a molecular switch. In addition to its activity as a cofactor, NS4A can also interact with cellular factors such as creatine kinase B and elongation factor 1A (Hara *et al*., 2009; Kou *et al*., 2006), interactions postulated to influence replication and translation respectively. Overexpression of NS4A in the absence of NS3 has also been demonstrated to inhibit cellular translation (Kato *et al*., 2002). However, the implications of these NS3-independent roles of NS4A in the HCV lifecycle are unclear and their prevalence *in vivo* is unknown.

The serine protease of NS3 is required for four cleavage events, acting *in cis* to release itself from the HCV polyprotein and *in trans* to produce the N-termini of NS4B, NS5A and NS5B (Bartenschlager *et al*., 1993; Grakoui *et al*., 1993; Lin *et al*., 1994b; Tomei *et al*., 1993). The C-terminal domain of NS4A aids cleavage of the downstream

polyprotein, being particularly necessary for accurate NS4B/5A cleavage (Bartenschlager *et al*., 1994). NS3-mediated cleavage occurs in a shallow binding pocket containing a catalytic triad formed by residues His 57, Asp 81 and Ser 139. Mutation of any of these amino acids abolishes NS3-mediated cleavage (Bartenschlager *et al*., 1993; Grakoui *et al*., 1993). In addition to processing viral proteins, the NS3/4A protease is also involved in blocking antiviral innate immune responses by interfering with double-stranded RNA signalling pathways. IPS-1 and TRIF are cellular targets cleaved by NS3/4A protease, subsequently impeding the innate responses triggered by RIG-I and TLR-3 and preventing induction of type-I IFNs (Foy *et al*., 2005; Li *et al*., 2005; Meylan *et al*., 2005).

The C-terminus of NS3 encodes a DexH/D-box RNA helicase. The crystal structure of the HCV helicase shows a Y-shaped molecule composed of 3 nearly equally sized subdomains (Kim *et al*., 1998; Tai *et al*., 1996; Yao *et al*., 1997). Although monomeric NS3 can bind RNA with high affinity, RNA unwinding requires an NS3 dimer (Serebrov & Pyle, 2004). The NS3 helicase unwinds RNA in an "inchworm" or "ratchet-like" fashion and is essential for HCV RNA replication and viral particle assembly (Murray *et al*., 2008), although its precise function in the viral lifecycle remains elusive. In line with this, studies have identified compensatory mutations within the NS3 helicase that promote the assembly of infectious virus particles independent of the role of the protein in HCV RNA replication (Ma *et al*., 2008; Phan *et al*., 2009; Yi *et al*., 2007). Adaptive mutations that enhance the RNA replication of subgenomic replicons (SGRs) have been observed in both the protease and helicase domains of NS3 (Lohmann *et al*., 2003).

1.9.7. NS4B

NS4B is a highly hydrophobic 27 kDa non-structural protein with at least four predicted TMDs, which are considered to anchor the protein to the ER membrane (Hugle *et al*., 2001; Lundin *et al*., 2003). The topology of a putative fifth transmembrane helix close to the N-terminal end is controversial, as this region may translocate to the luminal side of the ER membrane post-cleavage (Lundin et al., 2003; Lundin et al., 2006). NS4B is known to induce alterations to intracellular membranes. These altered membrane

structures are referred to as the "membranous web" (MW) (Egger *et al*., 2002; Gosert *et al*., 2003) or membrane-associated foci (MAF) (Gretton *et al*., 2005) and likely create an environment suitable for the formation on HCV replication complexes, where viral RNA replication can occur. Morphologically, the MW is a cytoplasmic accumulation of highly heterogeneous membranous vesicles that are embedded into an amorphous matrix. Amphipathic helical elements known to mediate membrane association have been found in the N-terminal and C-terminal regions of NS4B (Elazar *et al*., 2004; Gouttenoire *et al*., 2009a). A second amphipathic helix has been identified in the N-terminal domain of NS4B (referred to as AH2), immediately following the first helical element (Gouttenoire *et al*., 2009a; Gouttenoire *et al*., 2009b). Further analysis on the AH2 domain demonstrated it was a major determinant of NS4B oligomerization, a process required for the formation of MWs and functional HCV replication complexes (Gouttenoire *et al*., 2010; Paul *et al*., 2011). Replication-defective mutants generated by Paul *et al*. (2011) carrying substitutions in the highly conserved C-terminal region of NS4B were used for selection of pseudoreversions. These pseudoreversions restored both replication competence and heterotypic NS4B self-interactions disrupted by the primary mutation. While the majority of these pseudoreversions localised to the NS4B C-terminus, in one instance a compensatory intergenic mutation in NS5A was also required to restore efficient replication and accurate MW morphology in addition to the NS4B pseudoreversion. This indicates that, in addition to NS4B oligomerization, NS5A may also be important for accurate MW and replication complex formation (Paul *et al*., 2011).

While other NS proteins involved in replication are known to localise to these punctuate sites (Elazar *et al*., 2004; Hugle *et al*., 2001), disruption to the first N-terminal amphipathic helix domain of NS4B (AH1) prevents the correct localisation of these NS proteins in addition to abrogating replication of the HCV genome (Elazar *et al*., 2004). Analysis of the C-terminus of NS4B has uncovered two cysteine residues in the C-terminus of NS4B that are subjected to palmitoylation, a lipid modification that may be important for the formation of protein-protein interactions within viral replication complexes (Yu *et al*., 2006). While expression of NS4B protein alone is sufficient to cause formation of the MW structure (Egger *et al*., 2002; Gosert *et al*., 2003), the structure of these membranes is slightly distinct from the MWs observed when all the HCV proteins are present, suggesting that other components contribute to efficient

production of these membrane alterations (Egger *et al*., 2002). In addition to the report published by Paul *et al*. (2011), work by Romero-Brey *et al*. (2012) also postulates a role for NS5A in MW formation (Described further in section 1.11.2.2).

Mutagenesis studies in the replicon and HCVcc systems have clearly demonstrated the essential nature of NS4B in HCV RNA replication (Blight, 2007; Jones *et al*., 2009; Lindstrom *et al*., 2006). Indeed, the most effective single amino acid mutations associated with enhanced replication efficacy are located within the NS4B protein (Krieger *et al*., 2001; Lohmann *et al*., 2001; Lohmann *et al*., 2003; Namba *et al*., 2004). Furthermore, a nucleotide-binding motif (NBM) found in NS4B, involved in the binding and hydrolysis of GTP, is also essential for HCV RNA replication (Einav *et al*., 2004). An additional role for NS4B in viral assembly has also been determined, where a single amino acid substitution in the protein, N216A, was shown to increase JFH1 viral titres by five-fold without affecting HCV RNA replication (Jones *et al*., 2009). Additionally, site-directed mutagenesis experiments highlighted the multiple viral roles in NS4B function played by numerous charged residues found throughout the N- and C-terminus of NS4B, with three NS4B mutations disrupting the formation of replication complexes, another mutation altering NS4B stability and yet another significantly delaying NS4B/NS5A cleavage (Blight, 2011). Taken together, these studies clearly indicate that NS4B has roles in the formation of replication complexes, RNA replication and infectious particle production.

1.9.8. NS5A

NS5A is a hydrophilic non-structural protein that is peripherally anchored to membranes by an N-terminal amphipathic helix (Brass *et al*., 2002; Elazar *et al*., 2003). The protein is divided into three domains, separated by two repetitive low complexity sequence (LCS) stretches. Domain I is the most conserved region of NS5A and binds a single zinc atom per protein molecule, which is essential for HCV RNA replication (Tellinghuisen *et al*., 2004). The crystallographic structure of domain I is dimeric in nature. The dimer structure is believed to be orientated in such a way that a large groove exists between the two monomers and has been proposed as an RNA binding site (Tellinghuisen *et al*., 2005). In line with this, NS5A has been shown to bind the 3' ends

of both positive- and negative-strand HCV RNA (Huang *et al*., 2005). However, an alternative crystal structure of domain I has been generated that, although dimeric in nature, lacks the large groove at the proposed interface and does not contain any obvious RNA interaction surface in this region (Love *et al*., 2009). Despite this, it is conceivable that NS5A can assume two physiologically relevant dimer configurations, or potentially a multimeric structure. Four cysteine residues in domain I (C39, C57, C59 and C80) are critical for dimerization and have been proposed to form a zinc-binding motif. Mutagenesis studies on these residues reveal their essential nature in efficient binding of NS5A to RNA and viral replication in general, revealing a correlation between NS5A dimerization, RNA binding and HCV replication (Lim *et al*., 2012).

Unlike domain I, domains II and III of NS5A appear unfolded when examined in isolation (Hanoulle *et al*., 2009; Hanoulle *et al*., 2010; Liang *et al*., 2007). While domain II is required for HCV RNA replication, domain III is thought to be dispensible for this process (Appel *et al*., 2008; Tellinghuisen *et al*., 2008b). As a result, domain III can tolerate the insertion of molecules such as green fluorescent protein (GFP) without abrogating RNA replication. This has been exploited to show that NS5A is frequently localised with HCV RNA in cells actively replicating viral genomes (Jones *et al*., 2007; Moradpour *et al*., 2004; Targett-Adams *et al*., 2008a). However, a 19 residue insertion near the C terminus of domain III has been shown to result in a delay to RNA replication when deleted (Hughes *et al*., 2009). Furthermore, this study indicated that domain III of NS5A is also essential for infectious virus particle production, in line with a number of recent reports (Appel *et al*., 2008; Schaller *et al*., 2007; Tellinghuisen *et al*., 2008a). While mutations in domain I of NS5A can severely impair virus production by preventing its association with LDs (Miyanari *et al*., 2007), deletions in domain III did not alter NS5A-LD attachment but instead abrogated the association of core protein on LDs (Appel *et al*., 2008). A serine cluster in NS5A domain III (S2428, S2430, S2433) is a determinant of NS5A's interaction with core, with mutation of this cluster blocking the core-NS5A interaction and preventing production of infectious virus (Masaki *et al*., 2008).

NS5A is a phosphoprotein that exists in two distinct forms, a hypophosphorylated form of 56 kDa and a hyperphosphoylated form of 58 kDa (Tanji *et al*., 1995; Tellinghuisen *et al*., 2004). The functional role of NS5A phosphorylation in the HCV lifecycle is not

understood, nor have the precise identities of NS5A phosphorylation sites been determined unambiguously. Evidence from mutagenesis studies suggest that hypophosphorylation targets serine residues in domains II and III, whereas hyperphosphorylation sites cluster around domain I, domain II and the low complexity sequence (LCS I) between them (Appel *et al*., 2005; Katze *et al*., 2000; Neddermann *et al*., 2004; Reed & Rice, 1999; Tanji *et al*., 1995). Several studies have shown that reducing hyperphosphorylation in NS5A results in enhanced RNA synthesis (Appel *et al*., 2005; Evans *et al*., 2004; Neddermann *et al*., 2004). Furthermore, it has been noted that numerous cell culture adaptive mutations enhancing replication alter residues within NS5A domain II and LCS I, markedly reducing the protein's hyperphosphorylation state, even when mutations were not at serine residues (Blight *et al*., 2000; Tanji *et al*., 1995). From these results, a general theme has emerged in which hypophosphorylation is required for RNA replication, and hyperphosphorylation is a negative regulator of this process. In line with this, a recent study identifies a serine residue in the LCS I region of genotype 2a NS5A, S222, that functions as a negative regulator of RNA replication (LeMay *et al*., 2013). However, impairing NS5A hyperphosphorylation does not always lead to increased viral replication. A residue that diminished hyperphosphorylation in NS5A domain III, S457, had no effect on HCVcc RNA replication yet abolished virus production when mutated (Tellinghuisen *et al*., 2008a). This is in contrast to the serine cluster in domain III that mediate virus production through the core-NS5A interaction, which reduce hypophosphorylation if altered adversely (Masaki *et al*., 2008). Furthermore, mutations to the C-terminal acidic region of NS4A block both NS5A hyperphosphorylation and HCV RNA replication (Lindenbach *et al*., 2007). Taken together, these results suggest phosphorylation of NS5A plays key mediating roles in viral RNA replication and virus production through distinct mechanisms.

Besides roles in viral replication and assembly, NS5A also interacts with a range of cellular signalling pathways (Macdonald & Harris, 2004). For example, domain II contains a region referred to as the interferon sensitivity determining region, and this region combined with 26 adjacent C-terminal residues has been shown to be essential for interaction with the interferon-induced, double-stranded RNA-dependent protein kinase R (PKR). Normally, PKR can phosphorylate eIF-2α upon detection of dsRNA, shutting down protein translation. NS5A's interaction with PKR interferes with this

process, allowing HCV translation to continue unabated (Gale *et al*., 1997; Pawlotsky, 1999; Tan & Katze, 2001). NS5A can perturb epidermal growth factor (EGF)-stimulated activation of the Ras-Erk signalling pathway, a signalling cascade that mediates cell growth (Macdonald *et al*., 2003; Macdonald *et al*., 2005). The propensity of NS5A to bind host factors that include hVAP-A (Gao *et al*., 2004), hVAP-B (Hamamoto *et al*., 2005), FKBP8 (Okamoto *et al*., 2006), cyclophilin A (Waller *et al*., 2010) and FBL-2 (Wang *et al*., 2005) likely contributes to the protein's ability to perform multiple roles in the HCV lifecycle.

1.9.9. NS5B

HCV replication proceeds via the synthesis of a complementary minus-strand RNA using the genome as template, and subsequent synthesis of genomic plus-strand RNA from this minus-strand RNA template. The key enzyme in both these steps is NS5B, the HCV RNA-dependent RNA polymerase (RdRp). NS5B can initiate RNA synthesis *de novo*, a mechanism that is likely to operate *in vivo* (Bartenschlager *et al*., 2004). However, NS5B lacks a proofreading function, which contributes to the high genetic variability of HCV (Domingo *et al*., 1996). NS5B belongs to a class of membrane proteins termed tail-anchored proteins. It has a cytosolic orientation and attaches to the ER membrane via a highly conserved C-terminal TMD (Ivashkina *et al*., 2002; Schmidt-Mende *et al*., 2001), an association essential for HCV RNA replication (Moradpour *et al*., 2004).

RNA synthesis catalysed by NS5B is a multistep process involving initiation, elongation and product dissociation, followed by re-initiation for another round of polymerization. The initiation phase requires NS5B to catalyze the formation of a phosphodiester bond between two bound nucleotides, referred to as priming and initiating nucleotides. In the rate-limiting step that follows, the newly formed dinucleotide is used as a primer for the addition of a third nucleotide, whereupon the enzyme switches to the elongation mode which renders the reaction highly processive and enzyme dissociation is extremely slow (Dutartre *et al*., 2005; Harrus *et al*., 2010; Ferrari *et al*., 2008). To perform such an initiation step, polymerases contain structural features essential to the synthesis of their own short primers.

To investigate this, the crystal structure of NS5B has been determined by several groups (Ago *et al*., 1999; Biswal *et al*., 2005; Bressanelli *et al*., 1999; Lesburg *et al*., 1999; Simister *et al*., 2009). NS5B is described as a typical "right-hand" polymerase, showing a structural fold featuring palm, finger and thumb subdomains. The palm region contains the enzyme's catalytic GDD motif (enzyme active site), whereas the fingers and thumb subdomains modulate the interaction with the RNA chain. A special feature of NS5B is that the fingers subdomain contains an extension that interacts with the thumb subdomain and restricts the mobility of one region with respect to the other. This leaves the active site completely encircled and creates a channel in which a single-stranded RNA molecule is directly guided to the GDD motif, perhaps facilitating the initiation stage of viral RNA synthesis. Subsequently, NS5B must adopt an alternative conformation which allows elongation to occur, which involves removal of both a "β-flap" structure of the thumb domain and a 40-residue stretch between the catalytic core of NS5B and the C-terminal membrane anchor termed the "linker" region (Harrus *et al*., 2010). While it has been shown that an isoleucine residue at position 405 in NS5B promotes dinucleotide formation and the transition from the initiation stage of synthesis to elongation (Scrima *et al*., 2012), studies removing the autoinhibitory "β-flap" from genotype 2a HCV NS5B facilitated the determination of the first crystallographic structures of HCV polymerase in complex with RNA primer-template pairs (Mosley *et al*., 2012). These structures demonstrated the reordering of neighbouring residues, including I405, that occurs in the absence of this β-hairpin loop which allow transition from *de novo* initiation with GTP to the elongation of the growing primer-template RNA.

NS5B's interactions with other proteins, both viral and cellular, are important for modulating polymerase activity. NS5B is known to associate directly with NS5A, with a disruption of this interaction leading to inhibition of viral RNA replication (Shirota *et al*., 2002; Shimakami *et al*., 2004). NS3 and NS4B have also been touted as regulators of NS5B activity (Piccininni *et al*., 2002). Additionally, an interaction between NS5B and cyclophilin A has been established (Abe *et al*., 2009). Cyclophilin A, which also interacts with NS5A, is essential for HCV RNA replication and virus production and it was suggested that its association with viral proteins induced a conformation necessary for replicase formation and activity (Kaul *et al*., 2009). However, a later study

highlighted how cyclophilin A did not regulate NS5A or NS5B replication complex association (Chatterji *et al*., 2010), leaving the role of the NS5B-cyclophilin A interaction as yet undetermined. A recent report has shown via nuclear magnetic resonance (NMR) spectroscopy that NS5B and cyclophilin A share a common binding site on NS5A (Rosnoblet *et al*., 2012). NS5B can interact with another cyclophilin family member, cyclophilin B, although knockdown of cellular cyclophilin B alone failed to significantly affect HCV replication (Kaul *et al*., 2009). However, NS5B's interaction with nucleolin, a nucleolar phosphoprotein, enhances viral RNA synthesis (Shimakami *et al*., 2006).

1.9.10. The 3' UTR

The 3'UTR has a tripartite structure consisting of a variable region, which is poorly conserved among different HCV isolates, a poly (U/UC) tract, which is very heterogeneous in length, and a highly conserved 98 nucleotide sequence designated the 3' X-tail (Kolykhalov *et al*., 1996). Biochemical and structural analyses have confirmed the presence of two stem-loops in the variable region (VSL1 and VSL2) and three stem loops in the 3'X-tail (SL1, SL2 and SL3) (Blight & Rice, 1997; Ito & Lai, 1997; Tanaka *et al*., 1996). While VSL1 and VSL2 are dispensable for HCV RNA replication in cell culture and for HCV infectivity in chimpanzees (Friebe & Bartenschlager, 2002; Yanagi *et al*., 1999), removal of any of the 3' X-tail stem-loops is deleterious to both of these processes (Friebe & Bartenschlager, 2002; Yanagi *et al*., 1999; Yi & Lemon, 2003). The poly (U/UC) region is variable in length and composition, consisting of uridine residues that are interspersed with occasional cytidine residues. A minimum poly (U/UC) core length of 26 consecutive uridine nucleotides is required for HCV RNA replication (Friebe & Bartenschlager, 2002), while a core length of 33 uridine nucleotides is needed for optimal HCV RNA amplification in cell culture (You & Rice, 2008). This uridine rich-core of the poly (U/UC) has been identified as a PAMP motif that drives optimal RIG-I signalling (Schnell *et al*., 2012). HCV is unable to prevent RIG-I recognition via genomic sequence evolution due to the viral fitness costs involved in truncating a long uninterrupted poly-U nucleotide sequence.

Aside from roles in replication, the 3'UTR also stimulates IRES-mediated translation of viral RNA. This stimulation was stronger in hepatoma cell-lines such as Huh-7 and HepG2 cells compared to non-hepatoma cell-lines such as BHK and Hela cells (Song *et al*., 2006). It has been proposed that the 3'UTR enhances IRES-dependent translation by increasing the efficiency of termination, the process by which translating ribosomes that encounter an in frame stop codon associate with a complex of eukaryotic release factors to direct hydrolysis of the peptidyl-tRNA bond by the 60S ribosomal subunit, resulting in release of the translated polypeptide from the ribosome (the exact mechanism by which the 3'UTR performs this duty is as yet unclear) (Bradrick *et al*., 2006). Furthermore, a recent report has also highlighted the importance of the 3'UTR in accurate folding of the HCV IRES, a role it performs independently of protein factors (Romero-Lopez *et al*., 2012). However, cellular factors do interact with the 3'UTR, including the Polypyrimidine Tract Binding protein (PTB) and La autoantigen, both of whom also interact with the 5'UTR (Ito *et al*., 1998; Spangberg *et al*., 1999; Wood *et al*., 2001). Both of these cellular elements have been implicated in modulating HCV translation and replication (Ali & Siddiqui, 1995; Ali & Siddiqui, 1997), although a report discrediting the importance of PTB in the translation process has also been published (Brocard *et al*., 2007). Another host protein that interacts with the 3'UTR, Insulin-like growth factor-II mRNA-binding protein 1 (IGF2BP1), enhances HCV IRES-mediated translation initiation by recruiting the translation factor eIF3 (Weinlich *et al*., 2009).

1.10. Systems to Study HCV Replication

1.10.1. Animal Models

Humans and chimpanzees are the only species permissive to HCV infection. The basis for this highly restricted tropism is not fully understood, but may result from viral dependence on host factors present in only a few cell types. Years before the discovery of HCV, it was demonstrated that the etiological agent responsible for NANBH could be transmitted to chimpanzees, and the chimpanzee model was subsequently used to determine the physicochemical properties of the as yet unknown agent after inoculating

the animals with serum from infected patients (see section 1.1). As HCV virions in patient plasma are heterogenous, the generation of infectious molecular HCV clones was a welcome development, as they allowed monclonal HCV inoculation of prototype strains in chimpanzees and displayed viral kinetics indistinguishable from polyclonal natural infections (Bartenschlager & Sparacio, 2007; Kolykhalov *et al*., 1997; Yanagi *et al*., 1997). Furthermore, targeted deletion of selected regions of these infectious clones could be performed to reveal their role in infectivity and replication in chimpanzees.
The natural course of HCV infection is very similar between humans and chimpanzees, likely due to the close genetic relationship between the two. This has proven incredibly valuable when studying various molecular, immunological and clinical aspects of HCV infection. While it is nearly impossible to study the acute phase of infection in humans due to the general asymptomatic nature of patients, experimental HCV infections in chimpanzees allow close monitoring of viral kinetics of host responses during these early stages of infection (Meuleman & Leroux-Roels, 2009). Despite this, the chronicity rate for chimpanzees, while high (~ 60 %), is lower than in humans. The clinical course of infection also tends to be milder in chimpanzees compared to humans, with only one case of HCC reported using the chimpanzee model, and no instance of liver cirrhosis or fibrosis observed (Boonstra *et al*., 2009). However, in spite of the invaluable contribution this model has made to HCV research, experiments are generally performed with a limited number of animals owing to important ethical constraints, high costs and the outbred nature of chimpanzees as an endangered species.

Rodents are regarded as the most suitable alternative to chimpanzees due to their short gestation period, small size and low cost. Over the years, many transgenic mice have been generated that overexpressed specific HCV proteins in order to study various aspects of HCV biology. However, the transgene usually integrates at a random site in the host's genome at a high copy number and, in contrast to a natural infection, the viral proteins are typically overexpressed in an uncontrolled manner. Thus, qualities attributed to viral proteins gathered from these studies might be related to artificial overexpression or misregulation of host genes at the transgene integration site (Barth *et al*., 2008; Kremsdorf & Brezillon, 2007). The development of a rodent model in which HCV replicates and is infectious has proven complex and difficult. Although rodents are not naturally receptive to HCV infection, if maintained in an immunosuppressed state, they can undergo successful transplantation with human hepatocytes allowing viremia

to develop. The first mouse model that allowed successful HCV infection studies was the uPA transgenic mouse developed in mice with severe combined immunodeficiency (SCID). Overexpression of a urokinase plasminogen activator (uPA), expressed from an albumin (Alb) promoter, resulted in severe liver toxicity in murine systems (Heckel *et al*., 1990). The diseased mouse liver could be repopulated with non-transgenic human hepatocytes susceptible to HCV infection. Mice with these chimeric human livers that were inoculated with HCVcc or with serum from HCV-positive donors developed prolonged HCV infections with high viral titres and showed active replication of the virus in their livers (Mercer *et al*., 2001). However, this model has limitations, most notably an extremely high mortality rate, due to the need for intrasplenically-transplanted primary hepatocytes in each mouse within the first two weeks of life (Meuleman *et al*., 2005; Vanwolleghem *et al*., 2010).

Another rodent model with robust HCV propagation has been developed from immunodeficient mice with genetic alterations, where an impaired mouse liver is efficiently repopulated with human hepatocytes (Bissig *et al*., 2010). Up to 95 % of the liver in these mice (the *Fah*$^{-/-}$/*Rag2*$^{-/-}$/*IL2rg*$^{-/-}$ [FRG] model) can be engrafted with human hepatocytes. This is possible as, in these mice, the absence of Recombination activating gene 2 (*Rag2*), causes depletion of mature B and T lymphocytes, the absence of the interleukin 2 receptor gamma chain (*IL2rg*) abrogates T-cell and natural killer (NK)-cell differentiation, while the genetic knockdown of fumaryl acetoacetate hydrolase (*Fah*), a metabolic enzyme that catalyzes the last step of tyrosine catabolism, leads to an accumulation of toxic tyrosine catabolites within mouse hepatocytes (Bissig *et al*., 2007; Bissig *et al*., 2010). The advantage of this model is that the effect of genetic alteration that causes this degeneration of mouse hepatocytes can be blocked by oral administration of 2-(2-nitro-4-trifluoro-methylbenzoyl)-1,3-cyclohexanedione (NTBC), which blocks hydroxyphenylpyruvate dioxygenase activity upstream of FAH and prevents the accumulation of hepatotoxic metabolites, thus keeping mice healthy until engraftment. Human chimeric livers in these mice can then simply be generated by withdrawing the drug and injecting the mice with human hepatocytes, which stay healthy due to presence of the human FAH homologue (Bissig *et al*., 2010). An obvious shortcoming is that these mice and other earlier rodent models cannot be used in studies of the adaptive immune response to HCV. They therefore cannot be used to examine many aspects of immunity and pathogenesis or, more importantly, be used as challenge

models for vaccine studies (Bukh, 2012). This work has largely been confined to chimpanzees, but the recent development of two immunocompetent humanized mouse models has changed this (Dorner *et al*., 2011; Washburn *et al*., 2011). One genetically modified mouse model (AFC8-huHSC/hep mice) supports engraftment of human hepatocyte progenitor cells and hematopoietic stem cells, resulting in liver repopulation with human hepatocytes and immune reconstitution with human leukocytes (Washburn *et al*., 2011). In the other genetically humanized mouse model (Rosa26-Fluc mice), a subpopulation of liver cells from immunocompetent mice expressed human cell-surface receptors required for HCV entry. HCV entry was tracked in these liver cells because the virus was genetically engineered to induce luciferase expression upon infection (Dorner *et al*., 2011). This model will prove extremely useful in studying passive immunoprophylaxis against HCV challenge and protection against entry by recombinant vaccines. The use of both of these models is as yet restricted, however, by limited (AFC8-huHSC/hep) or absent (Rosa26-Fluc) viral replication. Furthermore, neither model displays detectable levels of viremia.

1.10.2. *In Vitro* Systems to Study HCV

Three major systems have been developed that are invaluable for the study of the HCV lifecycle in cell culture. These include the HCV cell culture infectious system (HCVcc), used for the study of the entire HCV lifecycle and HCV pseudoparticles (HCVpp) for insight into the complete HCV entry process. Replicons are necessary for analysis of viral RNA replication (Fig 1.3).

1.10.2.1. HCVpp

In 2003, several groups reported the production of infectious lentiviral particles known as HCVpp (Bartosch *et al*., 2003; Drummer *et al*., 2003; Hsu *et al*., 2003). HCVpp are produced in HEK-293T cells by co-transfecting plasmids encoding the HCV glycoproteins, retroviral or lentiviral core and polymerase proteins and a proviral genome harbouring a reporter gene such as luciferase or GFP. This allows the assembly and secretion of recombinant HCVpp that contain HCV envelope glycoproteins on their surface. These engineered viral particles are then harvested from transfected 293T cell

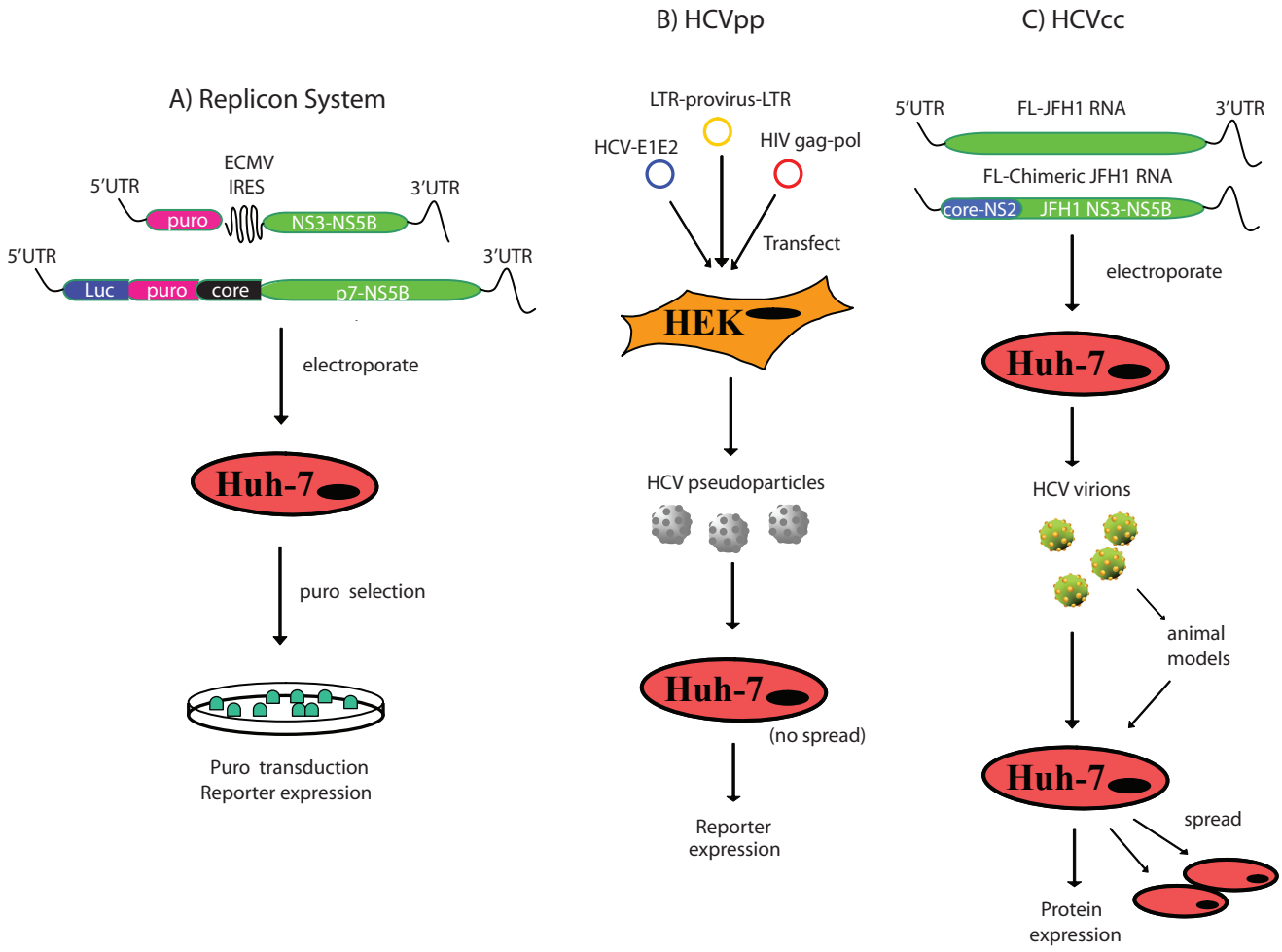

Figure 1.3. *In vitro* systems for the study of HCV replication, entry, and infectivity.

(A) HCV SGRs allow for the study of viral RNA replication in cell culture. Monocistroinic and bicistronic replicon RNAs, encoding selectable markers, are electroporated into Huh-7 cells and derived sub-lines. RNA replication results in the expression of the selectable marker and allows for selection of cell colonies that support viral RNA replication. (B) HCVpp allows for the study of HCV entry. Recombinant retrovirus particles that contain HCV envelope glycoproteins on their surface are produced in HEK-293T cells by co-transfecting plasmids encoding the HCV glycoproteins, retroviral or lentiviral core and polymerase proteins and a proviral genome harbouring a reporter gene. Following infection of permissive cell lines, the retrovirus genomes express a reporter gene, such as luciferase, allowing for a quantitative measure of cell entry. (C) HCVcc allows for the study of the entire HCV lifecycle. This system uses either JFH1 HCV genomic RNA or chimeric versions of this genome. Electroporation of these RNAs into permissive cell lines allows for viral RNA replication and the production of infectious particles that can infect naïve cells. Productive infection can be monitored by several methods allowing the detection of intracellular viral RNA or protein levels. Adapted from Tellinghuisen *et al*. (2007).

supernatant and used to infect permissive cell-lines such as human hepatoma Huh-7 cells. Following infection, the retrovirus genomes express a reporter gene such as luciferase. As HCVpp are replication deficient and support a single infection event only, reporter expression gives a quantitative measure of cell entry (Bartosch *et al*., 2003; Drummer *et al*., 2003; Lavillette *et al*., 2005). Many of the observations made with HCVpp regarding pH-dependent entry and the importance of CD81 in the entry process have now been confirmed with experiments performed in HCVcc, reflecting the similarity between HCVcc and HCVpp virions (Hsu *et al*., 2003; Sharma *et al*., 2011; Tscherne *et al*., 2006; Zhang *et al*., 2004). HCVpp has also been endorsed as a valid system for the study of HCV entry by the fact that these pseudoparticles can also be neutralized with anti-E1 or anti-E2 specific antibodies or sera from HCV-infected individuals (Bartosch *et al*., 2003; Hsu *et al*., 2003; Op De Beeck *et al*., 2004). Furthermore, HCVpp representing glycoproteins of all major HCV genotypes have been successfully generated (Lavillette *et al*., 2005; Owsianka *et al*., 2005), increasing the scope by which we can investigate virus binding, attachment and internalization.

1.10.2.2. Replicons

Despite the availability of HCV molecular clones that could infect chimpanzees, efficient and reproducible replication of these clones in cell culture could not be achieved. Thus, it was a major breakthrough in 1999 when a selectable, subgenomic (SGR) replicon system that allowed HCV RNA replication in cell culture was developed (Lohmann *et al*., 1999). SGRs were initially derived from Con1, a genotype 1b HCV strain. In this bicistronic construct, the coding region from core-NS2 was replaced with a gene encoding neomycin phosphotransferease (neo), translated under the control of the HCV IRES. The encephalomyocarditis virus (EMCV) IRES drives expression of the second cistron, encoding NS proteins NS3-NS5B followed by the 3'UTR. Electroporation of human hepatoma Huh-7 cells with *in vitro* transcribed RNA from this construct and then subjecting these cells to antibiotic selection pressure with the cytotoxic drug G418 produces a small number of resistant colonies supporting autonomously replicating HCV RNAs. The small number of colonies reflects the fact that this selection process allows only the survival of those cells that contain sufficient amounts of neomycin phosphotransferase to inactivate G418. However, this approach

allows cell-lines to be established that contain high levels of self-replicating HCV RNA and proteins (Lohmann *et al*., 1999).

Indeed, subsequent studies identified two reasons for the amplification of the small number of colonies that survived the antibiotic selection process, cell culture adapted mutations and host cell permissiveness. These adaptive mutations tend to cluster within the NS proteins NS3, NS4B, NS5A and NS5B (Blight *et al*., 2000; Krieger *et al*., 2001; Lohmann *et al*., 2001) and can increase viral replication to various extents if introduced separately into the parental genome. Another interesting feature from these studies is the observation that several of these replication-enhancing mutations resulted in a loss of NS5A hyperphosphoylation (Blight *et al*., 2000), leading to hypotheses postulating that reduced phosphorylation facilitated critical host-virus interactions stabilizing the replicase (Evans *et al*., 2004) or alternatively, that this change in the phosphorylation status of the protein disrupted interactions involved in dampening replication or potentiating the innate immune response (Sumpter *et al*., 2004). As stated earlier, the selection of highly HCV-permissive Huh-7-derived subclones can also increase the efficiency of replicon RNA replication. These cell-lines are usually generated by removal of replicon RNA from Huh-7 cells by treatment with IFN or selective antiviral drugs. These "cured" cell lines include Huh-7.5 cells, Huh-7.5.1 cells and Huh-7/Lunet cells. The phenotype of Huh-7.5 cells is believed to derive from a defective IFN response caused by a mutation in the RIG-I gene (Sumper *et al*., 2005), while Huh-7/Lunet cells maintain a bimodal level of CD81 expression (Koutsoudakis *et al*., 2007). With the advent of highly permissive cell clones and cell-culture adapted replicons, it was possible to develop transient RNA replication assays that avoided the cumbersome and time-consuming selection of antibiotic-resistant clones. Transient replication systems became available that were often based on replicons in which the neo gene was replaced by a reporter gene such as luciferase, allowing sensitive and accurate assessment of RNA replication at specific time points post-electroporation of viral RNA.

Despite exhibiting efficient HCV replication, autonomously replicating full-length genomic replicons that were generated harbouring the entire HCV ORF did not support the production of infectious HCV particles (Murray & Rice, 2011). This was because, during replication and antibiotic selection, replicon RNAs accumulate mutations that,

while enhancing replication by several orders of magnitude, generally interfere with assembly (Pietschmann *et al*., 2009). The most efficient increase of replication was achieved by mutations residing in NS5A or NS5B, either alone or in combination with NS3 mutations, although the latter were especially deleterious of viral assembly. One specific mutation in NS4B did not compromise infectivity as severely as the changes to NS3, NS5A and NS5B (Pietschmann *et al*., 2009). These findings are consistent with critical roles for certain NS proteins in regulating infectious viral assembly. They also suggest that mutations observed in replicons achieve cell culture adaptation by different mechanisms.

While the Con1 replicon system allowed detailed study of HCV RNA replication for the first time, the range of differences between genotypes and strains led to an urgency in developing replicons representing all the major HCV genotypes. Adapted mutations found in Con1 enhanced viral replication upon insertion in a number of other genotype 1b strains, including HCV-O (Abe *et al*., 2007, Ikeda *et al*., 2005), HCV-BK (Grobler *et al*., 2003) and AH1 (Mori *et al*., 2008). However, genotype 1b replicon HCV-N replicates in the absence of adaptive mutations, as long as a naturally occurring four-aa insertion in NS5A is present (Ikeda *et al*., 2002). SGRs derived from genotype 1a, such as the H77 replicon, were also developed (Yi & Lemon, 2004). While replication efficiency in genotype 1a replicons was not enhanced by introducing replication-enhancing mutations from 1b replicons, prolonged passaging experiments allowed genotype 1a-specific adaptive mutations to be isolated. In 2003, a SGR was developed based on a genotype 2a strain termed Japanese fulminant hepatitis-1 (JFH1), which was isolated from a patient with the highly unusual clinical presentation of acute fulminant hepatitis. This replicon was capable of highly efficient replication (Kato *et al*., 2003) without the need for cell selection or emergent mutations. The unique features of this unusual strain led to the establishment of the first cell culture infectious system for studying the complete HCV lifecycle.

Until very recently, efficient replicon systems were only developed from HCV genotypes 1 and 2. A number of recently published reports, however, were able to establish replicons derived from genotype 3 and 4 HCV isolates (Peng *et al*., 2013; Saeed *et al*., 2012; Saeed *et al*., 2013). The study by Saeed *et al*. (2013) used a consensus genotype 3a HCV isolate called S310, cloned from the high-titre serum of a

patient with recurrent hepatitis after transplantation, to generate a subgenomic replicon after selecting Huh-7.5.1 cells electroporated with this construct with G418. The replication-enhancing mutations generated by this selection process were observed in NS3, NS5A and NS5B and were similar (and in some cases identical) to mutations observed in Con1 replicons (Saeed *et al*., 2013). Peng *et al*. (2013) used the previously cloned consensus isolate ED43, which is infectious in chimpanzees, to design a genotype 4a SGR. After failing to generate sufficient colonies under selection in Huh-7/Lunet cells, a novel Huh-7 cell clone designated 1C was used instead. Using this cell-line, generated by curing a genotype 1a replicon derived from 51C cells (itself a previously cured Huh-7 cell-line), increased colony formation ~ 70-fold. While replication-enhancing mutations were observed in NS3 and NS4A, it was noted that an adaptive mutation in NS5A, S232I, was essential for replication of this replicon. Mutagenesis studies confirmed an absence of replication in genotype 4a replicons in its absence (Peng *et al*., 2013).

Another study also reported the generation of a genotype 4a replicon derived from the ED43 HCV isolate (Saeed *et al*., 2012). Furthermore, this report generated another genotype 3a replicon, although this construct was derived from the HCV S52 isolate. This study reported that, despite the huge genetic differences between the genotypes, replication-enhancing mutations were identified at identical positions in each replicon. These mutations were observed at the junction of the protease and helicase domains in NS3 and at the C-terminus of NS5B. This is in line with work stating that a mutation in NS5A (the genotype 4a mutation S232I, corresponding with S2204I in genotypes 1a and 1b and S2210I in genotype 3a) enhances RNA replication in genotypes 1a, 1b, 3a and 4a (Blight *et al*., 2000; Lohmann *et al*., 2003; Peng *et al*., 2013; Saeed *et al*., 2013).. This high conservation of certain cell culture replication-enhancing adaptive mutations will help to generate cell culture models for the remaining genotypes 5-7.

1.10.2.3. HCVcc

As stated previously, SGRs of the HCV genotype 2a JFH1 strain replicate efficiently in Huh-7 cells and do not require cell culture adapted mutations. Transfection of *in vitro* transcribed RNAs corresponding to the full-length JFH1 genome resulted in efficient HCV replication and secretion of viral particles. This secreted virus is infectious both *in*

vitro and *in vivo* and can be neutralized by CD81-specific antibodies (Wakita *et al*., 2005). A slightly later study reported that the infection kinetics of JFH1 could be improved using the Huh-7 clonal cell-line Huh-7.5.1 cells (Zhong *et al*., 2005). In the same year, a study reported the construction of a full-length chimeric genome that produced infectious particles. This genome, termed FL-J6/JFH1, made use of the core-NS2 gene regions from the infectious genotype 2a strain J6 fused to the JFH1 NS3-NS5B regions (Lindenbach *et al*., 2005). This chimeric HCVcc strain was found to be infectious *in vitro* (Lindenbach *et al*., 2005) and *in vivo* (Lindenbach *et al*., 2006). While FL-J6/JFH1 could establish long term infections in chimpanzees and in mice containing human liver grafts, it was also noted that virus recovered from these animals was highly infectious in cell culture, demonstrating efficient *ex vivo* culture of HCV (Lindenbach *et al*., 2006). Following these discoveries, a panel of intergenotypic and intragenotypic HCV chimeras was constructed and characterized, fusing the NS3-NS5B regions of JFH1 to the core-NS2 regions of genotype 1a, 1b, 2a and 3a strains (Pietschmann *et al*., 2006). This study reported that the efficiency of viral release for chimeric viruses could be improved by altering the fusion junction from the NS2/NS3 cleavage site to a crossover point that resides after the first TM segment of NS2. An intragenotypic chimera quite similar to FL-J6/JFH1, consisting of J6- and JFH1-derived sequences connected via this new junction, termed Jc1, was found to yield infectious titres up to 1000-fold higher than JFH1 (Pietschmann *et al*., 2006). Jc1 does not adapt during passage in cell culture however, possibly because of host cell factors limiting maximum achievable titres. On the other hand, titres for JFH1 can be enhanced from passaging experiments through adaptive mutations, with hotspots observed in E2, p7, NS2 and at the NS5A/NS5B junction (Murray & Rice, 2011). A panel of JFH1-based chimeras has since been developed representing all 7 HCV genotypes (Gottwein *et al*., 2009). While differential susceptibility to neutralization was found between the genotypes, no major genotype-specific differences were observed regarding intracellular lipid accumulation, response to IFN-α or interaction with cellular entry receptors.

Unlike JFH1, the full-length J6 clone was incapable of replication *in vitro*. However, through a systemic approach of culturing J6 with minimal JFH1 sequences, three mutations were identified (F1468L in NS3, A1676S in NS4A and D3001G in NS5B) that permitted culture replication and further adaptation of full-length J6. The most efficient recombinant, J6cc, expressed infectivity titres similar to JFH1-based systems

(Li *et al*., 2012a). This study also reported that the three J6-derived mutations also enabled culture adaptation of the genetically divergent isolate J8 (genotype 2b), allowing the development of an infectious full-length genotype 2b culture system, termed J8cc. Neither J6cc nor J8cc were genetically altered after viral passage experiments (Li *et al*., 2012a).

A full-length genotype 1a genome, H77-S, carrying mutations identified in the subgenomic replicon of the same strain has been reported to release relatively small amounts of virus particles (Yi *et al*., 2006). A full-length genotype 1b culture system has also been reported, but a very low level of replication has limited its utility (Pietschmann *et al*., 2009). However, following on from their work on J6cc and J8cc, Li and colleagues introduced mutations corresponding to the three J6-derived mutations into a replication deficient TN strain (genotype 1a) full-length virus. As in J6, these mutations enabled replication and cell culture adaptation, eventually leading to TNcc, a highly efficient full-length genotype 1a infectious culture system (Li *et al*., 2012b). The approach and identified mutations used in developing the J6cc, J8cc and TNcc models may facilitate the generation of HCV full-length systems for HCV isolates of all genotypes, which would not only be useful for HCV vaccine and drug developments but could also aid the introduction of more individualised treatment programmes.

A recently published report has demonstrated that a small set of defined host factors is sufficient to reconstitute the complete viral life cycle in a previously nonpermissive nonhepatic cell-line such as HEK-293T cells (Da Costa *et al*., 2012). Data presented here indicated that the exogenous expression of cellular receptors occludin (OCLN), CD81, claudin-1 (CLDN1) and SR-BI was sufficient for efficient HCV entry in these cells. Similar experiments confirmed that exogenous expression of miR-122 and apoE were sufficient for adequate viral replication and infectious virus production in this cell-line, respectively (Da Costa *et al*., 2012). Furthermore, it has recently been unearthed that supplementation with miR-122 allows recapitulation of the entire HCV lifecycle in nonpermissive hepatic cell-lines such as HepG2 (Narbus *et al*., 2011) and Hep3B cells (Thibault *et al*., 2013). Given that current *in vitro* HCV research is almost exclusively carried out in Huh-7-derived cell lines, which all bear similar host genetics, polymorphisms and cellular pathways, these new permissive cell-lines will increase our understanding of the complex host-virus interactions that occur *in vivo*. In line with this,

while stem cells and definitive endoderm resist HCV infection, it has been recently discovered that hepatic progenitor cells derived from these cell lines can be successfully infected by HCVcc or infectious patient sera (Wu *et al*., 2012). In contrast to the cell-lines derived from tumour tissues, these differentiated human hepatocye-like cells (DHHs) are non-cancerous and preserve important functions of primary hepatocytes while also retaining genetic malleability. The potentially unlimited supply of these cells adds to their enormous potential for expanding our understanding of HCV infection.

Despite the reported abilities of HCV in blunting the host IFN response, HCV infection is also capable of inducing antiviral cytokines in primary liver cell cultures. Induction of ISGs and γ-IFNs limit the growth and spread of HCV in primary cell cultures and the infected liver (Marukian *et al*., 2011). While HCV infection of primary cell cultures may provide a useful model for the study of gene induction by HCV, strategies aimed at dampening this response may lead to the development of new robust HCV cell culture systems. Pursuing this angle, Andrus *et al*. (2011) investigated the spread of HCVcc in human fetal liver cells (HFLC) transduced with paramyxovirus (PMV) V proteins, proteins known to block induction of type I IFNs and inhibit the STAT signalling pathway. They observed that V protein expression significantly enhanced productive HCV infection and protected these cultures from the HCV-inhibitory effects of type I and type III IFNs (Andrus *et al*., 2011).

1.11. The HCV Lifecycle

The HCV life cycle is entirely cytoplasmic and begins with the virus binding to specific receptors on the cell surface. Entry involves transit through an endosomal low pH compartment and fusion with the endosomal membrane, liberating the genome into the cytoplasm where it is then translated. Translation of the genome, directed by the HCV IRES, leads to a polyprotein precursor that is cleaved by cellular and viral proteases into mature HCV proteins. The mature non-structural HCV proteins co-ordinate viral replication by the formation of a membrane bound replication complex (RC). Virions are thought to form by plus-strand HCV RNA interacting with mature HCV structural proteins, becoming subsequently encapsidated and virus particles forming via budding

into the lumen of the ER. A hypothetical model of the complete replication lifecycle is schematically represented in Fig 1.4.

1.11.1. Virus Binding and Entry

HCV entry into hepatocytes is a highly coordinated and multistep process requiring numerous viral and host cell factors (Fig 1.5). Some of these cellular elements are thought to be attachment factors necessary for binding viral particles to the cell surface (glycosaminoglycans, LDL-receptor), while others are specific HCV entry factors believed to participate in the active steps of entry (CD81, SR-BI, claudin-1, occludin). However, before interacting with and entering hepatocytes, HCV particles need to cross the sinusoid barrier. Blood enters the liver via portal tracts before feeding into the parenchyma via the sinusoids. Endothelial cells line the sinusoids and are closely associated with hepatocytes and stellate cells within the space of Disse, which provides an extracellular matrix between cell types. The sinusoidal endothelium is highly fenestrated and may act as a molecular sieve that filters debris between the blood and hepatocytes (Meredith *et al*., 2012). The C-type lectins DC-SIGN and L-SIGN are proposed to be crucial factors in capture and delivery of virus from the circulating blood to liver hepatocytes.

1.11.1.1. Attachment Factors

The C-type Lectins

C-type lectins are membrane-anchored proteins that can bind to oligosaccharide structures on the surface of pathogens, facilitating uptake of these microorganisms for processing and presentation in antigen-presenting cells, inducing immune responses against these pathogens (Koppel *et al*., 2005). However, it is clear that HCV has evolved to subvert the function of some C-type lectins. DC-SIGN (dendritic-cell specific ICAM-3 grabbing non-integrin) and L-SIGN (liver/lymph node-specific ICAM-3 grabbing non integrin, also called DC-SIGNR - DC-SIGN related) are C-type lectins that specifically interact with the HCV E2 glycoprotein. Direct associations between L- or DC-SIGN expressed in heterologous cell systems and soluble E2

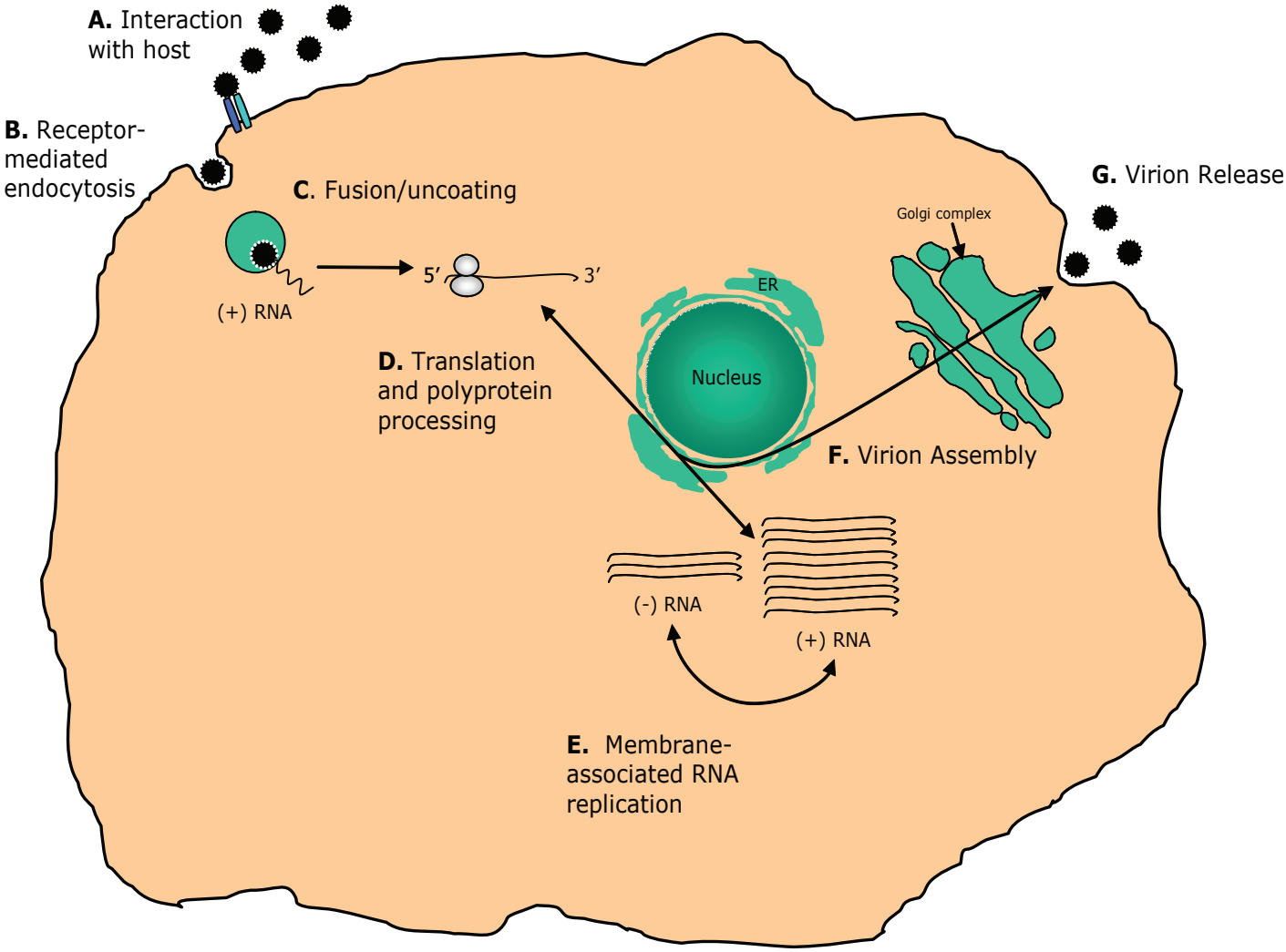

Figure 1.4. Model of the HCV lifecycle.

(a) HCV binding to cell-surface receptor molecules leads to (b) receptor-mediated endocytosis (c) into a low-pH vesicle. Following HCV glycoprotein mediated membrane fusion, the viral genome is liberated into the cytosol. (d) The viral RNA functions as a template for translation of the HCV ORF that is processed into the 10 mature HCV proteins. (e) Viral RNA replication occurs within membrane-associated replication complexes (membranous web). (f) Replication occurs through a positive-strand replicative intermediate to produce progeny RNA, a portion of which are encapsidated. Particles are enveloped by budding into the lumen of the ER where they are thought to follow the cellular secretory pathway, undergoing maturation during this transit. (g) Mature virions are secreted from the cell, completing the life cycle. Adapted from Tellinghuisen *et al*. (2007).

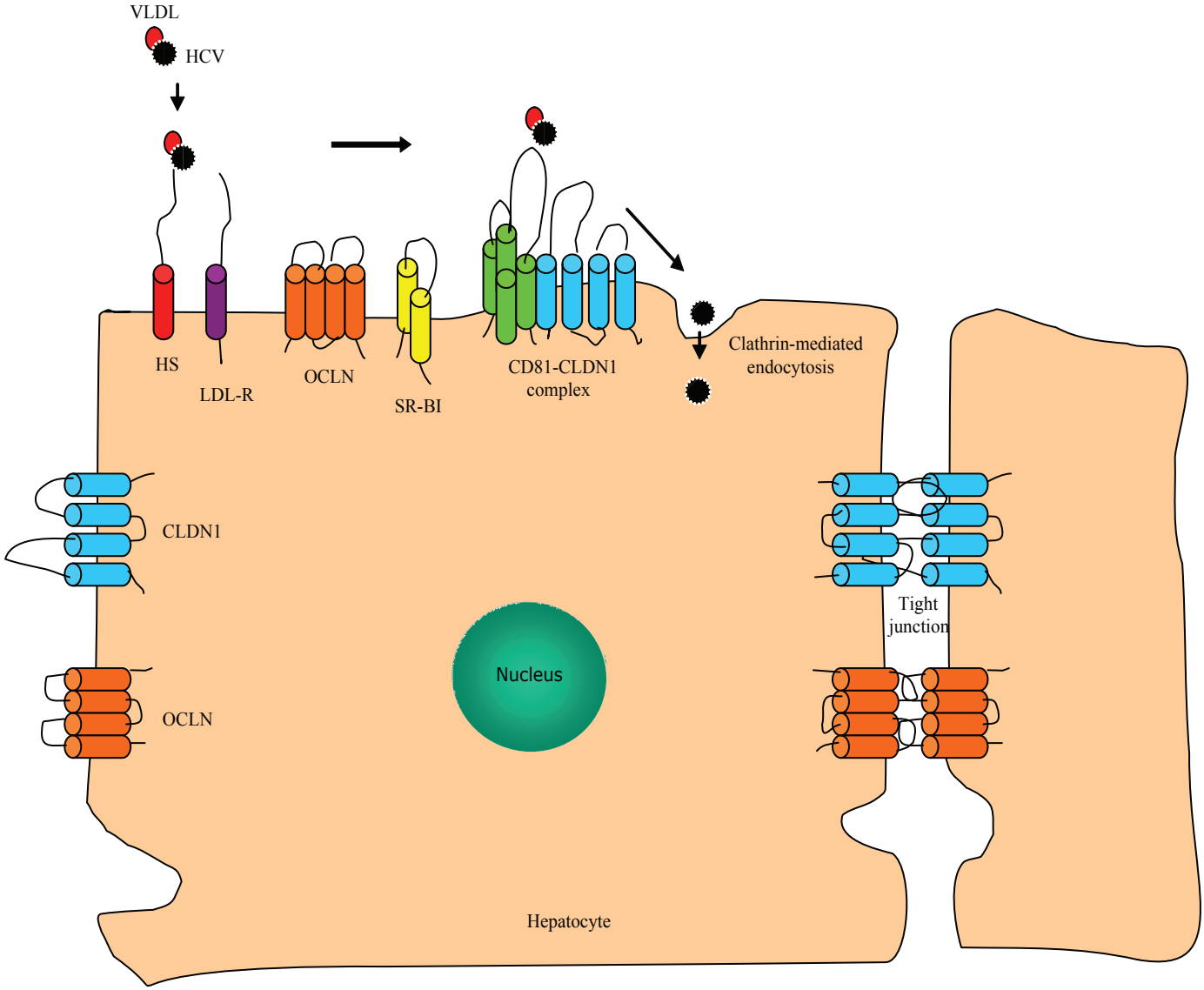

Figure 1.5. A model of HCV entry.

Initial host-cell attachment may involve glycosaminoglycans such as heparan sulfate (HS) binding to VLDL components on the virion surface. LDL-R may also play a part in this process, but this theory is controversial. Initial attachment occurs on the basolateral membrane surface to allow concentration of the virion. Subsequently, interaction with other host factors such as scavenger receptor class B member I (SR-BI), the tetraspanin CD81 and the tight junction proteins Claudin-1 (CLDN1) and Occludin (OCLN) ultimately leads to viral internalisation via clathrin-mediated endocytosis. Adapted from Meredith *et al*. (2012).

(Gardner *et al*., 2003; Lozach *et al*., 2003; Pöhlmann *et al*., 2003), HCVpp (Lozach *et al*., 2004) or serum particles (Gardner *et al*., 2003) have all been documented. L-SIGN and DC-SIGN are both expressed on sinusoidal endothelial cells (Lai *et al*., 2006). The interaction of E2 with these lectins on sinusoidal endothelial cells supports a mechanism for high affinity binding of circulating HCV within the liver sinusoids, allowing transfer of the virus to underlying hepatocytes (Cormier *et al.*, 2004a; Lai *et al*., 2006; Lozach *et al*., 2004). In addition, these lectins may provide a viral escape mechanism as uptake of HCV by L- and DC-SIGN has been reported to target nonlysosomal compartments in immature DCs, whereas Lewis X antigen, another ligand of DC-SIGN, was internalized to lysosomes (Ludwig *et al*., 2004). Thus, the process of capturing HCV particles may allow sinusoidal endothelial cells to act as reservoirs of HCV, enabling the virus to avoid immune detection.

Furthermore, it has been noted that virus can also be transferred to hepatocytes from non-permissive B cells. Antibodies specific for L- and DC-SIGN reduced B-cell transinfection, supporting a role for these molecules in B-cell association with HCV (Stamataki *et al*., 2009). While DC-SIGN is known to be internalised upon binding certain ligands and can traffic towards late endosomes and lysosomes (Engering *et al*., 2002, Khoo *et al*., 2008), on sinusoidal cells it is unable to support HCV entry, along with L-SIGN (Lai *et al*., 2006). Lastly, a study using virus-like particles produced in insect cells (baculovirus-expressed HCV glycoproteins) led to the suggestion that the asialoglycoprotein receptor, another C-type lectin highly expressed in the liver, could be another candidate receptor for HCV (Saunier *et al*., 2003). However, investigations with HCVpp and HCVcc are needed to determine the veracity of these postulations.

Glycosaminoglycans

Glycosaminoglycan (GAG) chains on cell surface proteoglycans provide primary docking sites for the binding of various viruses and other microorganisms to eukaryotic cells. GAGs are present almost ubiquitously on cell surfaces but vary with respect to their composition and quantity among different species, cell types, tissues and cellular development stages (Bernfield *et al*., 1999; Spillmann, 2001). The GAG heparan sulfate (HS) has been implicated as an initial cellular binding molecule for numerous viruses, including members of the *Flaviviridae* family such as dengue and TBE (Hilgard &

Stockert, 2000; Mandl *et al*., 2001). HS and heparin, a HS homologue naturally synthesised by mast cells, have been shown to bind soluble E2 and, to a lesser extent, E1 (Barth *et al*., 2003; Barth *et al*., 2006). Four viral epitopes overlapping the E2 HVR1 and E2-CD81 binding domains have been found to bind heparin, and the neutralizing mAb AP33 (which targets E2 close to HVR1) can markedly inhibit the HCV-heparin interaction. HCV-HS binding was also found to necessitate a specific HS configuration that included N-sulfated groups and a minimum of 10 to 14 saccharide units (Barth *et al*., 2006). Furthermore, treatment of cells with heparinase (an enzyme that can cleave HS) reduced recombinant E2 binding and HCVcc infectivity (Barth *et al*., 2003; Koutsoudakis *et al*., 2006; Morikawa *et al*., 2007). Similarly, virus incubation with increasing concentrations of heparin, but not other soluble GAGs which differ in their degree of sulfation and in their composition of disaccharide units, decreased levels of HCVcc infection, presumably because of competition between heparin and HCV particles (Basu *et al*., 2007; Germi *et al*., 2002; Koutsoudakis *et al*., 2006). These results indicated that a specific, highly sulphated type of GAG contributes to efficient HCV infection. In line with other reports examining the role of HS in *Flaviviridae*, heparin only inhibits HCV infection if administered before or during virus binding, clarifying that HS acts in the initial attachment of HCV to target cells (Koutsoudakis *et al*., 2006).

However, although liver-derived, highly sulphated HS can inhibit HCVpp infection (Barth *et al*., 2006) and heparin can effectively bind intracellular E1E2, no binding has been observed between heparin and HCVpp-derived envelope glycoproteins (Callens *et al*., 2005). This finding indicated that the heparin-binding domain of E2 is not accessible on the mature glycoprotein and that HCV interacts indirectly with HS through cellular or viral factors present in a HCVcc background but absent in HCVpp. This theory was confirmed by a recent publication indicating that apoE on the HCV virion mediates the HCV-HS interaction through specific interactions with cell surface HS (Jiang *et al*., 2012). Using a host protein on virions to bind HCV indirectly to a cellular protein for hepatocype attachment may make it much easier for viral particles to evade the host immune response and establish a persistent infection.

Low-Density Lipoprotein Receptor (LDL-R)

Hepatocytes acquire cholesterol via endocytosis involving low-density lipoprotein receptor (LDL-R). However, because of the physical association of HCV with LDL or VLDL in serum, forming LVPs (see section 1.2), LDLR has also been proposed as an attachment factor in HCV entry. The role of LDLR in viral attachment was first investigated in 1999, where HCV RNA accumulation was found to be inhibited by anti-LDLR antibodies (Agnello *et al*., 1999). Correlation has also been shown between the accumulation of HCV RNA into primary hepatocytes, expression of LDL-R RNA and LDL entry (Molina *et al*., 2007). Furthermore, knock down of LDL-R expression in target cells by small interfering RNA (siRNA) does inhibit HCVcc infectivity (Owen *et al*., 2009; Albecka *et al*., 2012).

However, data published by Albecka *et al*. (2012) indicated that, while LDL-R is important for optimal replication of the HCV genome, it is not essential for infectious HCV particle attachment and entry. This study showed that HCV binds to LDL-R and that this interaction and HCV uptake is increased through treatment with lipoprotein lipase (LPL), an enzyme that hydrolyzes the triglycerides in VLDLs. Despite this, they observed that this LPL treatment reduced the apoE content of the viral particle, leading to reduced infectivity, likely due to the necessity of apoE for efficient HCV binding to cellular GAGs. This decrease in infectivity, yet parallel increase in internalisation, suggests that LDL-R often leads to non-productive internalisation of HCV, possibly directing particles to a degradation pathway used in LDL or VLDL clearance. Neutralizing mAb experiments from this report revealed no decrease in infectivity at 2 h post-virus addition, but substantial reductions were observed at 24 h post-addition, implying LDLR is involved at a post-entry step of the HCV lifecycle, possibly maintaining specific levels of host cell lipids necessary for a suitable intracellular environment that can sustain viral replication events (Albecka *et al*., 2012).

1.11.1.2. Specific Entry Factors

SR-BI

The human scavenger receptor class B type I (SR-BI, also called CLA-1) is a 509 aa long multiligand receptor with multiple and flexible binding sites. SR-BI mediates both bidirectional flux of free cholesterol between cells and lipoproteins and selective uptake of cholesteryl esters into cells from high-density lipoprotein (HDL). SR-BI is known to influence cellular cholesterol mass and alter cholesterol distribution in plasma membrane domains. The protein's multiple functions in cholesterol metabolism, particularly those relating to HDL, are of greatest significance in liver and steroidogenic tissues, where it is most highly expressed (Kellner-Weibel *et al*., 2000; Krieger, 2001; Parathath *et al*., 2004; Rigotti *et al*., 2003).

SR-BI, which contains two TMDs, two cytoplasmic domains and a large extracellular loop with nine potential N-glycosylation sites (Rhainds & Brissette, 2004), was first proposed to act as a putative HCV entry molecule on the basis of its reactivity with sE2 through the HVR1 region (Scarselli *et al*., 2002). RNA interference results, as well as reports highlighting the ability of anti-SR-BI antibodies to block both HCVpp and HCVcc infections, have confirmed the involvement of SR-BI in the HCV entry process (Bartosch *et al*., 2003; Catanese *et al*., 2007; Kapadia *et al*., 2007; Lavillette *et al*., 2005). Furthermore, human non-hepatic and hepatic cell-lines could be rendered permissive for HCVpp and HCVcc infection upon *trans*-complementation with human SR-BI (Dreux *et al*., 2009a). Also, HCVcc is able to bind to Chinese hamster ovary (CHO) cells expressing SR-BI, but not to those expressing CD81, suggesting that HCV binds to SR-BI before interaction with other specific receptors involved in virus entry (Evans *et al*., 2007). Interestingly, SR-BI has also been demonstrated to mediate postbinding events during HCV entry such as the initiation of infection and viral dissemination (Haberstroh *et al*., 2008; Zahid *et al*., 2013; Zeisel *et al*., 2007). The role of SR-BI in postbinding steps occurs at similar time points to the HCV utilization of other specific entry receptors such as CD81 and claudin-1, suggesting that HCV entry may be mediated through the formation of co-receptor complexes (Zeisel *et al*., 2007).

Conflicting data has been published as to whether SR-BI binds HCV directly via the envelope glycoproteins or indirectly via virus-associated lipoproteins. Work by Maillard *et al*. (2006) stated that the interaction between CHO-SR-BI cells and HCV in serum was not sensitive to anti-E2 or anti-HVR1 antibodies but could be effectively inhibited by anti-βlipoprotein antibodies or competed out by apo-B-containing lipoproteins (Maillard *et al*., 2006). It has also been observed that the apolipoprotein serum amyloid A (SAA), a SR-BI ligand, can inhibit HCV infection (Cai *et al*., 2007; Lavie *et al*., 2006). In contrast, another SR-BI ligand, HDL, enhances HCVpp and HCVcc infectivity (Bartosch *et al*., 2005; Voisset *et al*., 2005). HDL-induced enhancement of infection was found to have no impact on the ability of anti-SR-BI antibodies to block HCV infection, and these antibodies were also seen to be effective in counteracting HCV infection even in the absence of lipoproteins (Catanese *at al*., 2010). Moreover, SR-BI mutants with impaired binding to sE2, which are incapable of restoring infectivity if introduced into an SR-BI-depleted Huh-7.5 cell-line, can still bind HDL and mediate cholesterol efflux (Catanese *at al*., 2010), findings which implied that distinct protein determinants in SR-BI are responsible for HCV interactions and HDL metabolism.

Recent papers by Dao Thi *et al*. (2012) and Guan *et al*. (2012) addressed the uncertainty over SR-BI's direct/indirect interaction with HCV. Guan *et al*. (2012) found five residues in the HVR1 of H77 (at positions 14, 15, 25, 26 and 27) that play a key role in binding E2 to SR-BI, with each residue indispensible for HCV cell entry (Guan *et al*., 2012). Meanwhile, work by Dao Thi *et al*. (2012) revealed three distinct HCV entry functions for SR-BI, a primary attachment function, an access function and an enhancement function that stimulates HCV infection activity. Although a functional E2/SR-BI interaction is essential for the postbinding enhancement role, the attachment and access functions progress without the need for a direct glycoprotein/receptor interaction (Dao Thi *et al*., 2012). The initial attachment of HCVcc particles to SR-BI is likely mediated by VLDL components such as apoE and cannot be inhibited by anti-E2 mAbs or by mutating those HVR1 residues which mediate E2/SR-BI binding. However, it was also noted in this study that very low density HCV particles did not use SR-BI as an attachment factor, utilizing a ligand that binds VLDL instead, possibly HS. Despite this, the lipid transfer activity of SR-BI was found to promote access function in HCV particles of all densities. Indeed, experiments blocking or altering the lipid transfer

activity of the receptor using small chemical inhibitors (Block Lipid Transfer - BLT - inhibitors) or by introducing specific mutations into SR-BI were shown to significantly impair HCVpp activity. Evidence was also produced which indicated that although HCV access progressed efficiently in the absence of direct E2/SR-BI binding, it did need an intact E2/CD81 interaction (Dao Thi *et al*., 2012).

CD81

The first identified and best characterised HCV receptor is CD81, a member of the tetraspanin family of transmembrane proteins. Tetraspanins are involved in various cellular processes such as adhesion, morphology, proliferation and differentiation (Boucheix & Rubinstein, 2001; Levy & Shoham, 2005). CD81 is a ubiquitously expressed 26 kDa protein containing four TMDs, one short cytoplasmic domain and two extracellular loops, one small (SEL) and one large (LEL). Early studies utilized sE2 to identify CD81 as a HCV receptor (Pileri *et al*., 1998). The subsequent development of the HCVpp and HCVcc model systems saw CD81 confirmed as an essential receptor for HCV entry, with anti-CD81 mAbs as well as a soluble form of CD81 LEL capable of inhibiting HCVpp and HCVcc infectivity (Bartosch *et al*., 2003; Cormier *et al*., 2004b; Kapadia *et al*., 2007; Zhang *et al*., 2004). Furthermore, hepatomas successfully targeted with siRNAs against CD81 were no longer permissive to HCVpp and HCVcc (Akazawa *et al*., 2007; Zhang *et al*., 2004). Also, hepatoma cells which do not express CD81, such as HepG2 or HH29, become permissive to HCVpp and HCVcc after ectopic expression of CD81 (Bartosch *et al*., 2003; Lavillette *et al*., 2005). Interestingly, inhibition of viral entry by anti-CD81 mAbs occurs only after HCV attachment to target cells, indicating that CD81 acts as a post-attachment entry co-receptor and that other factors function in concert with CD81 to mediate HCV entry (Cormier *et al*., 2004b).

The CD81-HCV binding site has been mapped. E2 binds the CD81 LEL (Drummer *et al*., 2002) via at least two distinct regions (~ residues 412-443 and 520-550) that can be brought together in E2 tertiary structure to form the binding site (Drummer *et al*., 2006; Krey *et al*., 2010; Owsianka *et al*., 2006). Mutagenesis experiments identified an additional region in E2 distant from the site of antibody recognition (residues 612-619) that is necessary for CD81 binding, although this region probably acts indirectly by inducing conformational changes within E2 (Iacob *et al*., 2008). The CD81 LEL

sequence essential for these E2 interactions is contained within residues 164-201 (Higginbottom *et al*., 2000). While access to the CD81-binding site on E2 is reduced by the presence of four glycans surrounding the binding site (Helle *et al*., 2010), soluble CD81 (hCD81-LEL) has been shown to neutralize and precipitate ΔHVR1 particles much more readily than wild-type particles, indicating that HVR1, which plays no role in E2 glycosylation, masks the viral CD81 binding site (Bankwitz *et al*., 2010). This suggests that the conserved CD81 binding site is hidden in wild-type particles, evading host immune responses, until host factor interactions elicit conformational changes that expose the binding site on E2 to this crucial receptor at a postbinding step. Moreover, susceptibility to infection is related not only to the expression level of CD81, but also to the proportions of CD81 and SR-BI on the cell surface (Akazawa *et al*., 2007; Kapadia *et al*., 2007; Koutsoudakis *et al*., 2007).

Members of the tetraspanin family are able to interact with each other and with a panel of protein partners to form tetraspanin-enriched microdomains (TEMs), also referred to as "tetraspanin webs". TEMs are cell-type specific, composed of different tetraspanins that participate in functions unique to the cell type (Bouchiex & Rubinstein, 2001; Levy & Shoham, 2005). As CD81 interacts with various different molecules in the TEM of liver cells, including itself (Drummer *et al*., 2005; Kitadokoro *et al*., 2001), it is possible that other tetraspanins, CD81 partner proteins or specific HCV receptors such as SR-BI may contribute to efficient HCV entry by participating in a receptor/co-receptor complex through direct or indirect recruitment into the TEM. It is also unclear whether these complexes pre-exist in cells or are induced by HCV infection. A major protein involved in CD81 complexes in TEMs is the immunoglobulin superfamily member EWI-2 (Charrin *et al*., 2003). A cleavage product of EWI-2, called EWI-2wint (corresponding to EWI-2 without its N-terminal immunoglobulin domain) can effectively block viral entry by inhibiting viral interaction with CD81. The absence of this natural inhibitor of CD81 in hepatic cells may thus enable viral entry to take place in these cells. This was confirmed by ectopic expression of constitutively cleaved EWI-2wint, which blocked HCVcc infectivity in Huh-7 cells (Rocha-Perugini *et al*., 2008), possibly by promoting changes in the membrane dynamics and partitioning of CD81, adversely altering cell-free transmission of HCV (Potel *et al*., 2013). These findings suggest that the narrow tissue tropism of HCV is due as much to the non-expression of

specific inhibitors as it is reliant on the expression of a specific set of cellular entry receptors.

Not only is CD81 essential for HCV entry, antibody or HCV-E2 engagement of CD81 has been reported to activate the Rho GTPase family members Rac, Rho and Cdc42 and the mitogen-activated protein kinase (MAPK) signalling cascade. Inhibition of these pathways reduced HCV infection (Brazzoli *et al*., 2008). Rho GTPase signalling stimulated by CD81 has been suggested to induce actin remodelling, allowing lateral movement of CD81 necessary for HCV entry, while CD81-mediated MAPK activation is believed to control an as yet unidentified post-entry event. Indeed, a role for CD81 in efficient replication of the HCV genome has been postulated (Zhang *et al*., 2010), as CD81 expression was found to positively correlate with the kinetics of HCV RNA synthesis but was found to be inversely related to the kinetics of viral protein production. This suggested that HCV RNA template function for RNA replication may be subjected to CD81 control. As members of the tetraspanin family are known to be involved in membrane-fusion processes, it is no surprise to learn that HCV is primed by CD81 for low pH-dependent fusion early in the entry process (Sharma *et al*., 2011). The fusion process will be discussed in more detail in section 1.11.1.4.

Tight Junction Proteins

Tight junctions are major components of cell-cell adhesion complexes that separate apical from basolateral membrane domains and maintain cell polarity by forming an intramembrane that regulates the diffusion of certain molecules (Shin *et al*., 2006). Tight junctions perform several important liver functions in hepatocytes, such as bile formation and secretion (Van Itallie & Anderson, 2004). Members of the claudin family, involved in the formation of tight junctions, have also been implicated in HCV entry. Claudin-1 (CLDN-1), which is most highly expressed in the liver and possesses four TMDs, two extracellular loops and three intracellular domains, was first postulated as a HCV entry receptor after ectopic expression of CLDN-1 rendered non-hepatic HEK-293T cell lines permissive to HCV infection (Evans *et al*., 2007). The same study also observed that siRNA knockdown of CLDN-1 inhibits HCV infection in Huh-7.5 cells. No interaction between the HCV glycoproteins and CLDN-1 has been demonstrated but a direct interaction between CD81 and CLDN-1 has been observed

(Harris *et al*., 2008; Harris *et al*., 2010). While CLDN-1's role in tight junction formation and maintenance is undisputed, CLDN-1 is seen to associate with CD81 at the basolateral surface of polarized hepatoma cells, suggesting a role for non-junctional pools of CLDN-1 in HCV entry (Harris *et al*., 2010). In line with this, the establishment of single particle tracking approaches to image fluorescent HCV particles in live cells demonstrated that virion entry generally occurred outside of cell-cell junctions (Coller *et al*., 2009). Mutagenesis of the first CLDN-1 extracellular loop (ECL1) (Cukierman *et al*., 2009; Evans *et al*., 2007; Harris *et al*., 2010) and antibodies specific for CLDN-1 ECL1 (Fofana *et al*., 2010; Krieger *et al*., 2010) both ablated the CLDN-1/CD81 interaction and impaired HCV entry. A homology model of CLDN-1 ECL1 predicts aa residues 33-35 and 62-66 of this region interact with CD81 ECL2 residues T149, E152 and T153 (Davis *et al*., 2012). Follow up Fluorescence Resonance Energy Transfer (FRET) assays confirmed the essential nature of these CD81 residues in CLDN-1 association and HCV infection, as well as confirming that they had no impact on protein conformation or HCV E2 binding. These studies imply that CLDN-1 and CD81 act in a co-operative manner during HCV entry. In addition to CLDN-1, two other claudin family members, CLDN-6 and CLDN-9, have also been reported to confer HCVpp entry (Meertens *et al*., 2008; Zheng *et al*., 2007), although ectopic expression of either protein could not *trans*-complement CLDN-1 silencing (Meertens *et al*., 2008).

However, numerous human cell lines and all non-primate cell-lines are resistant to HCV entry even when CD81, SR-BI and CLDN-1 are co-expressed, indicating that cellular factors essential for HCV entry were still undetermined (Evans *et al*., 2007). Another tight junction protein, occludin (OCLN), has been implicated in HCV entry, with siRNA knockdown of OCLN in cell-lines permissive for HCV entry significantly impairing both HCVpp and HCVcc infection (Ploss *et al*., 2009). OCLN is a 60 kDa protein with four TMDs and two extracellular loops, as well as a long C-terminal cytoplasmic domain and a short N-terminal cytoplasmic domain (Furuse *et al*., 1993; Furuse & Tsukita, 2006). Unlike CLDN-1, a direct OCLN-E2 interaction has been confirmed by co-immunoprecipitation assays (Liu *et al*., 2009). However, it has also been postulated that OCLN probably affects late entry events only, as expression and localisation of CD-81, SR-BI and CLDN-1 were unaffected by OCLN silencing, yet envelope glycoprotein fusion-associated events were impaired (Benedicto *et al*., 2009). It has also been noted that viral infection led to a decrease in the expression of OCLN,

as well as CLDN-1, implying that regulation of cell surface receptors may provide a mechanism preventing onset of superinfection (Liu *et al*., 2009).

1.11.1.3. Additional Cellular HCV Entry Factors

Co-expression of SR-BI, CD81, CLDN-1 and OCLN renders non-liver cells permissive for HCV entry, demonstrating that these four proteins constitute the minimal viral receptor requirement (Dorner *et al*., 2011; Ploss *et al*., 2009). Indeed, receptor complementation assays indicate that CD81 and OCLN usage by HCV is highly specific, as their mouse versions only ineffectively support HCV entry (Flint *et al*., 2006; Ploss *et al*., 2009). However, other cellular factors have been identified that are pivotal for efficient HCV entry. One of these newly-discovered elements is the Niemann-Pick C1-like 1 cholesterol absorption receptor (NPC1L1), a 13 TMD cell surface cholesterol-sensing receptor responsible for cellular cholesterol absorption and whole-body cholesterol homeostasis (Sainz Jr *et al*., 2012). Sainz Jr *et al*. (2012) observed downregulation of NPC1L1 in HCV-infected Huh-7 cells, similar to marked reductions previously reported concerning CLDN-1 and OCLN. This report also demonstrated that NPC1L1-silenced Huh-7 cells were significantly less susceptible to HCVcc infection and that NPC1L1-specific antibodies reduced HCV infection to a similar extent as CD81-specific antibodies. This study also analysed the role of the receptor *in vivo*, treating uPA-SCID mice with ezetimibe, an FDA-approved cholesterol-lowering drug that is a direct inhibitor of NPC1L1 internalization. Mice treated with this drug via oral gavage could subsequently delay HCV infection for two weeks. Another study using an RNAi screen to elucidate the functional role of host cell kinases within the HCV entry process identified EGFR and EphA2 as cofactors of the HCV entry process (Lupberger *et al*., 2011). EGFR is a receptor tyrosine kinase (RTK) that regulates key cellular processes including proliferation, survival, differentiation during development and tissue homeostasis (Schneider & Wolf, 2009), while EphA2 mediates cell positioning, morphology, polarity and motility (Lackmann & Boyd., 2008). Results obtained from Lupberger *et al*. (2011) highlight roles for these RTKs in the formation of HCV entry factor complexes and membrane fusion. Specifically, this report proposes that EGFR is important for HCV glycoprotein-dependent fusion with host membranes by regulating the CD81/CLDN-1 interaction. In contrast, a more recent

paper hypothesises that CD81/HCV binding induces EGFR activation and internalisation without any apparent involvement of CLDN-1 (Diao *et al*., 2012).

Analysis of a siRNA library that targeted 140 cellular membrane trafficking genes also identified 16 additional host cofactors of HCV entry (Coller *et al*., 2009). These factors function primarily in clathrin-mediated endocytosis, the key mechanism in HCV internalisation (see section 1.11.1.4)

1.11.1.4. Internalisation and Fusion

After binding to specific receptors, virus entry into host cells involves fusion of the lipid envelope with a cellular membrane. This process is tightly co-ordinated in time and space and requires drastic conformational changes in the fusion proteins, which are triggered by cellular factors. Enveloped viruses can enter target cells in two different ways. A number of viruses, notably retroviruses, can directly fuse their envelope with the plasma membrane, releasing the viral genome into the cytosol. Alternatively, viruses can enter target cells by endocytosis. In this instance, conformation changes to the envelope proteins triggered by the acidic pH of endosomes usually leads to fusion of the viral envelope with the endosomal membrane followed by release of the genome into the cytosol. HCV has been proposed to enter cells via the latter method. Subjecting cells to chlorpromazine treatment (which disrupts the formation of clathrin-coated pits) or siRNAs targeting clathrin greatly reduced HCVpp and HCVcc entry, confirming that HCV enters target cells via clathrin-mediated endocytosis (Blanchard *et al*., 2006; Meertens *et al*., 2006). RNA interference studies allowed Coller *et al*. (2009) to identify 16 host factors vital for HCV entry that were principally employed in clathrin-mediated endocytosis, including cellular elements involved in linking clathrin to the actin cytoskeleton, endosomal acidification, receptor internalization and sorting as well as structural components of the clathrin endocytosis machinery. Furthermore, HCVcc and HCVpp are sensitive to endosome acidification inhibitors such as bafilomycin A1, concanamycin A, ammonium chloride or chloroquine, indicating that HCV fusion is pH-dependent and occurs in early endosomes (Blanchard *et al*., 2006; Hsu *et al*., 2003; Koutsoudakis *et al*., 2006; Meertens *et al*., 2006; Tscherne *et al*., 2006). *In vitro* assay systems based on HCVpp and liposomes designed to better characterise the fusion process (Lavillette *et al*., 2006) determined a threshold pH of 6.3 and an optimum of

about 5.5. This assay system also determined that fusion is also dependent on temperature (no fusion was recorded at 4 ºC) and facilitated by the presence of cholesterol but does not require the presence of any protein at the surface of liposomes.

It is worth noting that exposing surface-bound virions to acidic pH followed by a return to neutral pH does not affect HCV infectivity (Meertens *et al*., 2006; Tscherne *et al*., 2006), indicating that HCV envelope proteins need an additional trigger to become sensitive to low pH. In line with this, a recent study implicated CD81 in priming HCV for low-pH-dependent fusion early in the entry process (Sharma *et al*., 2011), highlighting how E1E2 dimers undergo reversible temperature-dependent conformational changes at neutral pH following exposure to CD81 ECL2. Indeed, live cell imaging experiments further postulated a central role for CD81 in HCV internalisation and fusion, as CD81 and CLDN-1 undergo co-endocytosis and fusion with Rab5-expressing early endosomes in a clathrin- and dynamin-dependent process (Farquhar *et al*., 2012).

It is currently believed that HCV envelope proteins have a folding pattern similar to class II fusion proteins, a class of protein that are predominantly non-helical, having a β-sheet type structure instead. Unlike type I fusion proteins, they are not cleaved during biosynthesis and possess an internal fusion peptide with a loop conformation (Kielian & Rey, 2006). Class II fusion proteins are synthesised as a complex with a companion membrane glycoprotein, which acts as a chaperone. Cleavage of this companion protein activates the fusogenic potential of the fusion protein. Although there is no direct experimental evidence demonstrating the role of E2 as the HCV fusion protein, a model of the tertiary organisation of E2 highlighted the structural similarities of the protein to other class II fusion proteins in the *Flaviviridae* and *Togaviridae* families as well as determining the location of a candidate fusion loop in DII of the protein (see section 1.9.3) (Krey *et al*., 2010). The polypeptide segment in E2 implicated as the candidate region for the fusion loop, spanning residues 502-520, has all the principal characteristics associated with class II fusion loops. The segment is rich in glycine and other non-polar amino acids and is strictly conserved across all HCV genotypes. Work published by Krey *et al*. (2010) contradicted an earlier bioinformatics model of E1, which postulated that E1 was a truncated class II fusion protein with a fold similar to a flavivirus fusion protein DII domain (Garry & Dash, 2003). However, in class II fusion

proteins, DII must work in conjunction with two other domains covalently linked within the polypeptide to induce membrane fusion, a structure not observed in E1. Moreover, numerous structural studies have confirmed that most animal envelope viruses encode fusion proteins belonging to one of three currently characterized structural classes (Harrison, 2008), none of whom would be able to accommodate E1.

1.11.2. Genome Translation and RNA Replication

1.11.2.1. HCV IRES-mediated Translation

In mammalian cells, the two methods of translation initiation are cap-dependent and cap-independent (Fig 1.6). The prior represents the standard mode of translation for most cellular mRNAs and involves initiation-factor protein association with the 7-methyl guanosine moiety at the 5' end of mRNA, leading to 40S ribosome binding and scanning to the initiation codon. In contrast, cap-independent translation involves the direct interaction of ribosomes with an IRES, which is utilised by some cellular transcripts as well as some positive-strand RNA viruses including HCV (Shih *et al*., 2008). Indeed, the IRES located in the HCV 5'UTR (see section 1.9.1) directly recruits the 40S ribosomal subunit to the AUG codon and initiates protein translation without the need for ribosome scanning or those canonical translation initiation factors involved in scanning or unwinding secondary structures in mRNA (Honda *et al*., 1996b; Penin *et al*., 2004; Pestova *et al*., 2008; Reynolds *et al*., 1996; Terenin *et al*., 2008). In HCV-IRES directed translation initiation, however, localization of the initiator methionyl-tRNA (Met-tRNA) to the peptidyl (P) site on the surface of the 40S ribosomal subunit is dependent on the initiation factor eIF2. eIF5, the GTPase-activating protein of eIF2, is also required for this process. While the large multi-subunit initiation factor eIF3 does not play a role in accurate placement of the initiator tRNA, it has been implicated in stabilization of the eIF2-GTP-Met-tRNA complex, a stabilizing effect essential for the formation of a 48S translation initiation complex (Pestova *et al*., 1998; Ji *et al*., 2004). Subsequent association of a 60S ribosomal subunit to this complex (an event requiring the cellular initiation factor eIF5B) results in a translationally active 80S initiation complex. Inactivation of eIF2 by phosphorylation can occur as a result of host-cell responses to viral infection (Williams, 1999). This has been found to have a much

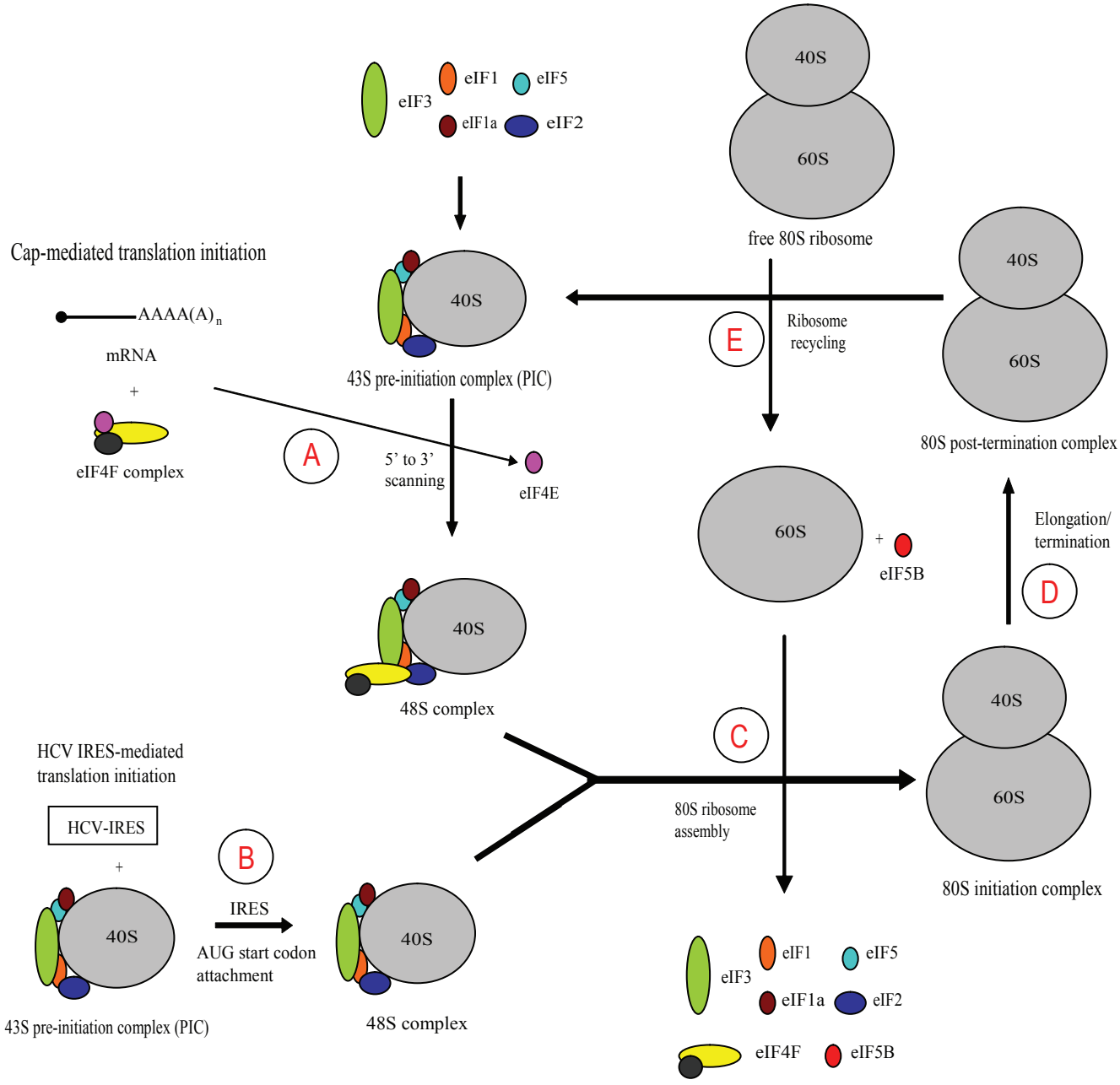

Figure 1.6. Models of cap- and HCV IRES-directed translation.

(A) Canonical (cap-mediated) translation begins with the binding of the 43S PIC and initiation factors to the 5'-end of mRNA and formation of the 48S complex. **(B)** In HCV IRES-directed translation, the 43S PIC binds directly to the AUG initiation codon and initiates protein translation in the absence of ribosome scanning and several canonical translation initiation factors. **(C)** The 48S complex generated in either instance then joins with the 60S ribosomal subunit, assembling the 80S translation initiation complex. **(D)** An elongation and termination phase follows, resulting in 80S post-termination complexes. **(E)** Post-elongation and termination, recycling of these complexes and free 80S ribosomes occurs. Adapted from Geissler *et al*. (2012).

smaller effect on HCV IRES-directed translation than on cap-dependent translation, as the HCV IRES can alternatively translate using a bacterial-like, eIF2-independent mechanism. This pathway requires only eIF5B and eIF3 and does not require GTP hydrolysis. In this instance, eIF5B can substitute for eIF2/eIF5 in promoting initiator tRNA binding to the 40S ribosome (Terenin *et al*., 2008). Translation occurs at ER membranes, which produces a single polyprotein that is processed by cellular and viral proteases to produce the mature structural and NS proteins. As with all positive-sense RNA viruses, once sufficient translation of HCV RNA has occurred, an undefined molecular switch is believed to direct the initiation of RNA replication within a membrane bound replication complex (Novak & Kirkegaard, 1994). The phosphorylation state of the viral protein NS5A has been implicated as having an important role in this process, but this theory is controversial and poorly understood (see also section 1.9.8).

1.11.2.2. HCV RNA Replication

A common feature of all positive-strand RNA viruses is the association of their replication machinery with the cytoplasmic surfaces of intracellular membranes, with numerous examples of replicase genes from these viruses encoding membrane-targeting sequences. These viruses also have an intrinsic capacity to remodel intracellular membranes, a process which serves to house viral replication complexes, thereby creating membrane-wrapped factories where RNA synthesis and eventually virion assembly take place. In the case of HCV, NS4B, at least in part, is known to induce membrane rearrangements that generate an intracellular platform for HCV RNA replication, referred to as the "membranous web" (MW) (Egger *et al*., 2002; Gosert *et al*., 2003) or membrane-associated foci (MAF) (Gretton *et al*., 2005). Recent papers used immunofluorescence- and EM-based methods to analyse the MWs induced by HCV in infected cells in greater detail (Ferraris *et al*., 2010; Romero-Brey *et al*., 2012). These reports illustrate how the morphology of the membranous rearrangements induced by HCV-infected cells resemble those of the unrelated picorna-, corona- and arteriviruses, but are clearly distinct from those of the closely related flaviviruses. From these studies, it was understood that the MW is derived primarily from the ER and contains markers of rough ER but also includes markers of early and late endosomes, COP vesicles, mitochondria and LDs. Indeed, the main constituents of the MW were

found to be single and double membrane vesicles (DMVs), the former induced by NS4B and the latter induced by NS5A (Romero-Brey *et al*., 2012), suggesting that a functional MW requires the concerted action of several HCV replicase proteins. DMVs predominate and were identified as protrusions from the ER membrane into the cytosol. Romero-Brey *et al*. (2012) also highlighted the appearance of multi-membrane vesicles late in infection, presumably as a result of a stress-induced reaction.

Both NS proteins and HCV RNA have been observed in close association with MWs. These viral RNAs and NS proteins are ribonuclease and protease resistant, indicating that the MW encloses and protects these replication components from the intracellular environment (Quinkert *et al*., 2005; Waris *et al*., 2004). HCV RNA replication begins rapidly after virus entry, given that negative-strand RNAs are detectable by Northern blot hybridisation at 4 h post-electroporation (Binder *et al*., 2007). Within these replication compartments, the instigation of HCV RNA synthesis occurs by an unknown mechanism but likely involves the *de novo* initiation of RNA replication by NS5B. Using the positive-strand genome, NS5B generates a negative-strand RNA genome that in turn serves as a template for the synthesis of excess amounts of plus-strand progeny (Lohmann *et al.*, 1999). During this process, the negative- and positive-strand RNAs are thought to form a dsRNA replicative intermediate, from which nascent strands are synthesized by strand-displacement (Targett-Adams *et al.*, 2008a). Quantitative analyses of replication complexes estimate that an active complex consists of minimally one negative-strand RNA template, up to ten positive-strand RNA copies and several hundred NS proteins (Quinkert *et al.*, 2005).

Numerous cellular factors have been identified with potential roles in HCV RNA replication. As discussed in section 1.10.2.3, supplementation with miR-122 allows efficient viral genome replication in previously nonpermissive cell-lines. The importance of host factors PTB, La autoantigen and PCBP2 in HCV RNA replication is highlighted in section 1.9.1. Several cellular NS5A-binding factors such as hVAP-A, FKBP8 and FBL2 (section 1.9.8) have also been implicated in this process. More recently, a study by Goueslain *et al*. (2010) identified GBF1, a guanine nucleotide exchange factor for small GTPases of the ADP-ribosylation factor (ARF) family, as another host factor involved in HCV replication. GBF1 is sensitive to brefeldin A (BFA), a lactone antibiotic known to exhibit a wide range of inhibitory actions on

membrane-associated mechanisms of the secretory and endocytic pathways through its ability to interfere with ARF activation processes (Goueslain *et al*., 2010). Goueslain *et al*. (2010) postulated that GBF1-associated mechanisms serve to deliver proteins or lipids to HCV replication complexes, thus contributing to functional activity of these complexes. DDX3, a DEAD-box RNA helicase, has also been reported to be essential for HCV RNA replication (Ariumi *et al*., 2007). This result will be discussed in greater detail in section 1.12.3.4.

1.11.3. HCV Assembly

The assembly and secretion of HCV particles is tightly linked with host cell lipid synthesis. In line with this, analysis of purified membrane vesicles containing HCV replication complexes isolated from human hepatoma cells harboring HCV replicons demonstrated that these organelles are highly enriched in proteins required for VLDL assembly, including apoB, apoE and microsomal triglyceride transfer protein (MTP) (Huang *et al*., 2007). Indeed, ApoB and apoE have both been identified as structural components of VLDL while MTP is known to be a key enzyme in VLDL production (Blasiole *et al*., 2007). ApoE has been observed to associate with HCVcc particles, and depletion of the protein in this system has been shown to adversely effect the production of infectious HCV (Benga *et al*., 2010; Chang *et al*., 2007; Hishiki *et al*., 2010; Jiang & Luo, 2009; Owen *et al*., 2009). ApoE is known to interact directly with NS5A (Benga *et al*., 2010; Cun *et al*., 2010), an association which suggests apoE functions at an early step of HCV assembly as NS5A is not a major constituent of HCV particles (Merz *et al*., 2011). A study in which virion-associated cholesterol was depleted and replenished with exogenous sterol analogues indicated that virion-association cholesterol contributes to an efficient HCV-apoE interaction (Yamamoto *et al*., 2011). ApoE is a polymorphic protein with three major isoforms: apoE2, apoE3 and apoE4. While ectopic expression of apoE3 and apoE4 enabled recovery of infectious HCV in cells depleted of endogenous apoE, expression of apoE2 had little influence on virus production in similar circumstances (Hishiki *et al*., 2010). This is in agreement with the results of an epidemiological study of Caucasians with persistent chronic hepatitis, which indicated a notable absence of the apoE2/apoE2 genotype in HCV antibody-positive individuals (Price *et al*., 2006).

The functional importance of apoB and MTP in the assembly and secretion of infectious HCV is as yet unclear. Two groups have reported greatly reduced HCV production in target cells upon treatment with an MTP inhibitor or exposure to siRNAs targeting apoB (Gastaminza *et al*., 2008; Huang *et al*., 2007). Furthermore, using an *in vitro* model system based on the lipoprotein-producing Caco-2 cell-line, where subviral particles can be produced when only E1 and E2 are expressed, it was noted that secretion of the HCV envelope glycoproteins could be reduced by MTP inhibition (Icard *et al*., 2009). In contrast, three other groups reported that depletion of apoE, but not of apoB, reduced virus production in a HCVcc background. They also noted that the level of MTP activity did not have any effect on HCVcc assembly or release (Benga *et al*., 2010; Chang *et al*., 2007; Jiang & Luo, 2009). The exact reason for these differences are unknown but may be partly related to the use of different cell culture systems. Nevertheless, all studies agree that the apoE component of the VLDL pathway is critical for infectious particle production. It still remains to be determined exactly how the apolipoproteins are incorporated into mature infectious particles. One possible model is described in Fig 1.7.

VLDL maturation occurs by acquisition of lipids from LDs either in the ER lumen or in the Golgi apparatus (Blasiole *et al*., 2007). Following cleavage, mature HCV core protein is targeted to LDs and it has been demonstrated that mutations which disrupt this localisation of core inhibit infectious virus production (Boulant *et al*., 2007). The role of core trafficking to LDs is not well understood, although previous investigation has shown that core recruits NS proteins and replication complexes to LD-associated membranes, suggesting an early step in virion morphogenesis occurs at these sites (Miyanari *et al*., 2007). Fluorescent labelling and functional imaging of core in living cells has recently been used to visualize core during HCV assembly. Core has been seen to move to the surface of large, immobile LDs soon after protein translation. During the peak of virus assembly, core forms polarized caps on these LDs that are frequently in close apposition to ER-localized core (Counihan *et al*., 2011). Presumably, these represent the sites of core protein transfer between the ER and LDs. Similar localizations of core-coated LDs were observed previously in fixed cells by IF staining (Boulant *et al*., 2007; Boulant *et al*., 2008). Core is known to induce the redistribution of LDs from their native diffuse cytoplasmic localisations to ER membranes in HCV-

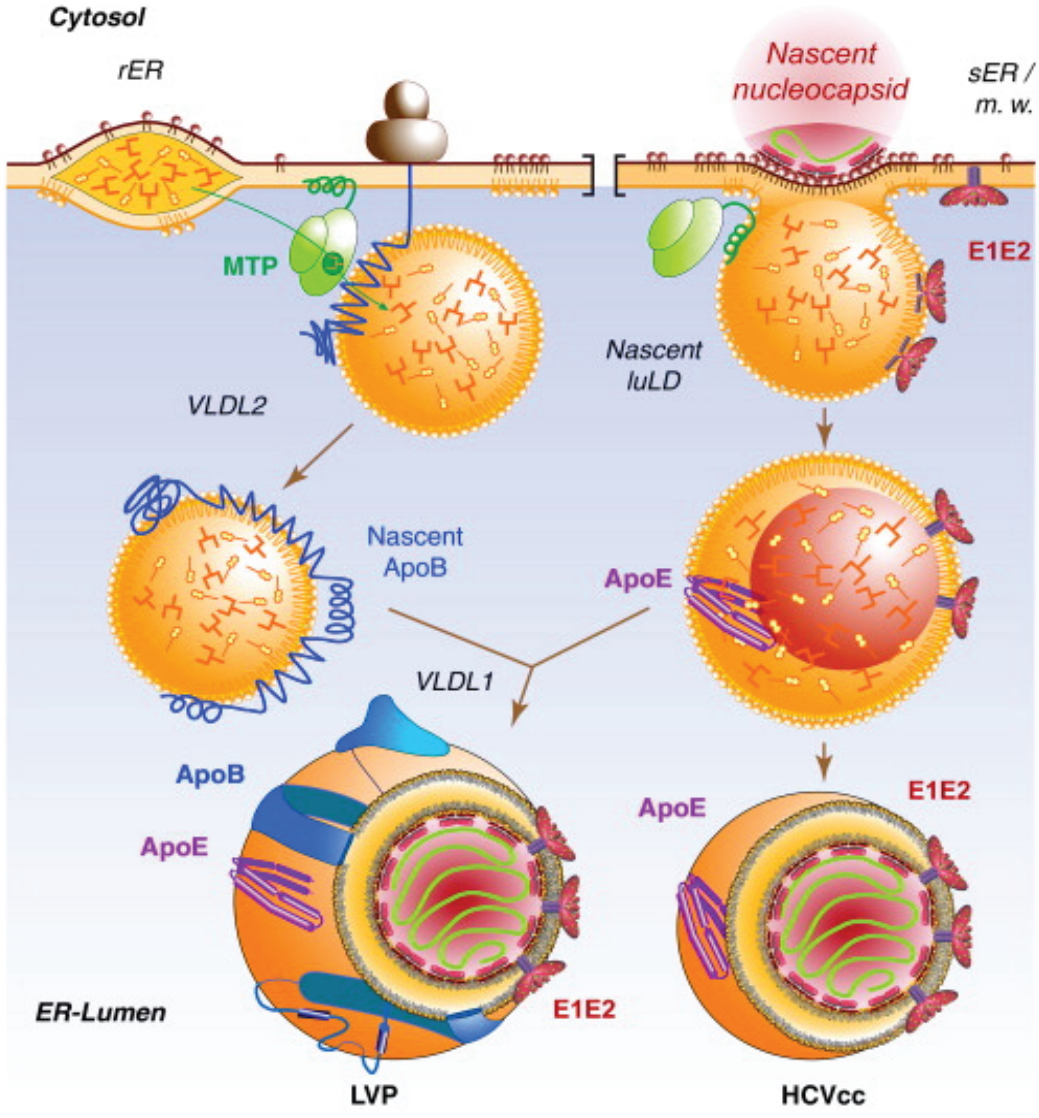

Figure 1.7. Model of infectious HCV particle structures and their biogenesis.

During translation at the rER, nascent apoB (blue line) is translocated into the ER lumen and loaded by MTP with phospholipids and triglycerides. This leads to the formation of a neutral lipid core that is converted into a spherical particle (*VLDL2*) acquiring exchangeable apoE and apoC (not shown for clarity). In the smooth ER (sER) or membranous web, a second precursor (the luminal LD; luLD) is formed from the ER membrane and by MTP-mediated triglyceride enrichment. E1 and E2 retained at the ER membrane might slide onto this luLD prior to pinching-off. The nucleocapsid would be inserted into the hydrophobic lipid core of the pinching-off luLD due to the hydrophobic nucleocapsid surface (formed by D2 of the core protein). In VLDL-competent cells such as primary human hepatocytes, this precursor could fuse with VLDL2 to form the LVP. In Huh-7 cells, where VLDL1 formation is inefficient, HCVcc is secreted predominantly as particles lacking apoB. Taken from Bartenschlager *et al*. (2011).

infected Huh-7 cells. This re-localisation of LDs in aggregates at ER membranes requires only core protein and is accompanied by reduced abundance of adipose differentiation-related protein (ADRP) on LD surfaces (Boulant *et al*., 2008), a cellular protein crucial in maintaining the disparate intracellular distribution of LDs in healthy uninfected cells. The redistribution of LDs is believed to coordinate interactions between the viral replication complexes and the assembly sites, allowing virion morphogenesis to proceed.

Viral NS proteins were first implicated in HCV production following the observation that JFH1-derived NS proteins are required to generate infectious virus from intra- and inter-genotype chimeric constructs (Lindenbach *et al*., 2005; Pietschmann *et al*., 2006). Evidence supporting important roles for NS2, NS3, NS4A, NS5A and p7 in the assembly and release of infectious HCV has come from mutational analyses. In addition to core protein, NS5A has been reported to associate with LDs, an event that is critical for infectious HCVcc assembly. It has been shown that mutations within domain I of NS5A prevent the proteins association with LDs, which impairs infectious virus production (Miyanari *et al*., 2007). A subsequent study classified domain III of NS5A as the primary "assembly determinant" and identified a NS5A-core association on the surface of LDs. Deletions to NS5A domain III impaired virus production by disrupting the NS5A-core protein association on LDs but did not alter NS5A-LD attachment (Appel *et al*., 2008). Another 2008 paper observed that substitutions at a serine cluster within NS5A domain III (aa 2428, 2430 and 2433), which have no impact on HCV RNA replication, inhibit the direct interaction between core and NS5A (Masaki *et al*., 2008). These studies suggest that the recruitment of NS5A to LDs enables its interaction with core protein for virion assembly. Since domain III of NS5A is one of the most variable regions in the HCV genome, these results also suggest how viral isolates may differ in their level of virion production and thus in their level of fitness and pathogenesis.

Numerous mutagenesis studies have identified regions or residues within NS2 that are important in infectious virus production (Dentzer *et al*., 2009; Jirasko *et al*., 2008, Jirasko *et al*., 2010; Jones *et al*., 2007; Ma *et al*., 2011; Phan *et al*., 2009; Popescu *et al*., 2011a; Yi *et al*., 2007, Yi *et al*., 2009). Indeed, both NS2 domains have been found to be essential for HCV assembly, but the protein's protease activity is not required in this

process (Jirasko *et al*., 2008; Jones *et al*., 2007). Genetic and biochemical data suggest NS2 directly interacts with multiple viral proteins including E1-E2, p7, NS3 and NS5A, with subsequent IF studies showing that NS2 recruits these proteins to assembly sites at the LD-ER interface (Boson *et al*., 2011; Jirasko *et al*., 2010; Popescu *et al*., 2011a). These results suggest that NS2 has a role in recruiting other viral proteins to sites in close proximity to LDs and/or acts as a scaffold promoting viral assembly. Since no direct interaction has been identified between NS2 and core (Jirasko *et al*., 2010; Ma *et al*., 2011; Stapleford & Lindenbach, 2011), it is possible that interplay exists between the core-NS5A interaction and NS2-NS5A interaction during assembly. p7 is known to be a vital element of virion production, as mutation of the basic residues required for its ion channel activity greatly reduces levels of virus production (Brohm *et al*., 2009; Jones *et al*., 2007; Steinmann *et al*., 2007). p7 has also been shown to recruit both core (Boson *et al*, 2011) and NS2 (Tedbury *et al*., 2011) to sites adjacent to replication complexes. The exact function of p7 during virion assembly remains to be elucidated but the possibility the protein controls multiple aspects of the process needs to be investigated in depth. Indeed, a recent study found that the proton-selective ion-channel activity of p7 prevented the acidification of intracellular virions during their transit through otherwise acidic intracellular compartments (Wozniak *et al*., 2010). This suggests that p7 is involved at a late stage of virus production, in contrast to an earlier report which postulated that p7 acted at an early stage of virion morphogenesis (Jones *et al*., 2007). In addition to these key players, various studies also indicate specific roles for NS3, NS4A and NS4B in HCV assembly (see sections 1.9.6 and 1.9.7). Thus, HCV assembly is a complex process that requires multiple interactions between the structural and NS viral proteins to be coordinated at LD-associated ER-membrane structures (Fig 1.8).

In addition to viral factors, a number of host proteins have been implicated in HCV morphogenesis, including heat shock cognate protein 70 (HSC70) (Parent *et al*., 2009), annexin A2 (ANXA2) (Backes *et al*., 2010) and the diacylglycerol acyl transferase 1 (DGAT1) enzyme (Herker *et al*., 2010). Proteomic analysis performed on highly purified HCV virions identified HSC70 as a component of the viral particle. Indeed, antibodies targeting HSC70 reduced infectivity, arguing that a fraction of HSC70 is accessible on the outside of the virion. Additionally, HSC was shown to colocalise with HCV proteins on LDs and found to be crucial for both LD size and efficient production

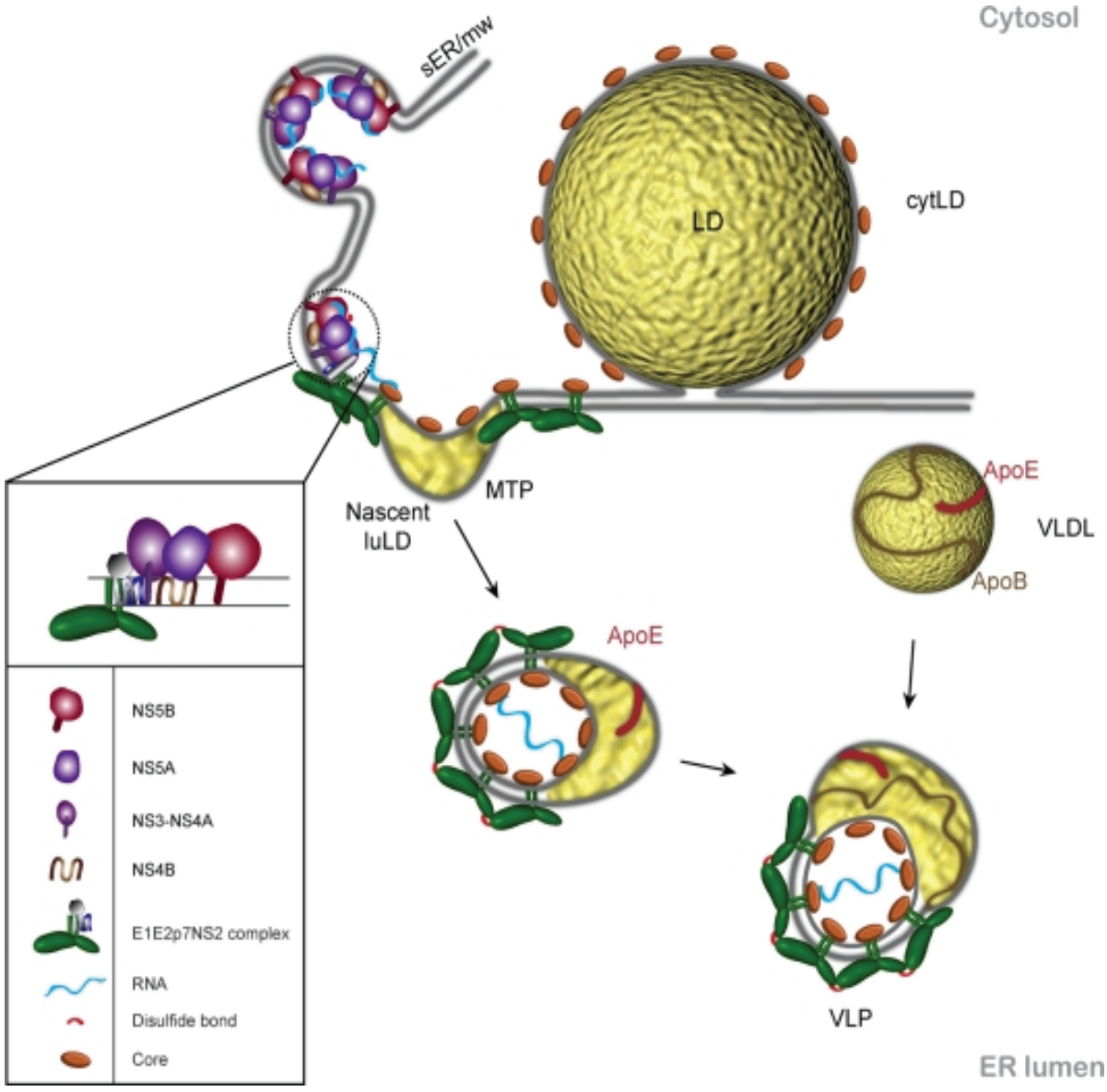

Figure 1.8. Working model of HCV assembly.

Viral assembly is triggered by the encounter of three modules: core, E1E2p7NS2 complex and the replication complex (RC). The assembly site is supposed to be in the membranous microenvironment of the lipid droplet (LD) and the endoplasmic reticulum (ER). The driving force of viral budding potentially comes from three directions: the pushing force of the nascent nucleocaspsid, the pulling force of envelope proteins which might stabilize the viral surface architecture by intermolecular disulfide bridges and the force of the nascent luminal LD (luLD) between the ER leaflets. The result is a hybrid lipoviroparticle, which acquires ApoE presumably by its lipid component. In primary hepatocytes, the lipoprotein moiety may mature into a VLDL-like structure. Taken from Popescu *et al*. (2011b).

of infectious virus particles (Parent *et al*., 2009). ANXA2 was identified after proteomic analysis of purified HCV replication complexes. Surprisingly, silencing of ANXA2 expression did not alter RNA replication but instead significantly reduced extra- and intracellular virus titres. Domain III of NS5A was found to specifically recruit ANXA2, probably by an indirect mechanism (Backes *et al*., 2010). How HSC70 and ANXA2 contribute to virion morphogenesis remains to be determined. The DGAT1 enzyme, which is essential for LD biogenesis, interacts with core protein and localizes it to LDs. Disrupting this process by depletion of the DGAT1 gene profoundly inhibits infectious virus assembly (Herker *et al*., 2010). A recent paper by Camus *et al*. (2013) identified NS5A as another binding partner of DGAT1. The authors propose a model whereby DGAT1 serves as a cellular "hub" for HCV core and NS5A proteins, guiding both onto the surface of LDs (Camus *et al*., 2013). Disrupting core-AP2M1 binding, however, leads to accumulation of core on LDs by altering AP2M1's recruitment to LDs, leading to decreased core localisation with E2 and elements of the trans-golgi network, suggesting the core-AP2M1 interaction mediates a later stage of assembly post-accumulation of core on LDs but before envelopment at ER sites (Neveu *et al*., 2012).

Finally, RNAi analysis performed by Coller *et al*. (2012) identified numerous other host cofactors that are required for infectious HCV secretion, but not HCV entry and replication. These factors included multiple components of the secretory pathway, such as cellular elements involved in ER to golgi trafficking (SAR1A), golgi structure and function (CYTH3), cargo sorting and vesicle budding (PRKD1, PI4KB, AP1M1) and exocytosis (RAB11A, RAB3D, VAMP1). Coller *et al*. (2012) also developed a live cell imaging approach to study HCV core trafficking using an infectious HCV that contains a tetracysteine (TC) tag insertion in the core protein (TC-core). TC-core movements dependent upon successful virion assembly were found to be microtubule-dependent and associated with a number of secretory-pathway compenents identified by siRNA (Coller *et al*., 2012).

1.12. DDX3

DDX3, a member of the DEAD-box family of RNA helicases, came to the attention of our research group through its ability to interact with HCV core protein. In 1999, three independent publications described this interaction, referring to the cellular helicase as DBX (Mamiya & Worman, 1999), CAP-Rf (Core-associated protein-RNA helicase full-length (You *et al*., 1999) and DDX3 (Owsianka & Patel, 1999) respectively. However, DDX3 is the name approved by the HUGO/GDB Nomenclature Committee and will therefore be used to describe the helicase for the remainder of this thesis. The interaction between core and DDX3 will be discussed in detail in section 1.12.3.4.

1.12.1. General Features of DEAD-box RNA Helicases

Nearly all aspects of RNA metabolism involve RNA helicases, which are enzymes that use ATP to bind or remodel RNA and RNA-protein complexes. In line with this, DEAD-box helicases have central and, in many cases, essential physiological roles in cellular RNA metabolism including transcription, pre-mRNA splicing, ribosome biogenesis, RNA export, translation and RNA decay (Cordin *et al*., 2006). DEAD-box proteins belong to helicase superfamily 2 (SF2). They share with other SF2 proteins a helicase core composed of two RecA-like domains. Within this helicase core, at least 12 characteristic sequence motifs are located at conserved positions (Fairman-Williams *et al*., 2010; Linder & Jankowsky, 2011). Motif II, also known as the walker B motif (Walker *et al*., 1982), contains the Asp-Glu-Ala-Asp (D-E-A-D) motif denominative for the entire family and is involved in binding the phosphates of ATP, alongside motif I (also known as the walker A motif) and motif VI. Motifs Ia, Ib, Ic, IVa, IV and V bind the RNA substrate while the Q motif specifically recognizes the adenine of ATP (Bleichert & Baserga, 2007; Cordin *et al*., 2006; Schutz *et al*., 2010). Motifs III and Va are thought to coordinate other motifs relative to the γ phosphate of ATP to create a high-affinity binding site for RNA. How this occurs is as yet unclear. In addition to motifs III and Va, other conserved elements in DEAD-box helicases may be important for this, with a phenylalanine residue in residue IV implicated in this process (Banroques *et al*., 2008). Deletion and chimera constructs tested both *in vivo* and *in vitro* confirmed the minimal functional unit of the DEAD-box helicase core starts two

amino acids before an isolated phenylalanine in the Q motif and extends to ~ 35 residues beyond motif VI (Banroques *et al*., 2011). In contrast, the N- and C-terminal extensions are highly variable in both sequence and length and are believed to confer functional specificity to individual DEAD-box helicases, with roles ranging from substrate interaction and subcellular localisation to interaction with cellular factors (Cordin *et al*., 2006).

1.12.2. Cellular Roles of DDX3

1.12.2.1. General Features

DDX3 was first identified in 1997 as one of five X-chromosomal genes that have homologues in the non-recombining region of the Y-chromosome. Unlike DDX3Y, which is expressed specifically in testes, the DDX3 (or more correctly DDX3X) gene escapes X-inactivation and is a ubiquitously expressed cellular protein (Kim *et al*., 2001; Lahn & Page, 1997). Known homologues of DDX3 include mouse PL10 (Leroy *et al.*, 1989), *Xenopus laevis* An3 (Gururajan *et al.*, 1991) and yeast Ded1p (Jamieson & Beggs, 1991). As well as being proposed as an RNA helicase due to its sequence homology with other DEAD-box helicases, DDX3 has also been shown to possess ATPase and helicase activities experimentally (Franca *et al*., 2007; Yedavalli *et al*., 2004). Although the precise biological function of DDX3 remains elusive, it is believed to play an important role in many cellular processes, including mRNA splicing, mRNA transport, mRNA degradation, protein translation, cell cycle regulation, cancer-related pathogenesis, immune response regulation and apoptosis (Rosner & Rinkevich, 2007; Schröder, 2010). DDX3 has also been implicated in various different viral lifecycles, including that of HCV. The following sections highlight the literature available on DDX3 to date.

1.12.2.2. Cellular Localisation

It has been demonstrated that DDX3 is a nucleo-cytoplasmic shuttling protein, with its export from the nucleus mediated by the importin-β family shuttling factor CRM1 (chromosome maintenance region 1) (Yedavalli *et al*., 2004). Subsequently, it was also

observed that DDX3 could directly interact with Tip-associated protein (TAP), the major nuclear mRNA export receptor (Lai *et al*., 2008). Inhibition of CRM1 or TAP results in nuclear accumulation of DDX3, suggesting that DDX3 could be exported from the nucleus through both pathways, although it is presently unclear whether DDX3 favours one pathway over the other or whether these two pathways are equally involved in DDX3 transport. Presumably due to the high rate of nuclear export, the majority of studies analysing intracellular DDX3 localisation have reported this protein as predominantly or exclusively cytoplasmic (Franca *et al*., 2007; Lai *et al*., 2008; Lee *et al*., 2008; Mamiya & Worman, 1999; Schröder *et al*., 2008; Yedavalli *et al*., 2004). In contrast, two studies reported a nuclear localisation of endogenous DDX3 in HeLa cells (Owsianka & Patel, 1999; You *et al*., 1999). The reason for this disparity is unclear. However, it has been reported that, while DDX3 localisation is cytoplasmic in skin tissue from cell carcinomas, it is mainly nuclear in healthy primary epidermis cells (Chao *et al*., 2006), suggesting discrepancies between transformed and non-transformed cell-lines.

1.12.2.3. Splicing

An arginine/serine rich RS-like domain of DDX3, encompassing aa's 582-632, was found to resemble the RS domains of splicing factors such as ASF/SF2 and SC-35 (Owsianka & Patel, 1999). Indeed, DDX3 was reported to be present in functional spliceosomal complexes (Deckert *et al*., 2006; Zhou *et al*., 2002) and the DDX3 homologue Ded1p was identified in the purified spliceosome in yeast (Stevens *et al*., 2002). However, DDX3 and Ded1p have been detected with spliced mRNA as part of mRNPs (messenger ribonucleoprotein particles) (Burckin *et al*., 2005; Merz *et al*., 2007) and it has been highlighted that DDX3 only associated with spliced mRNA in an Exon junction complex (EJC)-dependent manner (Merz *et al*., 2007). These findings suggest that DDX3 does not have an active role in splicing, but associates with mRNPs after splicing for roles such as RNA transport. The fact elements of the RNA export machinery associate with mRNPs after splicing gave credence to this hypothesis. Indeed, DDX3 was isolated from RNA-transporting granules (Kanai *et al*., 2004) and a recent paper by Choi & Lee (2012) described a novel interaction between DDX3 and DDX5 through the phosphorylation of both proteins which allowed a joint involvement for both proteins in mRNP export. This publication also reported on how DDX3 co-

localised with DDX5 in the cytoplasm during the G2/M phase of the cell cycle and the important role DDX3 played in shuttling DDX5 to the nucleus (Choi & Lee, 2012). A finding contradicting the importance of DDX3 in RNA transport has also been reported, where Kanai *et al*. (2004) observed how depletion of the cellular helicase by RNAi had little effect on RNA transport.

1.12.2.4. Innate Immune Response

DDX3 has been shown to interact with, and be phosphorylated by, TBK1 and IKKε, key kinases that phosphorylate IRF3/7 and subsequently activate the IFN-β gene (Soulat *et al*., 2008). This report also confirmed a role for DDX3 in PRR-induced IFN-β promoter activation and its subsequent function downstream of TBK1 and IKKε (Soulat *et al*., 2008). Observing an interaction between DDX3 and the IFN-β promoter after PRR stimulation, Soulat *et al*. (2008) suggested that DDX3 could act as a transcriptional cofactor at the promoter level. In line with work by Soulat *et al*. (2008), Schröder *et al*. (2008) also found DDX3 to be a positive regulator of IFN-β induction. Infection of HEK-293T with Sendai virus demonstrated a virus-induced transient association between endogenous DDX3 and endogenous IKKε, suggesting DDX3 contributes to IRF-3 activation (Schröder *et al*., 2008). A recent study by Gu *et al*. (2013) also postulated a role for DDX3 in IRF-3 activation, stating that DDX3 mediated the phosphorylation of IRF3 by IKKε. The authors reported that DDX3 directly interacted with IKKε, enhancing its autophosphorylation and activation. This led to the subsequent phosphorylation of a serine residue in the N-terminus of DDX3 by IKKε, allowing recruitment of IRF3 to DDX3 and facilitating its phosphorylation by IKKε. This report suggests that DDX3 may act as a downstream scaffolding adaptor that links IKKε and IRF3 (Gu *et al*., 2013).

In contrast, a paper by Oshiumi *et al*. (2010b) suggested DDX3 only marginally enhanced IFN-β promoter activation induced by TBK1 and IKKε and that the protein acts upstream of these kinases at the level of RIG-I and IPS-1 (Oshiumi *et al*., 2010b). This study observed that DDX3 directly interacted with the CARD (caspase recruitment domain) domain of IPS-1, a mitochondrial adaptor molecule that binds RIG-I following recognition of viral RNA in the cytoplasm. Findings gathered by Oshiumi *et al*. (2010b) lead the authors to postulate that DDX3 is an antiviral IPS-1 enhancer and that the

DDX3/IPS-1 interaction facilitates IFN-β induction, conferring high antiviral potential in the early phase of viral infection when RIG-I levels in the host cells are still low. Taken together, these disparate findings suggest DDX3 has multiple roles in innate immune signalling.

1.12.2.5. Apoptosis

So far, only two studies have presented data concerning DDX3's role in apoptosis. Chang *et al*. (2006) observed that DDX3 downregulation promoted cell proliferation and anti-apoptosis, with the authors also reporting preliminary findings indicating that key elements of the intrinsic apoptotic pathway, caspase-6 and caspase-9, cannot be activated in the absence of DDX3 (Chang *et al*., 2006). The anti-apoptotic effects of DDX3 depletion postulated by Chang *et al*. (2006) is in complete contrast to the findings published by Sun *et al*. (2008), who describe an anti-apoptotic death receptor complex comprising glycogen synthase kinase-3 (GSK3), cellular inhibitor of apoptosis protein-1 (c-IAP1) and DDX3. Stimulated death receptors can surmount this complex by inactivating GSK3 and cleaving DDX3 and c-IAP1, enabling progression of the apoptotic signalling cascade. This study also reported that DDX3 knockdown enhanced signalling through the death receptor TRAIL-R2 and activation of caspase-3 (Sun *et al*., 2008). Given the limited physiological sense derived if results by Chang *et al*. (2006) and Sun *et al*. (2008) are examined together, clarification of the role of DDX3 in apoptosis needs to be addressed by further studies.

1.12.2.6. Tumourigenesis

As stated in section 1.12.2.5, Chang *et al*. (2006) reported that DDX3 depletion promoted cell proliferation, with knockdown of the helicase by siRNA in the non-transformed mouse fibroblast cell-line NIH-3T3 resulting in premature entry into S-phase. This study also ascribed DDX3 knockdown as the reason behind lower expression levels of the tumour suppressor p21/waf in these cells. Furthermore, Chang *et al*. (2006) reported the differential deregulation of DDX3 expression in HCV-associated HCC, with samples from men and HBV-positive patients particularly affected. In line with this, a subsequent study by Chao *et al*. (2006) highlighted how DDX3 mRNA and protein expression were generally lower in HCC tissue specimens

compared to non-tumour samples. The vast majority of these samples with decreased DDX3 mRNA levels (77 %) also showed simultaneous p21/waf mRNA downregulation. The authors also demonstrated that overexpression of DDX3 in various different tumour cells inhibited their colony formation ability via upregulation of p21/waf. DDX3 was found to exert this transactivation function on the p21/waf promoter through an ATPase-dependent but helicase-independent mechanism by binding to the transcription factor Sp1 (Chao *et al*., 2006). A recent paper by Cruciat *et al*. (2013) implicated DDX3 as a novel regulator of the Wnt/β-catenin signalling network, which plays essential roles in embryonic development as well as tissue homoeostasis in adults and which leads to cancer if abnormally regulated. The authors found that DDX3 acts as a regulatory subunit of CK1ε (Casein kinase 1 subunit ε). DDX3 binds CK1ε in a Wnt-dependent manner and directly stimulates its kinase activity, as well as promoting phosphorylation of the scaffold protein Dishevelled. DDX3 is required for Wnt/β-catenin signalling in mammalian cells, and during *Xenopus* and *C. elegans* development (Cruciat *et al*., 2013)

While results by Chang *et al*. (2006), Chao *et al*. (2006) and Cruciat *et al*. (2013) suggest an important role for DDX3 in tumour suppression, numerous articles have been published implicating DDX3 in tumour promotion. Huang *et al*. (2004) found that DDX3 was overexpressed in ten different liver cancer cell lines showing anchorage independent growth (AIG), including Huh-7 cells. The activation of DDX3 by benzo(a)pyrene diol epoxide (BPDE), the active metabolite of benzo(a)pyrene present in tobacco smoke, promoted growth, proliferation and neoplastic transformation of breast epithelial cells (Botlagunta *et al*., 2008). A follow-up paper, published in 2011, found DDX3 was directly modulated by hypoxia inducible factor-1 (HIF-1) in these cells, suggesting hypoxia is an inducer of DDX3 mRNA and protein expression during breast tumourigenesis (Botlagunta *et al*., 2011). Sun *et al*. (2011) noted that DDX3 knockdown lead to synchronous reduction of protein and mRNA levels in the transcription factor Snail, a cellular element known to repress the expression of cellular adhesion proteins resulting in increased cell migration and metastasis. Treatment of cells with camptothecin, which inhibits the DNA enzyme topoisomerase I, increased Snail protein levels. This increase was significantly diminished in DDX3 knockdown cells, suggesting that DDX3 contributes to supporting the levels of Snail, which may have a regulatory role during cancer progression (Sun *et al*., 2011). DDX3 has also been

identified as a biomarker identifying gallbladder cancer after a study of the clinicopathological characteristics of adenocarcinoma (AC) and squamous cell/adenosquamous carcinoma (SC/ASC) specimens taken from patients suffering from this disease (Miao *et al*., 2013). Reasons for the contradictory results obtained regarding the role of DDX3 in tumourigenesis are as yet unforthcoming, although it may be the result of the different cell lines and cancer specimens analysed in each study.

1.12.2.7. Transcriptional Regulation

As alluded to in sections 1.12.2.4 and 1.12.2.6, there is increasing evidence that DDX3 can also function in transcriptional regulation of gene promoters. Promoter activation was upregulated by DDX3 in the case of the IFN-β promoter (Soulat *et al*., 2008) but downregulated in the case of the E-cadherin promoter (Botlagunta *et al*., 2008). In addition to supporting cellular levels of the transcription factor Snail (Sun *et al*., 2011), DDX3 can also bind to the transcription factor Sp1 and enhance the p21/waf promoter in a Sp1-dependent manner (Chao *et al*., 2006). As stated earlier, the effect of DDX3 on the p21/waf promoter appeared to require ATPase but not unwinding activity (Chao *et al*., 2006). In contrast, K230E, a variant of DDX3 without functional helicase or ATPase activity, was found to behave like wild-type DDX3 on the IFN-β promoter (Soulat *et al*., 2008). Thus, DDX3 may regulate different promoters in different ways. Although DDX3 was initially suggested to contain a leucine-zipper (Kim *et al*., 2001), there is little evidence for the existence of this motif in DDX3 or indeed, any ability to bind specific DNA sequences. It is more likely that DDX3 gets recruited to specific promoters by interacting with promoter-specific transcription factors or other co-activators, as seems to be the case for the p21/waf promoter.

1.12.2.8. Mitosis

Cyclin B/cdc2 kinases are key regulators in cell cycle progression in and out of mitosis. Sekiguchi *et al*. (2007) reported that DDX3 might be a novel cyclin B/cdc2 kinase substrate protein. Hamster DDX3 was found to be phosphorylated by cyclin B/cdc2 at residues T204 and T323 *in vitro*. These residues lie within conserved helicase motifs and are therefore likely to disrupt substrate binding and helicase activity. Indeed, the T204G DDX3 mutant protein causes a loss of DDX3 function. T204 could be

phosphorylated by cyclin B/cdc2 but not by cyclin A/cdk2, leading the authors to postulate that phosphorylation of DDX3 at T204 by cyclin B/cdc2 might have a role in repressing cyclin A expression and to decrease ribosome biogenesis and translation during mitosis (Sekiguchi *et al*., 2007). Ded1p has been implicated in similar processes in yeast, where a mutation to the helicase has been shown to inhibit translation and cell cycle progression of B-type cyclins Cdc13 and Cig2 (Grallert *et al*., 2000). Furthermore, the DDX3 *Drosophilia* homologue Belle has been found to promote mitotic chromosome segregation in *Drosophilia* somatic cells via the RNA interference pathway (Pek & Kai, 2011). During mitosis, *belle* promotes robust chromosomal localisation of Barr, a condensin I component, and chromosomal segregation. The localisation of Barr to condensing chromosomes was found to depend on *dicer-2* and *argonaute2*, while coimmunoprecipitation experiments determined that Belle interacted directly with Barr and Argonaute2 and is enriched at endogenous siRNA-generating loci. Work undertaken by the authors in HeLa cells found that *DDX3* and *DICER* are also required in promoting segregation and chromosomal localisation of hCAP-H, the human homologue of Barr, suggesting that Belle/DDX3 and the RNAi pathway exhibit a conserved function in regulating chromosome segregation in *Drosophilia* and human cells (Pek & Kai, 2011).

1.12.2.9. Translation

Data obtained with one of several yeast homologues, Ded1p, revealed its requirement for translation initiation (Chuang *et al*., 1997). It was also shown that human DDX3 can substitute for Ded1p in genetic complementation studies (Mamiya & Worman, 1999), suggesting a role for DDX3 in protein translation. Furthermore, it has been demonstrated that DDX3 interacts with several translation initiation factors such as eIF4E, eIF4A, eIF2α, eIF3, and PABP1 (Lai *et al*., 2008; Lee *et al*., 2008; Shih *et al*., 2008). However, initial studies by Shih *et al*. (2008) discovered that overexpression of DDX3 acted as a repressor rather than a facilitator of cap-dependent protein translation, despite enhancing IRES-dependent viral protein translation. In addition, the authors reported how knocking down DDX3 in HeLa cells increased cap-dependent translation but had no effect on cap-independent translation. In mammalian cells, cap-dependent translation initiation is the standard mode of translation for most cellular mRNAs and is facilitated by a cap-binding complex known as eIF4F. eIF4F is a complex whose

functions include the recognition of the mRNA 5' cap structure (mediated by subunit eIF4E), delivery of an RNA helicase to the 5' region (eIF4A), bridging of the mRNA and the ribosome (eIF4G), and circularization of the mRNA via interaction between eIF4G and the poly(A) binding protein (PABP) (Jackson *et al*., 2010) (for overview of cap-dependent vs cap-independent translation, see Fig 1. 6). Analysis of point mutations within the consensus eIF4E-binding motif in DDX3 that disrupted this interaction uncovered how eIF4E/DDX3 binding inhibited cap-dependent translation by blocking eIF4E/eIF4G complex formation in HEK-293T cells (Shih *et al*., 2008).

Subsequent publications proposed that DDX3 was not involved in general translation, but was required for translation driven by mRNA transcripts that contained secondary structures within their 5'UTRs, most likely by performing local destabilization of RNA structures allowing attachment of the 43S PIC to the 5' free extremity of the mRNA (Lee *et al*., 2008; Lai *et al*., 2008; Lai *et al*., 2010; Soto-Rifo *et al*., 2012). While Lee *et al*. (2008) uncovered the importance of eIF3 in regulating the translation of a β-globin mRNA, Soto-Rifo *et al*. (2012) indicated that DDX3 can be delivered to a target mRNA by direct binding or via the eIF4F complex through an eIF4G/PABP1 double interaction. In contrast to these studies, a 2012 report highlighted the involvement of DDX3 in promoting ribosomal subunit joining in an ATP-independent manner (Geissler *et al*., 2012).

Contradicting numerous other DDX3 translation studies, Geissler *et al*. (2012) published results commenting on the essential nature of DDX3 in general translation. DDX3 knockdown was found to deplete protein synthesis, irrespective of whether you introduced cap- or IRES- containing RNAs into cells, without consideration towards the length of these RNAs, regardless of whether the 5'UTRs of these RNAs were structured or not. A general role for DDX3 in protein translation was further supported by experiments where wild-type DDX3 and a variant with disrupted ATPase and helicase functions were transiently overexpressed in HEK-293T cells. Subsequent transfection of these cells with capped- or IRES- reporter RNAs revealed a positive stimulation of translation by the wild-type protein. Indeed, comparative stimulation was observed in the mutant protein also, indicating that the known enzymatic functions of DDX3 were not required for adequate translation (Geissler *et al*., 2012). This is in contrast to results

published by Shih *et al*. (2008), who observed that overexpression repressed cap-dependent translation, although a different cell-line was employed in that instance.

While previous studies, including that of Soto-Rifo *et al*. (2012), suggested DDX3 acted as a supportive translation factor that gave preference to mRNAs with structured 5'-UTRs, Geissler *et al*. (2012) highlighted no such role, finding similar reductions in protein expression between structured and non-structured mRNAs when DDX3 was depleted. Instead, the authors felt their results supported the notion that DDX3 functions in the second step of translation initiation, the formation of the 80S translation initiation complex. Initial indications for this hypothesis came from the observation that DDX3 is not part of "free" ribosomes and that a fraction of DDX3 specifically joins newly assembled (ie mRNA containing) 80S ribosomes. Analysis of translation-competent cytoplasmic extracts of Huh7 cells found disabled assembly of functional 80S ribosomes in DDX3-depleted cells. Further supporting evidence included the observation that purified DDX3 enhanced 80S assembly from individual translation initiation compounds (Geissler *et al*., 2012). This study also reported that DDX3 specifically bound to eIF3, in line with work by Lee *et al*. (2008), and the 40S ribosomal subunit, fuelling speculation that DDX3 is a component of the 43S PIC and, as such, also becomes part of 48S translation initiation complexes. This led to a potential model of DDX3 translation function being postulated by Geissler *et al*. (2012). DDX3, by interacting with eIF3 and the 40S subunit as part of the 43S PIC, enters the 48S complex on translatable mRNA. In conjunction with eIF3, DDX3 may then function as a conformational modulator of the 48S complex, supporting 80S assembly by protein–protein interactions. While eIF3 leaves the 48S complex during assembly of the 80S translation initiation complex, DDX3 remains bound to this complex but disassembles prior to the elongation process. It must be borne in mind, however, that differential experimental setups undertaken by the authors in the same report found that formation of 48S translation initiation complexes were unaffected by DDX3, so one can only speculate about the molecular activity of DDX3 in both cap-dependent and cap-independent translation.

DDX3 was found to associate with cytoplasmic stress granules, which are formed after exposure to environmental stress and contain stalled translation pre-initiation complexes (Lai *et al*., 2008). A recent study by Shih *et al*. (2012) suggested DDX3 should be

referred to as a core component of stress granules due to the fact that DDX3 interacts with translation initiation factors eIF4E and PABP1, coupled with the observation that DDX3 overexpression induced the formation of stress granules in a concentration-dependent manner. DDX3 depletion interfered with stress granule assembly, led to nuclear accumulation of PABP1 and reduced cell viability following stress. Interestingly, supplementation of a shRNA-resistant DDX3 into DDX3-deficient cells restored stress granule formation, allowed PABP1 translocation into these structures and increased cell survival (Shih *et al*., 2012). Thus, DDX3 may play a key role in co-ordinating translational regulation, stress granule dynamics and the cellular stress response.

1.12.3. DDX3 Interactions with Viral Proteins

Given the apparent multifunctional nature of DDX3 in the cell, it is thus no surprise to learn that DDX3 appears to be a prime target of viral manipulation, with numerous different viruses known to encode proteins that interact with the helicase and modulate its function (Schröder, 2011) (Fig 1.9).

1.12.3.1. VACV

While Schröder *et al*. (2008) found DDX3 expression enhanced Sendai virus-stimulated IFN-β promoter induction, they also reported that the vaccinia virus protein K7 interacted with DDX3 and inhibited its function in the IFN induction pathway. Interestingly, they found K7 bound to the N-terminal region of DDX3 (aa 1-139) required for the effect on the IFN-β promoter (Schröder *et al*., 2008). Follow-up studies narrowed down the binding site between aa's 61 and 90 of DDX3 and unearthed two phenylalanine residues in this region that are essential towards its effect on IFN activation (Kalverda *et al*., 2009; Oda *et al*., 2009). Taken together, these studies suggest that K7, through its interaction with DDX3, circumvents the IFN response by blocking downstream signaling events.

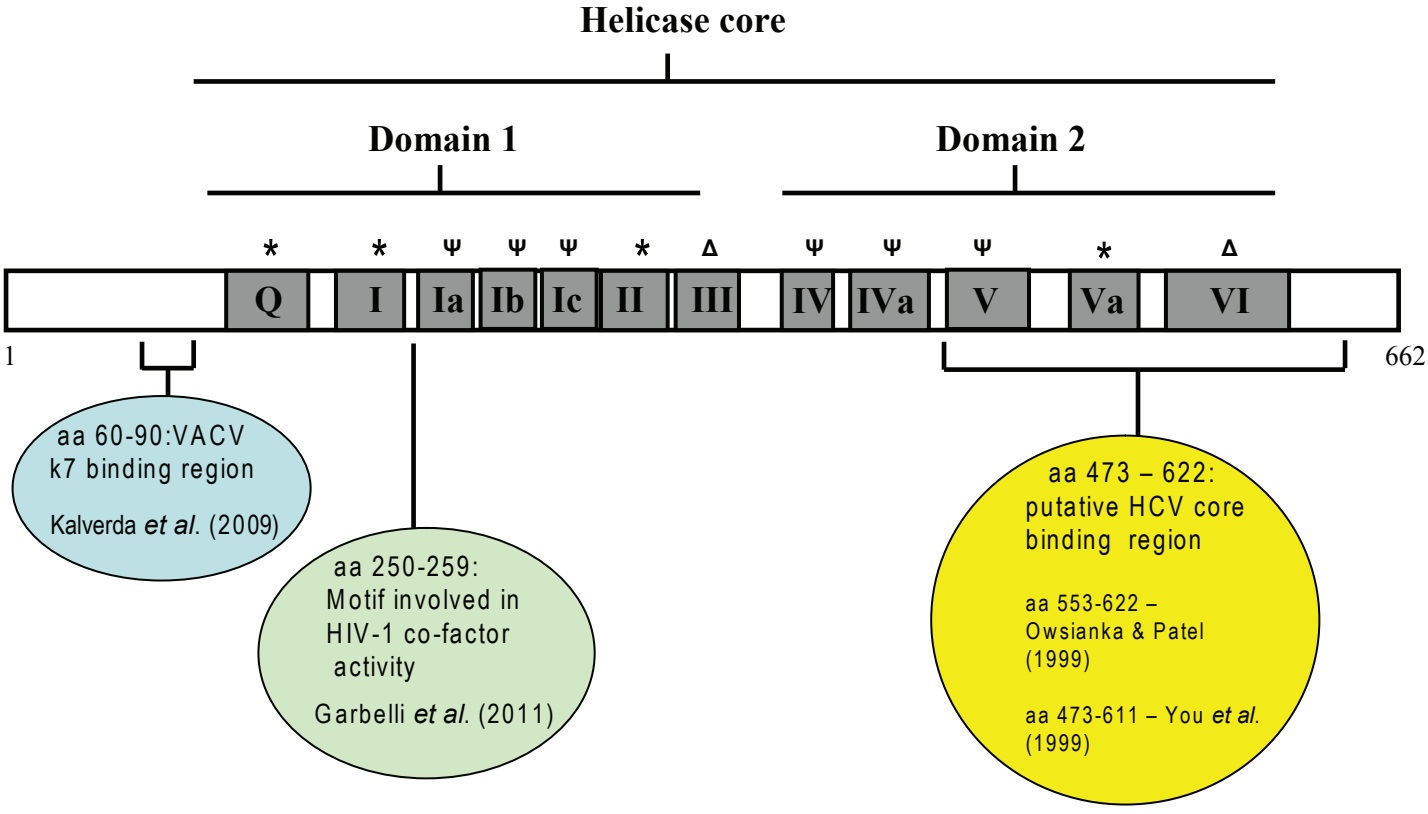

Figure 1.9. Conserved motifs and regions of interest of DDX3.

The helicase core region of DDX3 consists of two RecA-like helicase domains, domains 1 and 2. The conserved sequence motifs within these domains are shown, with highlighted symbols corresponding to the primary function of the domain (* corresponds to domains involved in ATP binding and ATP hydrolysis, Ψ signifies RNA binding domains and Δ symbolises domains involved in communication between ATP-binding and RNA-binding sites). Regions of the protein known to be involved in direct interactions with viral proteins are also highlighted. The distance between the conserved domains and regions of viral interaction is not drawn to scale. Adapted from Linder & Jankowsky (2011).

1.12.3.2. HIV-1

DDX3 has been found to be an essential host factor for HIV replication. HIV-1 gene expression is substantially governed post-transcriptionally by Rev-regulated export of unspliced and partially spliced RNAs from the nucleus into the cytoplasm. The Rev protein binds a highly structured RNA element called the Rev responsive element (RRE) that is present in all unspliced and partially spliced HIV transcripts. This binding specifically distinguishes, for purposes of nuclear export, viral transcripts from cellular RNAs. While performing this RNA transportation role, Rev interacts with the nuclear export receptor CRM1 (chromosome maintenance region 1). It has been shown that DDX3 functions specifically in Rev/RRE-dependent export of RNAs through its interaction with CRM1 (Yedavalli *et al*., 2004). Knockdown of DDX3 inhibited the export of these unspliced and partially spliced HIV RNAs from the nucleus, resulting in impaired HIV replication. It was also found that the function of DDX3 in this process was dependent on its helicase activity and that DDX3 interacted with nucleoporins and localised with the cytoplasmic side of nuclear pores. From their findings, the authors speculated that, following the initial delivery of the HIV RNAs by Rev/CRM1 into the nuclear pore, the enzymatic unwinding action of DDX3 facilitates the final release of the HIV-1 RNAs from the cytoplasmic side of the pore (Yedavalli *et al*., 2004). Follow up studies have confirmed that knockdown of DDX3 in cells inhibits HIV replication without affecting cell viability (Ishaq *et al*., 2008).

DDX3 contains a unique region between motifs I and Ia which has been proposed to bind the 3' end of an RNA substrate (Högbom *et al*., 2007). DDX3 mutants lacking this section bind HIV-1 RNA with lower affinity, and a specific peptide ligand to this region reduced the ability of DDX3 to support HIV-1 replication in infected HeLa cells (Garbelli *et al*., 2011). It is possible that, by binding the insertion between motifs I and Ia, the peptide prevented the correct assembly of the DDX3/CRM1/rev/HIV-RNA complex required for nuclear export. However, a recent study published results claiming that DDX3 exhibited a positive regulatory function in Rev-independent gene expression and HIV-1 IRES-mediated translation, implying other roles for the helicase in the viral lifecycle (Liu *et al*., 2011). The importance of DDX3 in the HIV lifecycle has led numerous researchers to target the helicase with antiviral compounds. Indeed, small-molecule inhibitors directed at the ATPase activity of DDX3 which inhibit HIV

replication have been successfully developed (Maga *et al*., 2008; Yedavalli *et al*., 2008), while a recent paper detailed the identification of the first small-molecules specifically designed to inhibit HIV-1 replication by targeting the RNA binding site of DDX3 (Radi *et al*., 2012).

1.12.3.3. HBV

Another viral protein that interacts with DDX3 is the hepatitis B virus (HBV) polymerase (pol). HBV is a hepadnavirus and replication of its genome occurs by reverse transcription of a pregenomic RNA template. This occurs entirely within nucleocapsids and is mediated by HBV pol (Beck & Nassal, 2007). DDX3 was found to bind HBV pol in an interaction that did not appear to be mediated by RNA (Wang *et al*., 2009a). The authors then demonstrated that overexpression of DDX3 in HBV replicating HepG2 cells decreased HBV DNA synthesis in a dose-dependent manner. Furthermore, knockdown of DDX3 from these cells resulted in a dose-dependent increase in HBV DNA synthesis. Mutational analysis revealed that mutant DDX3 with an inactive ATPase motif failed to inhibit viral DNA synthesis, in contrast to those mutants with inactive RNA helicase motifs. The impact of DDX3 overexpression or knockdown on HBV genome replication in HEK-293T cells was essentially identical to the results obtained with HepG2 cells, indicating that DDX3 inhibits HBV DNA synthesis in both hepatoma cells and non-hepatoma cells (Wang *et al*., 2009a). Although these results suggest DDX3 is a cellular host factor restricting HBV genome replication, the exact mechanism and physiological relevance behind these findings remain undetermined. The authors speculate their findings may be connected to results published by Chang *et al*. (2006), who report a decrease in DDX3 expression levels in HBV-induced HCC tissue samples (see section 1.12.2.6). In these instances, HBV might downregulate DDX3 expression during infection to relieve the inhibitory effect of DDX3 on its replication and thereby contribute to the development of HBV-induced HCC.

Interestingly, two independent studies published in 2010 highlighted how HBV pol acts in a similar manner to the VACV K7 protein, inhibiting IRF3 activation and IFN-β promoter induction by targeting DDX3 (Wang & Ryu, 2010; Yu *et al*., 2010). Both of these studies demonstrate that HBV achieves this by disrupting the interaction between

IKKε and DDX3. It is currently unclear whether this finding is linked with the effect of DDX3 on HBV genome replication. Indeed, it is now uncertain whether disrupting the HBV pol/DDX3 interaction would benefit the host (by restoring DDX3 function in the IFN induction pathway) or the virus (by relieving the inhibitory effect of DDX3 on genome replication).

1.12.3.4. HCV

HCV core protein was the first viral protein to be determined as a DDX3-interacting protein, with three independent publications describing the interaction (Owsianka & Patel, 1999; Mamiya & Worman, 1999; You *et al*., 1999). Owsianka & Patel (1999) reported that the regions of the proteins implicated in binding encompassed the N-terminal 59 aa's of core and a C-terminal RS-like domain of DDX3 comprising aa's 553-622, while You *et al*. (1999) stated that the interacting domains consisted of the first 40 residues of the viral capsid and aa's 473-611 of the cellular helicase. Colocalisation between core and DDX3 was observed following the expression of core in HeLa or COS-7 cells expressing c-myc-tagged DDX3 (Mamiya & Worman, 1999), in Huh-7 cells expressing FLAG-tagged DDX3 (You *et al*., 1999) and in HeLa cells expressing endogenous DDX3 (Owsianka & Patel, 1999).

It has been demonstrated that DDX3 is required for HCV RNA replication. In a study where a siRNA screen was designed targeting 62 host genes known to physically interact with HCV RNA or HCV-encoded proteins, knockdown of endogenous DDX3 resulted in significant reductions in RNA replication (1800-fold) and infectious virus release (42-fold) without affecting cell viability (Randall *et al*., 2007). A slightly later study confirmed that shRNA-mediated knockdown of cellular DDX3 led to severe impairments in intracellular RNA replication, core protein expression and colony formation in cells harbouring a replicative full-length genotype 1b HCV replicon (HCV-O) (Ariumi *et al*., 2007). This study also found that infection of DDX3-depleted cells with JFH1 virus resulted in significant reductions in both intracellular HCV RNA levels and core protein release into the culture supernatant compared to those obtained in wild-type cells. Despite observing more significant reductions to RNA replication levels in full-length genomes compared to SGRs that did not express core after DDX3 depletion,

Ariumi *et al*. (2007) were unable to find a link between DDX3's role in virus replication and the core-DDX3 interaction.

Investigating the core-DDX3 interaction in a JFH1 background, Angus *et al*., (2010) used alanine scanning mutagenesis to identify six residues (F24, G27, I30, G33, V34, and Y35) within domain 1 of the core protein that determined its interaction with DDX3. These residues are located between core amino acids 24 and 35, an area highly conserved across all HCV genotypes. The core substitution Y35A was found to abrogate the DDX3-core interaction. Interestingly, this mutation caused no alteration to HCV replication in cultured cells, indicating that the core-DDX3 interaction is dispensable for virus replication. Furthermore, DDX3 depletion studies revealed that the requirement of DDX3 for HCV replication is unrelated to its interaction with viral core protein (Angus *et al*., 2010). While results from Angus *et al*. (2010) suggest that HCV recruits DDX3 for its replication process in a core protein-independent manner, a subsequent study by Sun *et al*. (2010) published contradictory results, observing an inhibitory effect in a HCV replication system based on genotype 1b with peptides derived from the DDX3-binding site of HCV core protein. Furthermore, this inhibitory effect could be reversed by overexpression of DDX3 (Sun *et al*., 2010). Is it as yet unclear whether genotypic differences are responsible for these disparate findings.

Once HCV core has been introduced into cells, DDX3's cellular distribution has been shown to change from a diffuse cytoplasmic localisation into distinct cytoplasmic spots colocalised with core protein (Owsianka & Patel, 1999). This result suggests that core sequesters DDX3 from some of its cellular functions. In line with this, Oshiumi *et al*. (2010a) published results indicating that core protein participates in suppression of DDX3-augmented IPS-1-mediated IFN-β induction through its association with DDX3. Kang *et al*. (2012) discovered that core mutants generated during serial passage of JFH1 virus in cell culture could attenuate the type-I IFN pathway. In contrast to the findings published by Oshiumi *et al*. (2010a), however, Kang *et al*. (2012) observed that the activity of these mutants correlated with their differential interaction with DDX3, with reduced binding of core to the helicase corresponding to enhanced viral RNA replication and protein expression (Kang *et al*., 2012).

An RNA–protein interaction study confirmed that DDX3 interacts in an as yet unknown manner with the 3'UTR of the HCV RNA genome (Harris *et al*., 2006). During this study, Harris *et al*. (2006) discovered that several other DEAD-box family members, including DDX5 and DDX17, also interacted with the 3'UTR. The authors suggested that, although HCV encodes its own RNA helicase, cellular helicases such as DDX3 may greatly enhance plus-strand viral RNA synthesis by facilitating the unwinding of the negative strand RNA template. This hypothesis would help explain the decrease seen in HCV replication upon silencing of DDX3.

Another explanation is postulated by Geissler *et al*. (2012), who state that DDX3 is a functional determinant of HCV IRES-mediated translation. After comparing transiently and persistently transfected HCV RNAs, Geissler *et al*. (2012) observed significant reductions in viral protein expression levels in both cases. The fact that a reduction of cytoplasmic DDX3 inhibited the replication of transiently transfected HCV RNAs but not of persistently transfected replicons was attributed by the authors to different concentrations of viral replicase in the cells. This study also generated different types of luciferase-encoding reporter RNAs, including RNAs that contained the 5'UTR of HCV (+/- HCV 3'UTR). These HCV 5'UTR RNAs were transfected into naïve and DDX3-depleted Huh-7 cells and luciferase activity was measured in the cell lysates 1 h later. Luciferase readings were found to be reduced by between ~ 40-70 % in DDX3-null cells compared to control cells, further implying a role for DDX3 in HCV IRES-mediated translation. The results obtained in this publication also allowed the authors to state that DDX3 can regulate HCV translation efficiently in the absence of an authentic viral 3'UTR (Geissler *et al*., 2012).

1.12.3.5. Other Viruses

In addition to the viruses previously discussed, DDX3 has been shown to play important roles in many different viral lifecycles. Vashist *et al*. (2012) used riboproteomics to identify DDX3 as one of several host factors that interact with the extremeties of the Murine norovirus (MNV) genome, the only cultivatable norovirus identified to date. Indeed, siRNA targeting of DDX3, which interacts with the 3' extremity, was particularly effective at reducing MNV protein levels, viral titre, and viral RNA, with ~ 10-fold reductions observed in all cases (Vashist *et al*., 2012).

DDX3 has also been revealed to be an important host factor in *Herpesviridae* biology. From analysis of a siRNA functional screen, DDX3 was shown to be incorporated into Herpes simplex virus type 1 (HSV-1) virions (Stegen *et al*., 2013). Results published in this study suggest that both cellular and virion-incorporated pools of DDX3, in partnership with a large variety of host and viral proteins, participate in the HSV-1 replication cycle. Reinforcing this hypothesis is the fact that DDX3 has also been found in the viral particles of herpes family members human cytomegalovirus (HCMV) and Kaposi's sarcoma-associated herpesvirus (KSHV) (Varnum *et al*., 2004; Zhu *et al*., 2005).

Furthermore, the yeast homologue of DDX3, Ded1p, has been shown to be vital in the replication of the positive sense single-stranded RNA virus Tomato bushy stunt virus (TBSV), whose replication cycle mirrors that of other plus-strand RNA viruses such as HCV (Kovalev *et al*., 2012). Ded1p is shown to be recruited by TSBV, which does not encode its own helicase, into its replicase complex, with purified recombinant Ded1p seen to bind the 3' end of the complementary minus-strand RNA generated from the viral RNA. Kovalev *et al*. (2012) propose a model where Ded1p unwinds the 3' end of the TBSV minus-strand RNA, rendering the RNA compatible for initiation of plus-strand RNA synthesis.

1.13. Aims

The major aim of this project was to determine the exact stage of the HCV lifecycle at which DDX3 functions. To ascertain this, I investigated the effects of DDX3 depletion on a number of *in vitro* model systems, including HCV pseudoparticles (HCVpp), subgenomic replicons (SGR) and the HCV cell culture system (HCVcc). Furthermore, using a core mutant with abrogated DDX3 binding potential, I also investigated the importance of the core-DDX3 interaction at each stage of the viral lifecycle using the available lentiviral shRNA and model systems.

2. Materials and Methods

2.1. Materials

2.1.1. Chemicals

Chemical / Reagent	**Supplier**
Absolute ethanol	Bamford Laboratories, UK
30 % Acrylamide/bis solution 37.5:1	Bio-Rad laboratories
Agarose	Melford
2-Amino-2-(hydroxymethyl)-1,3-propanediol (TRIS)	BDH
Ammonium persulphate (APS)	Bio-Rad Laboratories
Ampicillin (Amp)	Melford
Bromophenol blue (BPB)	BDH
Calf intestinal phosphatase	NEB
Chloroform	Sigma-Aldrich
4',6-diamidino-2-phenylindole (DAPI)	Promega
Electroporation cuvettes (1 and 4 mm)	Apollo
Ethanol	Fisher Scientific
GelRed DNA stain	Biotium
Isopropanol	Fisher Scientific
β-Mercaptoethanol	Sigma-Aldrich
Methanol	Fisher Scientific
Mung Bean nuclease	NEB
Neomycin phosphotransferase	Melford
Phenol	Sigma-Aldrich
Phosphate-buffered saline (PBS)	Sigma-Aldrich
Pipette tips (RNase free)	Starlabs
Proteinase K	Invitrogen

Puromycin	Melford
Restriction enzymes	NEB
Sodium chloride (NaCl)	BDH
Sodium dodecyl sulphate (SDS)	BDH
Sucrose	BDH
T4 DNA ligase	NEB
N,N,N',N'-Tetramethylethylene-diamine (TEMED)	Sigma-Aldrich
Tween 20	Sigma-Aldrich

2.1.2. Kits

Kit	**Source**
Advantage® cDNA polymerase Kit	Clonetech
Calcium Phosphate Transfection Kit	Sigma-Aldrich
Bright-Glo™ Luciferase Assay System	Promega
MEGAscript High Yield Transcription Kit	Ambion
MEGAclear Purification Kit	Ambion
QIAprep Spin Miniprep Kit	Qiagen
QIAquick Gel Extraction Kit	Qiagen
Qiagen Plasmid Maxi Kit	Qiagen
QuikChange Site-Directed Mutagenesis Kit	Stratagene
SEAP Chemiluminescence Assay Kit	Applied Biosystems

2.1.3. Cells

Cells	Description	Source
Huh-7	Human Hepatoma cell line	Jean Dubuisson (CNRS, Institut de Biologie de Lille, Lille, France)
Huh7-J20	Human Hepatoma reporter cell line	Iro *et al*. (2009)
HEK-293T	Human Embryonic Kidney cell line	American Type Culture Collection
Huh-7 Lunet/CD81N#4 (Huh7L-#4)	Subclone of Huh-7 cells lacking cellular receptor CD81	Witteveldt *et al*. (2009); a kind gift from Thomas Pietschmann

2.1.4. Transfection Reagents

Reagent	Source
Calcium Phosphate Transfection Kit	Sigma-Aldrich
Lipofectamine 2000	Invitrogen
Opti-mem 1	Gibco

2.1.5. Cell Culture Growth Medium

All cell culture media components were supplied by Invitrogen. All cell lines used in this study were propagated in complete Dulbecco's modified Eagle's medium (DMEM) supplemented with 10 % fetal calf serum (FCS), 100 U/ml penicillin, 100 µg/ml streptomycin, 0.1 mM non-essential aas and 2 mM glutamine.

2.1.6. Primary Antibodies

Antibody	Name	Type	Raised in	Source
Anti-core	C7-50	mAb	Mouse	Bioreagents
Anti-NS5A	9E10	mAb	Mouse	Lindenbach *et al*. (2005); a kind gift from Charles M. Rice
Anti-DDX3	AO196	mAb	Mouse	Angus *et al*. (2010)
Anti-α-Tubulin	Anti-Tubulin	mAb	Mouse	Sigma-Aldrich
Anti-CD81	5A6	mAb	Mouse	Santa Cruz
Anti-DDX5	Clone 204	mAb	Mouse	Millipore

2.1.7. Secondary Antibodies

Antibody	Source
FITC-conjugated donkey anti-mouse IgG	Invitrogen
FITC-conjugated goat anti-rabbit IgG	Invitrogen
TRITC-conjugated goat anti-mouse IgG	Invitrogen
Anti-mouse-HRP conjugate	Sigma-Aldrich

2.1.8. Clones

Name	Details	Source
pJFH1	Full-length JFH1 cDNA downstream of the T7 RNA polymerase promoter.	Wakita *et al*. (2005); a kind gift from Tajaki Wakita
$pJFH1_{GND}$	As pJFH1, except carries a mutation in the NS5B GDD motif, downstream of the T7 RNA polymerase promoter.	Wakita *et al*. (2005); a kind gift from Tajaki Wakita
$pJFH1_{Y35A}$	As pJFH1, except carries a mutation in core (Y35A), downstream of the T7 RNA polymerase promoter.	Angus *et al*. (2010)
$pJFH1_{DSG}$	As pJFH1, except carries three adapted mutations (N415D, C1678S, A3222G), downstream of the T7 RNA polymerase promoter.	A. Angus, this work
pLKO.1-puro	Lentiviral vector backbone for selected shRNA sequences	Sigma-Aldrich
pCMV.DR.8.91	Lentivirus helper vector	Didier Trono
pVSV-G	For expression of VSV envelope protein for pseudotyped lentivirus production	BD biosciences
pcDNA3.1	Encoding E1E2 gps of HCV 2A genotype cloned downstream from a human CMV promoter	Lavillette *et al*. (2005)
MLV-Gag/Pol	Encoding MLV gag and pol genes cloned downstream of a human CMV promoter	Bartosch *et al*. (2003)

MLV-Luciferase	MLV based luciferase transfer construct under control of a human CMV promoter	Bartosch *et al*. (2003)
N17 SGR/JFH1$_{WT}$	Replicon construct encoding the firefly luciferase reporter and the puromycin resistance marker (separated by the foot-and-mouth-disease virus [FMDV] 2a self-cleavage site) in the JFH1 ΔE1E2 background.	Angus *et al*. (2012)
N17 SGR/JFH1$_{Y35A}$	As N17 SGR/JFH1$_{WT}$, except carries a mutation in core (Y35A), downstream of the T7 RNA polymerase promoter.	S. Stack, this work
N17 SGR/JFH1$_{GND}$	As N17 SGR/JFH1$_{WT}$, except carries a mutation in the NS5B GDD motif, downstream of the T7 RNA polymerase promoter.	Angus *et al*. (2012)
N17 SGR/JFH1$_{F130E}$	As N17 SGR/JFH1$_{WT}$, except carries a mutation in core (F130E), downstream of the T7 RNA polymerase promoter.	Angus *et al*. (2012)
NEO SGR/JFH1$_{WT}$	Bicistronic replicon containing HCV internal ribosome entry site (IRES), which directs expression of the neomycin resistance marker, and the encephalomyocarditis virus (EMCV) IRES, which directs the expression of the HCV nonstructural (NS) proteins NS3 to NS5B.	Kato *et al*. (2003); a kind gift from Tajaki Wakita

BLAST SGR/JFH1$_{WT}$	As NEO SGR/JFH1$_{WT,}$ except carries blasticidin resistance cassette instead of neomycin.	R. Adair & A. Patel, this work
pGL3-Control vector.	Plasmid containing SV40 promoter and enhancer sequences, with which you can accurately analyse cellular transcription in mammalian cells by measuring luciferase expression.	Promega
B3P7$_{WT}$	As N17 SGR/JFH1$_{WT}$, except it encodes in-frame E1E2 sequence.	A. Patel, this work
PQCXIP	Retroviral expression plasmid	Clontech
PQCXIP CE1E2$_{WT}$	PQCXIP vector expressing JFH1 structural proteins Core, E1 and E2.	A. Angus, this work
PQCXIP CE1E2$_{F24Y}$	As PQCXIP CE1E2$_{WT}$, except carries a mutation in core sequence (F24Y)	A. Angus, this work
PQCXIP CE1E2$_{Y35A}$	As PQCXIP CE1E2$_{WT}$, except carries a mutation in core sequence (Y35A)	S. Stack, this work

2.1.9. Bacterial Strains

Plasmids were manipulated and grown in the *Escherichia coli* strain JM109 (Promega) unless otherwise stated.

2.1.10. Solutions

2.1.10.1. Bacterial Expression

Solution	Components
L-Broth (LB)	170 mM NaCl, 10 g/l Bactopeptone, 5 g/l yeast extract
LB-agar	LB plus 1.5 % (w/v) agar

2.1.10.2. DNA Manipulation

Solution	Components
DNA loading dye	30 % glycerol; 0.25 % BPB, 0.25 % xylene cyanol
TBE (10x)	8.9 M Tris-borate, 8.9 M boric acid, 0.02 M EDTA (pH 8.0)

2.1.10.3. SDS-PAGE

Solution	Components
Running gel buffer	40 mM Tris, 185 mM Glycine, 0.1 % SDS
Resolving gel buffer	1.5 M Tris-HCl pH 8.9, 0.4 % SDS
Stacking gel buffer	0.5 M Tris-HCl pH 6.7, 0.4 % SDS
Sample loading buffer (reducing)	200 mM Tris-HCl, pH 6.7; 0.5 % SDS; 5 % β-mercaptoethanol; 10 % glycerol, 1 µg/ml bromophenol blue
Sample loading buffer (non-reducing)	30 mM Tris-HCl, pH 6.7; 1 % SDS; 5 % glycerol, 1 µg/ml BPB

2.1.10.4. Western Immunoblotting

Solution	Components
Towbin buffer	25 mM Tris-HCl (pH 8.0), 192 mM glycine, 20 % (v/v) methanol
PBS –Tween (PBST)	PBS, plus 0.05 % (v/v) Tween-20
Blocking buffer	PBST plus 5 % (w/v) dried milk (Marvel)

2.1.10.5. Tissue Culture

Solution	Components
Trypsin solution	0.25 % (w/v) Difco trypsin dissolved in PBS, 0.002 % (w/v) phenol red
Versene	0.6 mM EDTA in PBS, 0.002 % (w/v) phenol red

2.1.11. Oligonucleotides

Oligonucleotides used throughout the study were purchased from Sigma-Aldrich. All oligonucleotides were dissolved in deionised molecular biology grade water (dH2O) to a concentration of 100 μM by adding as the volume specified for each primer by the manufacturer.

2.2. Methods

2.2.1. Tissue Culture Maintenance

2.2.1.1. Cell Passaging

All cell lines were propagated at 37 °C in complete DMEM in an atmosphere of 5 % CO_2. Cell lines were typically grown in 80 cm^2 or 175 cm^2 tissue culture flasks (Nunc). Passage of cells was carried out when cells reached 90 % confluency by first gently washing cells in ice-cold PBS followed by their removal with trypsin (Sigma-Aldrich) diluted 1:100 in versene (E & O laboratories Ltd). Cells were then resuspended in 10 ml of complete DMEM before re-seeding or use in experiments.

2.2.1.2. Long Term Storage of Cells

Aliquoted cells were stored in DMEM containing 25 % FCS and 10 % DMSO. Aliquots were left overnight at -70 °C before being transferred to -180 °C for long-term storage.

2.2.2. DNA Manipulation

2.2.2.1. Quantitation of DNA

DNA aliquots were diluted 1:100 in dH_2O and the $OD_{260/280}$ measured using a BioPhotometer (Eppendorf).

2.2.2.2. Restriction Enzyme Digestion of DNA

All restriction enzyme digests of plasmid DNA were carried out at 37 °C for at least 1 h unless otherwise specified by the manufacturer. Typically, 10 U of each enzyme per μg DNA was used in a total volume of 50 μl. All reactions were performed using the appropriate enzyme buffers and BSA if necessary.

2.2.2.3. Ligation of DNA Fragments

Gel purified DNA fragments (Section 2.2.2.7) were ligated for 16 h at 4 °C in 15 µl reactions containing 1x ligase buffer and 2 U of T4 DNA ligase. Following ligation, 2 µl DNA was used for electroporation into competent *E. coli* bacteria (Section 2.2.2.4). Depending on the number of fragments used and the amount of DNA that could be gel purified, ligation mixes could be precipitated the day following ligation if required. This was done by adding 1/10 volume of 3M sodium acetate to the ligation before bringing the mixture up to a total volume of 400 µl with 100 % ethanol. This was then stored at -20 °C for 2 h before being centrifuged in a Sanyo MSE MicroCentaur at 13,000 r.p.m for 10 min. The resulting DNA pellet was washed with 70 % ethanol by 5 min centrifugation at 13000 r.p.m, air dried at room temperature and finally dissolved in 3-10 µl dH_2O depending on the size of the pellet. The purified DNA was used immediately for transformation of competent bacteria or stored at -20 °C.

2.2.2.4. Transformation of Chemically Competent Bacterial Cells

For transforming chemically competent JM109 cells (Promega), 50 µl aliquots were thawed on ice and mixed gently with an appropriate quantity of plasmid DNA. For re-transforming plasmid DNA, 5-10 ng of DNA mix was used. For transforming ligation mix (see Section 2.2.2.3), 2 µl DNA from a 15 µl ligation reaction was used. The mixture was incubated on ice for 30 min, transferred to a 42 °C water bath for 45 sec heat shock, placed back on ice for 2 min and mixed with 500 µl LB broth. Bacterial cells were allowed to recover at 37 °C for 1 h with horizontal shaking, with 200 µl of the mixture plated out on pre-warmed agar plates, supplied with appropriate antibiotic. Plates were incubated in a 37 °C incubator overnight and colonies were picked the following day for inoculating small scale cultures for plasmid miniprep analysis.

2.2.2.5. Small Scale Plasmid Preparation from Transformed Bacteria

A single colony from a freshly streaked selective agar plate was picked (Section 2.2.2.4) and used to inoculate a 5 ml culture of LB with ampicillin (LB-Amp). Following culture for 16 h at 37 ºC with vigorous shaking (180 r.p.m.), the bacteria were centrifuged in a

Sanyo MSE MicroCentaur at 13,000 r.p.m. and the DNA extracted from the bacterial pellet using the QIAprep miniprep kit according to the manufacturer's instructions.

2.2.2.6. Large Scale Plasmid Preparation from Transformed Bacteria

A single colony from a freshly streaked selective agar plate was picked (Section 2.2.2.4) and used to inoculate a 5 ml starter culture of LB-Amp. Following 8 h incubation, the starter culture was diluted 1:500 into 200 ml of LB-Amp and cultured for 16 h at 37 ºC with vigorous shaking (180 r.p.m.). The bacteria were then harvested by centrifugation at 3000 r.p.m. for 10 min at 4 ºC using a Sorval RC-5B Refrigerated Superspeed Centrifuge. A large scale DNA preparation was then made from the bacteria using the Qiagen HiSpeed plasmid Maxi kit according to the manufacturer's instructions.

2.2.2.7. Isolation and Purification of DNA from Agarose Gels

This method was employed to resolve DNA fragments produced by restriction enzyme digestion (Section 2.2.2.2). To separate fragments, slab gels containing 0.8 % agarose were prepared in 1 x TBE containing GelRed Nucleic acid stain (1 μg/ml). DNA fragments were run alongside TrackIt 1 Kb Plus (Invitrogen) or 100 bp (NEB) DNA ladders. DNA samples were mixed with 0.1 volumes of 10 x DNA loading dye before being loaded into the wells of the gel. Gels were typically run at 100 V in 0.5 x TBE buffer. To purify DNA, fragments were visualised with the aid of long wave UV light and then excised using a clean scalpel. Excised fragments were then purified using the QIAquick gel extraction kit (Qiagen) according to the manufacturer's instructions.

2.2.2.8. Site-Directed Mutagenesis

Mutagenesis reactions were performed using the QuikChange II XL Site-Directed Mutagenesis kit (Stratagene). Forward and reverse primers for mutagenesis (see Appendix) were designed to incorporate the desired mutation(s) in the middle of the primer sequence and were between 25 and 45 bases in length, according to the manufacturer's instructions. PCR reactions were performed in a GeneAmp PCR machine (Applied Biosystems) as follows:

Reaction components:

Component	**Amount**
DNA template	50.0 ng
Forward primer (10 Mm)	1.25 µl
Reverse primer (10 Mm)	1.25 µl
dNTP mix	1.0 µl
10x reaction buffer	5.0 µl
QuikSolution reagent	3.0 µl
dH_2O	Up to 50.0 µl

Reaction cycle:

Stage 1

- Hold at 95 °C for 30 s

Stage 2 (18 cycles)

- Hold at 95 ° C for 30 s
- Hold at 55 ° C for 1 min
- Hold at 68 ° C for 1 min/kb of plasmid length

Stage 3

- Hold at 68 °C for 7 min

Following PCR, each reaction was chilled on ice for 2 min followed by the addition of *Dpn*I (10 U) to digest the non-mutated dam-methylated parental DNA. Reactions were mixed by pipetting, then centrifuged in a Sanyo MSE MicroCentaur at 13,000 r.p.m. for 1 min, followed by incubation at 37 ºC for 1 h. *Dpn*I-treated DNA was transformed into 45 µl XL1-Blue Supercompetent bacteria (provided in SDM kit). Bacteria were thawed on ice and pre-treated with 2 µl of a β-Mercaptoethanol mix provided with the SDM kit for 10 min before 2 µl of mutant DNA was added to the competent cells, which were incubated on ice for a further 30 min. DNA-bacteria mixtures were then heat-pulsed at 42 ºC for 45 s and then incubated on ice for a further 2 min. 0.5 ml of LB broth pre-heated to 42 ºC was added to each mixture, followed by incubation at 37 ºC for 1 h with shaking at 180 r.p.m. Total cultures were pelleted at 4000 r.p.m using a Sanyo MSE MicroCentaur for 3 min, resuspended in 50 µl LB broth and plated onto LB-agar + Amp and incubated at 37 ºC overnight.

2.2.2.9. Nucleotide Sequencing

Nucleotide sequencing of plasmid and amplified cDNA was performed using specific primers by GATC biotech, Germany. A minimum of 30 µl of DNA (100 ng/µl) and primers (10 µM) were required for each reaction. Completed sequences were analyzed using NCBI alignment software.

2.2.2.10. Restriction Digestion of pJFH1 for *In Vitro* Transcription

Plasmids were linearised by *Xba*I digestion in a 100 µl reaction in an 1.5 ml RNase-free tube (Ambion) followed by treatment with Mung Bean nuclease to digest unpaired necleotides (30 °C for 30 min). To clean the template of proteins, Proteinase K (final concentration 100 µg/ml) and SDS (final concentration 0.5 %) were added and incubated at 50 °C for 30 min. The template was then treated with 100 µl of neutral phenol-chloroform (25 parts saturated neutral phenol: 24 parts chloroform: 1 part isoamylalcohol), vortexed for 1 min and centrifuged at 13,000 r.p.m. for 2 min using a Sanyo MSE MicroCentaur. The aqueous layer was placed in a fresh RNase-free centrifuge tube and 0.1 volumes 5 M NH_4OAc added along with 3 volumes 100 % ethanol. The sample was stored at -20 °C for 30 min before being centrifuged in a Sanyo MSE MicroCentaur at 13,000 r.p.m. for 15 min to pellet the precipitated DNA. The ethanol was carefully removed from the tube and the pellet dried at room temperature before being resuspended in 30 µl nuclease-free dH_2O. The concentration of linear DNA template was then determined (see Section 2.2.2.1).

2.2.2.11. Construction of Lentiviral Plasmids

The following short interfering hairpin RNA (shRNA) sequences were incorporated into lentivirus transfer plasmid pLKO.1-puro (Sigma-Aldrich)(Fig 2.1):

Name	**Sequence 5' – 3'**
shDDX3.1	GGAGGAAATTATAACTCCC
shDDX3.2	ACGAAAGCTGAGTGCATAG
shDDX3.3	GGCTGAGACTAGGGTTTTA
shDDX3.4	GGAACAAACACTCGCTTAG
shDDX3.5	CCGAGAAGCTACTAAAGGT
shDDX3.6	GGTGGAGTTCTAGCAAAGA
shControl	CCTAAGGTTAAGTCGCCCT
shHCV	CCCGGGAGGTCTCGTAGAC
shCD81	ACCTCAGTGCTCAAGAACA

These sequences were derived from siRNA (shDDX3.1 – Ariumi et al., 2007; shHCV – Jones et al., 2010) and shRNA sequences (shCD81 – Witteveldt et al., 2009) used in other publications, from plasmid websites (shControl – Addgene plasmid 1864 scramble shRNA) or were selected using the RNAi Target Sequence Selector online tool on the Clontech website (shDDX3.2 - shDDX3.6). These chosen sequences were then built into duplex oligonucleotides using the shRNA Sequence Designer tool on the Clontech website. These oligonucleotides contained the following elements: a *BamH*I cloning site at the 5′ end, the coding strand sequence of the hairpin (as in table), a loop region, the complementary noncoding strand sequence of the hairpin, an RNA polymerase III termination sequence, a marker *Mlu*I restriction site, and a 3′ *EcoR*I cloning site. Plasmid clones were identified by the presence of the *Mlu*I restriction site and then confirmed by DNA sequence analysis. The calcium phosphate transfection method was then used to introduce this plasmid DNA into HEK-293T cells (see Section 2.2.4.1).

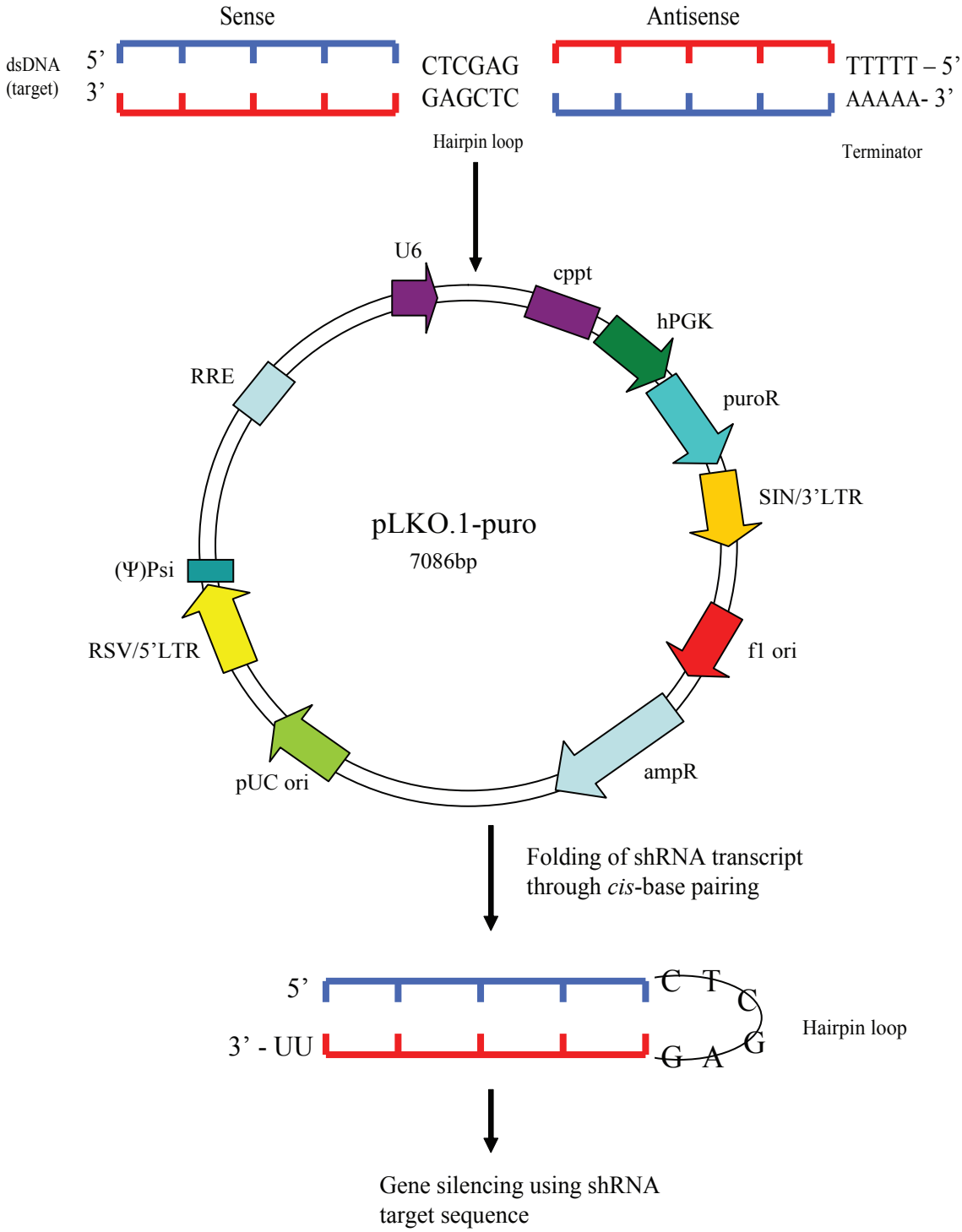

Figure 2.1. Lentiviral vector pLKO.1-puro.

DNA Map showing the features of the lentiviral vector pLKO.1-puro. Abbreviations of the features: RRE – rev response element, hPGK promoter – human phosphoglycerate kinase promoter, cPPT – polypurine tract, pUC Ori – pUC origin of replication, LTR – long terminal repeats, sin – self-inactivating, RSV – Rous sarcoma virus. The vector also bears a gene for puromycin resistance (PuroR) necessary for mammalian cell selection, a U6 promoter, an ampicillin resistance cassette (AmpR) for selective growth of transformed bacterial colonies and an RNA packaging signal (psi). With an shRNA insert (insertion site highlighted), the length of the pLKO.1-puro plasmid is 7,086 bp, as indicated. Without an shRNA insert, pLKO.1-puro vector has a length of 7,052 bp. The shRNA insert DNA sequence is transcribed to yield shRNA precursor molecules. Hairpin loop sequence allows folding through *cis*-base pairing to form an shRNA molecule that is recognized by Dicer which directs it for RISC assembly.

2.2.2.12. Transfection of DNA using Lipofectamine

Prior to DNA transfection, cells were plated at a density of 2.5 x 10^4/well on a 24-well cell culture dish and allowed to settle for 24 h at 37 ºC. The following day, 0.8 µg DNA and 2 µl Lipofectamine 2000 (Invitrogen) were diluted separately into individual 50 µl volumes of Opti-mem-I (Gibco) and incubated at room temperature for 5 min. The diluted DNA and Lipofectamine 2000 were combined and incubated at room temperature for a further 20 min. The DNA-Lipofectamine 2000 mixture was then added to the plated cells. Medium was changed after 6 h, and cells were incubated at 37 ºC for 48 h prior to testing for transgene expression.

2.2.3. RNA Manipulation

2.2.3.1. *In Vitro* Transcription

In vitro transcription was carried out using a T7 Megascript kit (Ambion) following the manufacturer's instructions using 1 µg of linear DNA template. The RNA was then purified using the MEGAclear kit to remove nucleotides, short oligonucleotides, proteins, and salts from the RNA. The amount of RNA was obtained by diluting an aliquot of the RNA 1:50 in dH_2O and reading the OD using a BioPhotometer (Eppendorf). Typically, this kit yielded RNA concentrations of 70-100 µg per reaction.

2.2.4. Introduction of DNA/RNA into Eukaryotic Cells

2.2.4.1. Generation of Lentivirus Medium Expressing shRNA (Transfection of DNA)

The calcium phosphate transfection method was used to introduce plasmid DNA into HEK-293T cells. This method is based upon the formation of a precipitate containing calcium phosphate and DNA. 1.4 million cells were seeded into 90 mm tissue culture dishes in 15 ml complete DMEM 24 h before transfection. The following day, cells were co-transfected with three different plasmids expressing (i) pLKO.1-puro lentivirus

transfer plasmid with incorporated shRNA oligonucleotides of interest (8 μg) (see Section 2.2.2.11), (ii) pVSV-G (3 μg) and (iii) packaging plasmid pCMVDR8.91 (8 μg) expressing lentivirus gag-pol using the Sigma-Aldrich Calcium Phosphate Transfection Kit. The plasmid DNA was mixed with dH_2O and 100 μl 2.5 M $CaCl_2$ in a total volume of 500 μl in a sterile 1.5 ml eppendorf. In a second sterile 1.5 ml tube, 500 μl of 2x HEPES-Buffered Saline (HeBS), pH 7.05 was added. To prepare the precipitate, the HeBS solution containing sodium phosphate was slowly mixed with the $CaCl_2$ solution containing the DNA. To do this, the HeBS was gently bubbled using an automatic pipette pump attached to a 1 ml sterile serological pipette during which time the $CaCl_2$/DNA solution was added dropwise with a sterile pipette tip. The precipitate was then incubated for 20 min at room temperature before being distributed over the cells in the culture dish in a dropwise fashion using a sterile pipette tip, followed by gentle agitation for mixing. This DNA-calcium phosphate co-precipitate adheres to the cell surface and is taken up by the cell, presumably by endocytosis. At 24 h post-transfection, medium was replaced with 8 ml fresh $DMEM_{complete}$. At 72 h post-transfection, culture media containing lentivirus particles was harvested by filtering through a 0.45 μm pore-sized membrane. This culture media could then be stored at 4 ° C or used to infect target cells. Target cells were infected with lentivirus supernatants for 48 or 72 h (as indicated in each separate experiment in results section), with silencing of target protein always monitored at transduction endpoint by SDS-PAGE and western blotting (see section 2.2.6). Depletion of endogenous protein expresssion was based on RNAi-mediated gene silencing (McManus & Sharp, 2002; Meister & Tuschl, 2004). An overview of the RNAi pathway is represented in Fig 2.2.

2.2.4.2. Generation of HCVpp (Transfection of DNA)

HCVpp were generated as described previously (Bartosch *et al*., 2003; Hsu *et al*., 2003; Owsianka *et al*., 2005). Typically, 1.4 million HEK 293-T cells were seeded into 100 mm tissue culture dishes in 15 ml complete DMEM 24 h before transfection. The following day, cells were co-transfected with three different plasmids expressing (i) replication deficient MLV gag/pol core (8 μg), (ii) HCV E1E2 glycoproteins (3 μg) and (iii) luciferase reporter gene (8 μg) using the Sigma-Aldrich Calcium Phosphate Transfection Kit as described above (Section 2.2.4.1). At 24 h post-transfection,

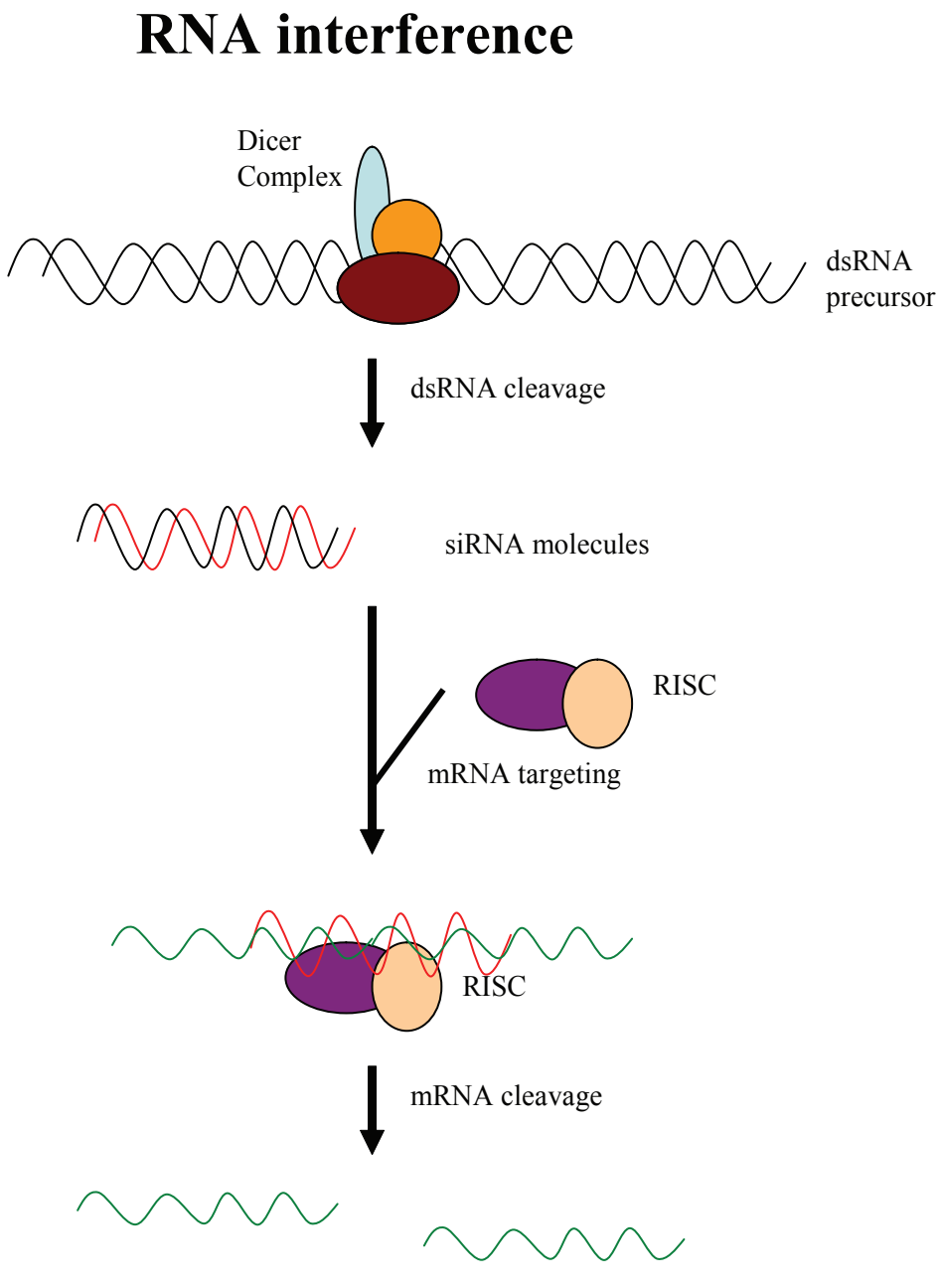

Figure 2.2. Posttranscriptional processing by RNA interference.

Double-stranded RNA (dsRNA) is recognized by the enzyme Dicer, which has a catalytic RNase III activity, and is cleaved into short double-stranded RNA molecules, called small interfering RNA (siRNA) molecules. SiRNA molecules associate with the protein complexes to form the RNA-induced silencing complex (RISC). Mature RISC contains the antisense single-stranded RNA molecules (red) that target the complementary sense sequence of the mRNA molecule (green). This results in mRNA cleavage and hence gene silencing. Adapted from McManus & Sharp, 2002.

medium was replaced with 8 ml fresh $DMEM_{complete}$. At 72 h post-transfection, culture media containing HCVpp was harvested by filtering through a 0.45 μm pore-sized membrane. Target cells could then be infected with HCVpp culture media (see Results). This culture media could then be stored at 4 ° C and used to infect target cells when appropriate. Vesicular stomatitis virus (VSV) pseudoparticles (VSVpp), which are used as control pseudoparticles, were generated in the exact same fashion as HCVpp, except that during co-transfection into HEK 293-T cells, 3 μg of plasmid encoding the VSV G protein was transfected into cells in place of HCV E1E2 glycoproteins (Bartosch *et al*., 2003).

2.2.4.3. Electroporation of RNA

Following trypsin treatment and counting, aliquots of 4 x 10^6 cells were centrifuged in 15 ml centrifuge tubes at 1000 r.p.m. for 5 min at room temperature using a Thermoscientific Heraeus Megafuge 16R. Media was decanted and pelleted cells were washed by resuspension in 10 ml PBS, and centrifuged as before. PBS was decanted and cell pellets were resuspended in a total volume of 400 μl PBS and added to a 4 mm gap cuvette along with 10 μg of *in vitro*-transcribed viral RNA. Electroporation was performed using a BioRad GenePulser Xcell (250 V, 950 μF), following the manufacturer's instructions. Cells were then diluted and resuspended in the indicated amount of complete DMEM and seeded into the appropriate tissue culture flask or plate.

2.2.5. Generation of JFH1 Virus

In vitro synthesized RNA (10 μg) was electroporated into Huh-7 cells (Section 2.2.5.2). The transfected cells were allowed to rest for 10 min before mixing with fresh medium and seeding into the indicated tissue culture dishes. Following incubation at 37 ^oC for the indicated time period, the medium containing the infectious virus progeny was filtered through a 0.45 μm pore-sized membrane before infectivity was determined (Section 2.2.5.1).

2.2.5.1 Measuring Virus Infectivity

Limiting dilution assays were used to quantify the amount of virus infectivity using the focus forming unit (FFU) assay (Zhong *et al*., 2005), which is calculated as FFU/ml by the average number of NS5A-positive foci detected at the highest dilution. To determine the virus titre by FFU assay, Huh-7 target cells were seeded at a concentration of 1000 cells per well on a 96-well plate in a total volume of 100 µl complete DMEM. At 24 h post-seeding, serial 5-fold dilutions of infectious cell medium were added, with three wells used per dilution. At 48 h post-infection, the infectious medium was removed and the cells were fixed with ice-cold methanol and incubated at -20 °C for 24 h. The cells were then washed three times with PBS and probed with anti-NS5A mAb 9E10 at a dilution of 1:10,000 in PBST for 1 h at room temperature. Cells were washed again three times with PBS and bound primary antibody was detected by incubation with the FITC-conjugated donkey anti-mouse IgG secondary antibody at a 1:500 dilution in PBST for 1 h at room temperature. After three washes in PBS, the cells were overlaid with 100 µl of dH_2O before visualization under a fluorescent microscope (Nikon Eclipse TS100). Clusters of infected cells identified by immunostaining for NS5A were considered to constitute a single infectious focus, and titres were calculated accordingly in terms of FFU/ml.

In experiments involving Huh7-J20 cells, the level of intracellular NS3/4A protease activity could also be measured by calculating the secreted alkaline phosphatase (SEAP) activity in the culture medium - as described by Iro *et al*. (2009), see also Fig 2.3 - using the SEAP Chemiluminescence Assay Kit (Applied Biosciences). To begin, 90 µl of culture medium was collected and mixed with 10 µl of 10-times concentrated lysis buffer to a final concentration of 50 mM Tris–HCl (pH 7.5), 1 mM EDTA, 10 mM NaCl and 0.5% Triton X-100 to inactivate the virus. In a 96-well plate, 30 µl of this mixture was then mixed 1:1 with 1x dilution buffer and incubated at 65 °C for 30 min. The plate was then cooled on ice to reach room temperature before 50 µl of the cooled reaction was mixed with 50 µl assay buffer in a white 96-well microplate. 50 µl of reaction buffer (prepared beforehand by diluting CSPD chemiluminescent substrate 1:20 with reaction buffer diluents) was then added to this plate before luminescence

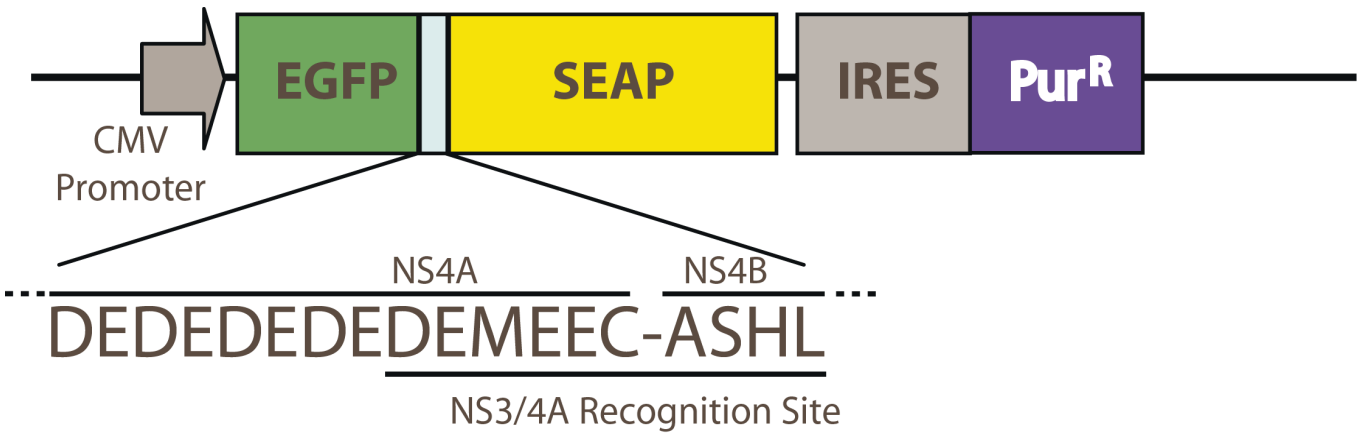

Figure 2.3. Schematic diagram of fusion protein construct stably expressed in Huh7-J20 cells.

Huh7-J20 cells stably express a fusion protein that contains the sequence encoding EGFP and SEAP linked by the octapeptide DEDEDEDE and the HCV genotype 1b NS4A/4B substrate sequence (representing the recognition site for the viral NS3/4A protease, which is underlined) cloned into a PQCXIP vector upstream of the internal ribosome entry site (IRES) and a puromycin resistance cassette. During HCV replication, the NS3/4A protease releases SEAP from the fusion protein, thus enabling its N-terminal signal peptide to direct its secretion into the extracellular culture medium. It has been observed that SEAP activity in culture medium correlates with the level of HCV RNA replication. Adapted from Iro *et al*. (2009).

could be measured. The SEAP activity was measured by using a Hidex Chameleon plate reader and expressed as relative light units (RLU).

Cell-associated virus was obtained using previously established methods (Gastaminza *et al*., 2006; Shavinskya *et al*., 2007). Cells were electroporated with viral RNA as before and reseeded into a T25 culture flask in 6 ml of complete DMEM for incubation at 37 °C. Forty-eight hours post-incubation, cells were washed once in PBS before being trypsinised, transferred to a 15 ml centrifuge tube and resuspended by rigorous pipetting in 10 ml complete DMEM. The cells were then centrifuged at 1000 r.p.m. for 5 min using a Thermoscientific Heraeus Megafuge 16R, after which the DMEM was decanted and cell pellet was resuspended in another 10 ml complete DMEM and recentrifuged under the same conditions. The cells were then resuspended in 0.8 ml complete DMEM, and freeze-thawed rapidly three times using dry ice/ethanol and a water bath set to 37 ºC. The samples were centrifuged at 4000 r.p.m. for 5 min using a Thermoscientific Heraeus Megafuge 16R to remove cell debris, and the supernatant assayed by FFU assay to determine virus infectivity.

2.2.5.2 Measuring Viral Replication by Luciferase Assay

To measure the luciferase activity of N17 SGR/JFH1$_{WT}$ (or equivalent luciferase-containing replicon), 4×10^6 Huh-7 cells or equivalent cell line were first plated onto a T80 culture flask in 15 ml of complete DMEM for incubation at 37 °C. At 24 h post-seeding, cells were transduced with lentivirus of interest. 48 h post-transduction, cells were electroporated with 10 μg of *in vitro* transcribed N17 SGR/JFH1$_{WT}$ RNA (see Section 2.2.4.3) and resuspended in 14 ml of culture medium. Aliquots of 500 μl were then seeded in triplicate over numerous 48-well cell culture dishes. Following incubation at 37 °C, cells were lysed for luciferase assay at 1, 2, 4, 8, 24 and 48 h post-electroporation. Luciferase activity was assayed with a Glomax® 20/20 Luminometer (Promega) using the Bright-Glo luciferase assay system (Promega) according to the manufacturer's instructions. Briefly, cells were washed with excess PBS and cell lysates were prepared by adding 150 μl of 1x lysis buffer to each well and the mix incubated with gentle shaking for 5 min at RT. Meanwhile, luciferase assay reagent was prepared by dissolving 17.1 mg lyophilized luciferase assay substrate into 1 ml luciferase assay

buffer. 100 µl of cell lysate was then mixed with equal volume of luciferase assay reagent in a 1.5 ml eppendorf and luminescence measured immediately.

2.2.6. Detection of Cellular and Viral Proteins

2.2.6.1. Sample Lysis for SDS-PAGE Analysis

To detect intracellular antigens, cultured cells were washed once in phosphate-buffered saline (PBS) and lysed directly in SDS-PAGE sample loading buffer (reducing). However, as CD81 protein could not be detected in cellular extracts lysed in sample loading buffer (reducing) using the available antibody, cells to be analyzed for CD81 expression were lysed in SDS-PAGE sample loading buffer (non-reducing). Extracellular antigens were detected by concentrating virus at 48 h post-JFH1 electroporation by ultracentrifugation of the culture medium for 16 h at 36,000 rpm (135,000 × *g*) in a SW60Ti rotor at 4 °C in a Beckman L8-80 M preparative ultracentrifuge. The viral pellets were lysed directly in SDS-PAGE sample loading buffer (reducing). For the remainder of this thesis, SDS-PAGE sample loading buffer (reducing) will be referred to simply as sample buffer (SB) while SDS-PAGE sample loading buffer (non-reducing) will be referred to as NR-SB.

2.2.6.2. Denaturing Polyacrylamide Gel Electrophoresis (SDS-PAGE)

Resolving gels were prepared using acrylamide solution at a final concentration of 7.5 - 10 % in 1x resolving gel buffer. Addition of APS (to 0.1 %) and TEMED (to 0.08 %) initiated polymerisation and the solution was immediately poured into the gel assembly apparatus, leaving a gap of ~ 2 cm from the top. The solution was then overlaid with 1 ml of dH_2O. When polymerisation was complete, the dH_2O was discarded. Stacking gels were prepared using acrylamide at a final concentration of 5 % in 1x stacking gel buffer. Again, polymerisation was initiated upon the addition of APS (to 0.1 %) and TEMED (to 0.08 %) before the solution was overlaid onto the resolving gel. A 10-tooth Teflon comb was typically used to form wells in the stacking gel. The gel was allowed to polymerise before removal of the comb. Gels were then loaded into a tank and submerged in running gel buffer. Denatured protein samples were then loaded into each

well. Protein markers (Amersham) were also included for protein size determination and empty wells were filled with an equal volume of SDS-PAGE sample loading buffer. Electrophoresis was performed at 100 V until the required separation of protein markers and samples was achieved. Gels were then removed from the apparatus for western immunoblotting (Section 2.2.6.3).

2.2.6.3. Western Immunoblotting

Proteins separated on polyacrylamide gels were transferred to Hybond^{TM}-ECL^{TM} nitrocellulose membranes using a BioRad transblot Semi-Dry blotting device. Transfer was carried out at 25 V for 15 min and membranes were incubated in PBST containing 5 % milk powder to block non-specific binding of antibody. Membranes were washed three times in PBST at room tempertaure and probed with the appropriate antibody (diluted in PBST) for 1 h at room temperature. The membrane was again washed three times with PBST and incubated with the appropriate secondary antibody (diluted in PBST) conjugated to HRP for 1 h at room temperature. Finally the membrane was washed three times in PBST and bound antibody was detected using enhanced chemiluminescence reagents (Millipore). Bands were visualized by autoradiography using Kodak X-OMAT film and a Konica SRX-101-A film processor.

2.2.7. Indirect Immunofluorescence (IF)

To examine the intracellular expression of HCV proteins, cells on coverslips were fixed in methanol, washed with PBS, blocked for 10 min with PBS containing 2 % FCS and incubated at room temperature for 1 h with primary antibody in the blocking buffer. Cells were washed with PBS, stained with secondary antibody conjugated with either FITC or TRITC in blocking buffer for 1 h, washed with PBS, and the coverslips mounted on a glass slide and examined with a Zeiss Laser Scanning LSM510 META inverted confocal microscope (Carl Zeiss Ltd., UK). The images were analyzed using LSM510 software.

2.2.8. Colony Forming Assay

To determine the effect of gene knockdown on viral replication during prolonged culture, 3×10^6 shRNA-transduced Huh-7 cells were electroporated with 10 μg of SGR RNA (see Section 2.2.4.3), resuspended in complete DMEM and plated onto 6-well culture dishes at specific densities in duplicate. At 24 h post-seeding, one set of cells (test cells) were treated with drug at appropriate concentrations (depending on antibiotic resistance cassette of SGR) while another set of cells (control cells) were left to grow in the absence of drug. Media was changed twice weekly for three weeks. At three weeks post-electroporation, media was removed, cells were washed twice in PBS and remaining cell colonies were fixed and stained with Giesma's stain solution (VWR).

2.2.9. Generation of Retrovirus Particles Containing HCV Structural Proteins

Typically, 2 x 10^6 HEK 293-T cells were seeded into 100 mm tissue culture dishes in 15 ml complete DMEM 24 h before transfection. The following day, cells were transfected with 30 μg of the retrovirus vector PQCXIP expressing HCV structural proteins (PQCXIP $CE1E2_{WT}$) or mutant derivative (PQCXIP $CE1E2_{Y35A}$ or PQCXIP $CE1E2_{F24Y}$) using the Sigma-Aldrich Calcium Phosphate Transfection Kit as described earlier (Section 2.2.4.1). At 24 h post-transfection, medium was removed and cells were lysed in 400 μl lysis buffer A.

2.2.10. Co-immunoprecipitation of HCV Core Protein

2 x 10^6 HEK-293T cells were seeded into 100 mm tissue culture dishes. At 24 h post-seeding, cells transduced with retrovirus virus PQCXIP $CE1E2_{WT}$ or mutant derivatives (see section 2.2) using the calcium phosphate precipitation method. At 24 h post-transfection, cells were washed once in PBS (A) and lysed in 400 μl lysis buffer A. The lysates were spun briefly to remove nuclei. After pre-clearing, the clarified lysate was immunoprecipitated overnight with 30 μl of Protein G-sepharose beads that had been

pre-incubated overnight with 6 µl of the anti-DDX3 antiserum R648. The immune complex was precipitated with the beads by centrifugation using a Sanyo MSE MicroCentaur at 2000 r.p.m. for 2 min, washed 3 times with 1 ml lysis buffer A. Beads were resuspended in 25 µl of non-reducing sample buffer, subjected to 12 % SDS-PAGE electrophoresis followed by western immunoblotting using the anti-core mAb C7-50 (1:20,000 dilution).

2.2.11. Two-Dimensional SDS-PAGE Gel Electrophoresis

JFH1 cellular extracts lysed in lysis buffer A and treated with non-reducing sample buffer. Samples were run in the first dimension in a 7.5 % SDS-PAGE gel (see section 2.2.6.2). After sufficient separation of proteins, the gel strip (lane) containing the sample of interest was excised (each sample was run between two stained protein ladders for ease of excision) and transferred to a sterile 15 ml conical tube. Here, the sample was reduced with NuPage 1 × reducing agent (Invitrogen) in NuPAGE® LDS sample buffer (Invitrogen) for 30 min before being alkylated for 15 with LDS sample buffer supplemented with 50 mM N,N-Dimethylacrylamide (DMA) (Sigma). Sample was then treated with quenching buffer composed of LDS sample buffer, 5 mM DTT and 20% ethanol. After buffer treatment, the whole gel strip was loaded onto a second dimension NuPAGE® Novex® 4-12% Bis-Tris Gel (Invitrogen) and SDS-PAGE was run according to appropriate parameters (see section 2.2.6.2). Prior to transfer of the proteins to membranes, the PVDF membrane was wetted in methanol. Proteins were transferred to PVDF membranes using a semi-dry blotting apparatus (XCell II™ Blot Module , Invitrogen) for 1 h at 25 V. After transfer, proteins were examined with antibodies of interest.

3. Results

3.1. Investigating the Role of the Cellular RNA Helicase DDX3 in the HCV Lifecycle in Huh-7 cells

3.1.1. Introduction

Two separate studies have confirmed that HCV replication is greatly decreased in DDX3-depleted cells (Ariumi *et al*., 2007; Randall *et al*., 2007), but the exact stage(s) of the HCV lifecycle at which DDX3 functions remains unclear. After I had confirmed the important role DDX3 plays in HCV replication by shRNA-directed intracellular depletion of DDX3, I used this DDX3 knockdown system on a number of *in vitro* cell systems available to me, namely the subgenomic replicon (SGR), HCV pseudoparticle (HCVpp) and HCV cell culture (HCVcc) systems, to determine what effect DDX3 depletion in Huh-7 cells had on the different stages of the viral lifecycle, in an attempt to pinpoint its exact function. Together, the data collected from these experiments indicated that DDX3 acts at an early, post-translation stage of the HCV lifecycle in Huh-7 cells, facilitating some as yet undetermined element of HCV RNA replication. Results obtained also suggested that it is possible that DDX3 influences the HCV replication complex (RCs) machinery to perform this important role, although whether DDX3 performs this task through direct incorporation into the RC or via a indirect mechanism is not yet understood. The fact that DDX3-deficient replicon cells cannot be maintained in culture was also established, indicating that construction of a stably replicating DDX3-depleted Huh-7 cell line was impossible and that studies of the HCV lifecycle must be limited to transient assays in DDX3-depleted cells.

Our lab and others have previously shown that DDX3 binds directly with domain 1 of HCV core (Mamiya & Worman, 1999; Owsianka & Patel, 1999; You *et al.*, 1999). Further investigation of this interaction was performed using alanine scanning mutagenesis, which allowed our lab to identify six residues within this region of core that determined its association with DDX3. These residues were located between core amino acids 24 and 35, an area highly conserved across all HCV genotypes. Alanine

substitution of these residues revealed that the Y35A change abrogated the DDX3-core interaction. However, this mutation caused no alteration to the replication of the HCV JFH1 cell culture infectious virus (HCVcc), indicating that the core-DDX3 interaction is dispensable for HCV replication (Angus *et al*., 2010). The study by Angus *et al*., (2010) also demonstrated that siRNA-led knockdown of DDX3 decreased virus production and RNA replication levels in a Y35A background to a similar extent as that seen in a WT background. Thus, I looked at the effects of shRNA-mediated DDX3 depletion in a Y35A setting in a number of relevant *in vitro* cell systems to establish the stage of the lifecycle at which DDX3 acted upon in this environment and determine if there were any specific effects the abrogation of the DDX3-core interaction had on the HCV lifecycle in Huh-7 cells. Data collected from this study entrenched the view that the core-DDX3 interaction is dispensable in the HCV lifecycle. This section also investigated the effect of DDX3 depletion in Huh-7.5 cells, a subclone of Huh-7 cells which have a defective RIG-I response to viral challenges. No significant differences were observed between results obtained in a Huh-7 or Huh-7.5 background.

3.1.2. Knockdown of DDX3 Expression in Huh-7 Cells

A common way to analyse the role of a specific cellular protein in the viral life cycle is to use RNAi to produce cells depleted of the protein of interest. Therefore, DDX3-depleted cells were generated where protein levels were severely suppressed by expression of shRNA molecules targeting endogenously expressed DDX3. Generation and analysis of these cells was performed as follows. First, six distinct short interfering hairpin RNA (shRNA) sequences were designed against different regions of DDX3 and incorporated into lentivirus transfer plasmid pLKO.1-puro (Fig 3.1A, see also Materials and Methods, section 2.2.2.11). In order to produce lentiviral stocks, each of these pLKO-shDDX3 plasmids (shDDX3.1 through to shDDX3.6) were transfected in parallel into HEK-293T cells, together with plasmids encoding for lentivirus components, as described in Materials and Methods, section 2.2.4.1. pLKO-shControl plasmid was also transfected in parallel together with helper plasmids. At 72 h post-transfection, the supernatants were harvested and used to transduce Huh-7 cells. In order to determine the efficiency of DDX3 protein knockdown in Huh-7 cells, 4 x 10^4 cells were seeded into a 24-well plate, transduced with lentiviral stocks of interest, then

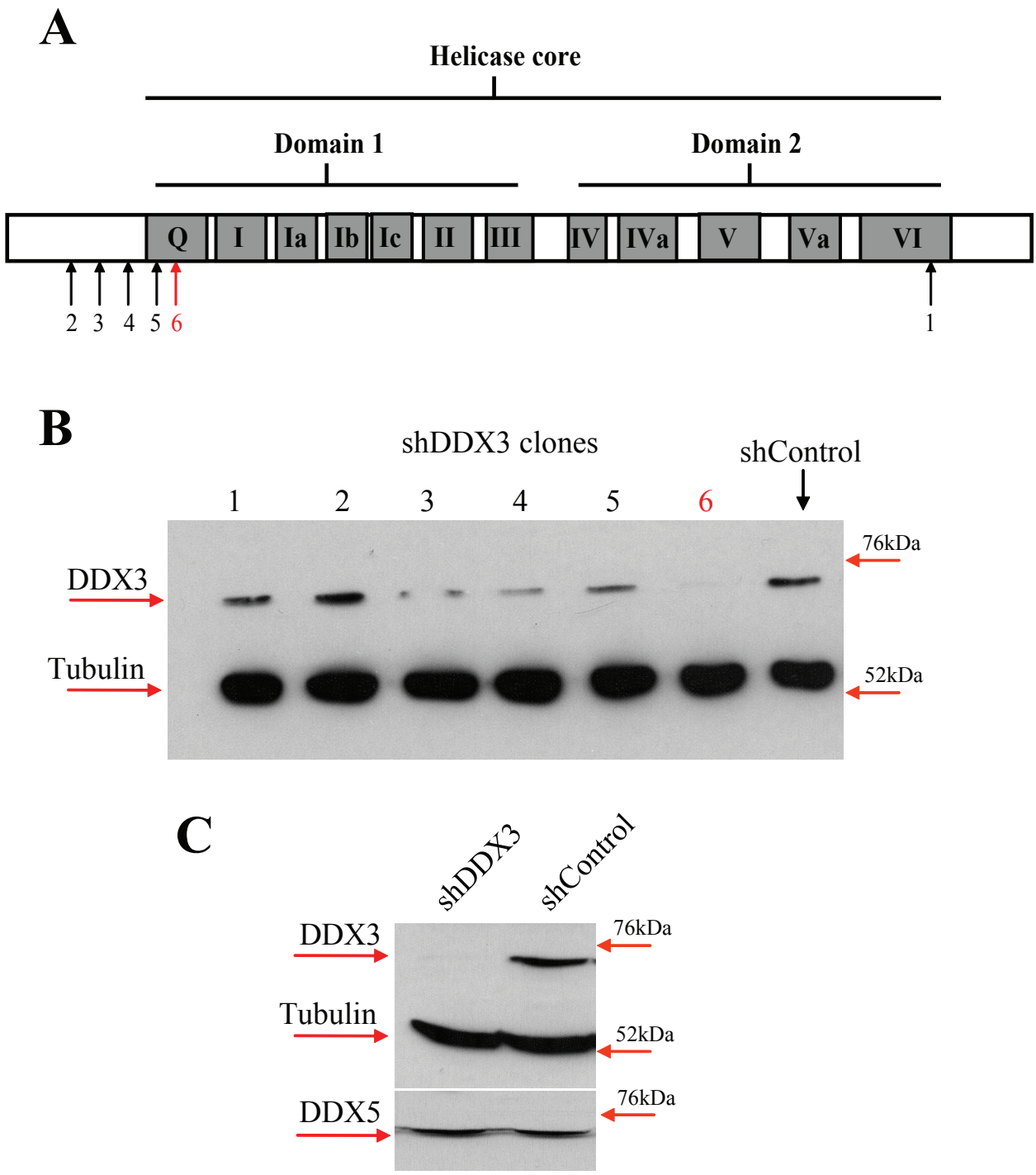

Figure 3.1. Depletion of DDX3 expression using shRNA technology.

(A) Schematic illustrating the conserved motifs of DDX3. Six shRNAs were designed against different regions of the gene. Arrows indicate target sites for each individual shRNA. **(B)** Western blot analysis of cellular lysates from Huh-7 cells expressing various shRNAs against DDX3, as well as analysis of Huh-7 cells transduced with a control lentivirus vector (shControl). Lysates were probed with anti-DDX3 mAb AO196 and an anti-α-Tubulin mAb. **(C)** Lysates from Huh-7 cells expressing shRNA against DDX3.6 (shDDX3) and Huh-7 cells expressing shControl were analysed by immunoblotting for DDX3, Tubulin and DDX5 proteins to determine specificity of DDX3 knockdown.

wells were harvested for analysis by western blotting at 48 h post-transduction. According to the data presented in Figure 3.1B, DDX3 levels in lysates from shDDX3.6 cells were undetectable by western blot analysis. Tubulin was used as a loading control, and as expected, its levels were unchanged between DDX3-depleted and control cell lines. Reduction in DDX3 expression was also prominent in shDDX3.4 cells, but not as significant as those levels seen in shDDX3.6 cells. Analysis of lysates with the monoclonal anti-DDX5 antibody Clone 204 showed no depletion to the cellular DEAD-box helicase family member DDX5, indicating that the DDX3 knockdown achieved in shDDX3.6 Huh-7 cells is highly specific (Fig 3.1C).

3.1.3. Effect of DDX3 Knockdown on HCVcc

Previous reports have shown that siRNA-mediated knockdown of DDX3 reduces HCVcc replication in infected cells (Ariumi *et al*., 2007; Randall *et al*., 2007). To assess the influence of DDX3 abundance on virus infection, I measured the replication of $JFH1_{WT}$ virus by SEAP assay (see Materials and Methods, section 2.2.5.1) following infection of Huh7-J20 cells that had previously undergone 48 h transduction with lentivirus expressing shDDX3.6 (hereafter referred to simply as shDDX3). $JFH1_{WT}$ replication levels in shControl-transduced cells and in cells expressing shRNA against the 5'UTR of HCV (shHCV) were determined in parallel, serving as negative and positive controls, respectively. Untransduced Huh7-J20 cells (mock) were also infected with $JFH1_{WT}$ virus at the same time as each set of transduced cells. In line with previous studies, virus replication levels were found to be substantially less in DDX3-depleted cells compared to shControl- and mock-transduced cells following infection with $JFH1_{WT}$ virus, with a reduction of almost 75 % observed. Infection was almost totally abrogated in the positive control shHCV-transduced cells, where a replication decrease of almost 98 % was detected in this assay (Fig 3.2). Furthermore, viral protein expression could not be observed by immunoblot analysis in lysates extracted from DDX3-depleted cells and shHCV-transduced cells at 48 hours post-infection, while lysates from shControl and mock-transduced cells extracted at the same time were found to express considerable quantities of NS5A and Core protein. Protein samples lysed just before HCVcc infection found DDX3 silencing in shDDX3 cells but undiminished DDX3 levels in the different sets of control cells, a test carried out to

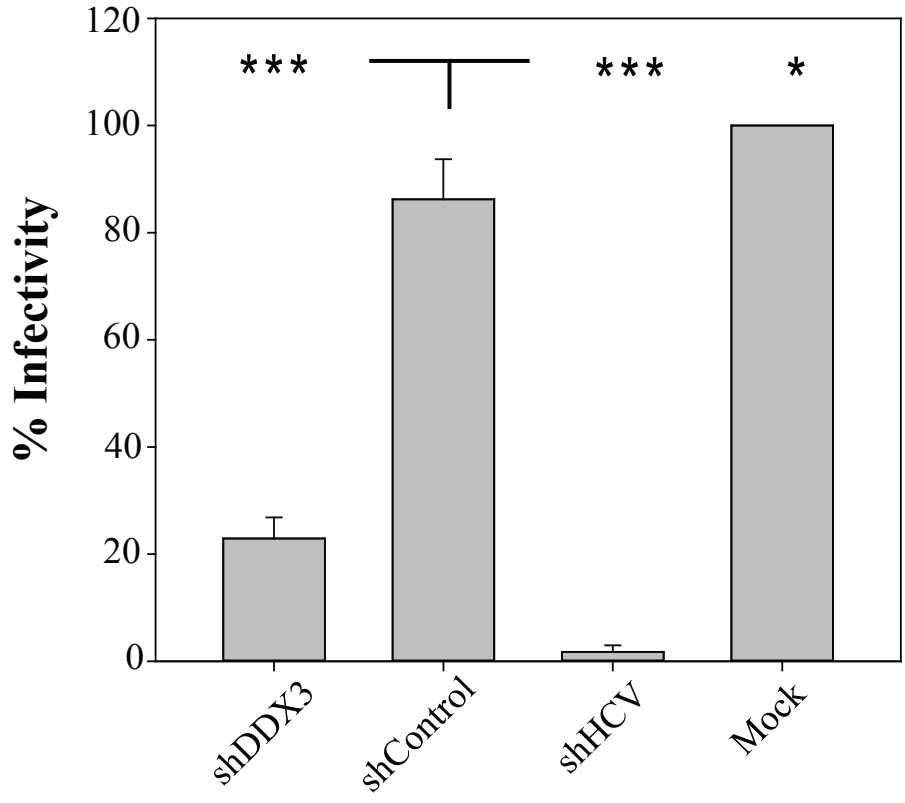
120
100
80
60
40
20
0
% Infectivity
***
***
*
shDDX3
shControl
shHCV
Mock

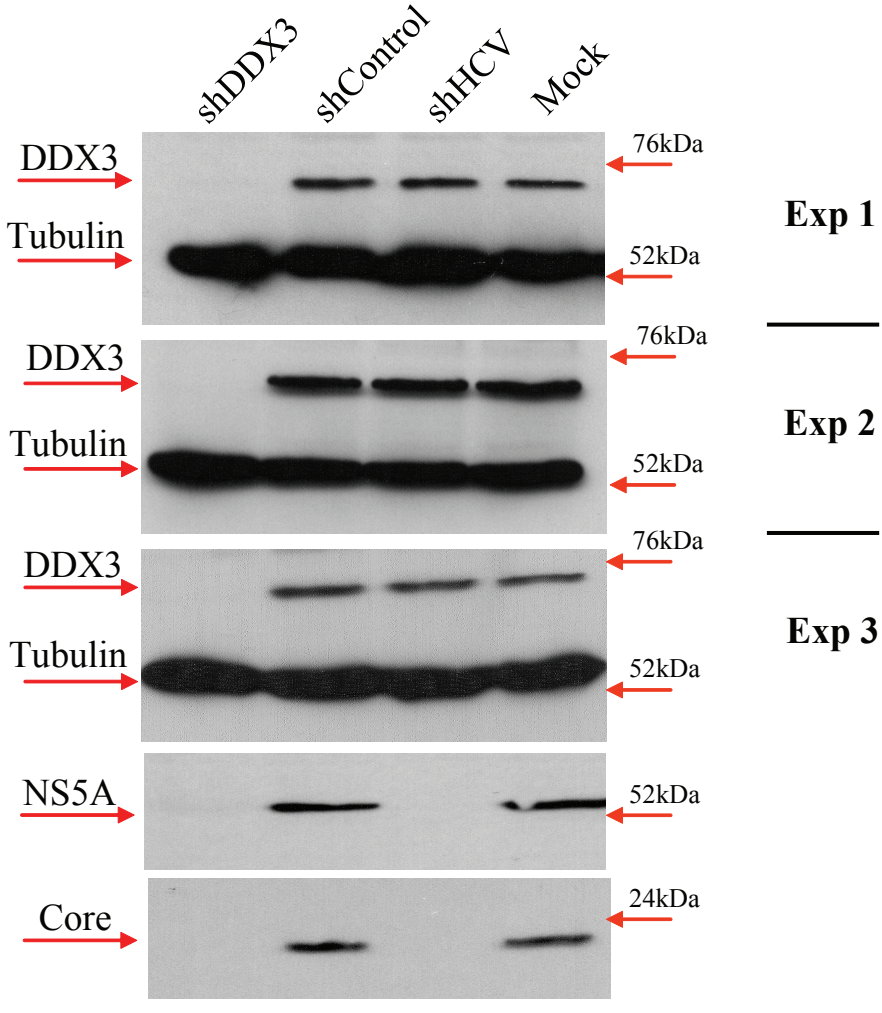
shDDX3
shControl
shHCV
Mock
DDX3
Tubulin
76kDa
52kDa
Exp 1
DDX3
Tubulin
76kDa
52kDa
Exp 2
DDX3
Tubulin
76kDa
52kDa
Exp 3
NS5A
52kDa
Core
24kDa

Figure 3.2. Effect of DDX3 knockdown on HCV infectivity measured by SEAP assay.

Huh7-J20 cells transduced with indicated lentivirus for 48 h were subsequently infected with $JFH1_{WT}$ virus at an m.o.i. of 0.1 FFU/cell. At 48 h post-infection, HCV infectivity was determined for each set of transduced cells by SEAP assay. Error bars indicate the standard deviation of the mean of three independent experiments. Student's t-test was performed to determine the P value. * $P < 0.05$, ** $P < 0.01$, *** $P < 0.001$, NS, not significant. A portion of cells from each set of transduced cells were harvested in SB at 48 h post-transduction for each independent experiment. Lysates were immunoblotted with anti-DDX3 mAb A0196 and an anti-α-Tubulin mAb. In the third repeat experiment, a portion of cells from each set of transduced cells were harvested in SB at 48 h post-infection also. NS5A and Core expression were measured in these lysates using the anti-NS5A mAb 9e10 and the anti-Core mAb C7-50.

determine lentivirus efficiency that was performed before every experiment undertaken in this study. Similar reductions were found in shDDX3- and shHCV- transduced cells compared to shControl-transduced cells when infectivity was measured using a focus forming assay (Fig 3.3). These results confirm an important role for DDX3 in HCV replication.

This data showing that RNAi silencing of DDX3 impairs $JFH1_{WT}$ infection is in accordance with previous studies (Ariumi *et al*., 2007; Randall *et al*., 2007). In addition to reproducing the deleterious effects of DDX3 knockdown on $JFH1_{WT}$ infection, a similar phenotype was observed in DDX3-depleted cells infected with $JFH1_{Y35A}$ virus by SEAP (Fig 3.4) and focus forming assay (Fig 3.5). These findings are in agreement with work published in a recent report by our group (Angus *et al*., 2010), which states that the requirement of DDX3 for HCV replication is unrelated to its interaction with the viral core protein.

3.1.4. Effect of DDX3 Knockdown on HCVpp

While it was confirmed that DDX3 is essential for HCVcc replication, it remains unclear at what stage of the HCV life cycle DDX3 is acting upon. To begin, I wished to determine whether DDX3 was important for viral entry. To do this, I generated retrovirus-based HCV pseudoparticles (HCVpp) (see Materials and Methods, section 2.2.4.2) that can recapitulate envelope glycoprotein-mediated receptor binding, particle internalisation and low-pH-mediated membrane fusion (Bartosch *et al*., 2003). Huh-7 cells were transduced with different lentivirus for 48 h before undergoing HCVpp infection, with luciferase activity measured at 48 h post-infection an indication of the efficiency of cell entry. The absence of DDX3 did not interfere significantly with HCVpp infection (Fig 3.6) compared to shControl- or mock-transduced Huh-7 cells, in contrast to the positive control cells, which were transduced with shRNA targeting the HCV-specific entry receptor CD81, which selectively reduced HCVpp infection by ~ 98 %. These results indicate that DDX3 interferes with a step downstream of glycoprotein-mediated fusion. To determine if this was a HCV-specific effect, I repeated this experiment using VSVpp (Fig 3.7), which recapitulate the entry process of vesicular stomatitis virus (VSV)(see Materials and Methods, section 2.2.4.2). No significant

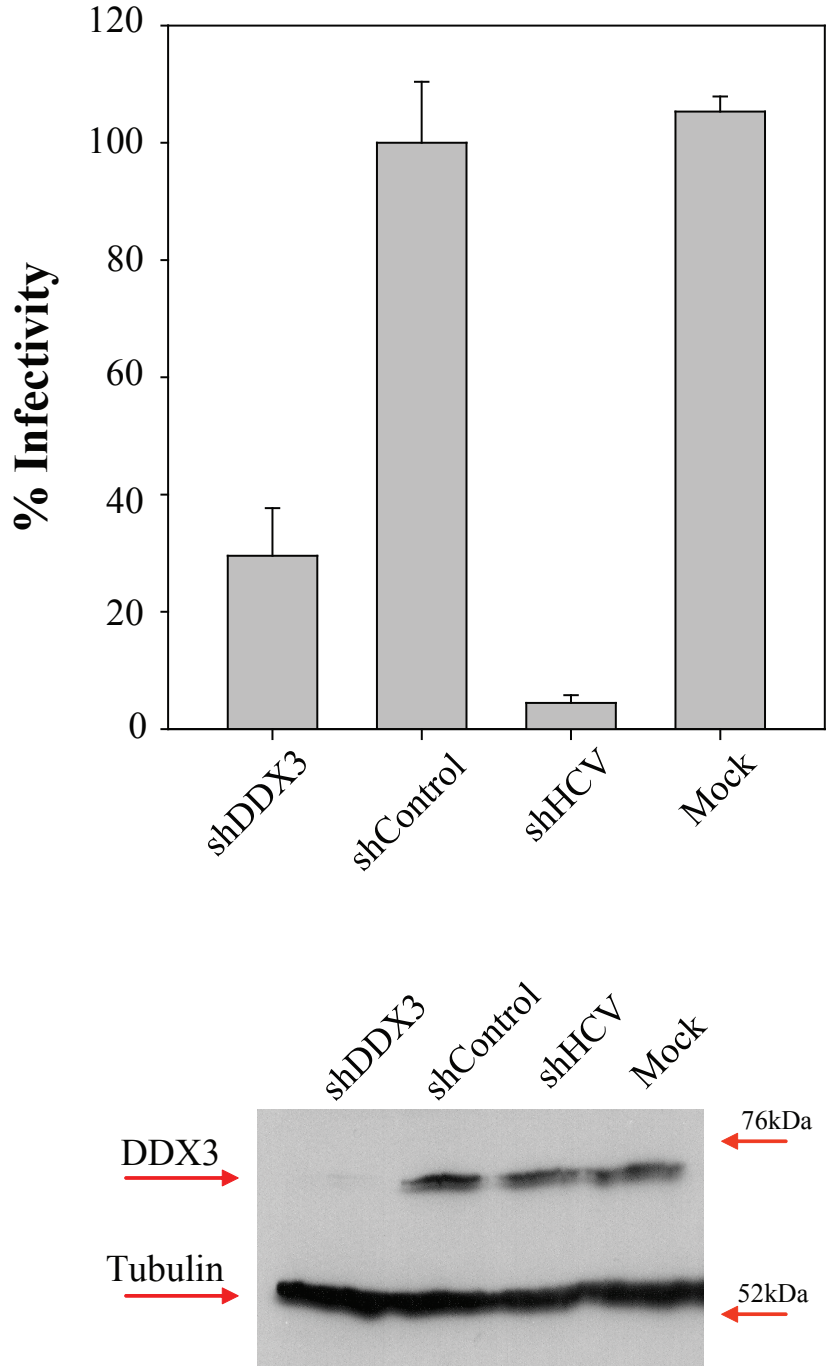

Figure 3.3. Effect of DDX3 knockdown on HCV replication measured by focus forming assay.

Huh-7 cells transduced with indicated lentivirus for 48 h were subsequently infected with $JFH1_{WT}$ virus at an m.o.i. of 0.1 FFU/cell. At 48 h post-infection, cells were fixed and probed for NS5A protein using 9e10 mAb. Mean values and standard deviations represent a single experiment performed with three technical repeats. A portion of cells from each set of transduced cells were harvested in SB at 48 h post-transduction and examined using the anti-DDX3 mAb AO196. Anti-α-Tubulin mAb used as a loading control.

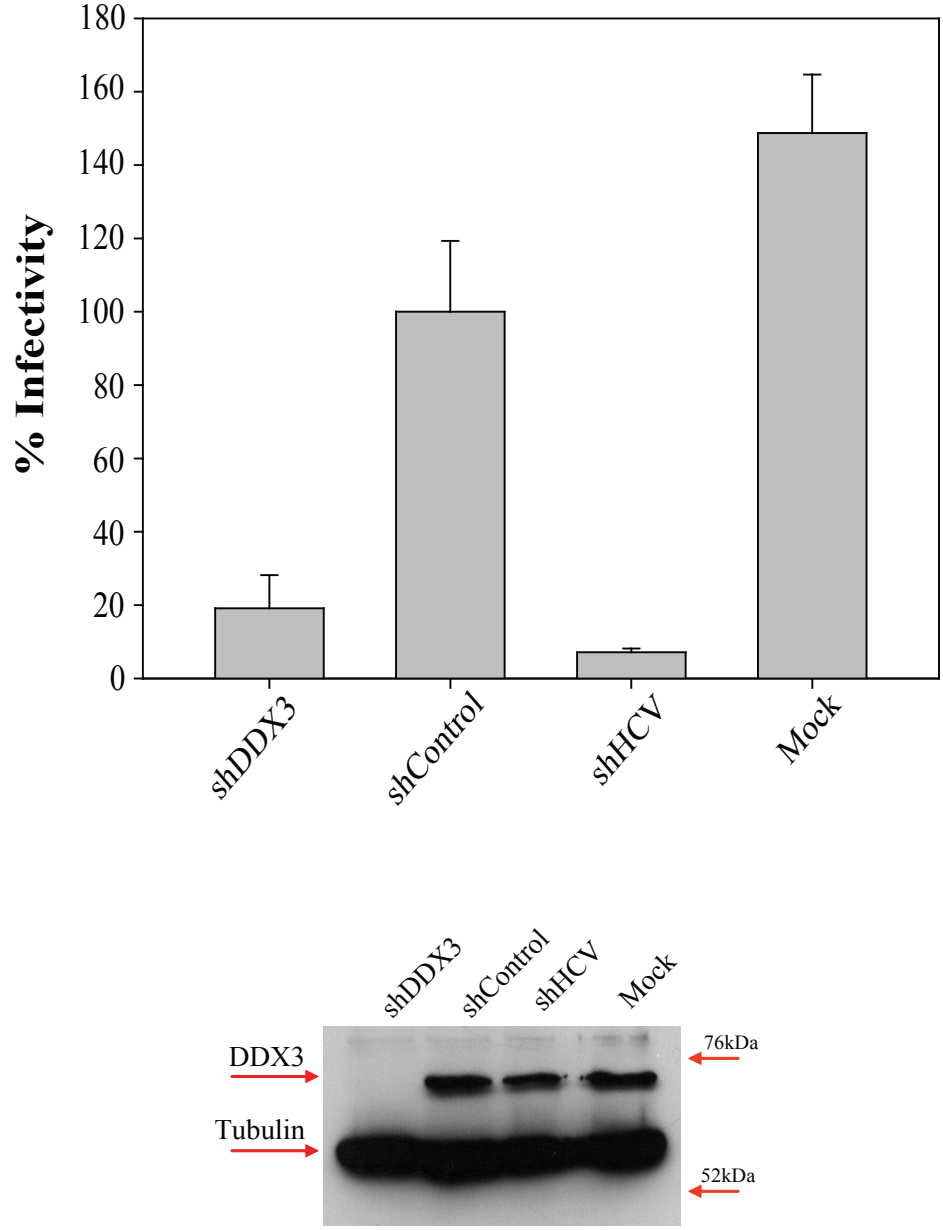

Figure 3.4. Effect of DDX3 knockdown on Core mutant HCV replication measured by SEAP assay.

Huh7-J20 cells transduced with indicated lentivirus for 48 h were subsequently infected with $JFH1_{Y35A}$ virus at an m.o.i. of 0.1 FFU/cell. At 48 h post-infection, HCV infectivity was determined for each set of transduced cells by SEAP assay. Mean values and standard deviations represent a single experiment performed with three technical repeats. A portion of cells from each set of transduced cells were harvested in SB at 48 h post-transduction. Lysates were immunoblotted with anti-DDX3 mAb A0196 and an anti-α-Tubulin mAb.

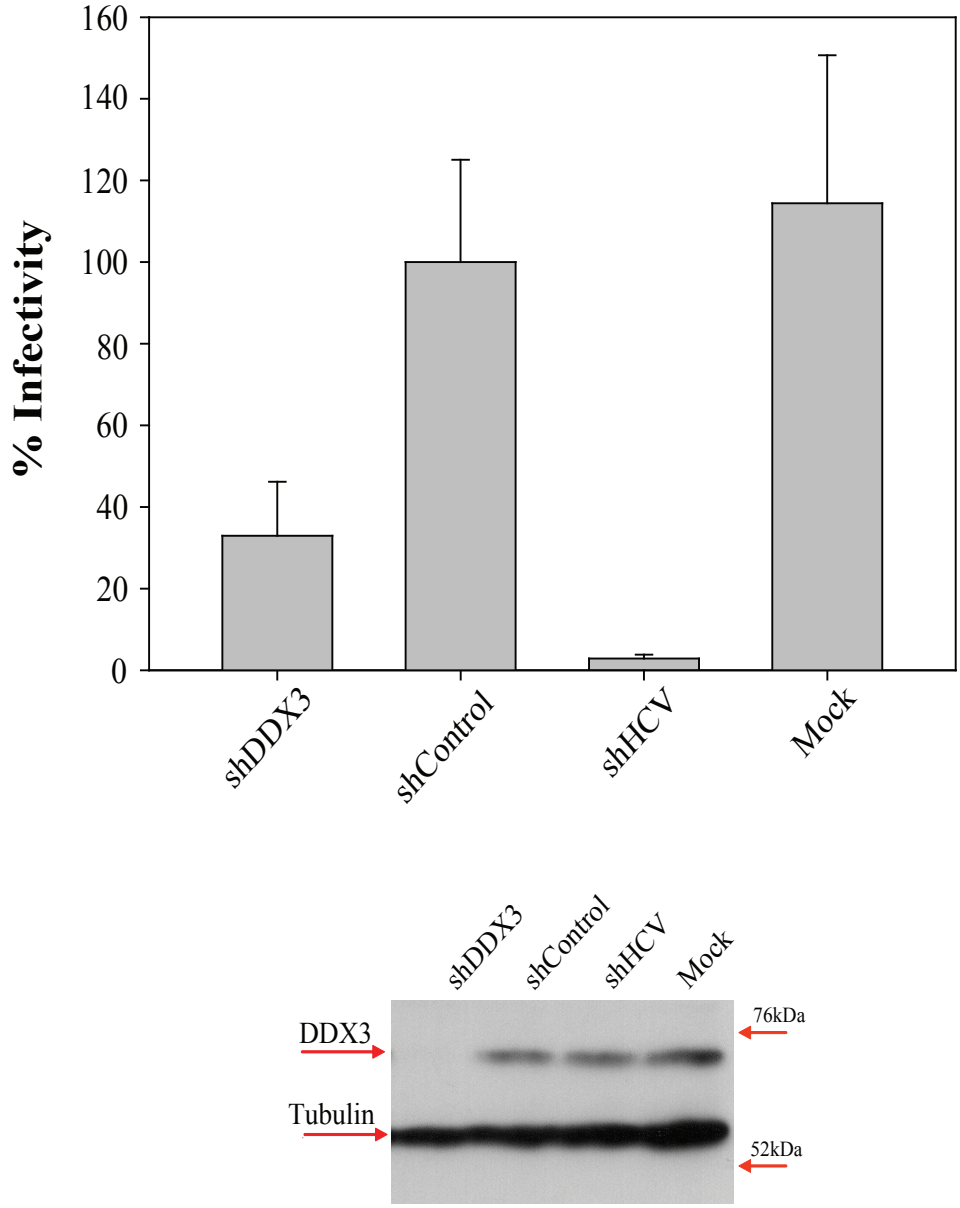

Figure 3.5. Effect of DDX3 knockdown on Core mutant HCV replication measured by focus forming assay.

Huh-7 cells transduced with indicated lentivirus for 48 h were subsequently infected with $JFH1_{Y35A}$ virus at an m.o.i. of 0.1 FFU/cell. At 48 h post-infection, cells were fixed and probed for NS5A protein using 9e10 mAb. Mean values and standard deviations represent a single experiment performed with three technical repeats. A portion of cells from each set of transduced cells were harvested in SB at 48 h post-transduction and examined using the anti-DDX3 mAb AO196. Anti-α-Tubulin mAb used as a loading control.

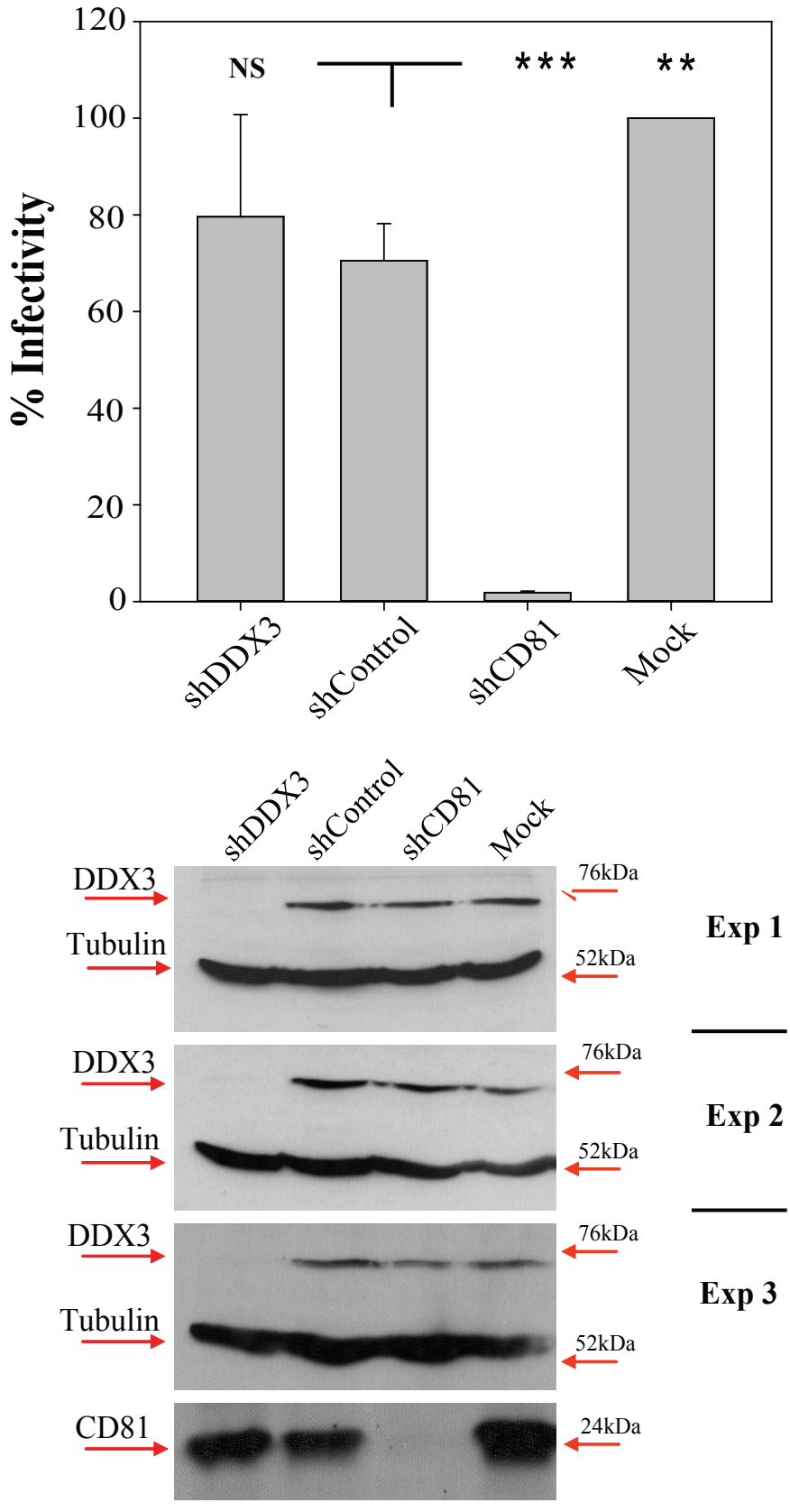

Figure 3.6. Effect of DDX3 knockdown on HCVpp infectivity.

Huh-7 cells transduced with different lentivirus for 48 h were subsequently infected with HCVpp. At 48 h post-infection, HCVpp infectivity was quantified by luciferase assay. Error bars indicate the standard deviation of the mean of three independent experiments. Student's t-test was performed to determine the P value. * $P < 0.05$, ** $P < 0.01$, *** $P < 0.001$, NS, not significant. A portion of cells from each cell-line were harvested in SB at 48 h post-transduction from each independent experiment and probed using the anti-DDX3 mAb AO196 and an anti-α-Tubulin mAb. CD81 expression was measured in the third repeat only using anti-CD81 mAb 5A6.

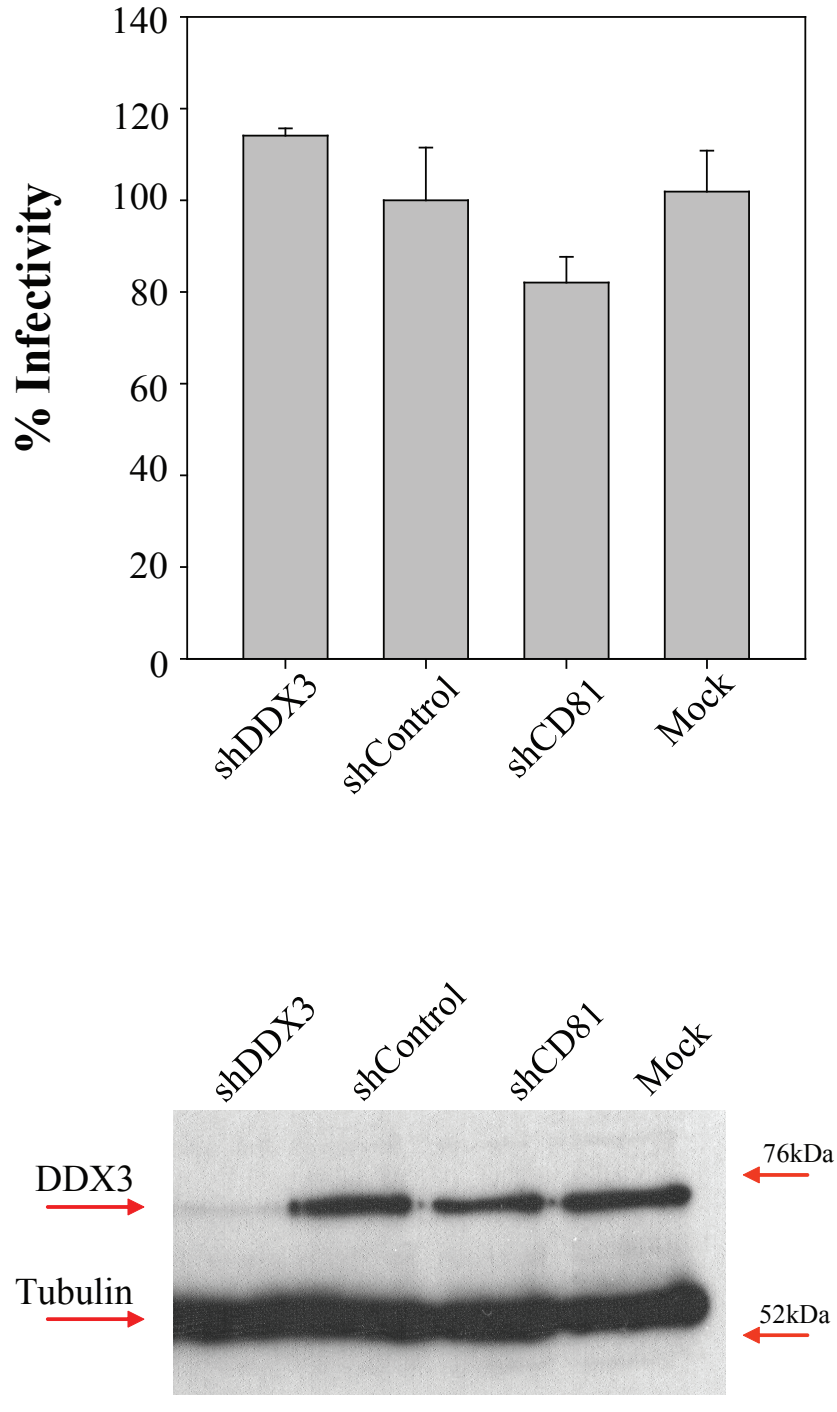

Figure 3.7. Effect of DDX3 knockdown on VSVpp infectivity.

Huh-7 cells transduced with different lentivirus for 48 h were subsequently infected with VSVpp. At 48 h post-infection, VSVpp infectivity was quantified by luciferase assay. Mean values and standard deviations represent a single experiment performed with three technical repeats. A portion of cells from each set of transduced cells were harvested in SB at 48 h post-transduction and examined using the anti-DDX3 mAb AO196. Anti-α-Tubulin mAb used as a loading control.

differences in luciferase activity were observed between shDDX3- and shContol-transduced cells, and VSVpp entry was also unperturbed in shCD81-transduced cells.

3.1.5. Effect of DDX3 Knockdown on Viral Replication in Cells Stably Harbouring HCV Subgenomic Replicon RNA

To determine if DDX3 plays a role in HCV RNA replication, I used Huh-7 cells that were persistently replicating a subgenomic, monocistronic, HCV replicon RNA (N17 SGR/JFH1$_{WT}$; Fig 3.8A). In this replicon, the HCV IRES directs the synthesis of a single polyprotein carrying a firefly luciferase reporter and a puromycin resistance marker (separated by the foot-and-mouth-disease virus [FMDV] 2a protease, the inclusion of which allows the self-cleavage of the puromycin resistance marker during translation) in the JFH1 ΔE1E2 background. Initially, selection and culturing of Huh-7 cells that were electroporated with N17 SGR/JFH1$_{WT}$ RNA was performed with culture medium containing 1 μg puromycin/ml to generate a population of cells that autonomously replicated this replicon RNA. Once this was performed successfully, the effect of DDX3 knockdown on these replicon-containing cells was analysed by transducing cells with different lentivirus for 72 h. Luciferase readings were found to be very similar between DDX3-depleted cells, shControl-tranduced cells and mock cells, while a large drop in luciferase expression (> 80 %) was observed in cells transduced with shRNA against the 5'UTR of HCV (Fig 3.8B). NS5A protein expression was also found to be greatly depleted in these shHCV-transduced replicon cells. No such reduction was observed in DDX3-knockdown replicon cells, where viral protein expression was in line with levels detected in shControl and mock-transduced replicon cells.

Similar results were obtained using cells stably expressing N17 SGR/JFH1$_{Y35A}$ and N17 SGR/JFH1$_{F130E}$ RNA. These mutations in core protein were introduced into the N17 SGR/JFH1$_{WT}$ DNA sequence by site-directed mutagenesis. Successful generation of Huh-7 cells that stably replicated these mutant replicons involved an identical procedure to that undertaken upon introducing N17 SGR/JFH1$_{WT}$ RNA into Huh-7 cells. The fact that luciferase activity was unchanged in a DDX3-deficient background where the core-DDX3 interaction is abrogated (Y35A, Fig 3.9) or where core protein is known to be

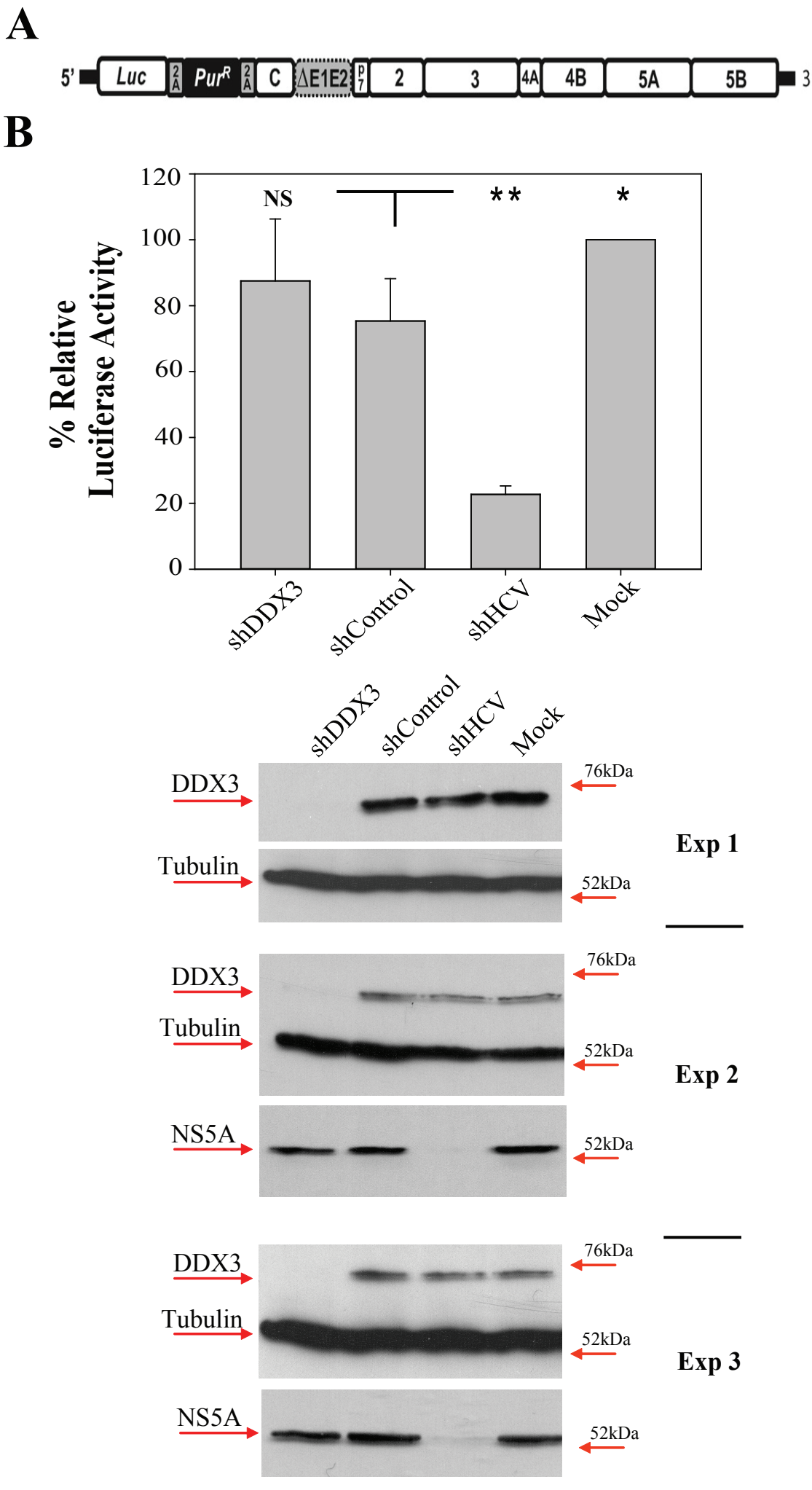
A
5'
Luc
2A
Pur^R
2A
C
ΔE1E2
p7
2
3
4A
4B
5A
5B
3'
B
% Relative Luciferase Activity
120
100
80
60
40
20
0
NS
**
*
shDDX3
shControl
shHCV
Mock
shDDX3
shControl
shHCV
Mock
DDX3
76kDa
Tubulin
52kDa
Exp 1
DDX3
76kDa
Tubulin
52kDa
NS5A
52kDa
Exp 2
DDX3
76kDa
Tubulin
52kDa
NS5A
52kDa
Exp 3

Figure 3.8. DDX3 knockdown in Huh-7 cells stably replicating N17 SGR/JFH1$_{WT}$.

(A) Schematic illustrating the principal features of the monocistronic N17 SGR/JFH1$_{WT}$ replicon. This construct encodes the firefly luciferase reporter and the puromycin resistance marker (separated by the foot-and-mouth-disease virus [FMDV] 2a self-cleavage site) in the JFH1 ΔE1E2 background. **(B)** Huh-7 cells stably replicating N17 SGR/JFH1$_{WT}$ replicon RNA were transduced with indicated shRNAs. At 72 h post-transduction, luciferase activity was measured. Error bars indicate the standard deviation of the mean of three independent experiments. Student's t-test was performed to determine the P value. * $P < 0.05$, ** $P < 0.01$, *** $P < 0.001$, NS, not significant. A portion of cells from each set of transduced cells were harvested in SB at 72 h post-transduction in each independent experiment. Lysates were immunoblotted with anti-DDX3 mAb A0196 and an anti-α-Tubulin mAb. NS5A expression was also measured in the second and third repeat using the anti-NS5A mAb 9e10.

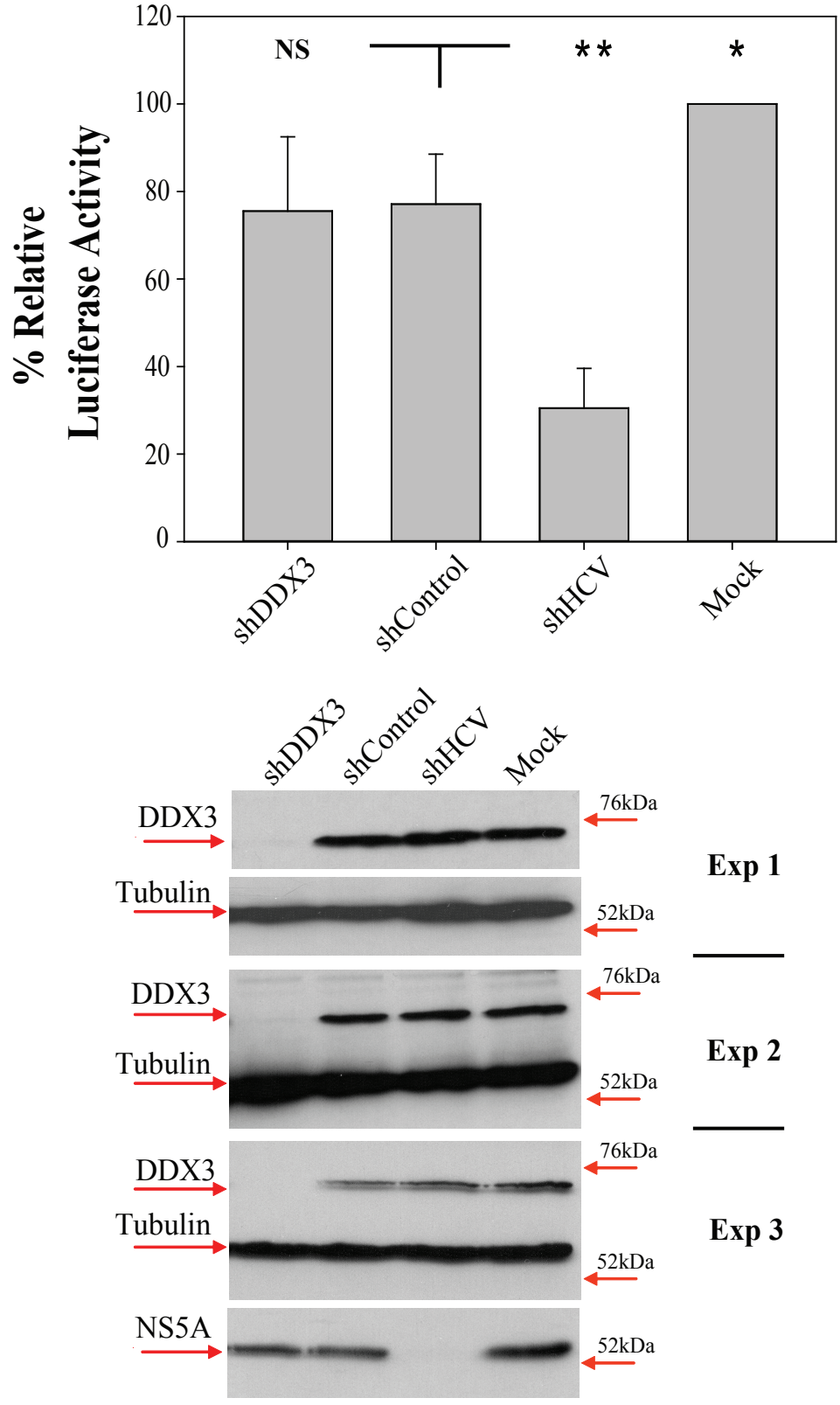

Figure 3.9. DDX3 knockdown in Huh-7 cells stably replicating N17 SGR/JFH1$_{Y35A}$.

Huh-7 cells stably replicating N17 SGR/JFH1$_{Y35A}$ replicon RNA were transduced with indicated shRNAs. At 72 h post-transduction, luciferase activity was measured. Error bars indicate the standard deviation of the mean of three independent experiments. Student's t-test was performed to determine the P value. * $P < 0.05$, ** $P < 0.01$, *** $P < 0.001$, NS, not significant. A portion of cells from each set of transduced cells were harvested in SB at 72 h post-transduction in each independent experiment. Lysates were immunoblotted with anti-DDX3 mAb A0196 and an anti-α-Tubulin mAb. NS5A expression was measured in the third repeat only using the anti-NS5A mAb 9e10.

susceptible to complete degradation (F130E, Fig 3.10) (Boulant *et al*., 2006) indicates that the core-DDX3 interaction is not required for stages of the HCV lifecycle up to and including RNA replication in stable replicon-containing cells. This was further clarified during analysis of DDX3 depletion in Huh7-J20 cells stably replicating the bicistronic BLAST SGR/JFH1$_{WT}$ replicon, which does not express core protein (Fig 3.11A). This construct contains the HCV internal ribosome entry site (IRES), which directs expression of the blasticidin resistance marker, and the encephalomyocarditis virus (EMCV) IRES, which directs the expression of the HCV nonstructural (NS) proteins NS3 to NS5B. Assay readings revealed that DDX3 depletion in these cells had no effect on SEAP levels compared to shControl- and mock-transduced cells (Fig 3.11B), a result further suggesting that the absence of core has no effect on DDX3-deficient cells stably replicating HCV SGR RNA. Meanwhile, reductions in SEAP activity were found in shHCV-transduced cells, but the reductions observed (> 40 %) were found to be smaller than those observed between shHCV- and shControl-transduced cells stably expressing N17 SGR/JFH1 RNA. The reason for this discrepancy is unclear, as the 5'UTR sequence in the BLAST SGR/JFH1$_{WT}$ replicon is the same as that in the monocistronic N17 SGR/JFH1$_{WT}$ replicon. However, it is possible that the different components and smaller size of the BLAST SGR/JFH1$_{WT}$ replicon may mean that the secondary structure of this replicon could be significantly different to that of N17 SGR/JFH1$_{WT}$. Thus, it could be harder for shHCV to target the BLAST SGR/JFH1$_{WT}$ mRNA efficiently.

3.1.6. Effect of DDX3 Knockdown on Viral Replication in Cells Transiently Transfected with HCV Subgenomic Replicon RNA.

Previous reports have shown that in DDX3-depleted cells, replication in cells transiently transfected with full-length HCV genomic RNA was greatly reduced, while this effect was less pronounced in cells stably expressing subgenomic replicon RNA (Ariumi *et al*., 2007; Randall *et al*., 2007). Accordingly, I investigated the effect of DDX3 knockdown on the replication of transiently transfected N17 SGR/JFH1$_{WT}$ replicon. Huh-7 cells were transduced with different lentivirus for 48 h before each cell-line was electroporated with 10 μg of replicon RNA. 48 h later, the cells were harvested and the luciferase activity and protein content were analysed. In contrast to cells

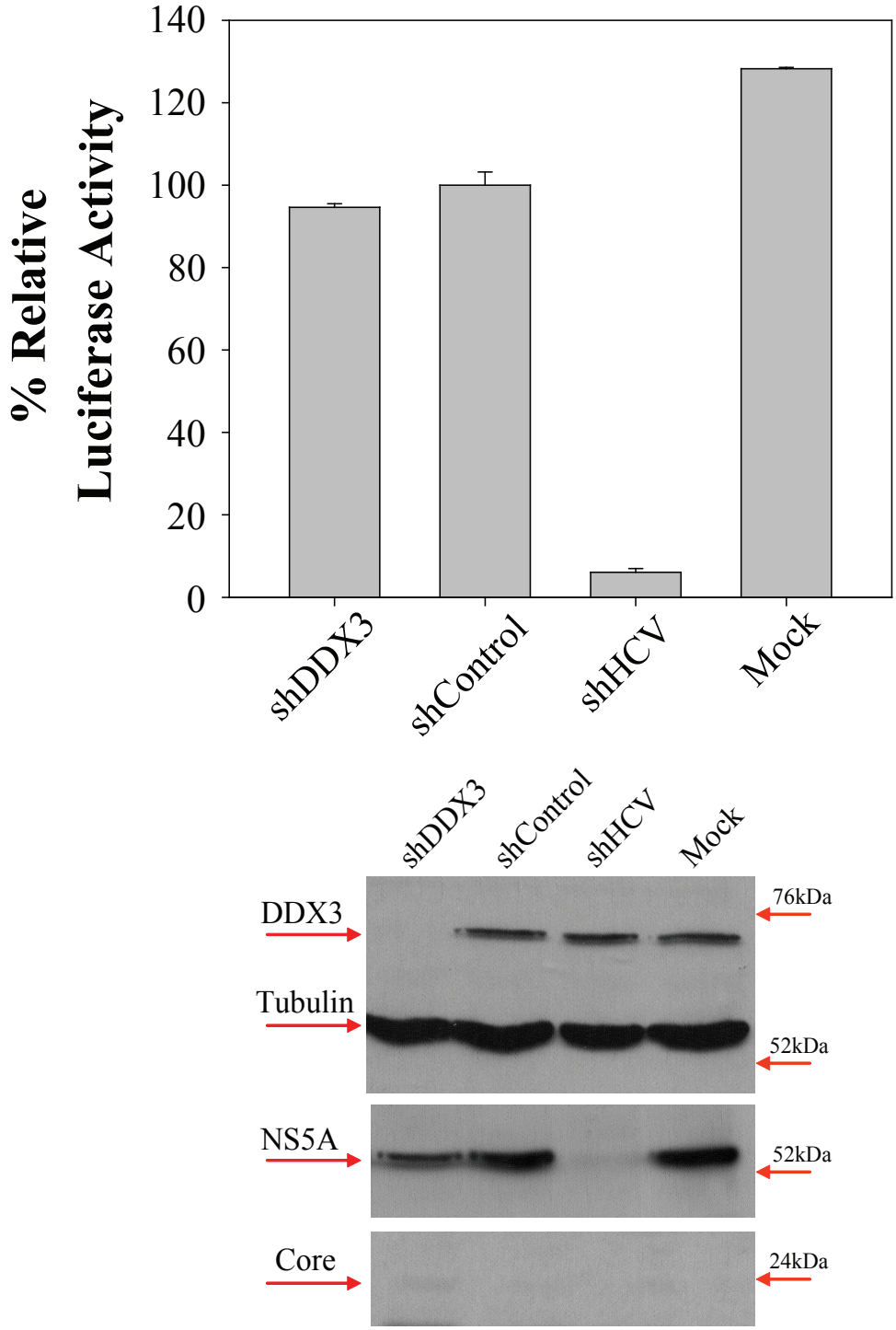

Figure 3.10. DDX3 knockdown in Huh-7 cells stably replicating N17 SGR/JFH1$_{F130E}$.

Huh-7 cells stably replicating N17 SGR/JFH1$_{F130E}$ replicon RNA were transduced with indicated shRNAs. At 72 h post-transduction, luciferase activity was determined in each set of transduced cells. Mean values and standard deviations represent a single experiment performed with three technical repeats. A portion of cells from each set of transduced cells were harvested in SB at 72 h post-transduction and examined using the anti-DDX3 mAb AO196, the anti-NS5A mAb 9e10 and the anti-Core mAb C7-50. Anti-α-Tubulin mAb used as a loading control.

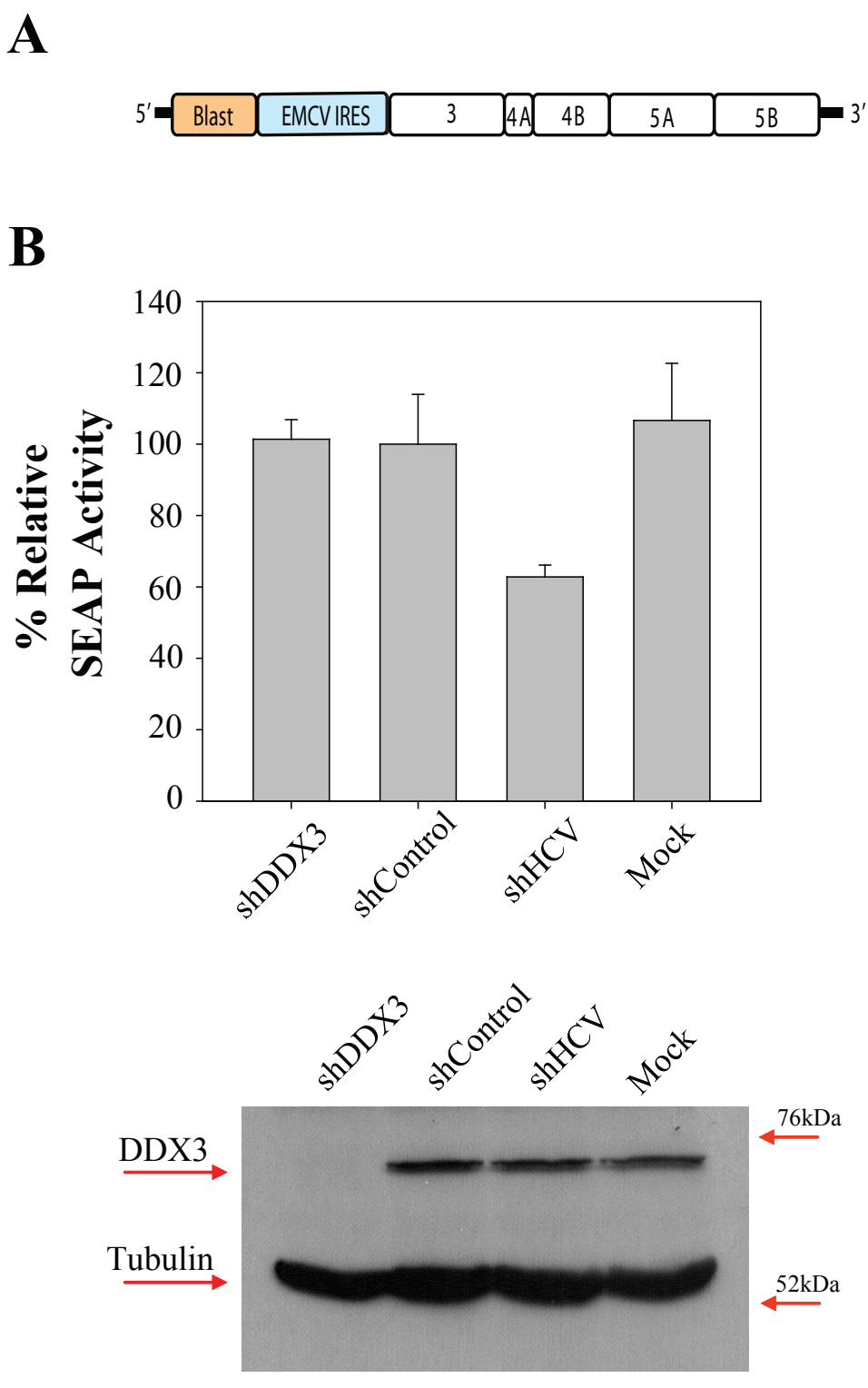

Figure 3.11. DDX3 knockdown in Huh7-J20 cells stably replicating BLAST SGR/JFH1$_{WT}$.

(A) Schematic illustrating the principal features of the bicistronic BLAST SGR/JFH1$_{WT}$ replicon. This construct contains the HCV internal ribosome entry site (IRES), which directs expression of the blasticidin resistance marker, and the encephalomyocarditis virus (EMCV) IRES, which directs the expression of the HCV nonstructural (NS) proteins NS3 to NS5B. **(B)** Huh7-J20 cells persistently replicating BLAST SGR/JFH1$_{WT}$ bicistronic replicon were transduced with indicated lentivirus. At 72 h post-transduction, replication levels were determined in each set of transduced cells by SEAP assay. Mean values and standard deviations represent a single experiment performed with three technical repeats. Cellular extracts from each set of transduced cells were lysed in SB at 72 h post-transduction and immunoblotted with anti-DDX3 mAb A0196 and an anti-α-Tubulin mAb.

persistently expressing SGR RNA, I found a strong reduction in luciferase expression in DDX3 knockdown cells that had been transiently transfected with N17 SGR/JFH1$_{WT}$ replicon. Again, it was not as pronounced a reduction as that observed in cells transduced with shHCV, but luciferase readings were found to be approximately 70 % lower than in mock cells or in cells transduced with shControl (Fig 3.12), a similar reduction as that observed in my HCVcc experiments (see Fig 3.2). The irrelevance of the absence of core in these cells transiently replicating SGR RNA was also demonstrated, with similar results observed between shDDX3- and shControl-transduced Huh7-J20 cells transiently transfected with BLAST SGR/JFH1$_{WT}$ RNA (Fig 3.13) and shDDX3- and shControl-transduced Huh-7 cells transiently transfected with N17 SGR/JFH1$_{WT}$ RNA. As in Fig 3.11 where the BLAST SGR/JFH1$_{WT}$ replicon was also employed, reductions between shHCV- and shControl-transduced cells were much smaller than those observed by luciferase assay in Huh-7 cells stably or transiently replicating N17 SGR/JFH1 replicons. Indeed, SEAP assay and western immunoblot analysis revealed that more viral protease cleavage activity and NS5A expression were observed in shHCV-transduced cells compared to DDX3-knockdown cells (It must be borne in mind that this experiment was only performed once, so a poor lentiviral transduction efficiency must not be ruled out for these aberrant findings).

To gain further insight into the role of DDX3 in HCV RNA replication, I repeated the experiments shown in Fig 3.12, but this time measured the luciferase readings at various time points post-electroporation (1, 2, 4, 8, 24 and 48 h post-electroporation) (Fig 3.14A, B and C). Luciferase readings indicated no significant difference between DDX3-deficient cells and any of the control cells lines during the first four timepoints (up to 8 h post-electroporation) (see appendix 3 for statistical analysis of individual timepoints based on the three independent experiments). However, at 24 h post-electroporation, luciferase readings were seen to be reduced by an average of ~ 60 % in shDDX3-transduced cells compared to shControl-transduced cells. The difference in luciferase activity actually increased between shDDX3- and shControl-transduced cells at 48 h post-electroporation, with the drop in replication between them found to be approaching 70 %, a reduction consistent with the earlier result obtained in Fig 3.12. Statistical analysis revealed the difference in luciferase activity between shDDX3- and shControl-transduced cells to be significant at both the 24 h and 48 h post-electroporation time points (see appendix 3). Luciferase activity in shHCV-transduced

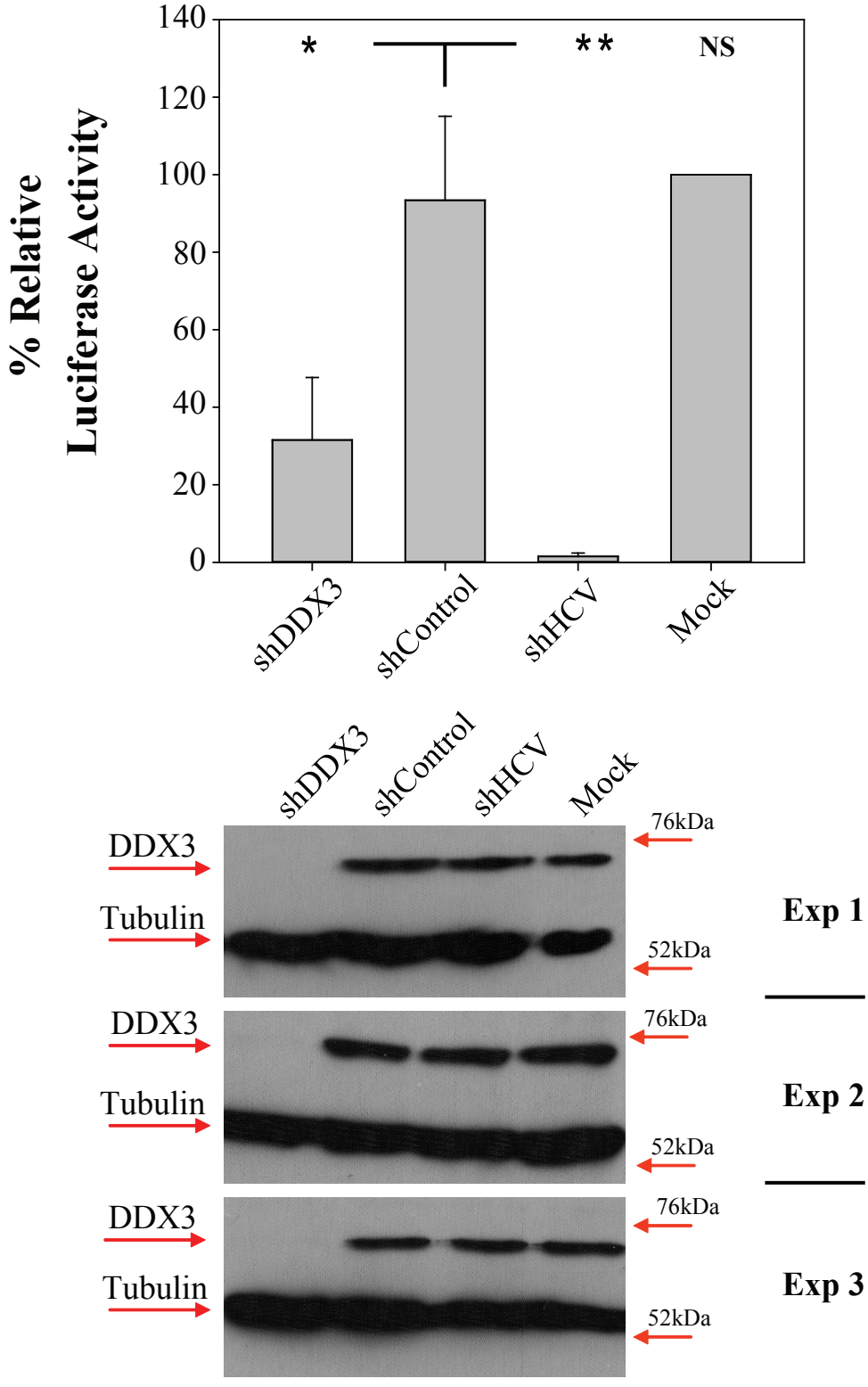

Figure 3.12. Effect of DDX3 knockdown in Huh-7 cells transiently replicating N17 SGR/JFH1$_{WT}$ replicon RNA.

Huh-7 cells were transduced with the relevant shRNAs. At 48 h post-transduction, 10 µg of N17 SGR/JFH1$_{WT}$ replicon RNA was electroporated into each set of transduced cells. At 48 h post-electroporation, luciferase activity was measured. Error bars indicate the standard deviation of the mean of three independent experiments. Student's t-test was performed to determine the P value. * $P < 0.05$, ** $P < 0.01$, *** $P < 0.001$, NS, not significant. In each experiment, a portion of Huh-7 cells were harvested from each cell-line in SB at 48 h post-transduction and examined using the anti-DDX3 mAb AO196. Anti-α-Tubulin mAb was used as a loading control.

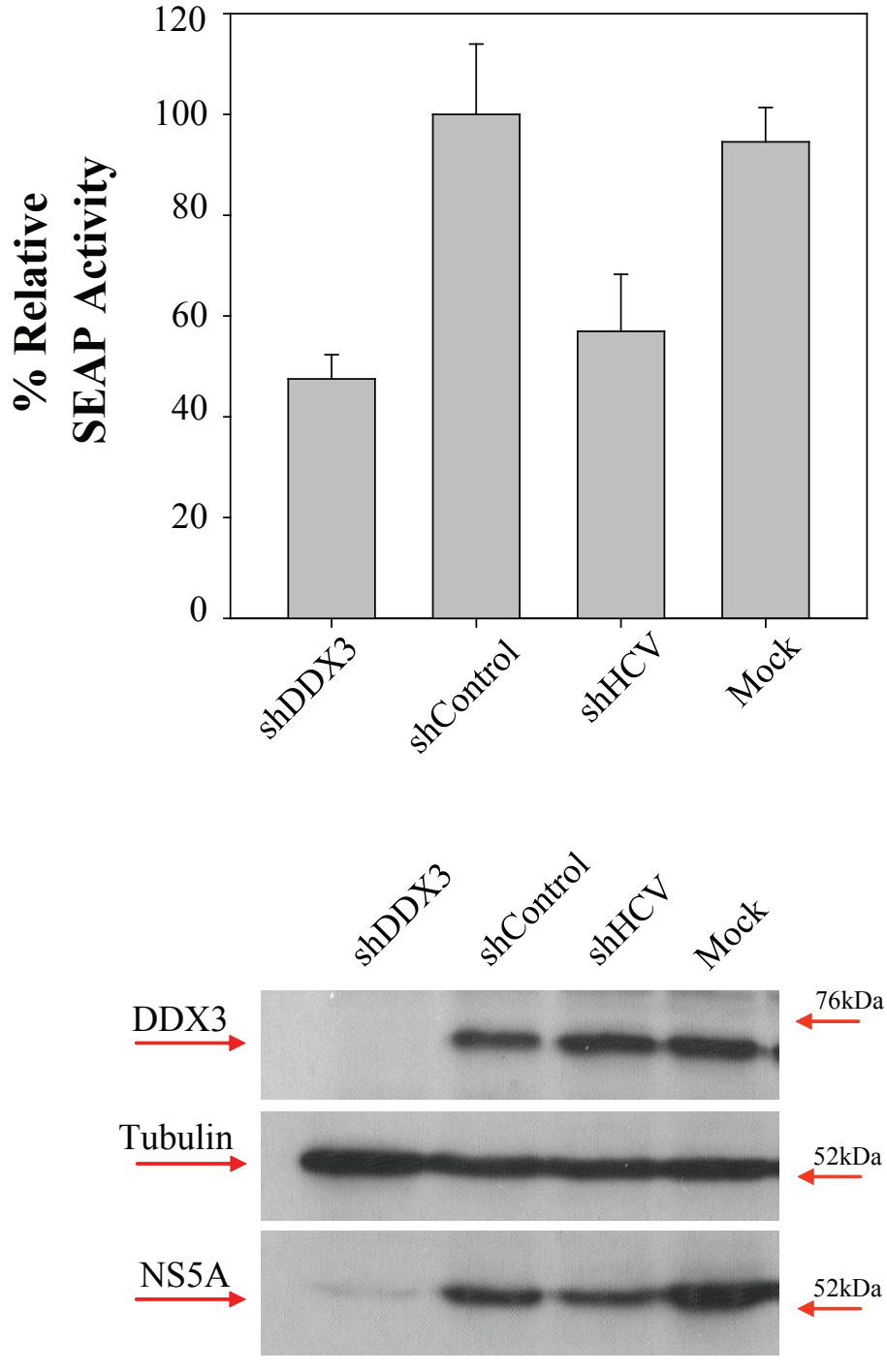

Figure 3.13. Effect of DDX3 knockdown in Huh7-J20 cells transiently replicating SGR/ JFH1$_{WT}$.

Huh7-J20 cells were transduced with the indicated shRNAs. At 48 h post-transduction, each set of transduced cells were electroporated with 10 µg of SGR/JFH1$_{WT}$ RNA. At 48 h post-electroporation, SEAP activity was measured in each set of transduced cells. Mean values and standard deviations represent a single experiment performed with three technical repeats. A portion of cells from each set of transduced cells were harvested in SB at 72 h post-transduction and lysates were immunoblotted with anti-DDX3 mAb AO196, an anti-α-Tubulin mAb and the anti-NS5A mAb 9e10.

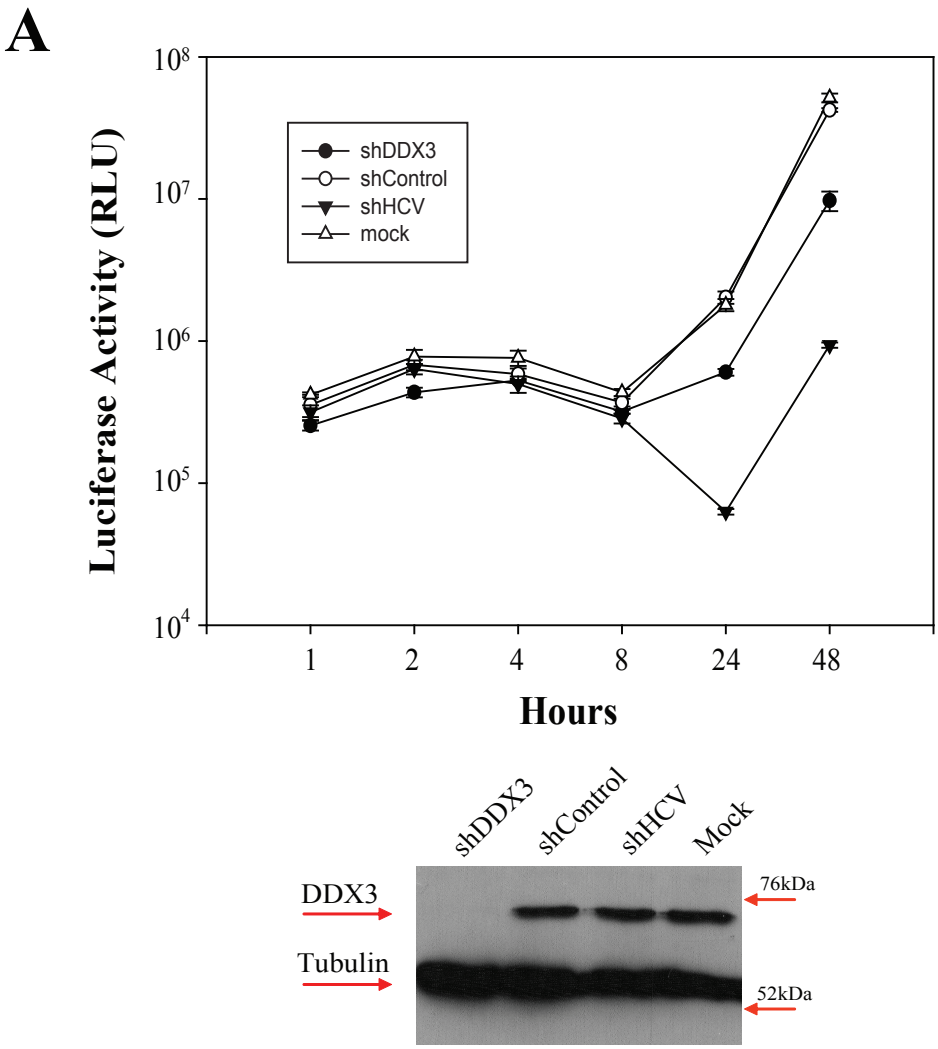
A
Luciferase Activity (RLU)
10^8
10^7
10^6
10^5
10^4
shDDX3
shControl
shHCV
mock
1
2
4
8
24
48
Hours
shDDX3
shControl
shHCV
Mock
DDX3
Tubulin
76kDa
52kDa

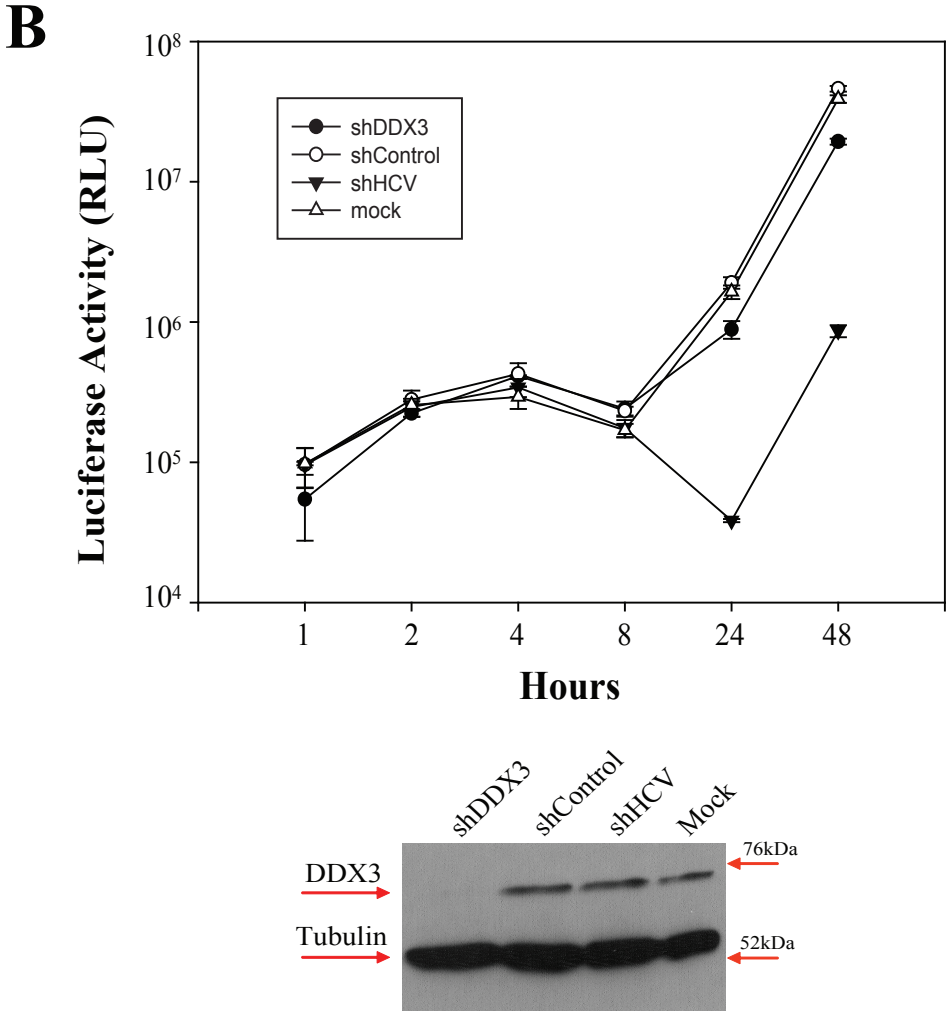
B
Luciferase Activity (RLU)
10^8
10^7
10^6
10^5
10^4
shDDX3
shControl
shHCV
mock
1
2
4
8
24
48
Hours
shDDX3
shControl
shHCV
Mock
DDX3
Tubulin
76kDa
52kDa

C

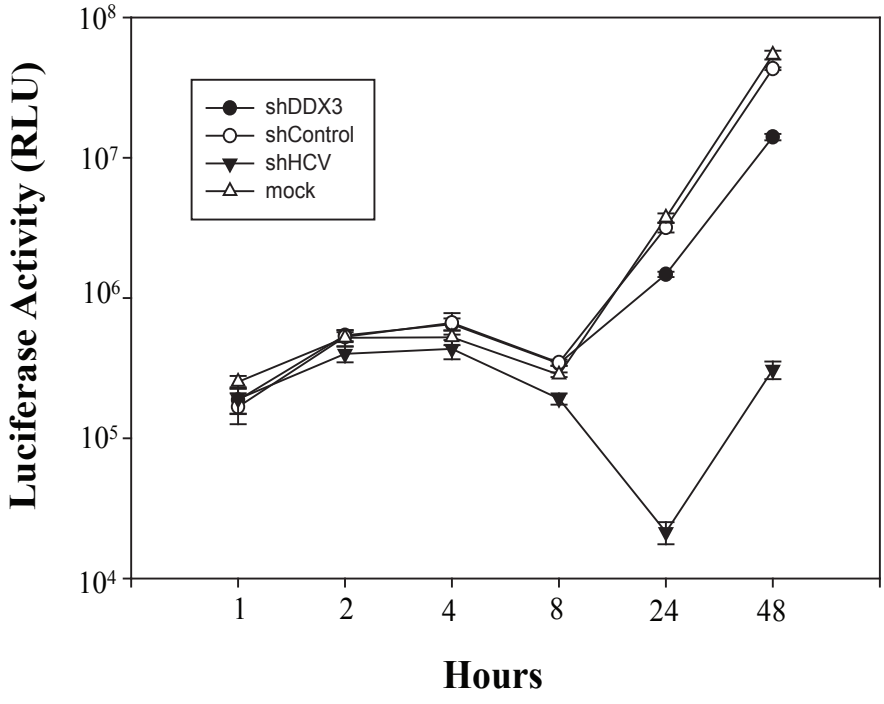

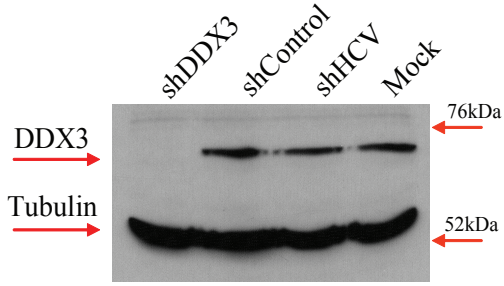

D

Fold change from shControl		
	24hrs	**48hrs**
shDDX3	- 2.55 +/- 0.69	- 3.26 +/- 0.99
shHCV	- 48.95 +/- 1.29	- 52.22 +/- 2.20
mock	+ 0.04 +/- 0.16	- 0.07 +/- 0.21

Figure 3.14. Effect of DDX3 Knockdown in Huh-7 cells transiently replicating N17 SGR/JFH1$_{WT}$ replicon RNA at various timepoints.

Three independent experiments represented by **A, B** and **C.** In each case**,** Huh-7 cells were electroporated with 10 µg N17 SGR/JFH1$_{WT}$ replicon RNA at 48 h post-transduction with indicated lentivirus. Cell lysates were assayed at the indicated time points post-electroporation for luciferase activity. Error bars indicate the standard deviation of the mean of three technical repeats in each individual experiment. A portion of transduced cells from each set of transduced cells were lysed in SB in each experiment and probed with anti-DDX3 and anti-α-Tubulin antibodies to determine protein levels at time of electroporation. **(D)** Table showing the fold-changes in luciferase activity from the three experiments compared to cells transduced with shControl.

cells, while consistent with the other sets of transduced cells until the 8 h timepoint, was almost abrogated compared to shControl cells at both the 24 h and 48 h time points. Results observed in a Y35A (Fig 3.15) and a F130E (Fig 3.16) background indicate that the core-DDX3 interaction is dispensable in Huh-7 cells transiently transfected with SGR RNA, in line with results shown in Fig 3.13.

To ensure that the phenotype observed in DDX3-depleted cells transiently transfected with SGR in Figs 3.12 and 3.14 was accurate and that minimal levels of DDX3 still present in shDDX3-transduced cells at 48 h post-transduction were not masking the genuine effects of DDX3 knockdown on HCV replication, Huh-7 cells were transduced with selected lentivirus for 72 h before undergoing N17 SGR/JFH1$_{WT}$ electroporation. In DDX3-deficient cells that had undergone this longer transduction, fold-reductions in luciferase activity between shDDX3- and shControl-transduced cells at 24 and 48 h post-electroporation were similar to those seen in cells that had been transduced for 48 h, indicating that levels of DDX3 depletion at 48 h post-transduction were sufficient for DDX3 knockdown phenotypes to be accurately observed in Huh-7 cells (Fig 3.17). I was also aware of the possibility that the replication phenotype in DDX3-deficient Huh-7 cells may be due to overloading target cells with viral RNA, which could create high background levels of luciferase and therefore obscure the effects of DDX3 on aspects of the viral lifecycle at early time points post-electroporation. To prove that this was not the case, I repeated the experiments shown in Fig 3.14, but in this instance, I electroporated 0.1 μg of N17 SGR/JFH1$_{WT}$ RNA into each transduced set of cells instead of 10 μg. Luciferase readings were far lower in each set of cells at each time point, as expected, and no significant changes were observed between DDX3-depleted cells and shControl-transduced cells up to 8 h post-electroporation. Furthermore, similar declines in luciferase activity were found between DDX3-depleted cells and shControl-transduced cells at the 24 and 48 h timepoints as were seen when 10 μg of RNA was introduced into each set of transduced cells (Fig 3.18). The control experiments depicted in Figs 3.17 and 3.18 confirmed that the reduction in luciferase activity seen in DDX3 knockdown cells is an accurate phenotype and highlights the importance of DDX3 at an early stage of the HCV lifecycle.

While we were conducting our experiments, a paper was published by Geissler *et al*. (2012) stating that the role of DDX3 in HCV replication is to translate the viral genome.

A

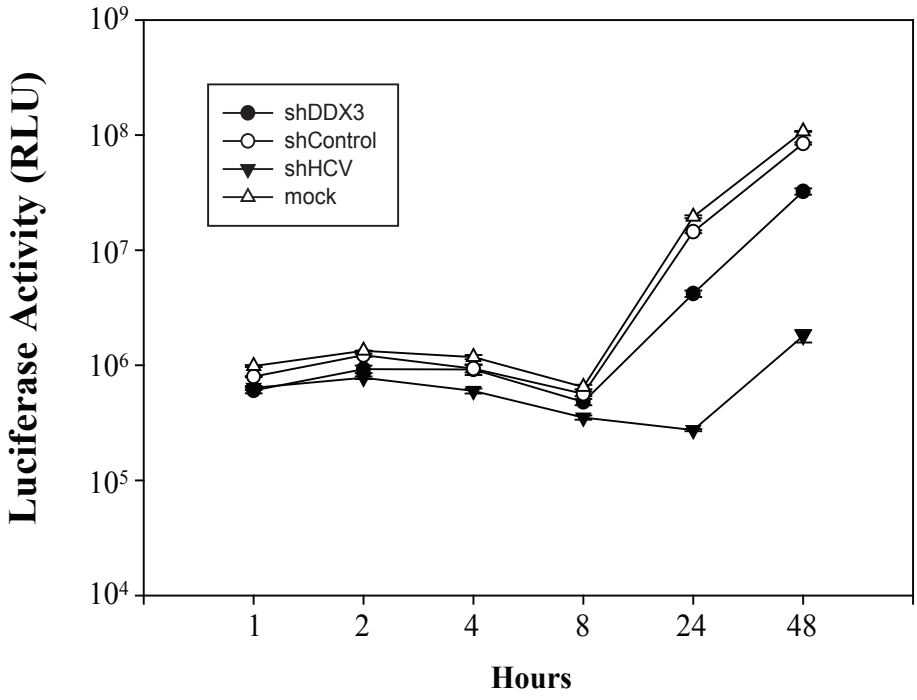

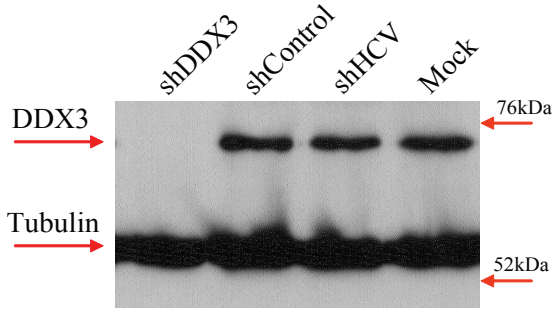

B

Fold change from shControl		
	24hrs	**48hrs**
shDDX3	- 3.45	- 2.61
shHCV	- 52.93	- 46.97
mock	+ 0.34	+ 0.27

Figure 3.15. Effect of DDX3 Knockdown in Huh-7 cells transiently replicating N17 SGR/JFH1$_{Y35A}$ replicon RNA at various timepoints.

(A) Huh-7 cells were electroporated with 10 µg N17 SGR/JFH1$_{Y35A}$ replicon RNA at 48 h post-transduction with indicated lentivirus. Cell lysates were assayed at the indicated time points post-electroporation for luciferase activity. Mean values and standard deviations represent a single experiment performed with three technical repeats. A portion of cells from each set of transduced cells were lysed in SB at 48 h post-transduction and probed with the anti-DDX3 mAb AO196. Anti-α-Tubulin mAb was used as a loading control. **(B)** Table showing the fold-changes in luciferase activity in cells transduced with indicated lentivirus compared to cells transduced with shControl.

A

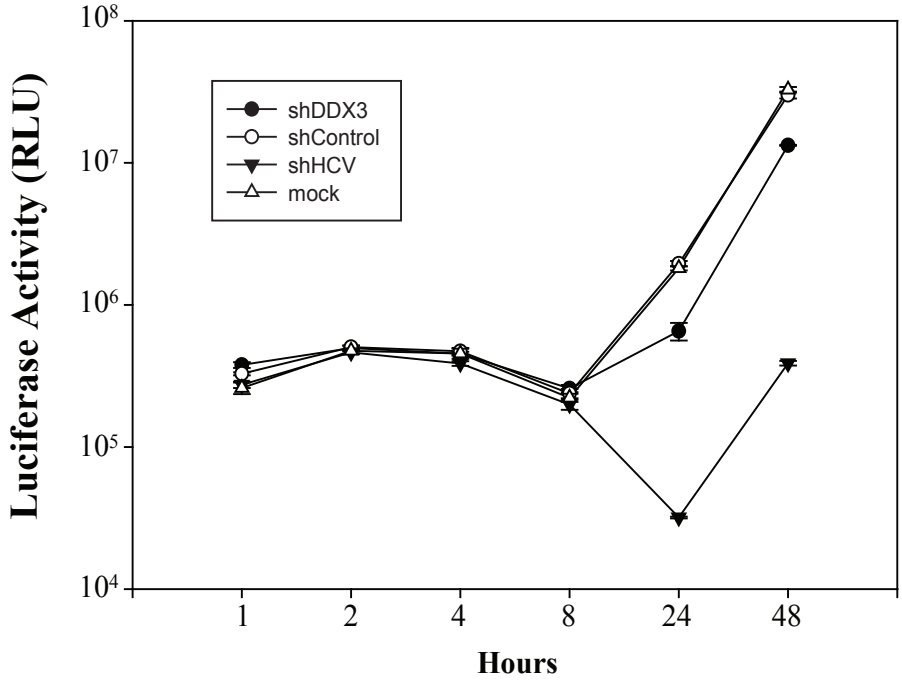

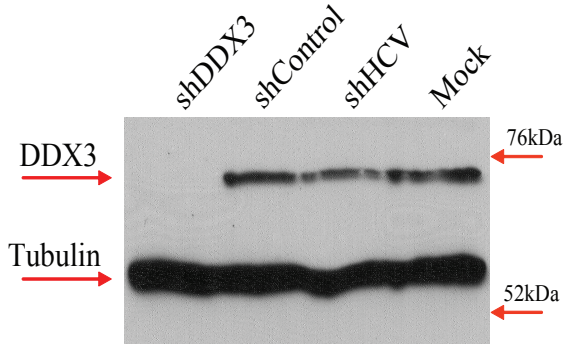

B

Fold change from shControl		
	24hrs	**48hrs**
shDDX3	- 2.97	- 2.26
shHCV	- 61.15	- 77.35
mock	- 0.07	+ 0.08

Figure 3.16. Effect of DDX3 Knockdown in Huh-7 cells transiently replicating N17 SGR/JFH1$_{F130E}$ replicon RNA at various timepoints.

(A) Huh-7 cells were electroporated with 10 µg N17 SGR/JFH1$_{F130E}$ replicon RNA at 48 h post-transduction with indicated lentivirus. Cell lysates were assayed at the indicated time points post-electroporation for luciferase activity. Mean values and standard deviations represent a single experiment performed with three technical repeats. A portion of cells from each set of transduced cells were lysed in SB at 48 h post-transduction and probed with the anti-DDX3 mAb AO196. Anti-α-Tubulin mAb was used as a loading control. **(B)** Table showing the fold-changes in luciferase activity in cells transduced with indicated lentivirus compared to cells transduced with shControl.

A

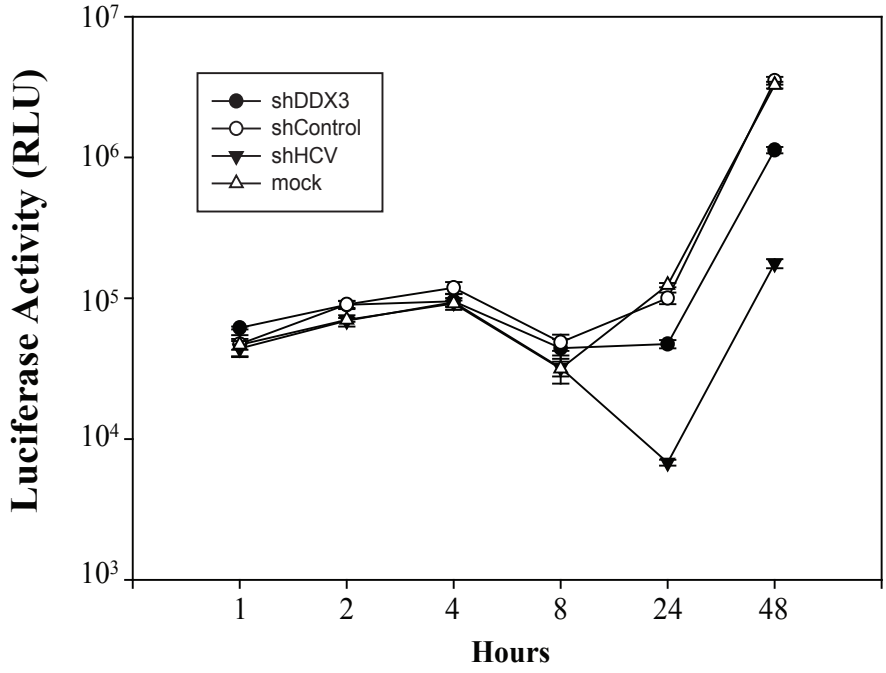

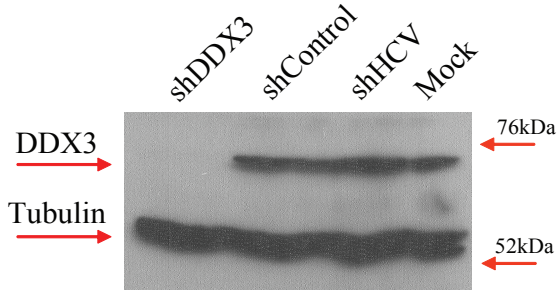

B

Fold change from shControl		
	24hrs	**48hrs**
shDDX3	- 2.12	- 3.11
shHCV	- 14.70	- 19.92
mock	+ 0.20	- 0.07

Figure 3.17. Effect of DDX3 Knockdown in Huh-7 cells transiently replicating N17 SGR/JFH1$_{WT}$ replicon RNA at various timepoints after 72hr shRNA transduction.

(A) Huh-7 cells were electroporated with 10 µg N17 SGR/JFH1$_{WT}$ replicon RNA at 72 h post-transduction with indicated lentivirus. Cell lysates were assayed at the indicated time points post-electroporation for luciferase activity. Mean values and standard deviations represent a single experiment performed with three technical repeats. A portion of cells from each set of transduced cells were lysed in SB at 72 h post-transduction and probed with the anti-DDX3 mAb AO196. Anti-α-Tubulin mAb was used as a loading control. **(B)** Table showing the fold-changes in luciferase activity in cells transduced with indicated lentivirus compared to cells transduced with shControl.

A

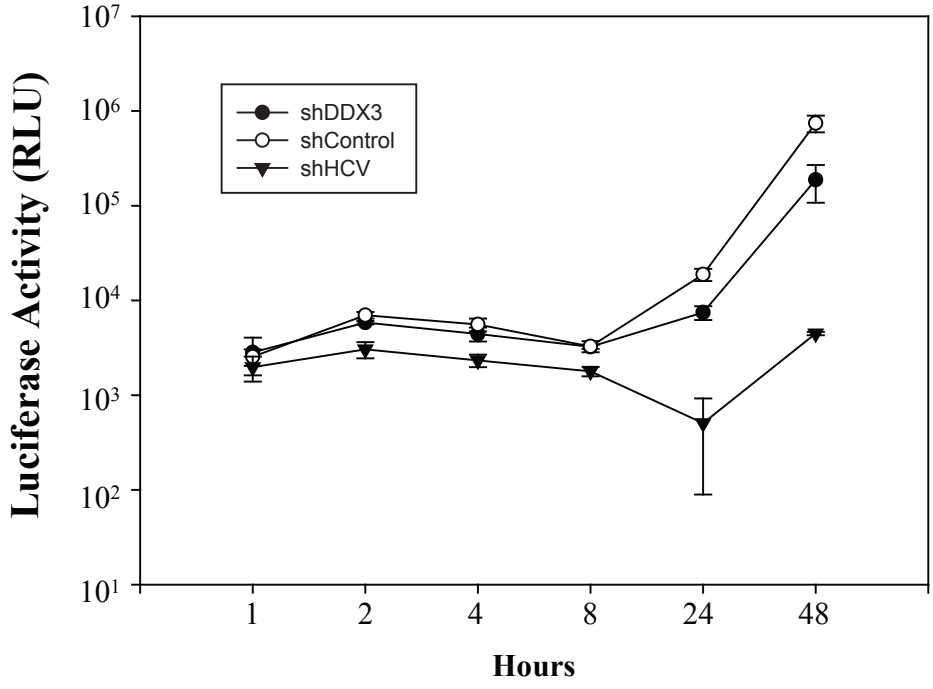

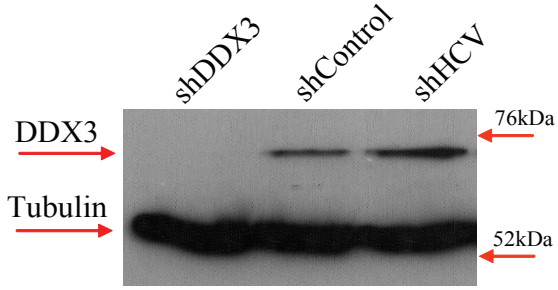

B

Fold change from shControl		
	24hr	**48hr**
shDDX3	- 2.51	- 3.90
shHCV	- 37.13	- 166.17

Figure 3.18. Effect of DDX3 Knockdown on N17 SGR/JFH1$_{WT}$ replication using lower input RNA levels.

(A) Huh-7 cells were electroporated with 0.1 µg N17 SGR/JFH1$_{WT}$ replicon RNA at 48 h post-transduction with indicated lentivirus. Cell lysates were assayed at the indicated time points post-electroporation for luciferase activity. Mean values and standard deviations represent a single experiment performed with three technical repeats. A portion of cells from each set of transduced cells were lysed in SB at 48 h post-transduction and probed with anti-DDX3 and anti-α-Tubulin mAbs to determine protein levels at time of electroporation. **(B)** Table showing the fold-changes in luciferase activity in cells transduced with indicated lentivirus compared to cells transduced with shControl.

Thus, I wished to test the effects of DDX3 knockdown on translation of the replication-deficient N17 SGR/JFH1$_{GND}$ replicon. This construct was generated by digesting pJFH1$_{GND}$ with *Hind*III and *Sfi*I, excising the NS5B GND motif and subsequently inserting this fragment between the *Hind*III and *Sfi*I sites of the N17 SGR/JFH1$_{WT}$ plasmid. The replication profile of this replicon was determined by electroporating 10 μg of N17 SGR/JFH1$_{GND}$ and N17 SGR/JFH1$_{WT}$ RNA into Huh-7 cells in parallel and comparing luciferase readings at selected timepoints post-electroporation from both sets of cells. Luciferase readings in cell lysates from the two sets of cells were almost identical up to 8 h post-electroporation, whereupon readings begin to decline dramatically in N17 SGR/JFH1$_{GND}$ cells and increase significantly in N17 SGR/JFH1$_{WT}$ cells (Fig 3.19). To determine a potential role for DDX3 in HCV translation, N17 SGR/JFH1$_{GND}$ RNA was electroporated into DDX3-depleted cells and the various control sets of transduced cells in parallel and cell extracts lysed for luciferase analysis at 1, 2, 4, 8, 24 and 48 h post-electroporation from each set of cells (Fig 3.20A, B and C). No significant difference in luciferase expression was observed between any two sets of transduced cells at any of the numerous time points (see appendix 4 for statistical analysis of data from Fig 3.20), indicating that DDX3 knockdown does not impair genome translation. It was perhaps surprising to note that luciferase activity was unperturbed in shHCV-transduced cells compared to shControl-transduced cells at any of the early time points post-electroporation, given that these cells produce RNA molecules that target the 5'UTR directly. One possible explanation for this result is that, at these early timepoints post-electroporation, the rate of replicon translation occurs at a far faster rate than that of mRNA cleavage and gene silencing by the shRNA machinery, which may lead to insignificant reductions in luciferase activity in these transduced cells.

Next, I wished to determine the effects of DDX3 knockdown on SGR replication during prolonged culture. To do this, I began by testing the efficiency of colony formation in DDX3-depleted Huh-7 cells transfected with RNA from the bicistronic BLAST SGR/JFH1$_{WT}$ replicon (described earlier in Fig 3.11A). 10 μg of this RNA was electroporated into DDX3-deficient Huh-7 cells (transduced with shDDX3 lentivirus for 48 h beforehand), which were subsequently plated onto separate 6-well culture dishes at a density of 100,000 cells per well. Similar work was performed with shControl-, shHCV- and shCD81-transduced Huh-7 cells. Once plated, all cells were treated with

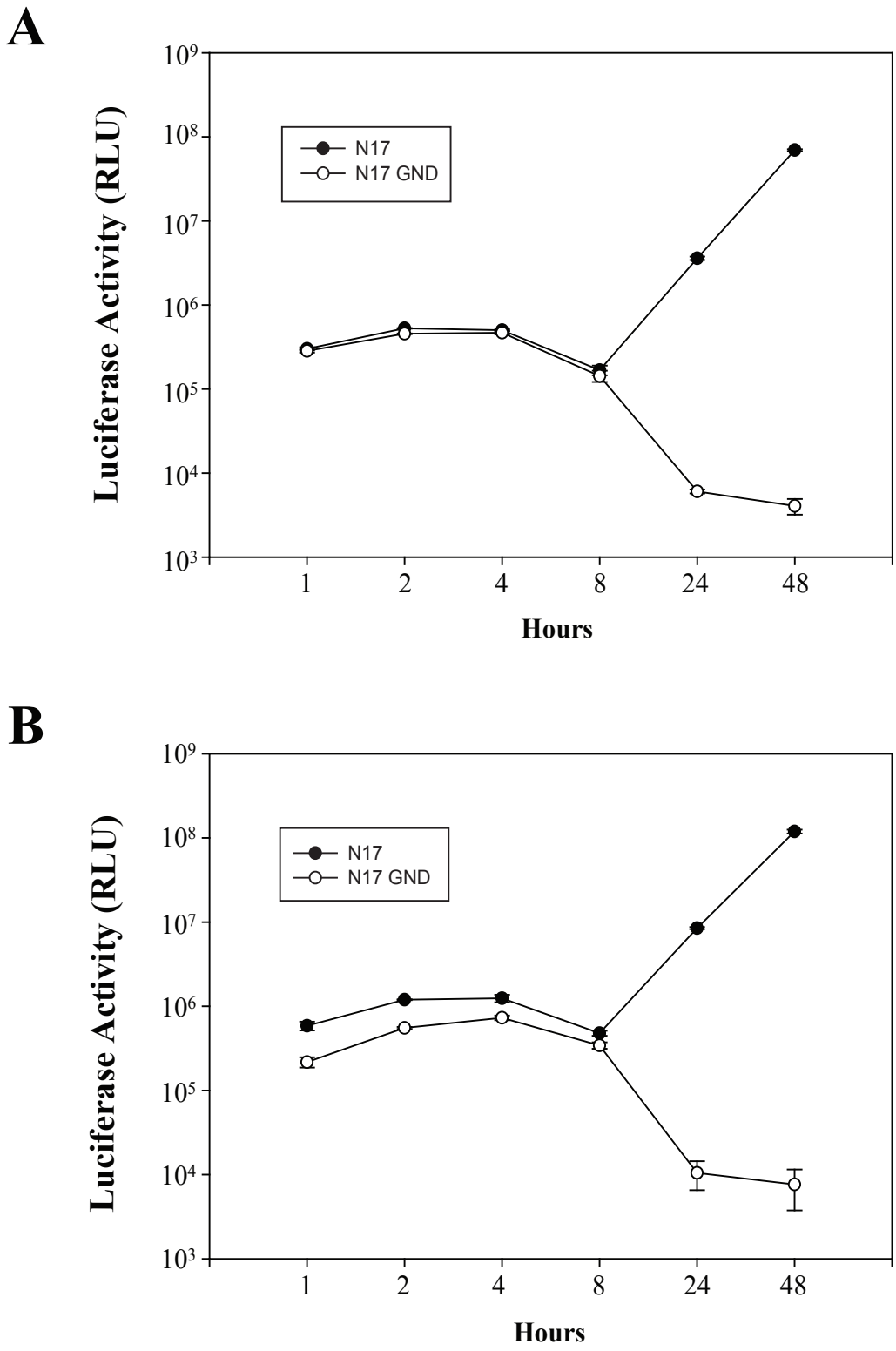

Figure 3.19. Replication profile of N17 SGR/JFH1$_{WT}$ compared to N17 SGR/JFH1$_{GND}$.

Two independent experiments represented by **A** and **B**. In each case, Huh-7 cells were electroporated with either 10 µg N17 SGR/JFH1$_{WT}$ replicon RNA or 10 µg replication-deficient N17 SGR/JFH1$_{GND}$ replicon RNA. Cell lysates were assayed at the indicated time points post-electroporation for luciferase activity. Error bars indicate the standard deviation of the mean of three technical repeats in each individual experiment.

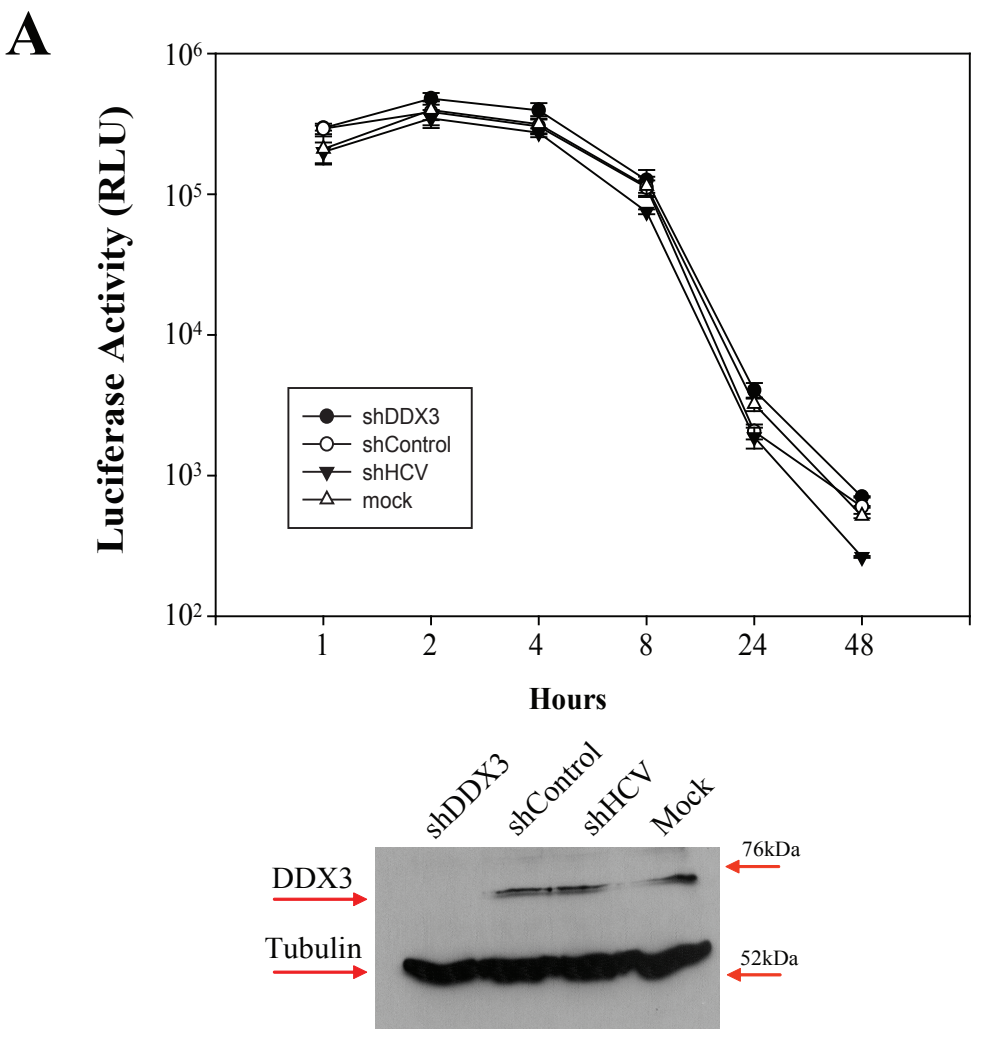
A
Luciferase Activity (RLU)
10^6
10^5
10^4
10^3
10^2
shDDX3
shControl
shHCV
mock
1
2
4
8
24
48
Hours
shDDX3
shControl
shHCV
Mock
DDX3
Tubulin
76kDa
52kDa

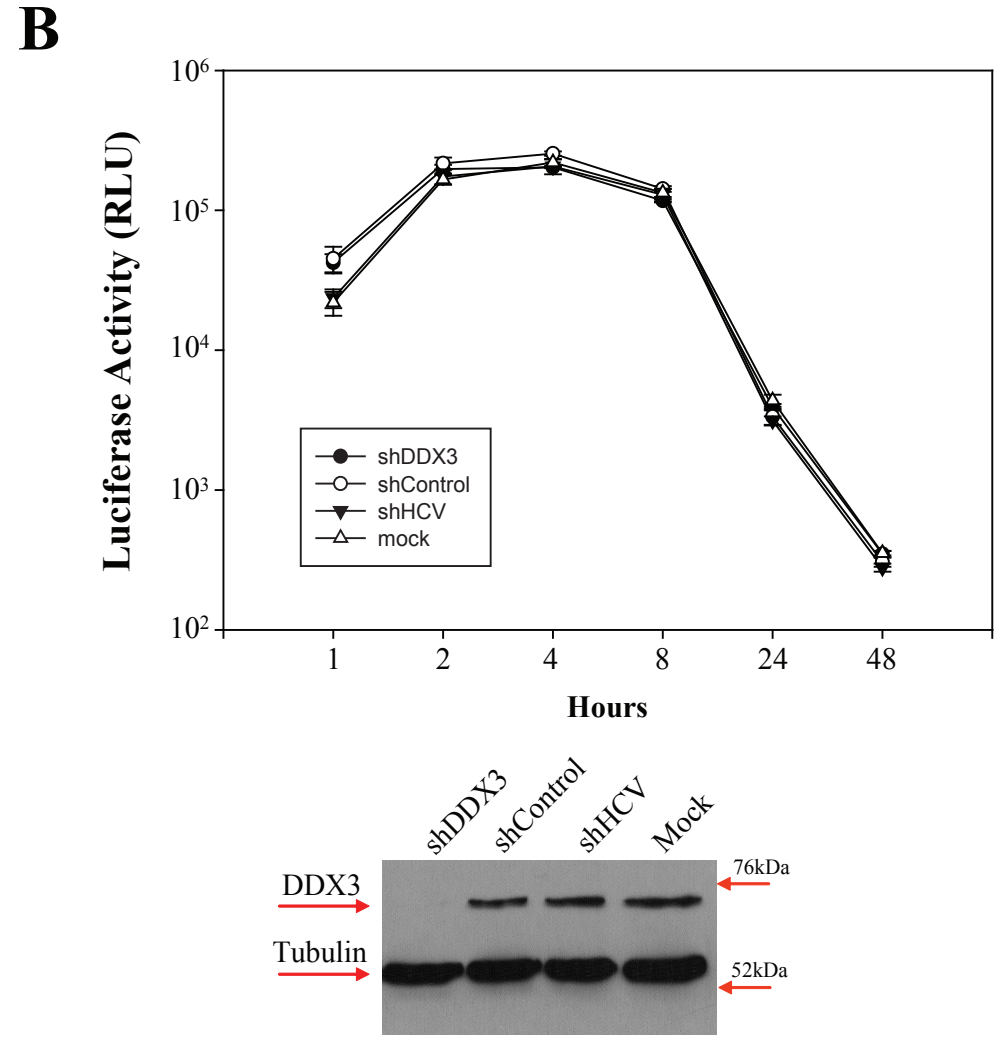
B
Luciferase Activity (RLU)
10^6
10^5
10^4
10^3
10^2
shDDX3
shControl
shHCV
mock
1
2
4
8
24
48
Hours
shDDX3
shControl
shHCV
Mock
DDX3
Tubulin
76kDa
52kDa

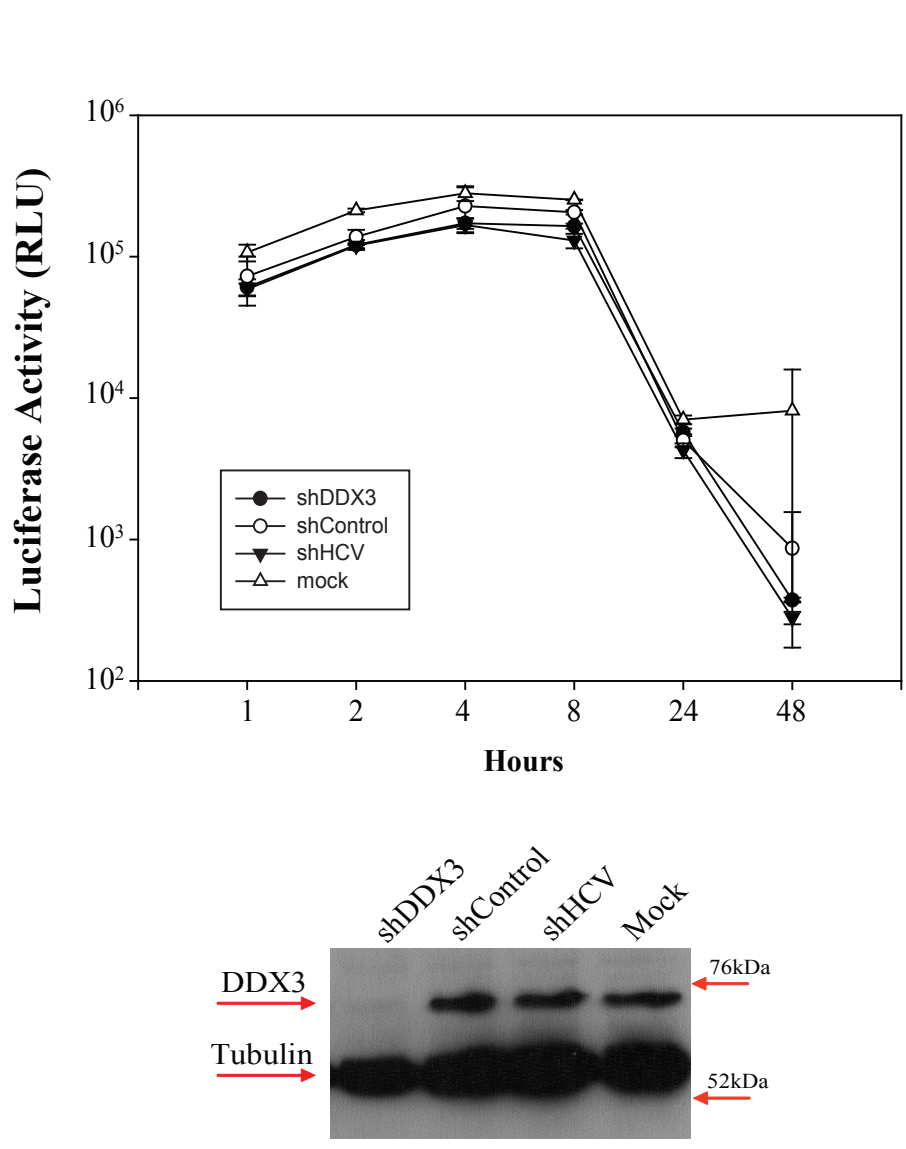

Figure 3.20. Effect of DDX3 knockdown on HCV translation.

Three independent experiments represented by **A, B** and **C.** In each case, Huh-7 cells were electroporated with 10 µg N17 SGR/JFH1$_{GND}$ replicon RNA at 48 h post-transduction with indicated lentivirus. Cell lysates were assayed at the indicated time points post-electroporation for luciferase activity. Error bars indicate the standard deviation of the mean of three technical repeats in each individual experiment. A portion of cells from each set of transduced cells were lysed in SB in each experiment and probed with anti-DDX3 and anti-α-Tubulin mAbs to determine protein levels at time of electroporation.

blasticidin at 100 μg/ml. Samples from each transduced set of cells were stained with Giesma's stain solution at specific time points (2, 4, 6 and 8 days) post-electroporation of RNA. A steady decline in blasticidin-resistant cells was observed in shDDX3-transduced cells, with very few remaining at 8 days post-electroporation, while cell growth in all other sets of transduced cells was unperturbed by the presence of drug (Fig 3.21).

While these results indicated that replicons cannot survive in culture without DDX3, the speed at which DDX3-depleted cells died indicated that blasticidin may be too toxic to cell growth in a DDX3-deficient environment to perform this experiment accurately. Thus, the experiment was repeated but in this instance, I transfected the different sets of transduced cells with 5 μg NEO SGR/JFH1$_{WT}$ RNA. This replicon is essentially identical to BLAST SGR/JFH1$_{WT}$, except that the IRES of this construct directs expression of a neomycin resistance marker in place of a blasticidin cassette, as it was hoped that neomycin would not kill DDX3-depleted cells as quickly (Fig 3.22A). Each electroporated set of transduced cells was plated out at different densities onto 6-well culture dishes. Once plated, dishes with the same cell density were divided into two sets, with one set of cells (test cells) treated with neomycin at 500 μg/ml, and another set (control cells) left to grow in the absence of drug. After three weeks of culture, very few colonies were observed in the shDDX3-transduced test and control cells at any cell density, indicating that Huh-7 cells stably replicating replicon RNA cannot survive in culture for sustained periods of time without DDX3, even without the effects of antibiotic selection pressure. Slight toxic effects were observed in test and control samples of shHCV- and shCD81-transduced cells, but levels of death were negligible compared to shDDX3-transduced cells (Fig 3.22B). The toxic effects observed in control samples, where no antibiotic selection pressure had been applied for three weeks, may be due to the high level of integration of the plasmids introduced by calcium phosphate transfection into these cells post-transduction.

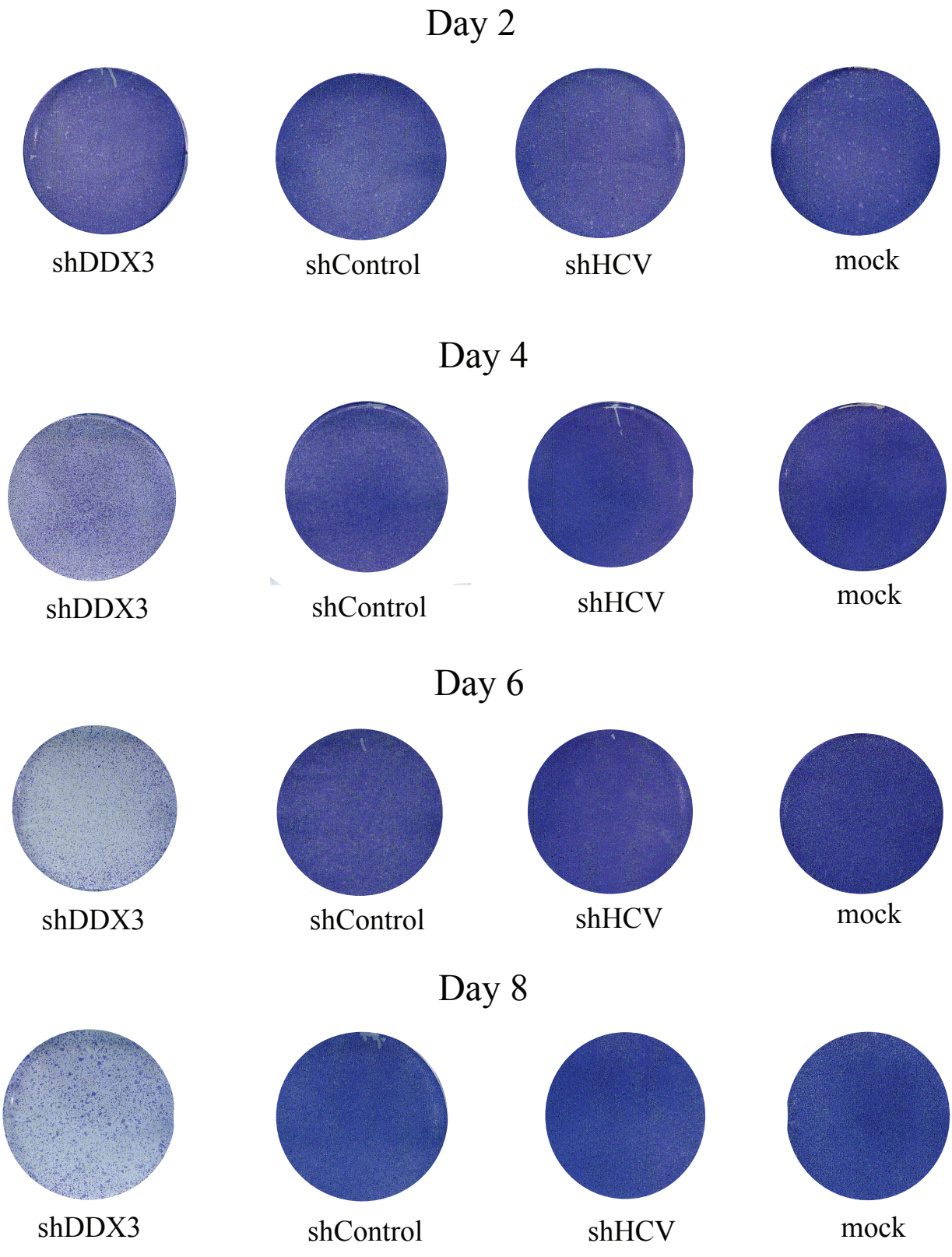

Figure 3.21. Efficiency of colony formation in DDX3 knockdown cells using BLAST SGR/JFH1$_{WT}$ replicon RNA.

Huh-7 cells were electroporated with 10 µg of BLAST SGR/JFH1$_{WT}$ replicon RNA at 48 h post-transduction with indicated lentivirus and plated onto 6-well culture dishes at a density of 100,000 cells per well. Blasticidin-resistant colonies were stained with Giesma's stain solution at specific time points (2, 4, 6 and 8 days) post-electroporation of RNA.

A

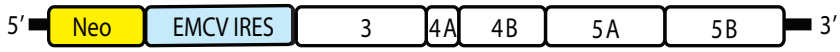

B

Neo

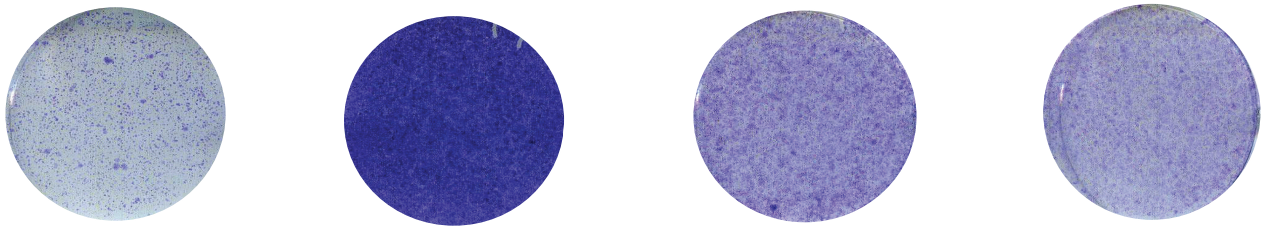

shDDX3 shControl shHCV shCD81

No drug

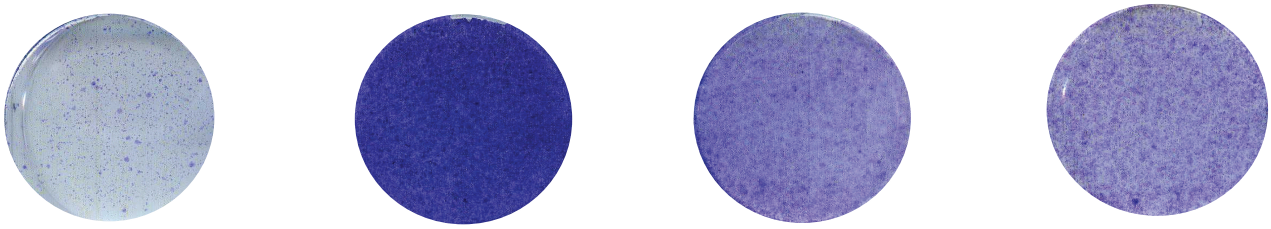

shDDX3 shControl shHCV shCD81

C

Neo

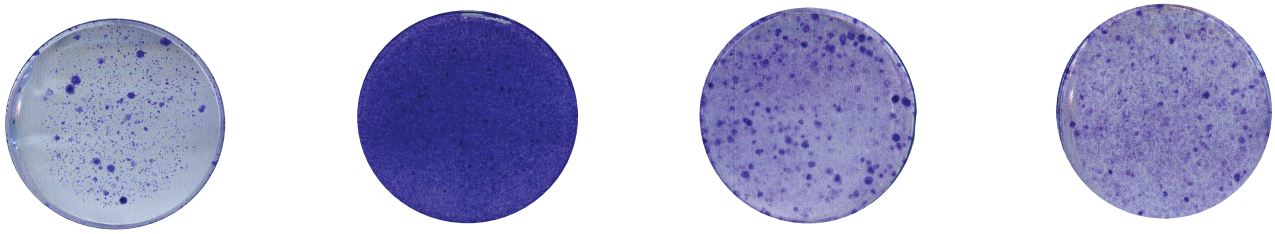

shDDX3 shControl shHCV shCD81

No drug

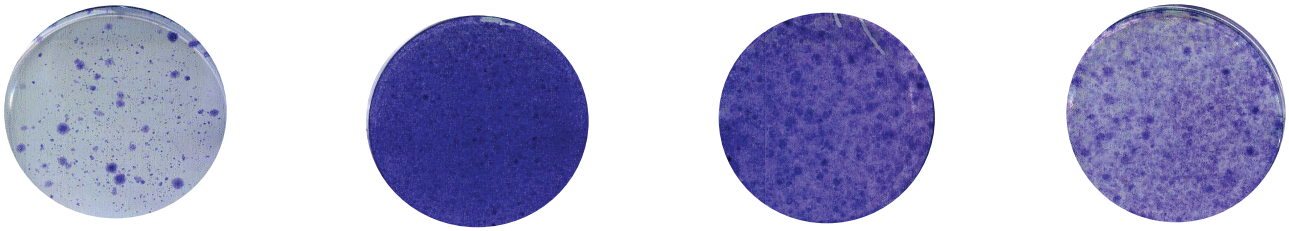

shDDX3 shControl shHCV shCD81

D

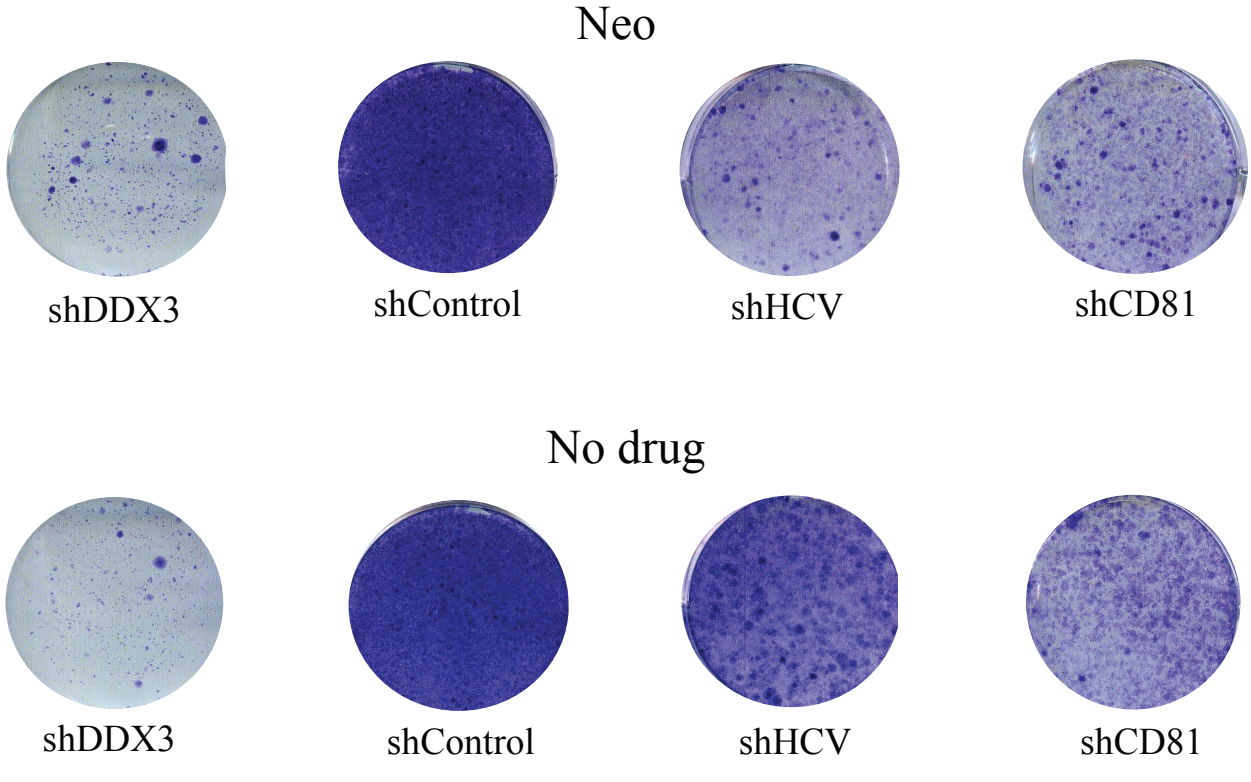
Neo
shDDX3
shControl
shHCV
shCD81
No drug
shDDX3
shControl
shHCV
shCD81

E

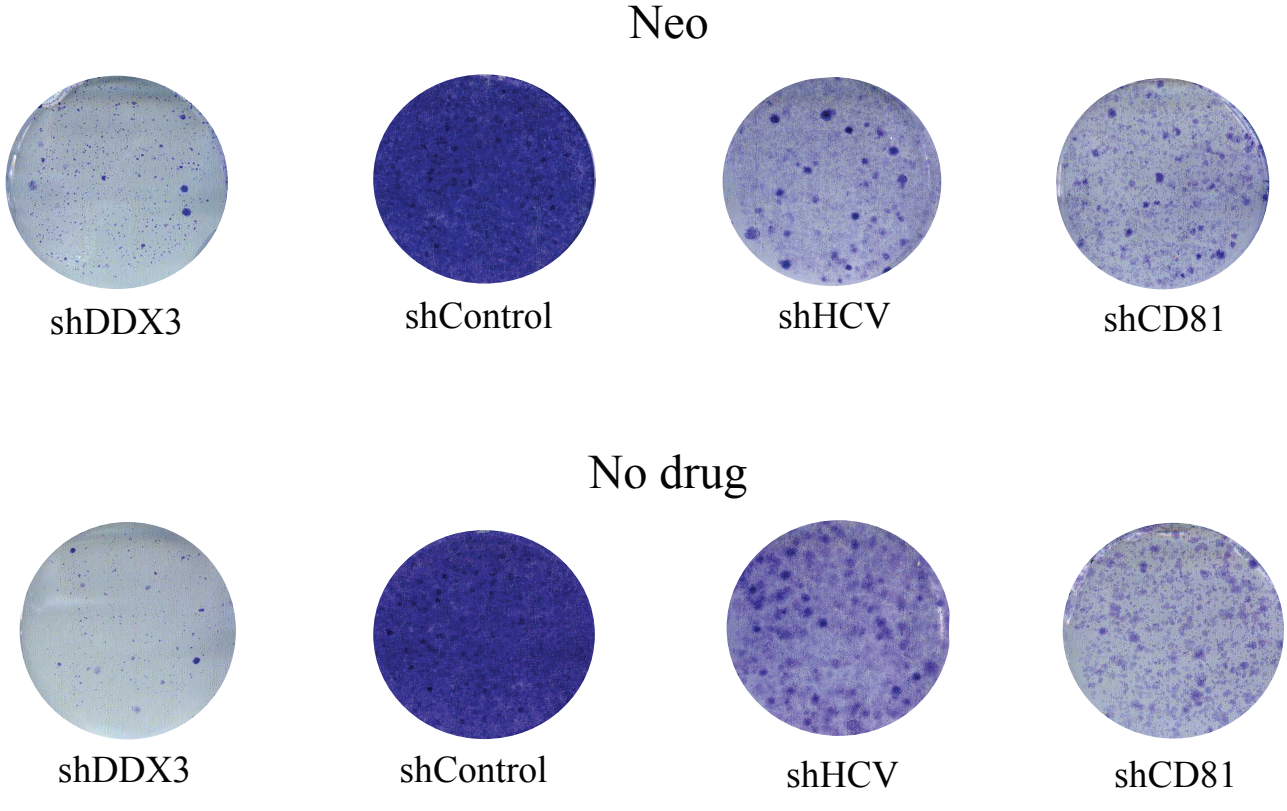
Neo
shDDX3
shControl
shHCV
shCD81
No drug
shDDX3
shControl
shHCV
shCD81

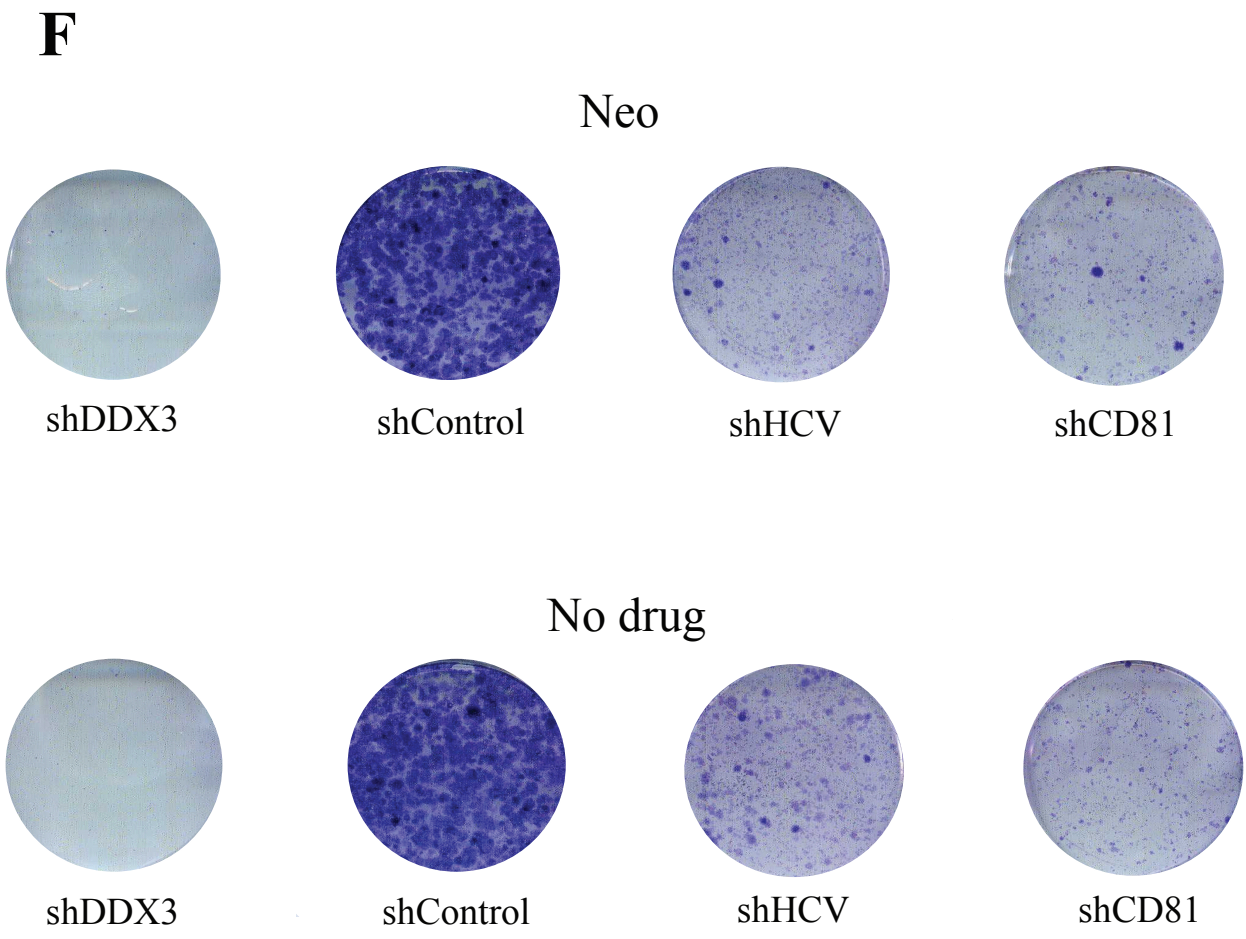

Figure 3.22. Efficiency of colony formation in DDX3 knockdown cells using NEO SGR/JFH1$_{WT}$ replicon RNA.

(A) Schematic illustrating the principal features of the bicistronic NEO SGR/JFH1$_{WT}$ replicon. This construct contains the HCV internal ribosome entry site (IRES), which directs expression of the neomycin resistance marker, and the encephalomyocarditis virus (EMCV) IRES, which directs the expression of the HCV nonstructural (NS) proteins NS3 to NS5B. **(B)** Huh-7 cells were electroporated with 10 µg of NEO SGR/JFH1$_{WT}$ replicon RNA at 48 h post-transduction with indicated lentivirus, and plated onto 6-well culture dishes at specific denstities. Neomycin-resistant colonies were stained with Giesma's stain solution at 3 weeks post-electroporation of RNA. The starting cell population in each well in this experiment was 100,000 cells. Repeats of this experiment with starting cell populations in each well of 75,000 **(C)**, 50,000 **(D)**, 25,000 **(E)** and 10,000 **(F)** cells were also performed.

3.1.7. DDX3 does not Colocalise with HCV Replication Complex Component NS5A

Previous studies have shown that the HCV non-structural protein NS5A plays an integral role in the formation and composition of the HCV replication complex. To test whether DDX3 is relocalised to replication complexes during HCV RNA replication, I measured its intracellular localization in SGR-containing cells expressing endogenous levels of DDX3 as well as cells depleted by shRNA knockdown. Huh-7 cells that had been transduced for 48 h with lentivirus expressing shDDX3 or shControl were electroporated with 10 µg of SGR/JFH1$_{WT}$ RNA before being seeded on coverslips at a volume of 4 x 10^4 cells/well in a 24-well plate. At 48 h post-electroporation, cells were fixed and labelled with antibodies specific for DDX3 and NS5A and analysed under the microscope. No colocalisation of these two proteins was observed in shControl-transduced cells. DDX3-deficient cells gave similar results, despite a lower signal intensity for DDX3 (Fig 3.23A and B), an intensity drop confirmed by western blot (Fig 3.23I). The lack of colocalisation was confirmed by quantitative pixel analysis of these confocal microscopic images (shDDX3: Fig 3.23 C, D and E, shControl: Fig 3.23 F, G and H). Correlation coefficients were calculated for each couple of intensity values (*R*_values of 0.36, 0.04 and 0.16 were observed for three different DDX3-depleted cell samples, *R*_values of 0.11, 0.11 and - 0.11 in three separate shControl-transduced cell samples). These low correlation coefficients further demonstrated the lack of colocalisation between NS5A and DDX3. These results indicate that DDX3 may not be recruited into replication complexes. However, it is also possible that only a few molecules of the protein are present at these sites and cannot be detected by IF analysis.

3.1.8. Effect of DDX3 Knockdown on Huh-7.5 Cells

Removal of a replicon from Huh-7 cells by treatment with IFN or a selective drug frequently results in cell clones that support higher levels of HCV RNA replication as compared to naïve Huh-7 cells. The underlying reason for the higher permissiveness is largely unknown, but for one particular cell clone, designated Huh-7.5 cells, a single point mutation in the dsRNA sensor RIG-I, T55I, was found to be involved in higher permissiveness for HCV RNA replication (Blight *et al*., 2002; Sumpter *et al*., 2005). I

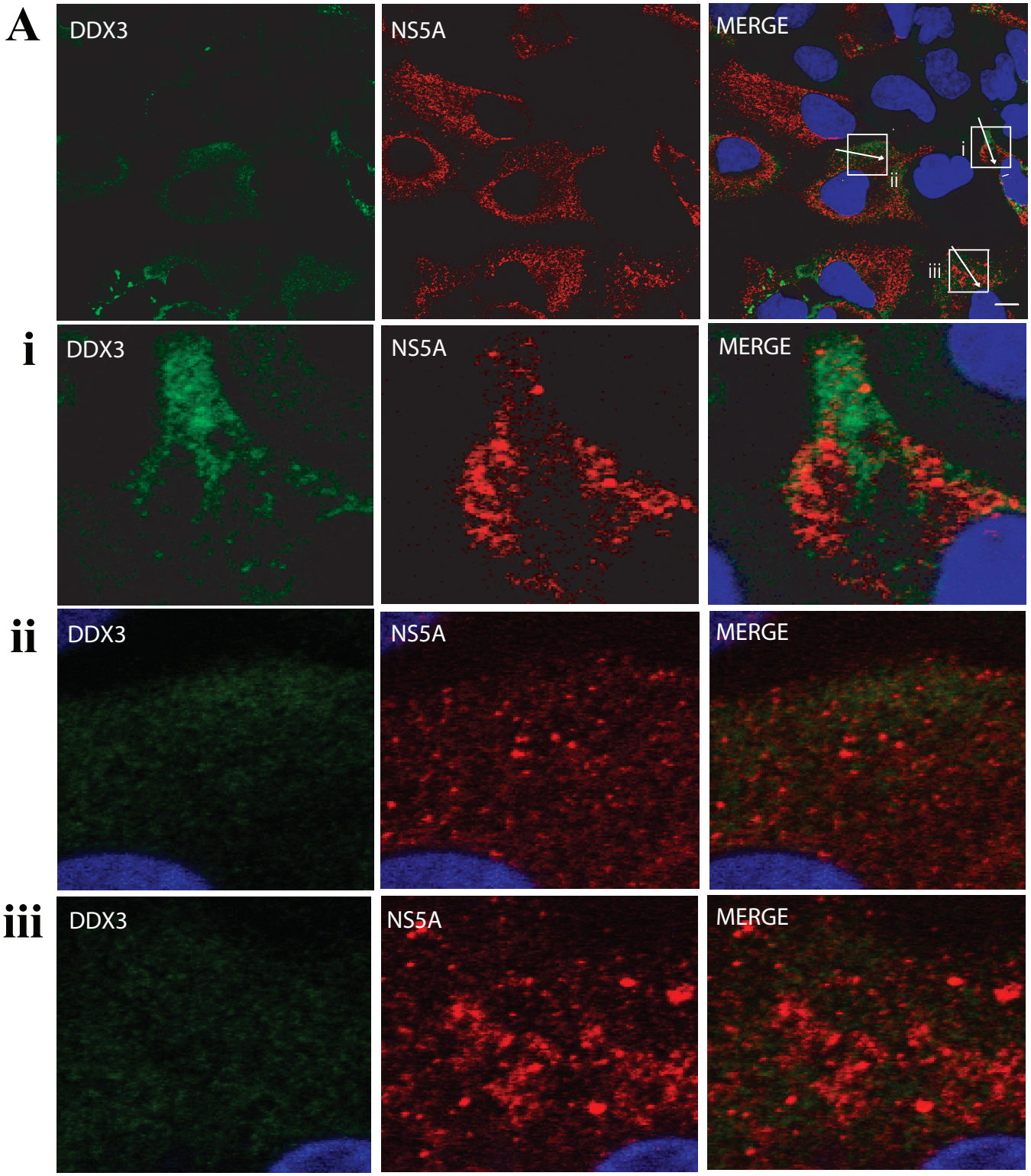
A
DDX3
NS5A
MERGE
i
ii
iii
i
DDX3
NS5A
MERGE
ii
DDX3
NS5A
MERGE
iii
DDX3
NS5A
MERGE

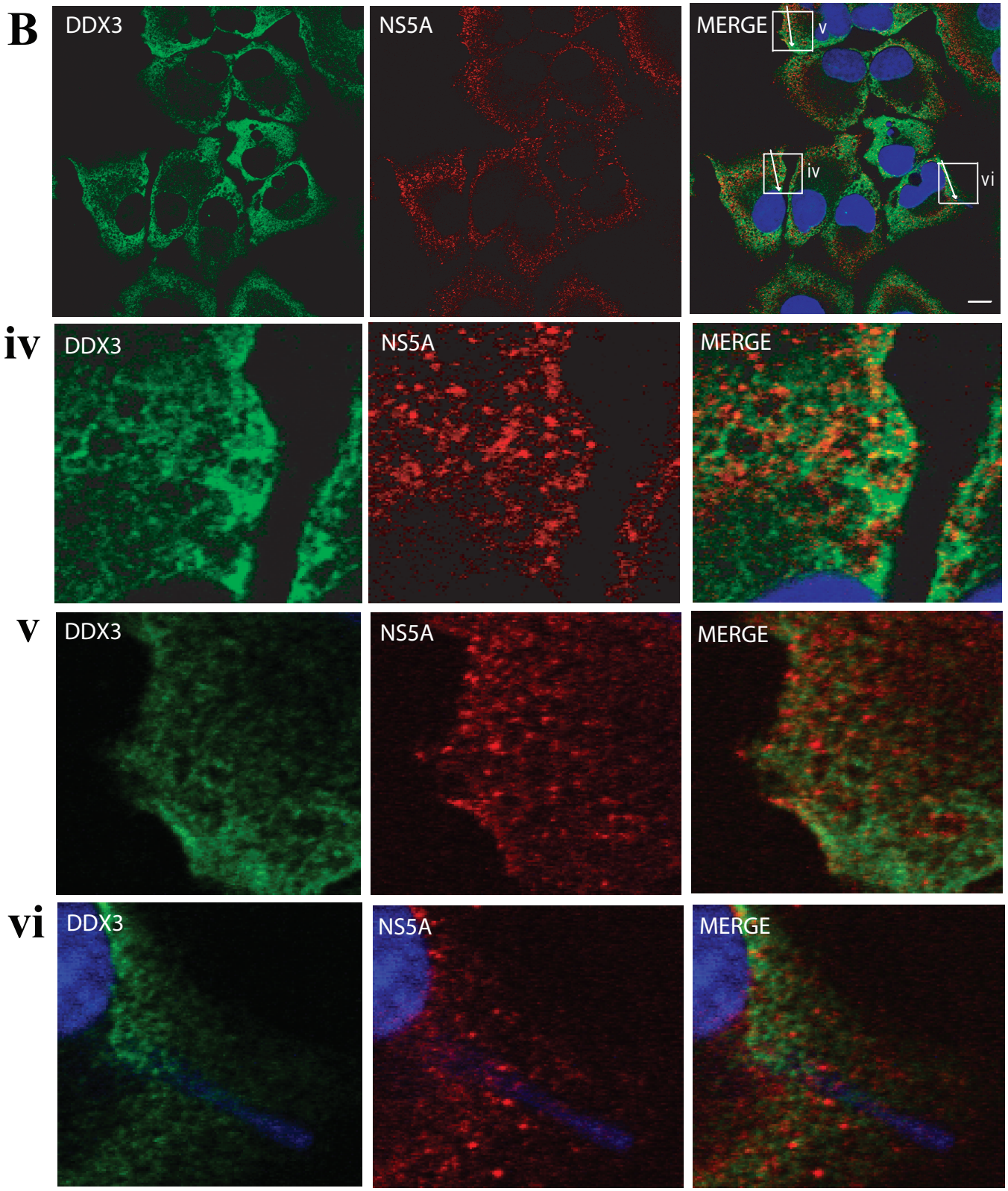
B
DDX3
NS5A
MERGE
v
iv
vi
iv
DDX3
NS5A
MERGE
v
DDX3
NS5A
MERGE
vi
DDX3
NS5A
MERGE

C

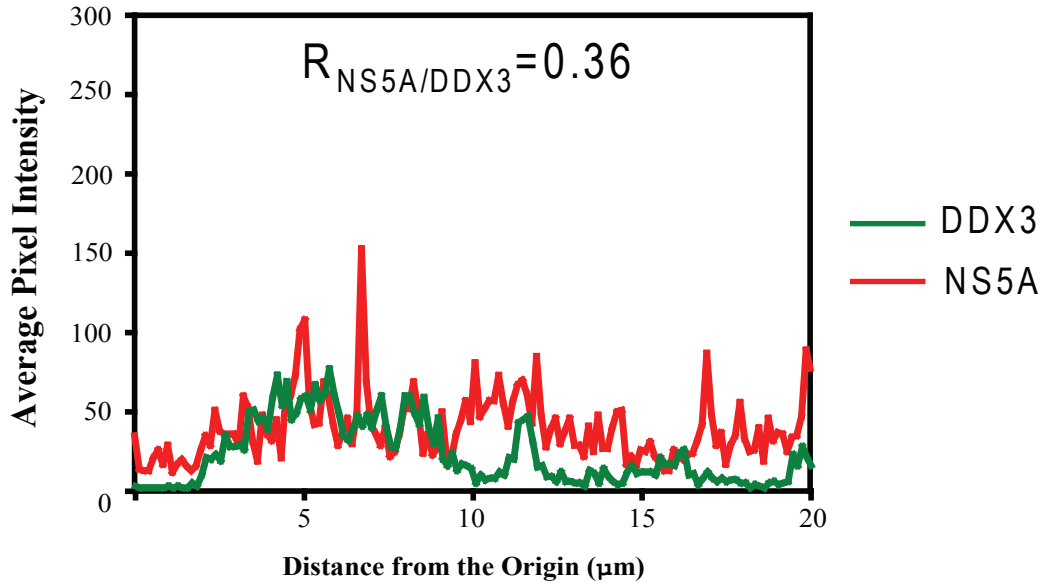
R NS5A/DDX3=0.36
Average Pixel Intensity
300
250
200
150
100
50
0
5
10
15
20
Distance from the Origin (µm)
DDX3
NS5A

D

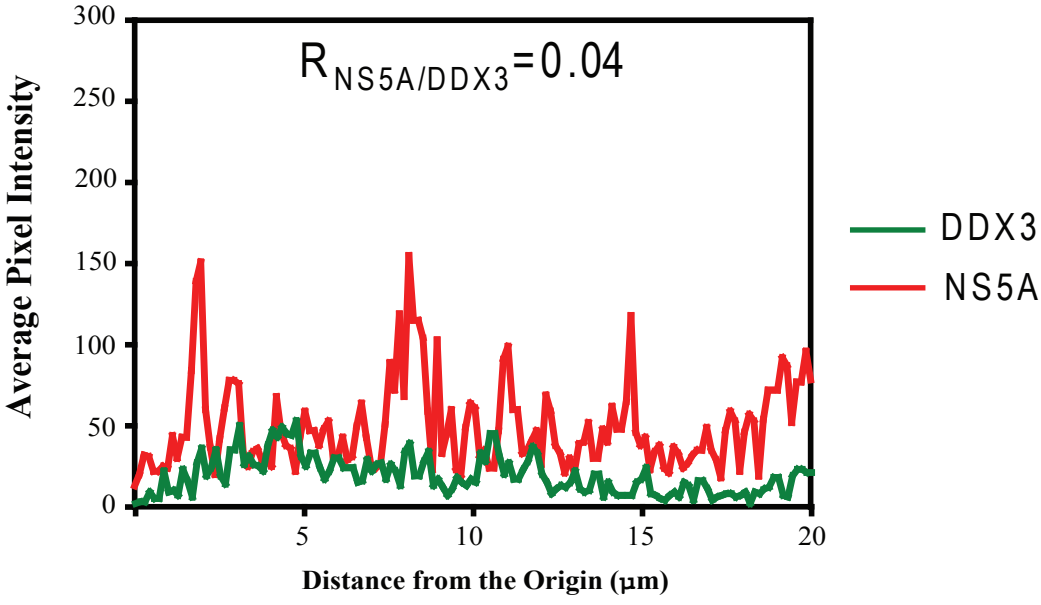
R NS5A/DDX3=0.04
Average Pixel Intensity
300
250
200
150
100
50
0
5
10
15
20
Distance from the Origin (µm)
DDX3
NS5A

E

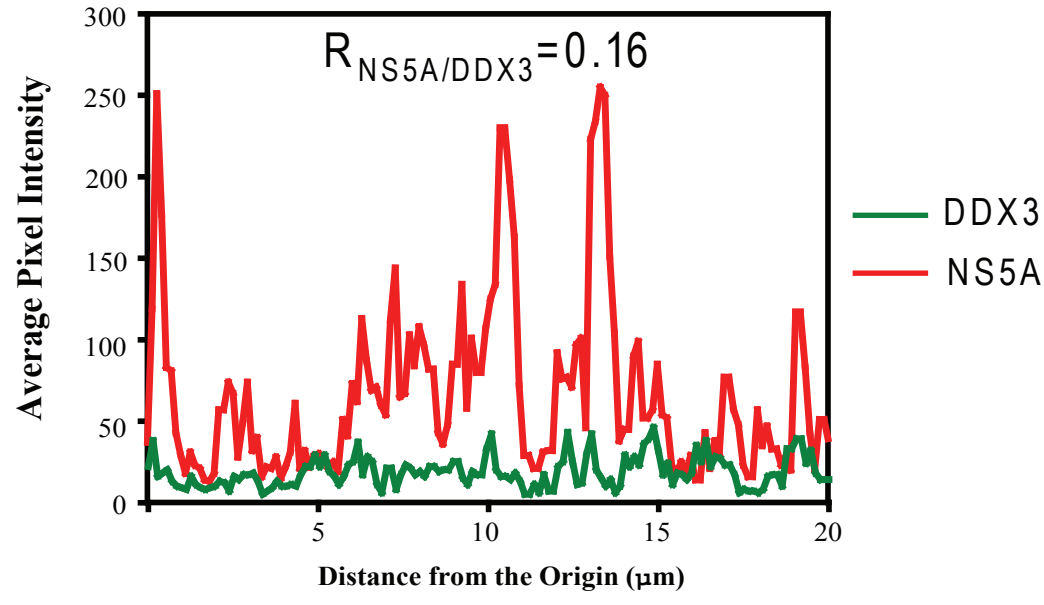
R NS5A/DDX3=0.16
Average Pixel Intensity
300
250
200
150
100
50
0
5
10
15
20
Distance from the Origin (µm)
DDX3
NS5A

F

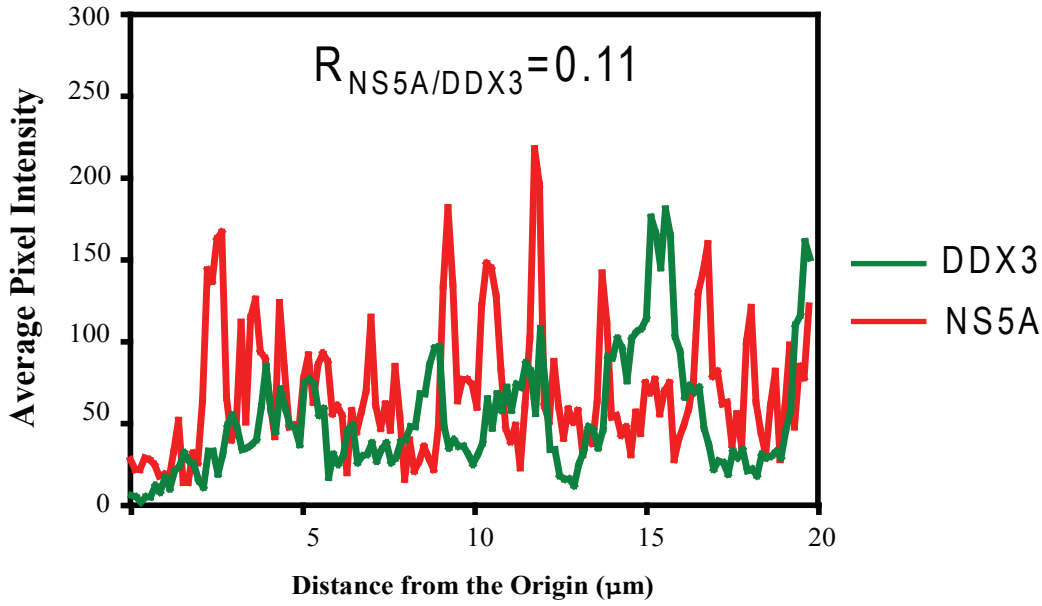
$R_{NS5A/DDX3}$=0.11
Average Pixel Intensity
300
250
200
150
100
50
0
5
10
15
20
Distance from the Origin (µm)
DDX3
NS5A

G

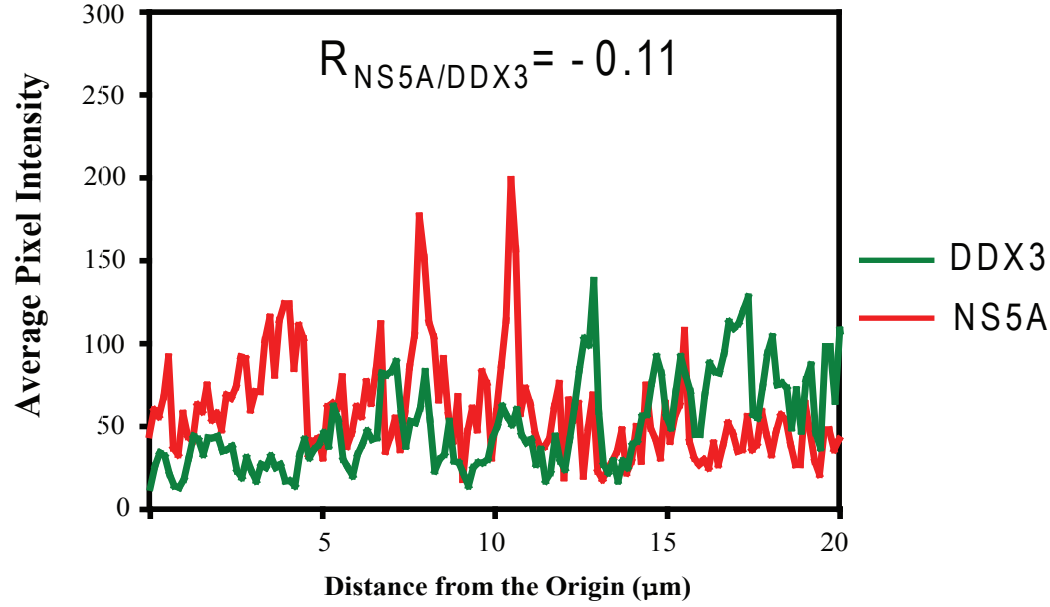
$R_{NS5A/DDX3}$= - 0.11
Average Pixel Intensity
300
250
200
150
100
50
0
5
10
15
20
Distance from the Origin (µm)
DDX3
NS5A

H

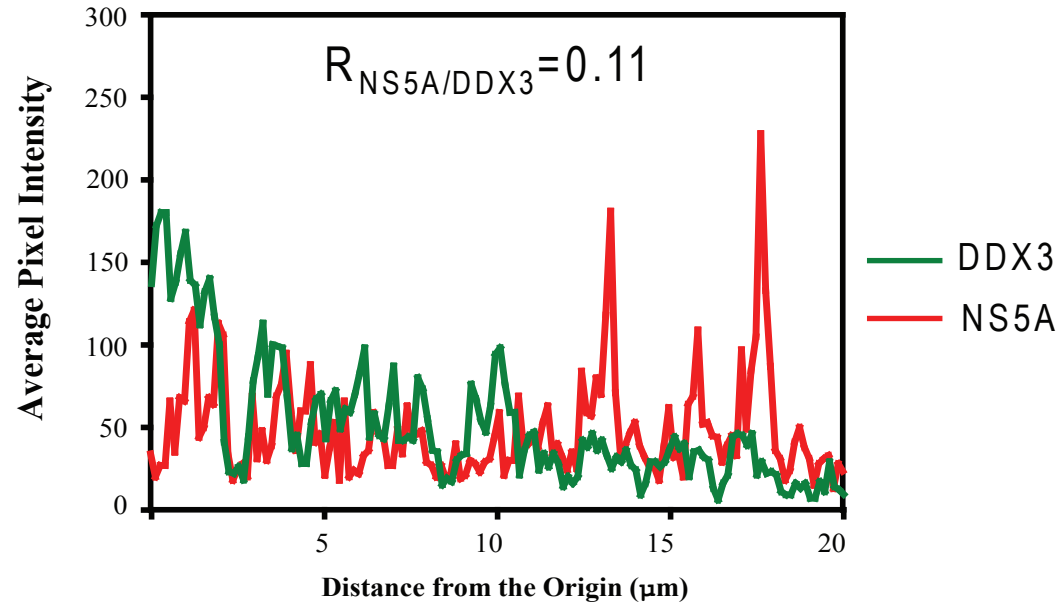
$R_{NS5A/DDX3}$=0.11
Average Pixel Intensity
300
250
200
150
100
50
0
5
10
15
20
Distance from the Origin (µm)
DDX3
NS5A

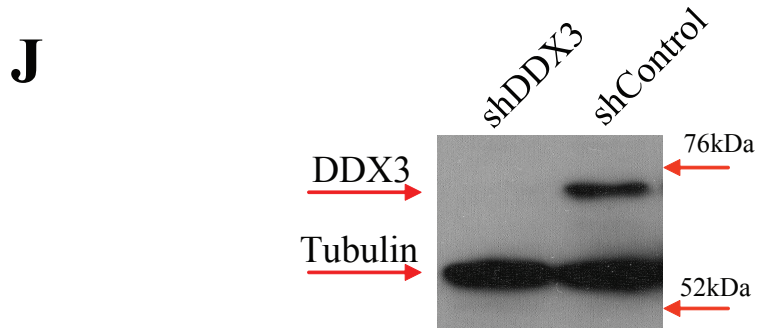

Figure 3.23. Localisation of DDX3 in Huh-7 cells harbouring a subgenomic replicon.

Huh-7 cells were transduced with either shDDX3 **(A)** or shControl **(B)** lentivirus. At 48 h post-transduction, both shDDX3- and shControl-transduced cells were electroporated with 10 µg of SGR/JFH1$_{WT}$ RNA. At 48 h post-electroporation, cells were fixed and labelled with antibodies specific for DDX3 (green) and NS5A (red). Slides of Huh-7 cells transduced with shDDX3 and shControl were subsequently examined with a Zeiss Laser Scanning LSM 510 Meta microscope. Scale bar, 10 µm. Higher magnification analysis of shDDX3 (**i, ii and iii**) and shControl (**iv, v and vi**) were also undertaken. Line scan results of each of these higher magnification images were generated for shDDX3 **(C, D** and **E,** corresponding to areas **i, ii and iii respectively)** and shControl **(F, G** and **H,** corresponding to areas **iv, v and iv respectively)**, depicting a linear trace of the fluorescence intensity of individual pixels along a segment of the white arrow overlaying the merged image. Red and green traces correspond to the colour of the fluorophores shown in merged images. Correlation coefficients (also referred to as **R**) for each couple of intensity values are shown in each graph. **(J)** A portion of cells from each cell-line were lysed in SB at 48 h post-transduction and probed with the anti-DDX3 mAb AO196. Anti-α-Tubulin mAb was used as a loading control.

wished to determine what effect the defective RIG-I response in Huh-7.5 cells would have on the role of DDX3 in the HCV lifecycle. I began by assessing the influence of DDX3 abundance on virus infection in Huh-7.5 cells. This was done by measuring the replication of $JFH1_{WT}$ virus by focus forming assay following infection of Huh-7.5 cells that had previously undergone 48 h transduction with selected lentivirus. Huh-7 cells were also transduced and infected in parallel. Virus replication levels were found to be substantially lower in DDX3-deficient Huh-7.5 cells compared to shControl-transduced Huh-7.5 cells, while almost all replication was ceased in Huh-7.5 cells transduced with shHCV. Indeed, analysis by focus forming assay revealed that there were no significant difference in infectivity between shDDX3- and shControl-transduced Huh-7 cells (22/97 foci observed = 77.3 % decrease) and shDDX3- and shControl-transduced Huh-7.5 cells (37/118 foci observed = 68 % decrease) (Fig 3.24A and B), while western blot analysis showed DDX3 was undetectable in both shDDX3-transduced Huh-7.5 and Huh-7 cells at 48 h post-transduction (Fig 3.24C). Next, I investigated the effect of DDX3 knockdown on the replication of transiently transfected N17 SGR/$JFH1_{WT}$ replicon in Huh-7.5 cells. An experiment was performed identical to that presented in Fig 3.14, except in this case Huh-7.5 cells were transduced with different lentivirus and electroporated with replicon RNA. Results obtained were not significantly different to those detected in Huh-7 cells, with reductions in shDDX3-transduced Huh-7.5 cells only observed at 24 and 48 h post-electroporation and at levels similar to those observed in Huh-7 experiments (Fig 3.25). These results suggest that the proviral role of DDX3 is not influenced by the T55I RIG-I mutation.

3.1.9. Effect of DDX3 Knockdown on Viral Promoter Transcription

We wished to determine if DDX3 had any general effect on viral promoter transcription and its subsequent translation. We could not use N17 SGR/JFH1 DNA to examine transcription as it does not contain the necessary polymerase factors required. Huh-7 cells were transduced with different lentivirus for 48 h before each set of transduced cells was transfected with 10 µg pGL3-Control Vector DNA (Promega). The pGL3-Control Vector (Fig 3.26A) contains SV40 promoter and enhancer sequences, which results in strong luciferase expression in healthy mammalian cells.. Cells were harvested

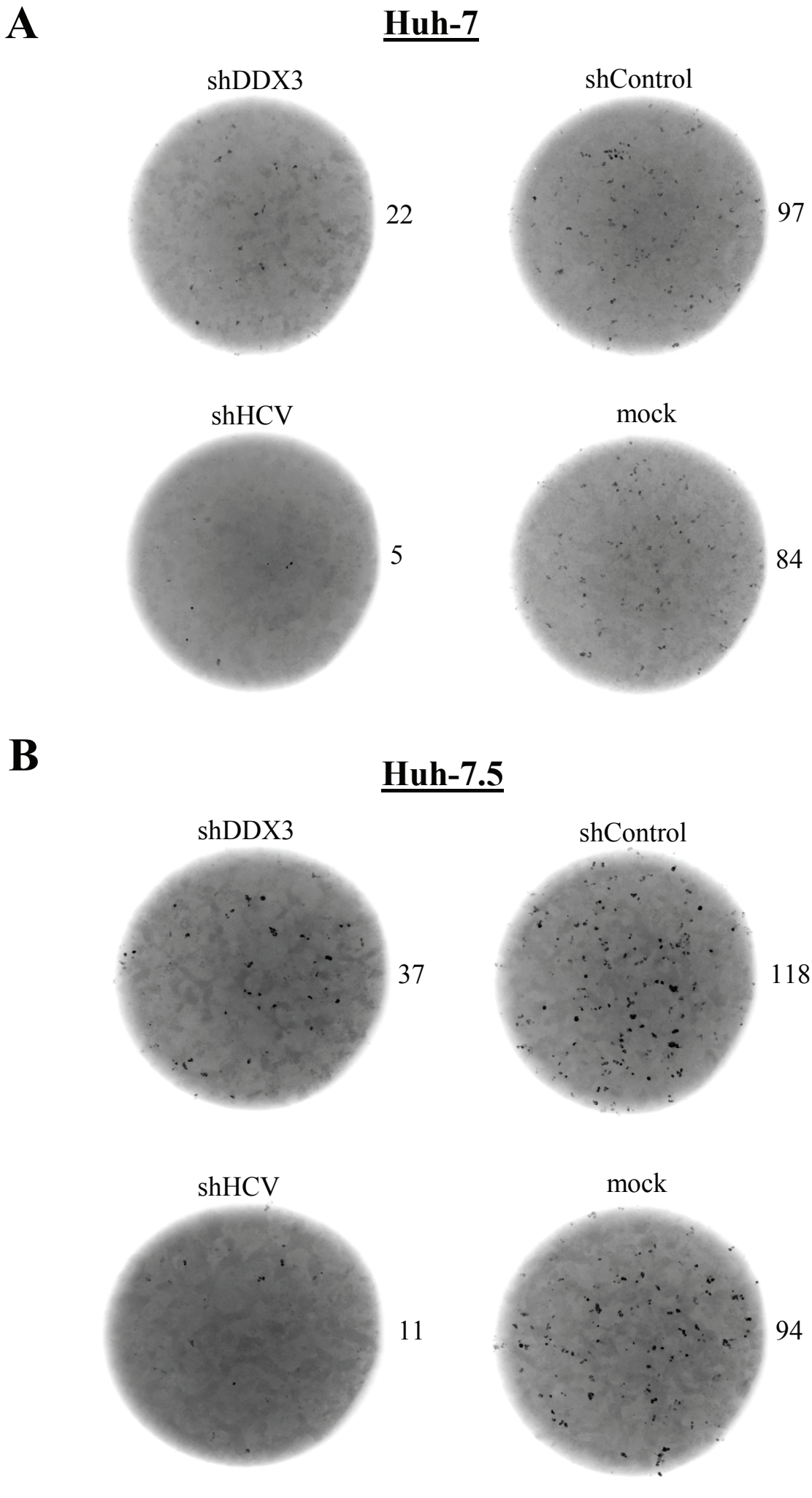
A
Huh-7
shDDX3
22
shControl
97
shHCV
5
mock
84
B
Huh-7.5
shDDX3
37
shControl
118
shHCV
11
mock
94

C

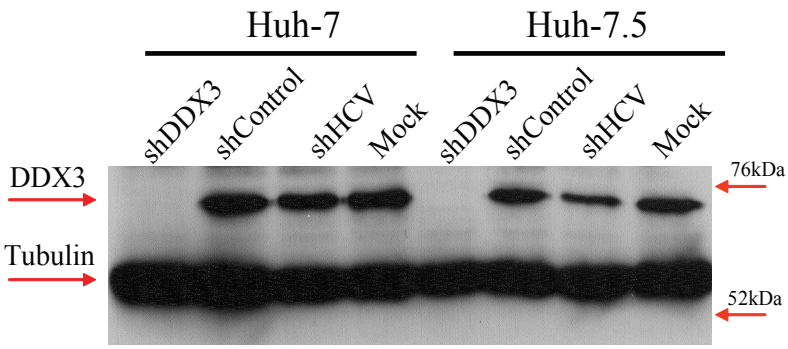

Figure 3.24. Effect of DDX3 knockdown on HCV infectivity in Huh-7 cells and Huh-7.5 cells.

An equal number of Huh-7 **(A)** and Huh-7.5 cells **(B)** were plated evenly onto 24-well culture dishes before being transduced with indicated lentivirus. At 48 h post-transduction, cells were infected with $JFH1_{WT}$ virus at an m.o.i. of 0.1 FFU/cell. At 48 h post-infection, cells were fixed and probed for NS5A protein using 9e10 mAb. Images were obtained and converted into greyscale to improve clarity. Naïve cells are in grey and infected cells are indicated by black dots. The number of foci observed in each well is indicated beside the relevant image. **(C)** Cells were harvested in SB at 48 h post-transduction and examined using the anti-DDX3 mAb AO196. Anti-α-Tubulin mAb used as a loading control.

A

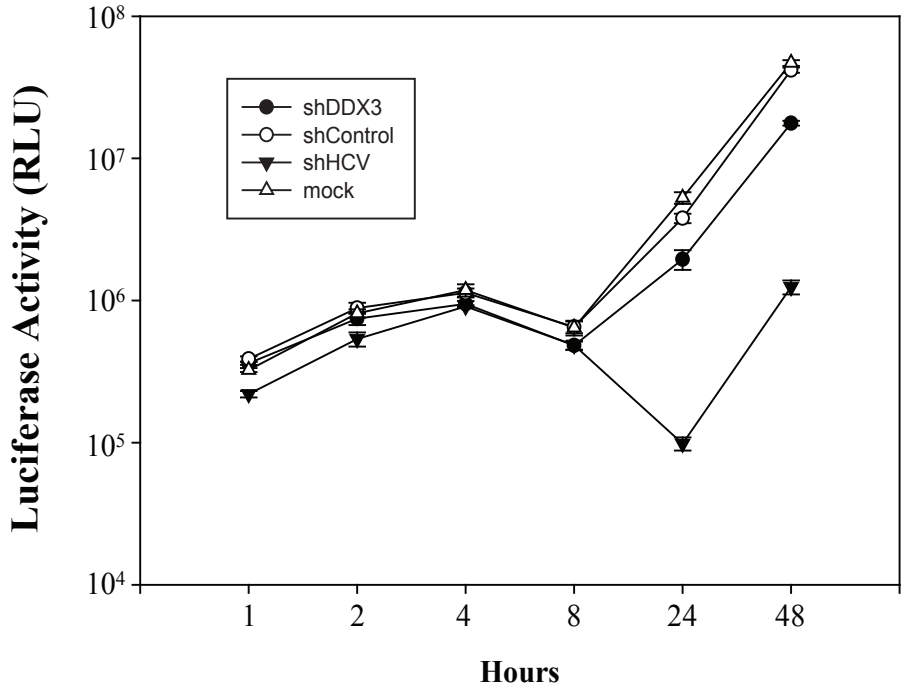

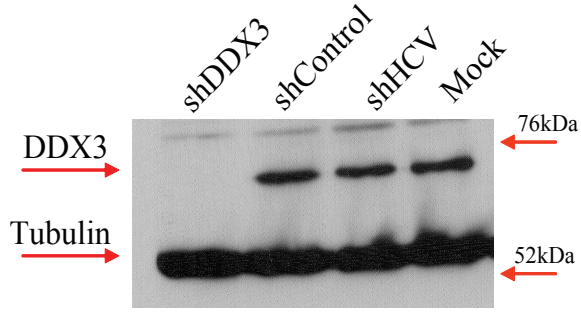

B

Fold change from shControl		
	24hrs	**48hrs**
shDDX3	- 1.94	- 2.36
shHCV	- 38.49	- 33.56
mock	+ 0.39	+ 0.12

Figure 3.25. Effect of DDX3 Knockdown in Huh-7.5 cells transiently replicating N17 SGR/JFH1$_{WT}$ replicon RNA at various timepoints.

(A) Huh-7.5 cells were electroporated with 10 µg N17 SGR/JFH1$_{WT}$ replicon RNA at 48 h post-transduction with indicated lentivirus. Cell lysates were assayed at the indicated time points post-electroporation for luciferase activity. Mean values and standard deviations represent a single experiment performed with three technical repeats. A portion of cells from each set of transduced cells were lysed in SB at 48 h post-transduction and probed with the anti-DDX3 mAb AO196. Anti-α-Tubulin mAb was used as a loading control. **(B)** Table showing the fold-changes in luciferase activity in cells transduced with indicated lentivirus compared to cells transduced with shControl.

A

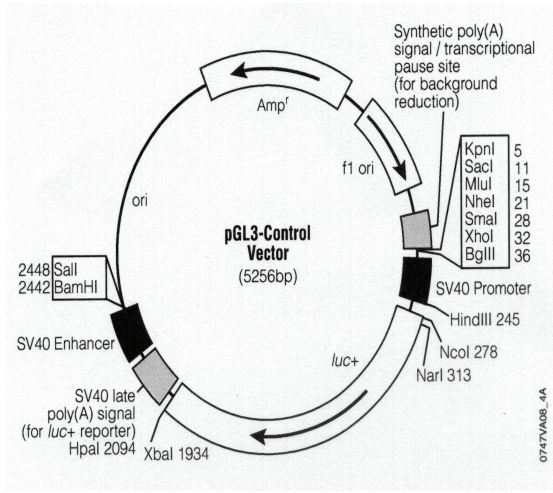

B

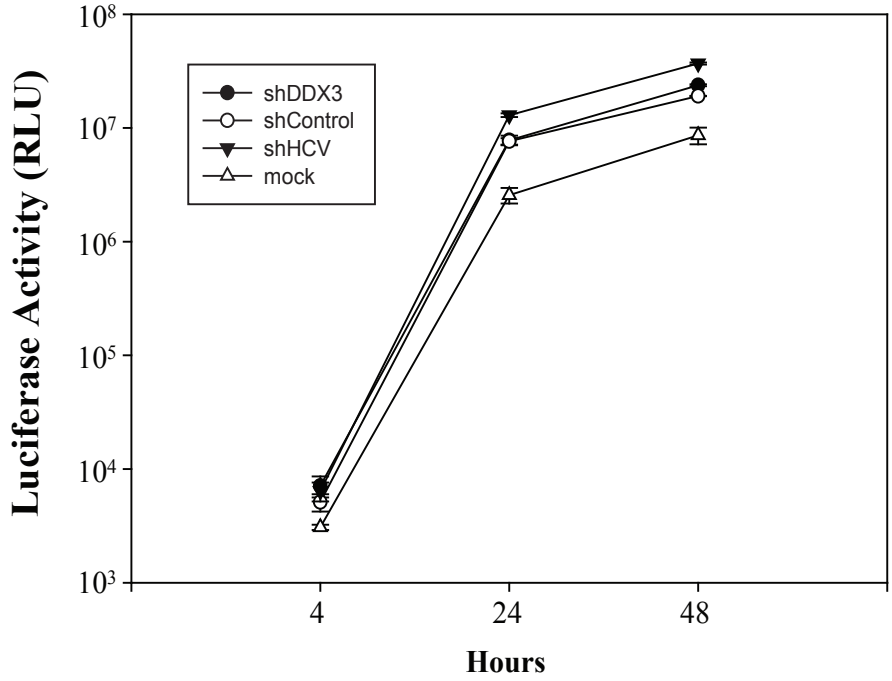

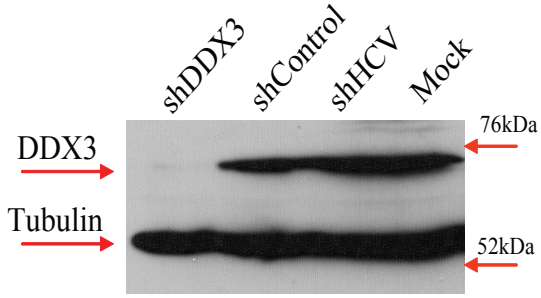

Figure 3.26. Effect of DDX3 depletion on viral promoter transcription.

(A) Schematic illustrating the principal features of the Promega$_{TM}$ pGL3-Control vector. This plasmid contains SV40 promoter and enhancer sequences, which direct accurate luciferase expression when introduced into mammalian cells. **(B)** Huh-7 cells were transfected with 10 µg pGL3-Control vector RNA at 48 h post-transduction with indicated lentivirus. Cell lysates were assayed at the indicated time points post-electroporation for luciferase activity. Mean values and standard deviations represent a single experiment performed with three technical repeats. A portion of cells from each set of transduced cell lines were harvested in SB at 48 h post-transduction and examined using the anti-DDX3 mAb AO196. Anti-α-Tubulin mAb used as a loading control.

for luciferase activity at specific time points post-lipofection, with readings indicating that luciferase expression is unaltered in a DDX3-deficient background compared to shControl-transduced cells and other controls at any stage up to 48 h post-lipofection of DNA (Fig 3.26B). This result suggests that knockdown of DDX3 does not generally alter viral promoter transcription.

3.1.10. Design of HCV Minigenome

While my results indicate that DDX3 is important at an early stage of the HCV lifecycle, pinpointing the exact function of DDX3 remains unclear. Recent studies have used synthetic HCV minigenomes as a tool to study *cis*- and *trans*-acting factors involved in HCV RNA replication (Zhang *et al*., 2007a, Yang *et al*., 2010). I designed my own HCV minigenome along similar lines to these studies, with the construct containing the antisense sequences of a luciferase reporter gene and an EMCV IRES flanked by the 5' and 3'- end regions of HCV. Zhang *et al*. (2007a) and Yang *et al*. (2010) have shown that minigenome RNA can act as a functional template for the HCV replication complex, which subsequently produces negative strand HCV mingenome RNA that directs luciferase expression in cells expressing RNA dependent RNA polymerase (Fig 3.27). The negative strand of the minigenome RNA not only allows expression of the reporter gene, but also acts as a template for synthesis of positive strand minigenome RNA. I wished to determine if DDX3 was involved in the initiation of HCV RNA replication by introducing minigenome RNA into cells stably expressing BLAST SGR/JFH1$_{WT}$ RNA that had previously been transduced with selected lentivirus. I could then compare luciferase readings in shDDX3- and shControl-transduced cells. If DDX3 was involved in the initiation of HCV RNA replication, negative strand minigenome RNA production would be diminished if DDX3 was depleted and thus, minimal luciferase activity would be detected compared to shControl-transduced cells. Unfortunately, I was unable to establish this system effectively in replicon cells, with no luciferase activity observed in shControl-transduced replicon cells up to 72 h post-electroporation of minigenome RNA.

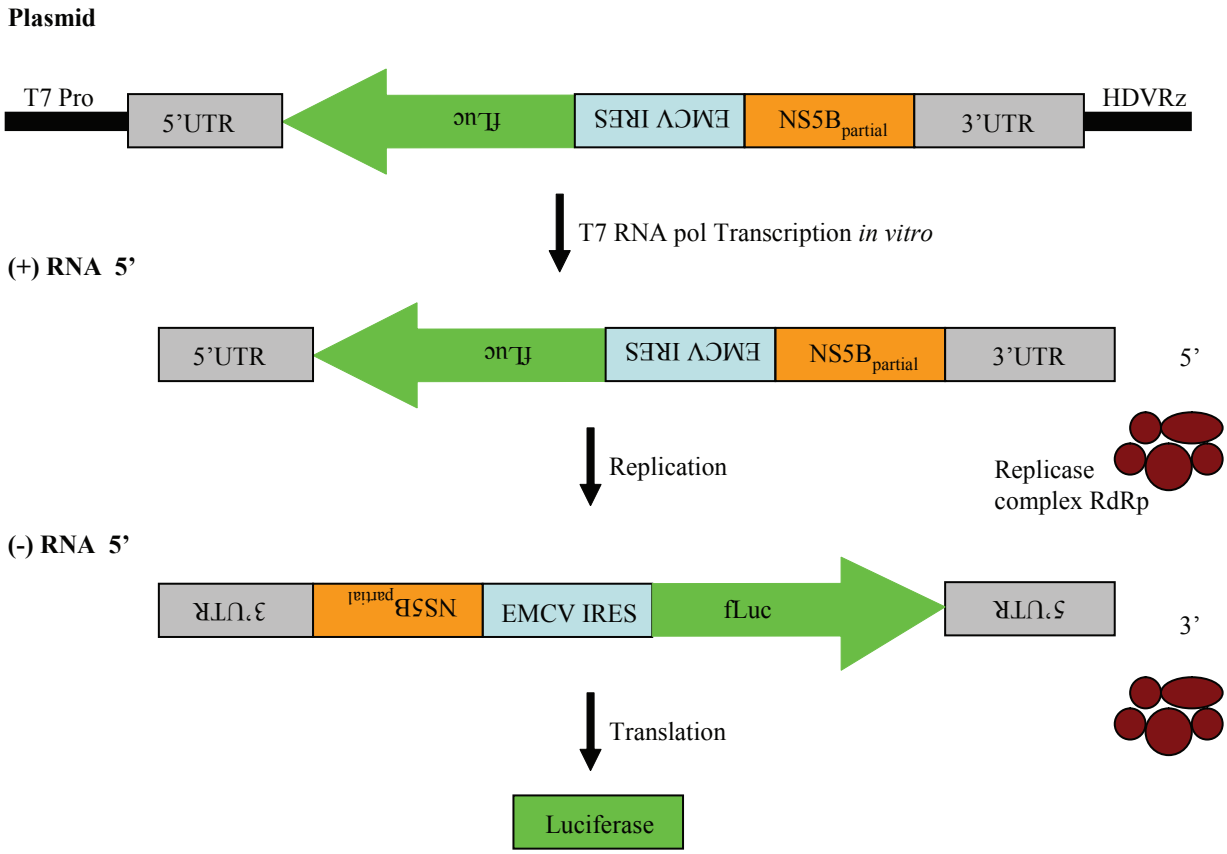

Figure 3.27. Characteristics of HCV minigenome.

Schematic illustrating a T7-driven cDNA minigenome and how it can be transcribed, replicated and expressed. This construct contains the antisense sequence of a firefly luciferase and an EMCV IRES, flanked by 5' and 3' HCV sequences that contain cis-acting replication elements.

3.1.11. Discussion

Previous studies have shown substantial reductions to HCVcc replication when DDX3 is depleted from target cells by RNAi (Ariumi *et al*., 2007; Randall *et al*., 2007). As well as confirming this finding, my overall goal in this section was to determine the role of DDX3 in the HCV lifecycle in Huh-7 cells. I used a number of *in vitro* cell systems available to me to analyse how depletion of DDX3 affected numerous cellular and molecular events vital to an efficient viral lifecycle. Towards this end, I confirmed the importance of DDX3 in the HCV lifecycle and deduced that DDX3 acts at an early, post-translation stage of the HCV lifecycle in Huh-7 cells, impeding some as yet undetermined element of HCV RNA replication. This finding is in conflict with the results published by Geissler *et al*. (2012), who observed that DDX3 was a functional determinant of IRES-mediated translation. Although I found no evidence for a role in translation in my work, this disparity may be due to differences in experimental conditions, particularly the use of shRNA technology instead of siRNA. I initially believed that my findings were different from that of Geissler *et al*. (2012) due to overloading my target cells with viral RNA during the electroporation procedure or because of insufficient depletion of endogenous DDX3 during the transduction process. However, my results were unchanged in experiments where less RNA was added or where transduction was lengthened, discounting these theories. Nevertheless, the important role of DDX3 in an early stage of the HCV lifecycle is clear. It is possible that DDX3 manipulates the HCV replication complex (RC) machinery to play this proviral role. This concept is supported by my results, which show diminished replication in DDX3-depleted cells transiently transfected with SGR RNA compared to control cells, yet when DDX3 is depleted in cells stably replicating SGR RNA, such an effect is not observed. Although I could not find evidence for DDX3's presence in RCs by IF analysis, it is possible that the protein may function in these structures at a level undetectable by this assay. Alternatively, DDX3 may influence RC function through an indirect mechanism.

Another interesting point to note in this section is that my colony forming assays indicate that DDX3-deficient replicon cells cannot be maintained in culture. Therefore, studies of the HCV lifecycle are limited to transient assays on early time points after

infection in order to avoid disrupting additional host factors necessary for efficient cellular function. Experiments performed in a Y35A and Δcore background give similar phenotypes to those completed in a WT background, which confirms work published by Angus *et al*. (2010) stating that the requirement of DDX3 for HCV replication is unrelated to its interaction with the viral core protein. These results confirm the clear and important distinction between the effects of shRNA knockdown of DDX3 from target cells and disruption of the core-DDX3 interaction on HCV replication. Depleting DDX3 in a Huh-7.5 background also indicated that the ablated IFN-response caused by the RIG-I T55I mutation in these cells did not influence the proviral effects of DDX3.

From the evidence provided in this section, I have identified an important role for DDX3 at an early stage of the HCV lifecycle

3.2. Investigating the Effects of DDX3 Knockdown on the Production of Infectious HCV

3.2.1. Introduction

My experimental data in the previous chapter confirmed that DDX3 acts at an early stage of the HCV lifecycle in Huh-7 cells. As well as determining if the drop in viral replication observed in DDX3-depleted Huh-7 cells impaired infectious virus production, my aim in this section was also to ascertain if DDX3 knockdown had any specific effect on the HCV assembly process. It is essential to separate the steps of the HCV life cycle to determine any exclusive assembly effects accurately. Single-cycle infectious virus production experiments are the best method of determining specific effects of HCV assembly as they allow comparison of virus production from different cell-lines without bias from viral spread through limiting the replication cycle of HCV to one round (Russell *et al*., 2008). Huh-7 cells are perceived as unsuitable for such experiments due to the possibility of direct viral cell-to-cell spread and the potential capacity these cells have to support multiple rounds of the complete HCV lifecycle,. Therefore, a cell-line was sought that was resistant to infection with cell-free virus but released infectious HCV after transfection. The level of cell surface-expressed CD81 molecules has been shown to modulate host cell permissiveness and is a key determinant of productive infection by HCV (Koutsoudakis *et al*., 2007). Thus, to delineate the effects of DDX3 on HCV assembly, I enlisted a subclone of Huh-7 cells with depleted CD81 levels called Huh7L-#4 cells (Witteveldt *et al*., 2009) for use in these single-cycle assays.

An approximate ten-fold reduction in infectious HCV production was observed in DDX3-depleted Huh7L-#4 cells compared to Huh-7 cells. However unlike Huh-7 cells, luciferase activity was unaltered in DDX3-depleted Huh7L-#4 cells compared to shControl-transduced Huh7L-#4 cells at 48 h post-electroporation of N17 SGR/JFH1$_{WT}$ RNA. Subsequent analysis of infectious virus production and replicon activity in DDX3-depleted shCD81 cells was performed to investigate if the unusual phenotype seen in Huh7L-#4 cells may be related to the absence of CD81. My results confirmed

that this was not the case. The data presented in this section suggest DDX3 plays a pleiotropic role in the HCV lifecycle, with distinct yet undetermined roles for the protein in both RNA replication and virus production.

3.2.2. Effect of DDX3 Knockdown on Infectious HCV Production in Huh-7 Cells.

To determine if the drop in viral replication observed in DDX3-depleted cells also impaired infectious virus production in Huh-7 cells, I electroporated 10 μg $JFH1_{WT}$ RNA into Huh-7 cells transduced for 48 h with different lentivirus. Two days after the introduction of RNA, the extracellular and intracellular virus titres were analysed by FFU assay. As shown in Fig 3.28, both the cell-free and cell-associated infectivity of $JFH1_{WT}$ were lower in DDX3-depleted cells compared to control cells, with results indicating production of infectious virus reduced by half in DDX3-depleted cells compared to control cells, indicating that DDX3 knockdown does alter infectious HCV production in Huh-7 cells. This drop was potentially due to the effect of reduced RNA replication in DDX3-depleted cells as observed in the reductions in luciferase activity in DDX3-depleted Huh-7 cells at 48 h post-N17 SGR/$JFH1_{WT}$ RNA electroporation. Infectious virus assembly was also reduced in shHCV-transduced cells, although not substantially lower than in DDX3-knockdown cells (~ 30 % less particles observed), which was surprising given the large fold-difference in luciferase activity between shDDX3-transduced cells and shHCV-transduced cells at 48 h post-N17 SGR/$JFH1_{WT}$ RNA electroporation.

However, it is important to note that Huh-7 cells may be unsuitable for the accurate assessment of DDX3 knockdown on virus production because of the possibility of viral spread occurring in each set of transduced cells, which may explain the difference in viral titres observed between shHCV- and shDDX3-transduced Huh-7 cells. I performed a single cycle infection assay in Huh-7 cells to try and overcome this potential problem. Huh7-J20 cells were infected at a high m.o.i.(100 FFU/cell) with the JFH1 variant virus $JFH1_{DSG}$, a cell-culture adapted virus that can produce far higher quantities of virus particles than $JFH1_{WT}$ (~ 10^7 particles/ml) at 48 h post-electroporation (Fig 3.29A). At 24 h post-infection, cells were transduced with different lentivirus of interest. Analysis

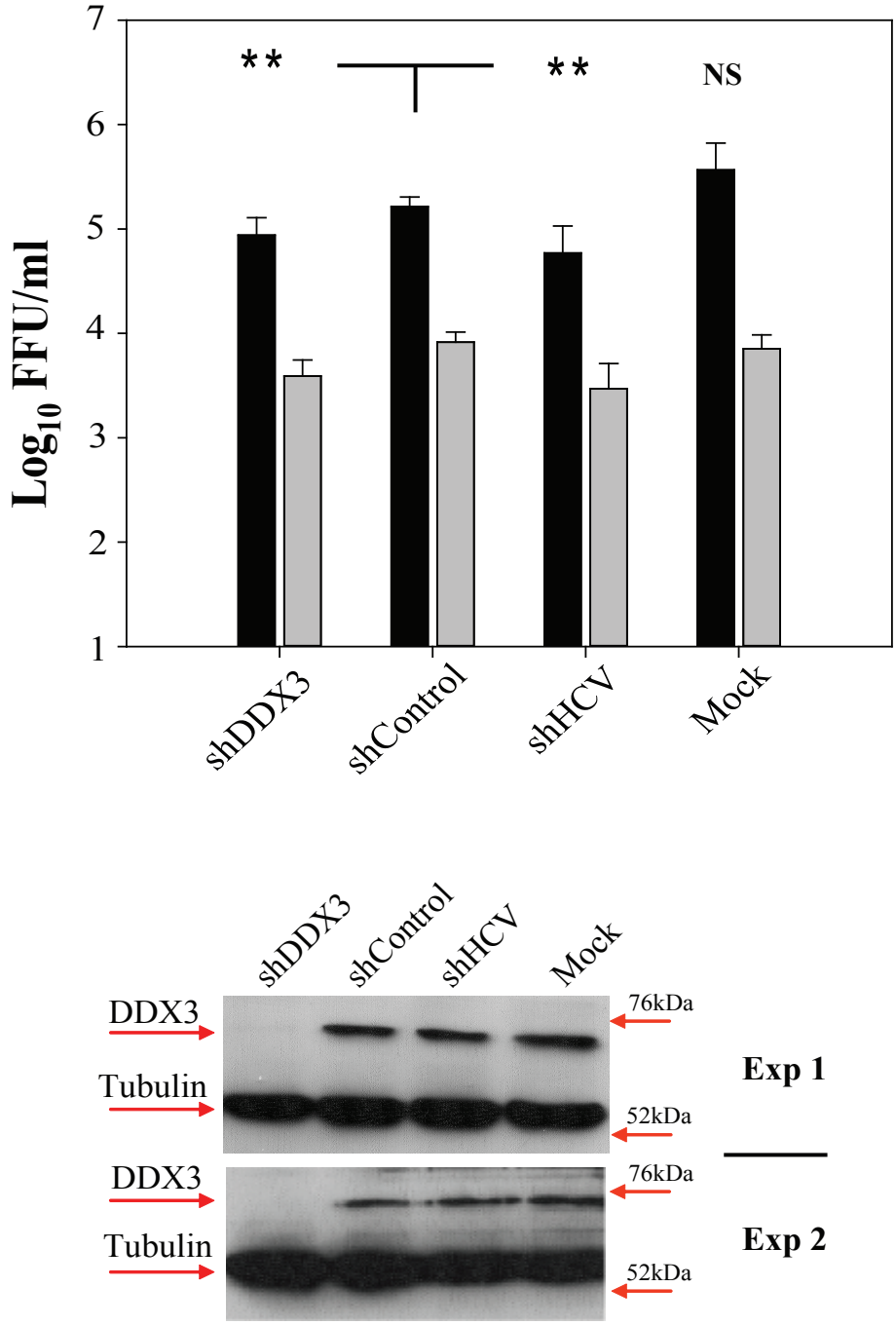

Figure 3.28. Infectious virus production in DDX3-depleted Huh-7 cells.

Huh-7 cells were electroporated with 10 µg $JFH1_{WT}$ RNA at 48 h post-transduction with indicated lentivirus. At 48 h post-electroporation, the cell-released (black bars) and cell-associated (grey bars) infectivity were determined by FFU assay. Error bars indicate the standard deviation of the mean of six technical repeats derived from two independent experiments. Student's t-test was performed to determine the P value. * $P < 0.05$, ** $P < 0.01$, *** $P < 0.001$, NS, not significant. A portion of cells from each set of transduced cells were lysed in SB in each experiment and probed with anti-DDX3 and anti-tubulin antibodies to determine protein levels at time of electroporation.

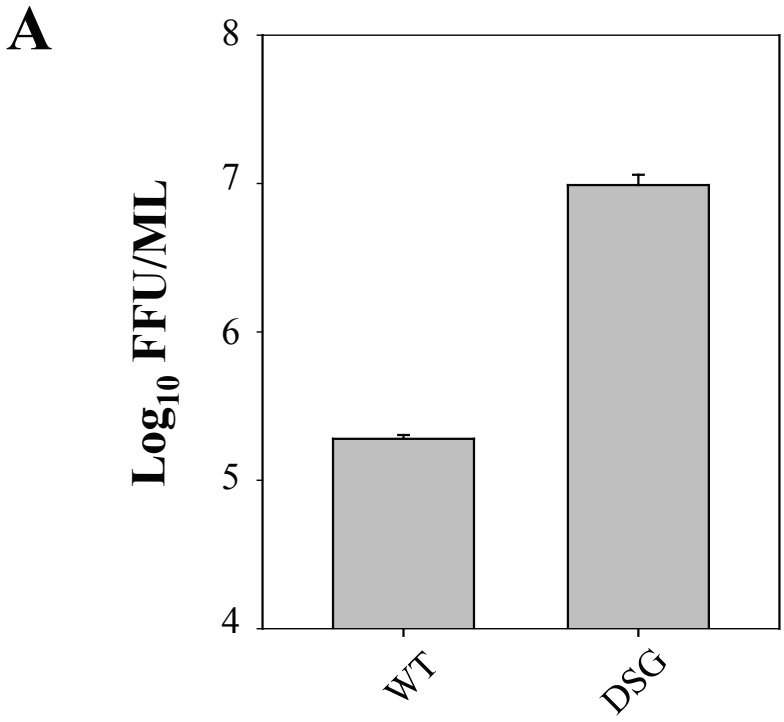
A
8
7
6
5
4
Log10 FFU/ML
WT
DSG

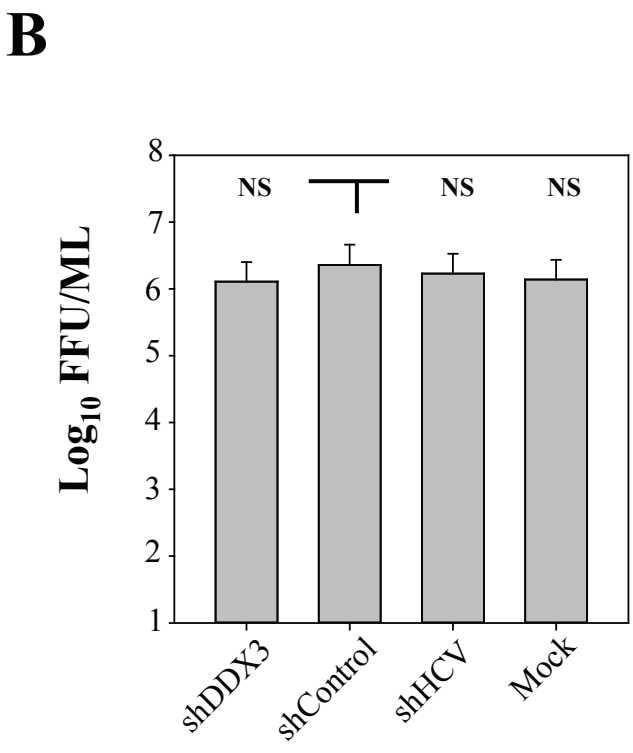
B
8
7
6
5
4
3
2
1
Log10 FFU/ML
NS
NS
NS
shDDX3
shControl
shHCV
Mock

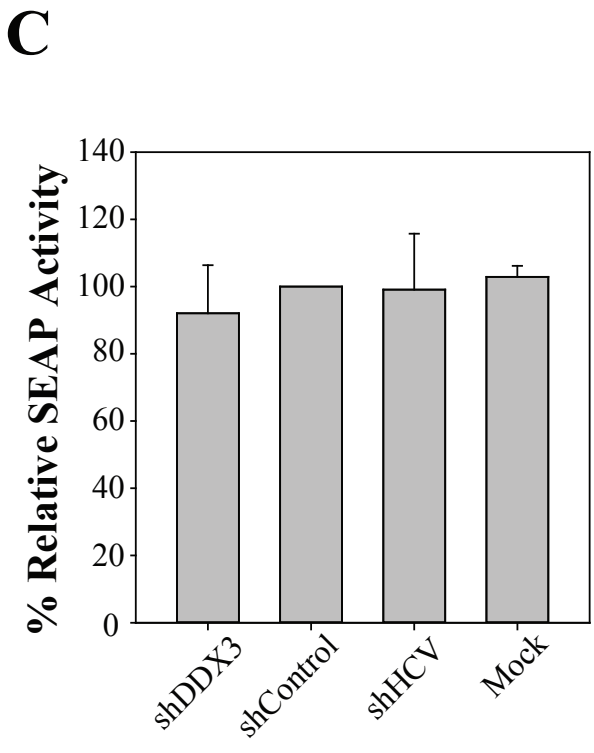
C
140
120
100
80
60
40
20
0
% Relative SEAP Activity
shDDX3
shControl
shHCV
Mock

D

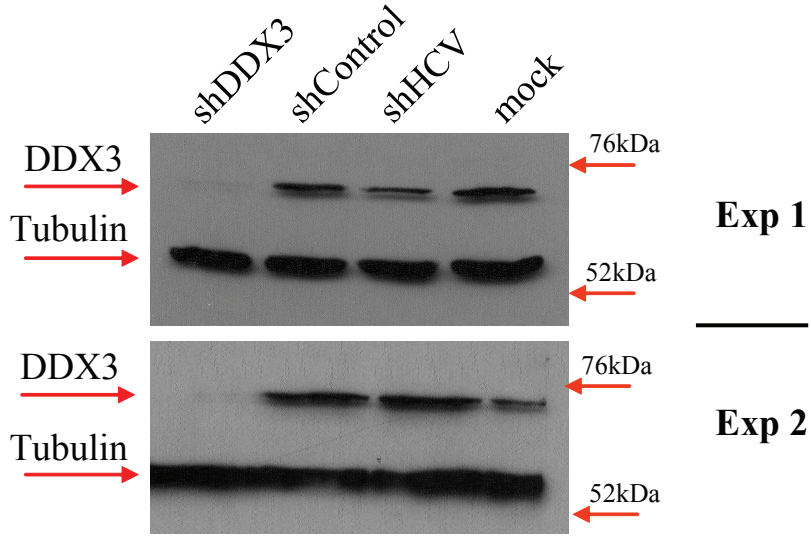

Figure 3.29. Effect of DDX3 knockdown on single cycle infection assay using Huh-7/J20 cells.

Huh-7 cells were electroporated with 10 µg of $JFH1_{WT}$ RNA or $JFH1_{DSG}$ RNA. At 48 h post-electroporation, the cell-released infectivity was determined by FFU assay. Mean values and standard deviations represent a single experiment performed with three technical repeats. **(A)**. Huh-7/J20 cells were plated at an equal density onto 24-well culture dishes before being infected with $JFH1_{DSG}$ virus at an m.o.i. of 100 FFU/cell. At 24 h post-infection, cells were transduced with indicated lentivirus. At 48 h post-transduction, infectious virus release **(B)** and SEAP activity **(C)** were determined in each cell line by FFU and SEAP assay respectively. In the FFU assay, the error bars indicate the standard deviation of the mean of six technical repeats derived from two independent experiments. Student's t-test was performed to determine the P value. * $P < 0.05$, ** $P < 0.01$, *** $P < 0.001$, NS, not significant. In the SEAP assay, error bars indicate the standard deviation of the mean of two independent experiments. **(D)** A portion of cells from each set of transduced cells were lysed in SB at 48 h post-transduction for each independent experiment. Samples were immunoblotted with anti-DDX3 mAb A0196 and an anti-α-Tubulin mAb.

of virus production levels and intracellular NS3/4A protease activity at 48 h post-transduction revealed that DDX3 depletion had little effect on infectious virus production in this instance (Fig 3.29B and C).

3.2.3. Huh-7 Lunet/CD81N#4 cells.

Given the potential for direct cell-cell spread to adversely alter the accuracy of infectious virus production experiments involving Huh-7 cells, I measured the effect of DDX3 knockdown in a single cycle production assay using an individual subclone species of Huh-7/Lunet cells with depleted CD81 levels called Huh-7 Lunet/CD81N#4 (Huh7L-#4) cells (Witteveldt *et al*., 2009). Huh-7/Lunet cells represent a subclone of Huh-7 cells that are highly permissive for HCV RNA replication and display a bimodal expression level of the cell surface entry receptor CD81 (Koutsoudakis *et al*., 2007). Huh7L-#4 cells produce infectious virus following $JFH1_{WT}$ electroporation (Fig 3.30A), but are virtually uninfectable with cell-free virus due to the minimal levels of CD81 they contain (Fig 3.30B). Thus, Huh7L-#4 cells were found to display characteristics that were suitable for single-cycle infectious virus production experiments, which measure virus titres released from transfected (primary) cells rather than from cells infected by spreading (secondary) virus – measured in my earlier single cycle infection assay (Fig 3.29B & C) - as they allow comparison of virus production from different sets of transduced cells without bias from viral spread through limiting the replication cycle of HCV to one round.

Because of these characteristics, I wished to observe infectious virus production in DDX3-deficient Huh7L-#4 cells. I electroporated 10 µg $JFH1_{WT}$ RNA into Huh7L-#4 cells transduced for 48 h with different lentivirus. Extracellular and intracellular virus titres were analysed by FFU assay at 48 h post-electroporation from each set of transduced cells. Surprisingly, both the cell-free and cell-associated infectivity of $JFH1_{WT}$ were found to be over 20-fold lower in DDX3-deficient cells compared to shControl- and mock-transduced Huh7L-#4 cells, indicating that DDX3 knockdown greatly alters infectious HCV production in Huh7L-#4 cells (Fig 3.31A). Huh7L-#4 cells transduced with shHCV were found to show reductions in extracellular and intracellular virus titres similar to those observed in DDX3-depleted cells.

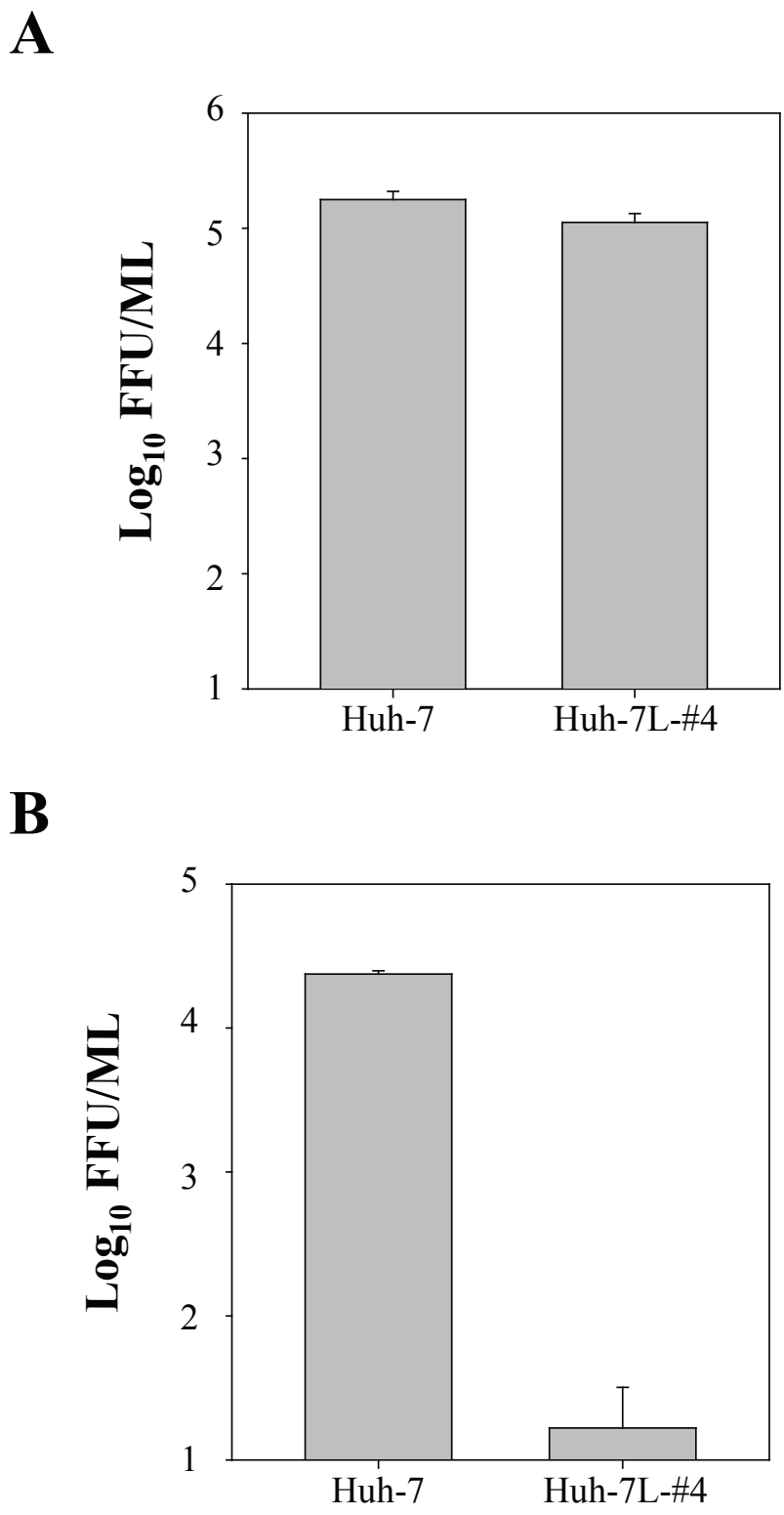

Figure 3.30. Characteristics of Huh-7 Lunet/CD81N#4 cells.

(A) Huh-7 cells and Huh-7L-#4 cells were each electroporated with 10 µg $JFH1_{WT}$ RNA. At 48 h post-electroporation, cell-released infectivity in both cell lines was determined by FFU assay. Mean values and standard deviations represent a single experiment performed with three technical repeats. **(B)** $JFH1_{WT}$ virus was titrated on Huh-7 cells and Huh-7 Lunet/CD81N#4 (Huh7L-#4) cells. At 48 h post-infection, cells were fixed and the levels of infectivity were determined by FFU assay. Mean values and standard deviations represent a single experiment performed with three technical repeats.

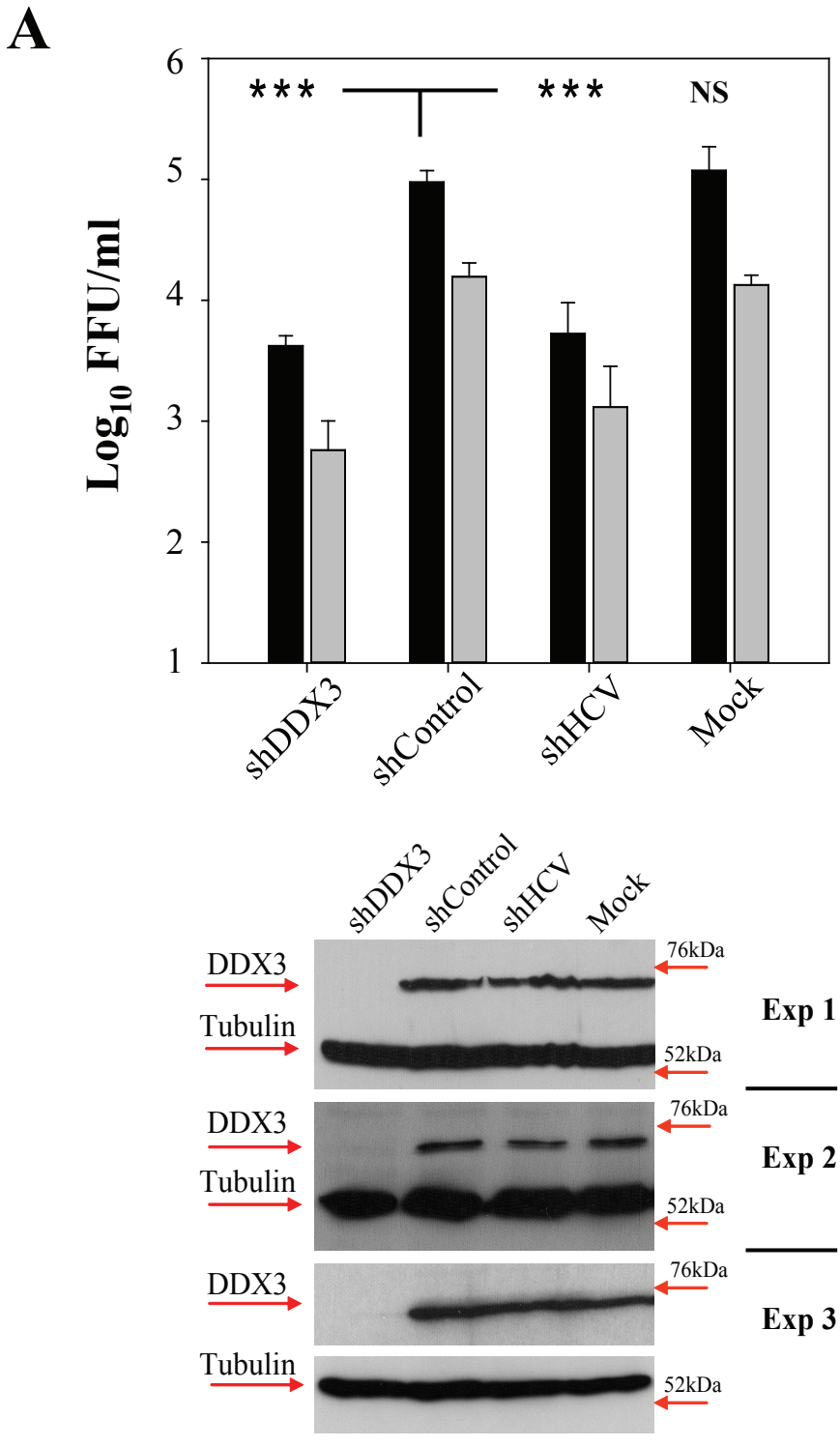
A
6
5
4
3
2
1
Log10 FFU/ml
***
***
NS
shDDX3
shControl
shHCV
Mock
shDDX3
shControl
shHCV
Mock
DDX3
Tubulin
76kDa
52kDa
Exp 1
DDX3
Tubulin
76kDa
52kDa
Exp 2
DDX3
Tubulin
76kDa
52kDa
Exp 3
B
shDDX3
shControl
shHCV
Mock
Core
24kDa
Core
24kDa

Figure 3.31. Effect of DDX3 depletion on single cycle infection assay using Huh7L-#4 cells.

(A) Huh7L-#4 cells were electroporated with 10 µg $JFH1_{WT}$ RNA at 48 h post-transduction with indicated lentivirus. At 48 h post-electroporation, the cell-released (black bars) and cell-associated (grey bars) infectivity were determined by FFU assay. Error bars indicate the standard deviation of the mean of nine technical repeats derived from three independent experiments. Student's t-test was performed to determine the P value. * $P < 0.05$, ** $P < 0.01$, *** $P < 0.001$, NS, not significant. A portion of transduced cells from each set of transduced cells were lysed in SB in each experiment and probed with anti-DDX3 and anti-α-Tubulin mAbs to determine protein levels at time of electroporation. **(B)** HCV extracellular particles from each set of transduced cells were collected at 48 h post-electroporation. Pellets were suspended in SB and probed with anti-Core mAb C7-50. Western blot analysis from two independent experiments are shown.

Immunoblotting indicated minimal levels of extracellular core in samples from shDDX3- and shHCV-transduced Huh7L-#4 cells compared to shControl- and mock-transduced Huh7L-#4 cells, indicating that DDX3 knockdown impairs HCV particle secretion as a whole (Fig 3.31B). Similar levels of particle production impairment was observed in DDX3-deficient Huh7L-#4 cells infected with $JFH1_{Y35A}$ virus instead of $JFH1_{WT}$ virus, indicating that the core-DDX3 interaction, as well as being dispensable in the context of HCV RNA replication, plays no role in regulating infectious virus production either (Fig 3.32). I also determined that DDX3 depletion in Huh7L-#4 cells already replicating $JFH1_{WT}$ RNA did not diminish infectious virus production levels compared to control cells (Fig 3.33).

Given the adverse effect of DDX3 knockdown on infectious virus particle production in Huh7L-#4 cells, I wished to determine if this effect was caused by greatly reduced replication of replicon RNA, a phenotype I observed post-RNA replication in Huh-7 cells. Thus, N17 SGR/$JFH1_{WT}$ replicon RNA was transiently transfected into DDX3-depleted Huh7L-#4 cells and luciferase readings were taken at specific time points post-RNA electroporation to determine replication kinetics. Interestingly, luciferase readings indicated no substantial difference in luciferase activity between DDX3-deficient cells and shControl- or mock-transduced cells at any of the time points analysed, while luciferase readings in shHCV-transduced cells declined dramatically at the 24 and 48 h time points (Fig 3.34). Interestingly, this result indicates that DDX3 is not important for efficient HCV replication in Huh7L-#4 cells, but seems to have a critical role in infectious particle assembly. Repeating the experiment highlighted in Fig 3.34 but replacing N17 SGR/$JFH1_{WT}$ RNA with $B3P7_{WT}$ RNA (N17 SGR/$JFH1_{WT}$ replicon that also encodes E1E2) gave similar results, with similar luciferase readings observed between shDDX3- and shControl-transduced cells at all analysed time points post-RNA electroporation (Appendix 2). This further illustrates that DDX3 is not required for efficient HCV replication in Huh7L-#4 cells.

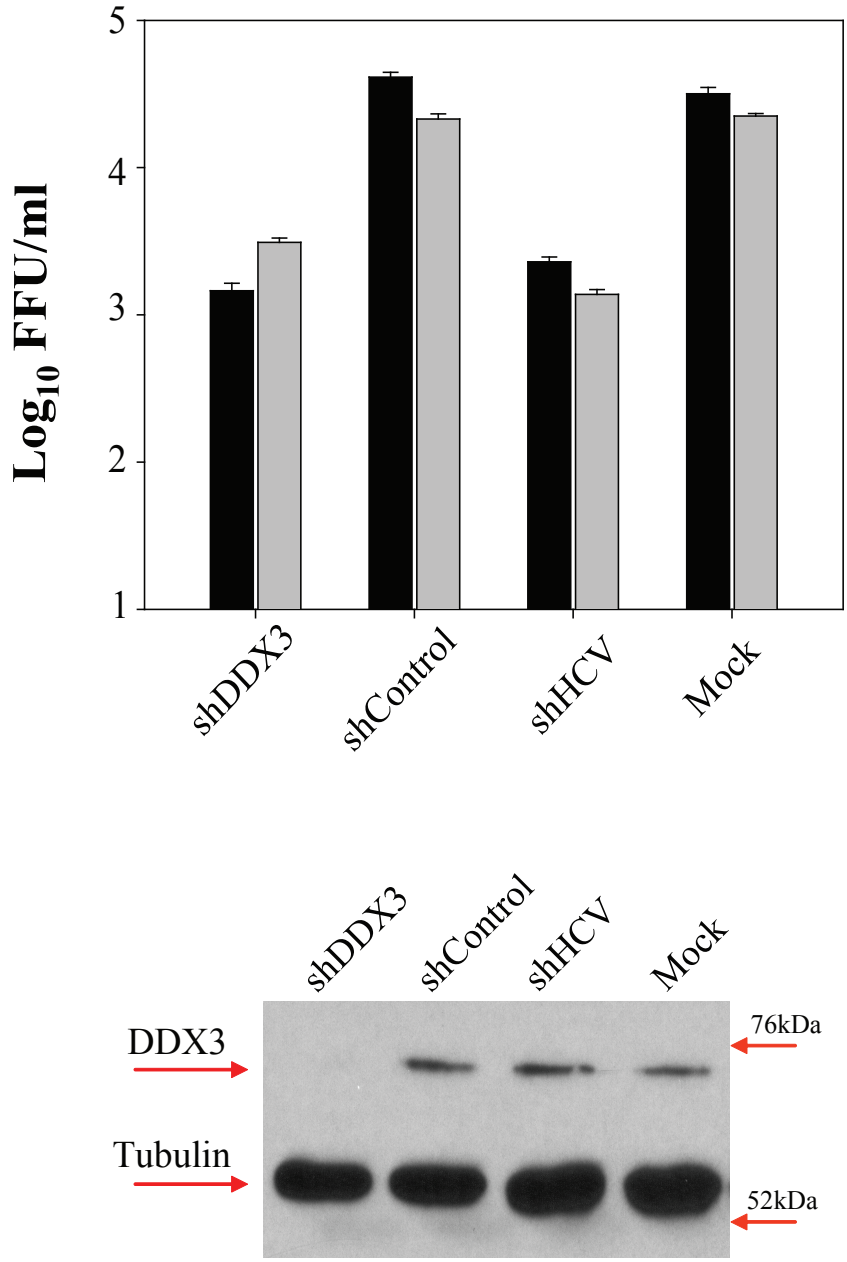

Figure 3.32. Infectious Core mutant virus production in DDX3-depleted Huh7L-#4 cells.

Huh7L-#4 cells were electroporated with 10 µg $JFH1_{Y35A}$ RNA at 48 h post-transduction with indicated lentivirus. At 48 h post-electroporation, the cell-released (black bars) and cell-associated (grey bars) infectivity were determined by FFU assay. Mean values and standard deviations represent a single experiment performed with three technical repeats. . A portion of cells from each set of transduced cells were harvested in SB at 48 h post-transduction and examined using the anti-DDX3 mAb AO196. Anti-α-Tubulin mAb used as a loading control.

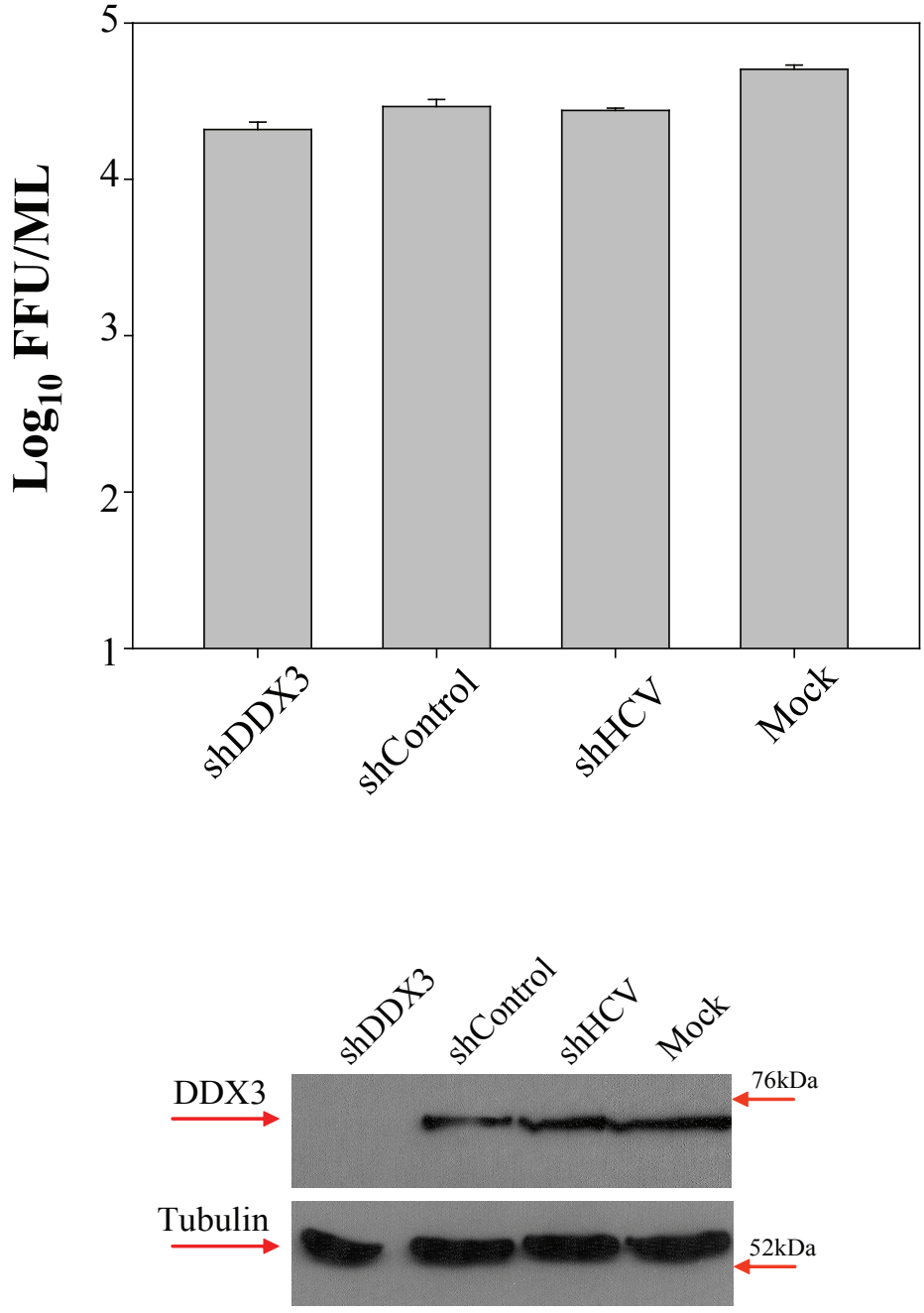

Figure 3.33. Effect of DDX3 knockdown in cells replicating $JFH1_{WT}$.

Huh7L-#4 cells were electroporated with 10 µg $JFH1_{WT}$ RNA and plated evenly onto 24-well culture dishes. At 24 h post-electroporation, cells were transduced with indicated lentivirus. At 48 h post-transduction, the infectivity of the cell-culture supernatant for each set of transduced cells was determined by FFU assay. Mean values and standard deviations represent a single experiment performed with three technical repeats. A portion of cells from each set of transduced cells were lysed in SB at 48 h post-transduction and probed with anti-DDX3 mAb AO196. Anti-α-Tubulin mAb was used as a loading control.

A

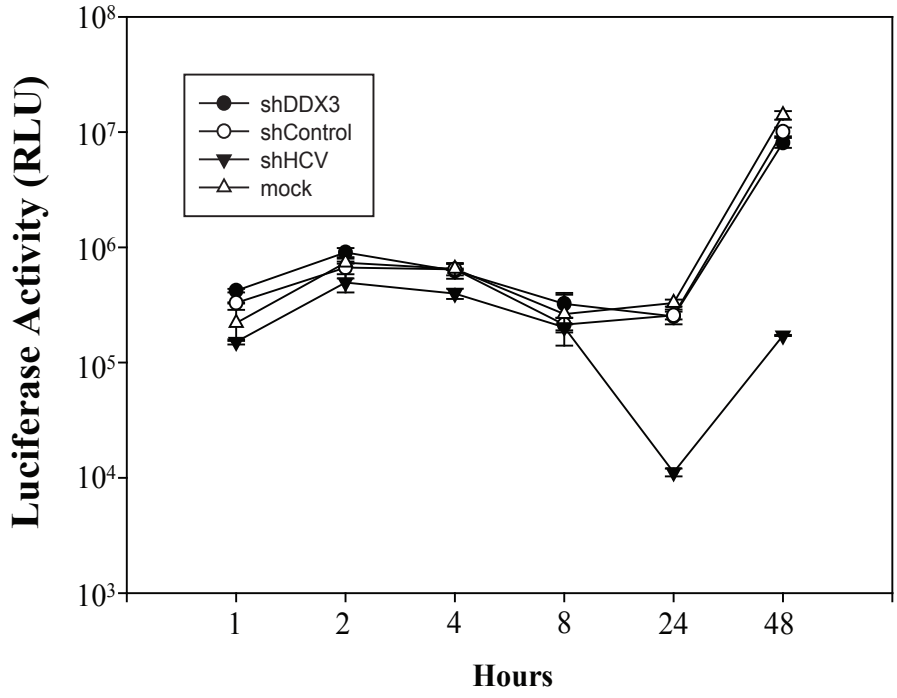

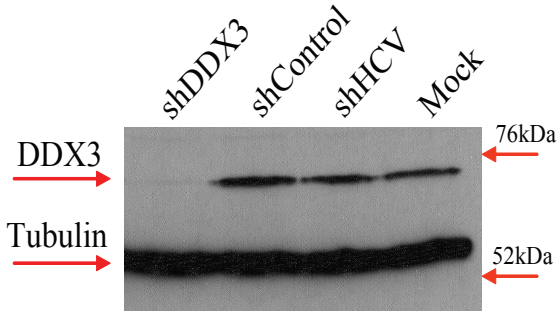

B

Fold change from shControl		
	24hrs	**48hrs**
shDDX3	- 0.02	- 0.24
shHCV	- 22.99	- 58.62
mock	+ 0.22	+ 0.29

Figure 3.34. Effect of DDX3 Knockdown in Huh7L-#4 cells transiently replicating N17 SGR/JFH1$_{WT}$ replicon RNA at various timepoints.

(A) Huh7L-#4 cells were electroporated with 10 µg N17 SGR/JFH1$_{WT}$ replicon RNA at 48 h post-transduction with indicated lentivirus. Cell lysates were assayed at the indicated time points post-electroporation for luciferase activity. Mean values and standard deviations represent a single experiment performed with three technical repeats. A portion of cells from each set of transduced cells were lysed in SB at 48 h post-transduction and probed with the anti-DDX3 mAb AO196. Anti-α-Tubulin mAb was used as a loading control. **(B)** Table showing the fold-changes in luciferase activity in cells transduced with indicated lentivirus compared to cells transduced with shControl.

3.2.4. shCD81 cells.

A recent study showed that CD81 is an important host factor required for HCV RNA replication (Zhang *et al*., 2010). Therefore, it is possible that the different replication levels observed after DDX3 knockdown may be related to the absence of CD81 expression in Huh7L-#4 cells. To investigate this possibility, I compared N17 SGR/JFH1$_{WT}$ replication in Huh-7 cells and Huh7L-#4 cells alongside Huh-7 cells transduced with shRNA against CD81 (shCD81 cells). While no prominent difference was observed in luciferase expression between all three cell-lines from addition of RNA until the 8 h time point, differences were observed between the cell-lines at 24 and 48 h post-electroporation. Similar luciferase readings were observed in Huh7L-#4 and shCD81 cells at these time points but viral RNA replicated far more slowly in these cells compared to Huh-7 cells. Indeed, luciferase readings from Huh-7 cells were found to be almost 10-fold higher than Huh7L-#4 and shCD81 cells at these later time points (Fig 3.35). However, the similar replication levels of the Huh7L-#4 and shCD81 cells indicated that the unusual phenotype of the Huh7L-#4 cells could indeed be related to the absence of CD81.

To confirm if this is the case, infectious virus production and replicon luciferase activity were determined in DDX3-depleted shCD81 cells. It was established that shCD81 cells can also produce infectious virus following JFH1$_{WT}$ electroporation (Fig 3.36A), but are more susceptible to cell-free JFH1$_{WT}$ virus infection than Huh7L-#4 cells, despite being ~ 100 fold less permissive for infection than Huh-7 cells (Fig 3.36B). Both the cell-free and cell-associated infectivity of JFH1$_{WT}$ were found to be much lower in DDX3-depleted shCD81 cells compared to shCD81 cells transduced with shControl and mock cells, with reductions in infectious HCV production at similar levels to those observed in Huh7L-#4 cells (Fig 3.37). However, substantial changes in luciferase activity were found in DDX3-deficient shCD81 cells at 48 h post-N17 SGR/JFH1$_{WT}$ RNA electroporation compared to shControl- and mock-transduced cells. Levels of luciferase activity in DDX3-depleted shCD81 cells were found to be almost as low as those seen in shCD81 cells transduced with shHCV at 48 h post-RNA electroporation. Indeed luciferase readings in DDX3-knockdown cells were found to be almost 30-fold lower than shControl-transduced shCD81 cells at this time point (Fig 3.38). The impaired

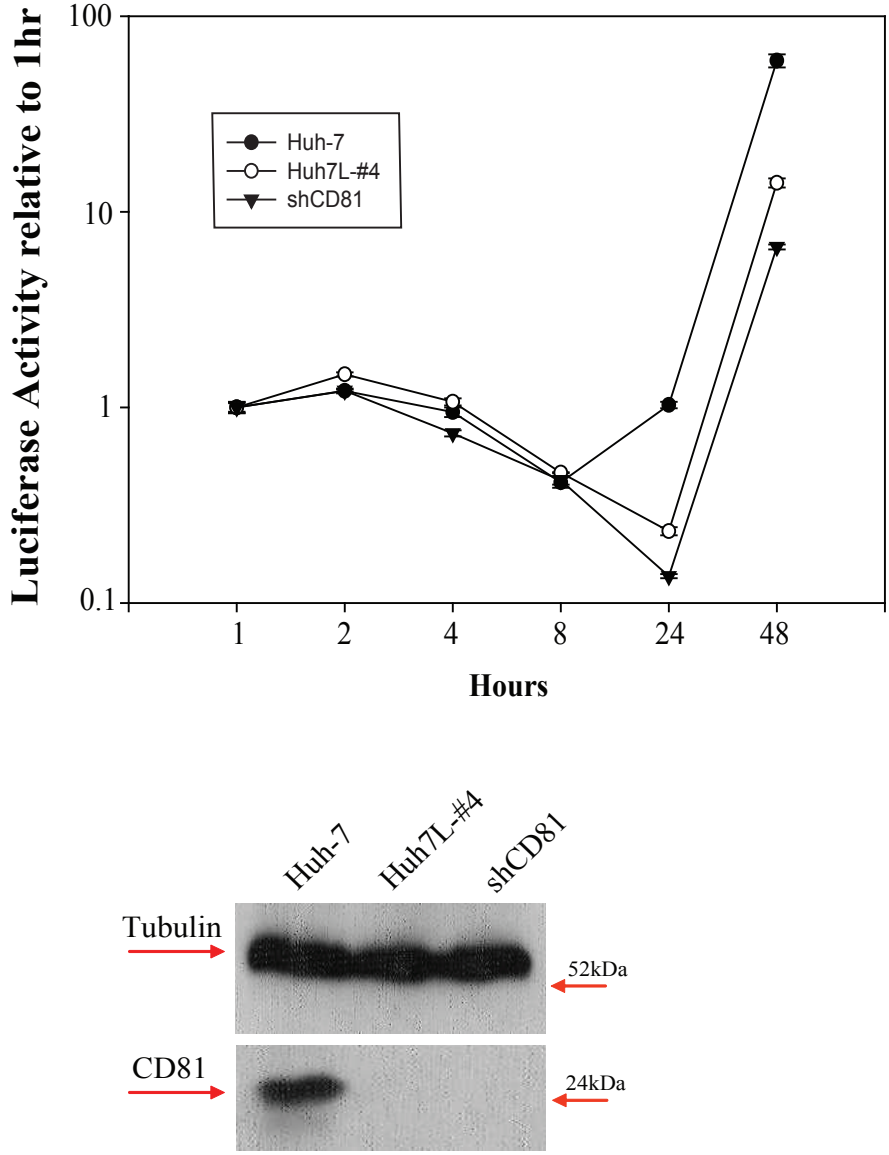

Figure 3.35. Replication profile of N17 SGR/JFH1$_{WT}$ in various cell-lines.

An equal number of Huh-7 cells, Huh7L-#4 cells and shCD81 cells were each electroporated with 10 µg N17 SGR/JFH1$_{WT}$ replicon RNA. Cell lysates were assayed at the indicated time points post-electroporation for luciferase activity. Mean values and standard deviations represent a single experiment performed with three technical repeats. Results of one representative experiment out of two independent repetitions are shown. A portion of cells from each cell-line were lysed in SB at 48 h post-electroporation and were immunoblotted with an anti-α-Tubulin mAb and the anti-CD81 mAb 5A6 to determine relative protein levels.

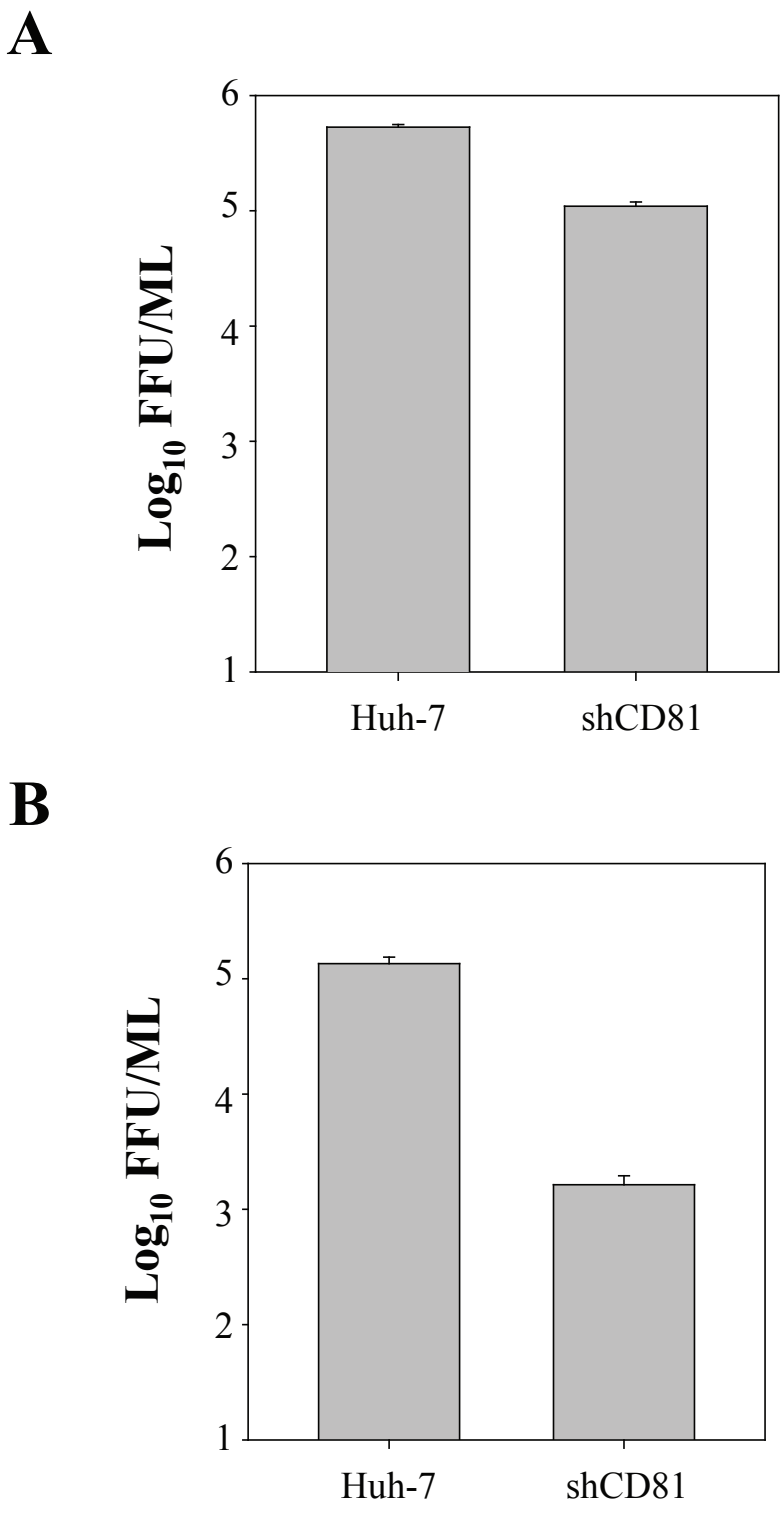

Figure 3.36. Characteristics of shCD81 cells.

(A) Huh-7 cells and shCD81 cells were each electroporated with 10 µg $JFH1_{WT}$ RNA. At 48 h post-electroporation, cell-released infectivity in both cell lines was determined by FFU assay. Mean values and standard deviations represent a single experiment performed with three technical repeats. **(B)** $JFH1_{WT}$ virus was titrated on Huh-7 cells and shCD81 cells. At 48 h post-infection, cells were fixed and the levels of infectivity were determined by FFU assay. Mean values and standard deviations represent a single experiment performed with three technical repeats.

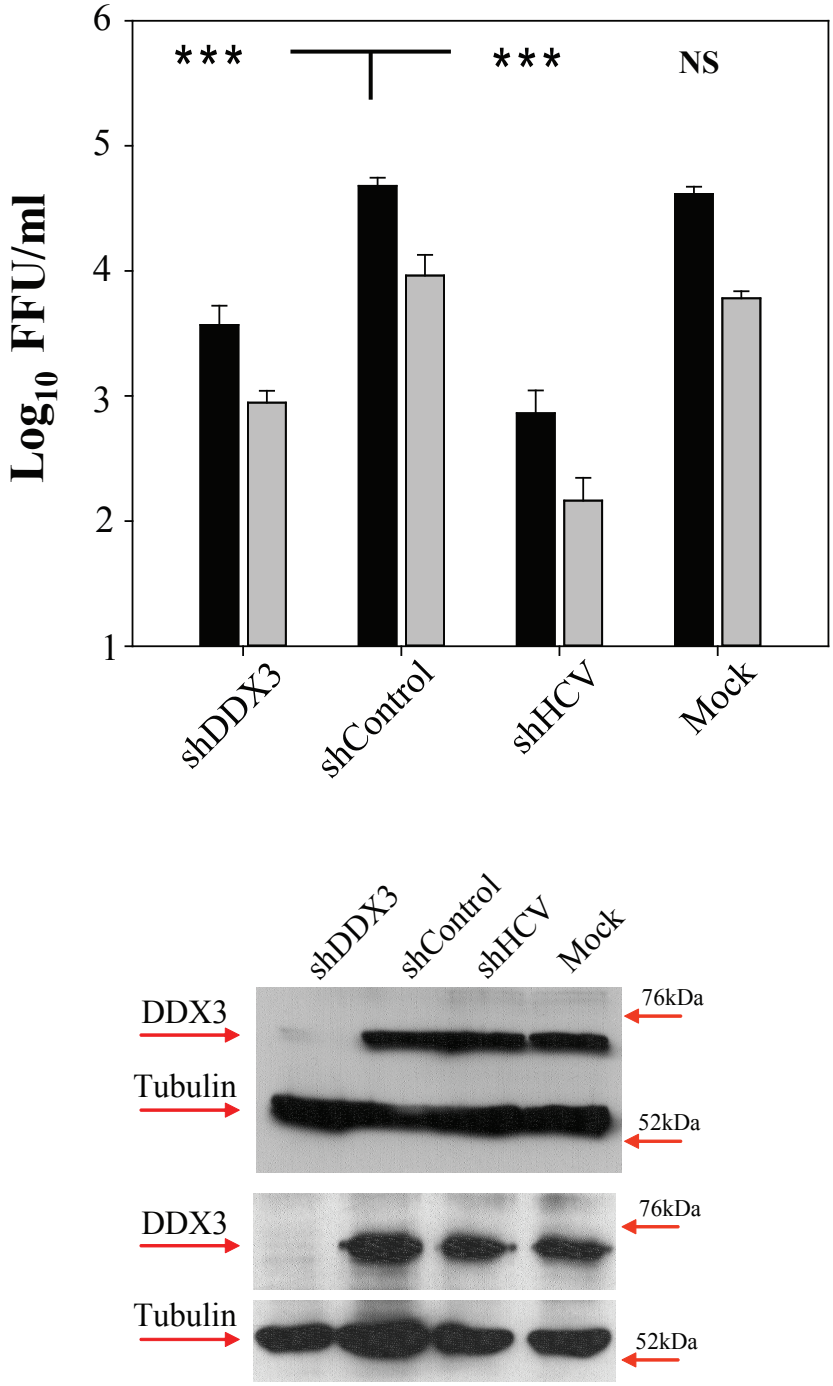

Figure 3.37. Effect of DDX3 depletion on single cycle infection assay using shCD81 cells.

ShCD81 cells were electroporated with 10 µg $JFH1_{WT}$ RNA at 48 h post-transduction with indicated lentivirus. At 48 h post-electroporation, the cell-released (black bars) and cell-associated (grey bars) infectivity were determined by FFU assay. Error bars indicate the standard deviation of the mean of six technical repeats derived from two independent experiments. Student's t-test was performed to determine the P value. * $P < 0.05$, ** $P < 0.01$, *** $P < 0.001$, NS, not significant. A portion of transduced cells from each cell-line were lysed in SB in each experiment and probed with anti-DDX3 and anti-α-Tubulin mAbs to determine protein levels at time of electroporation.

A

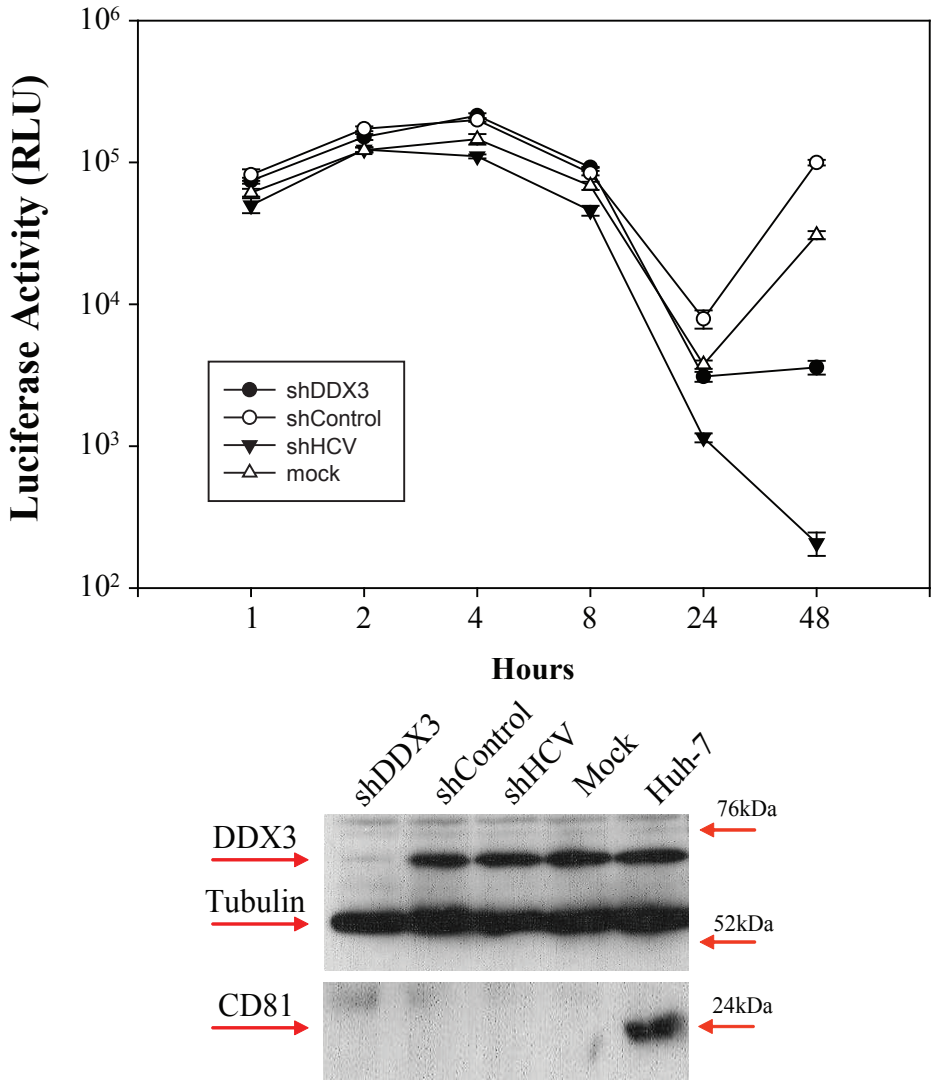

B

Fold change from shControl		
	24hrs	**48hrs**
shDDX3	- 2.55	- 27.74
shHCV	- 6.80	- 48.10
mock	- 2.55	- 3.24

Figure 3.38. Effect of DDX3 Knockdown in shCD81 cells transiently replicating N17 SGR/JFH1$_{WT}$ replicon RNA at various timepoints.

(A) shCD81 cells were electroporated with 10 µg N17 SGR/JFH1$_{WT}$ replicon RNA at 48 h post-transduction with indicated lentivirus. Cell lysates were assayed at the indicated time points post-electroporation for luciferase activity. Mean values and standard deviations represent a single experiment performed with three technical repeats. A portion of cells from each set of transduced cells were lysed in SB (or NR-SB, if analysing CD81) at 48 h post-transduction and were immunoblotted with anti-DDX3 mAb A0196, an anti-α-Tubulin mAb and the anti-CD81 mAb 5A6 to determine relative protein levels. **(B)** Table showing the fold-changes in luciferase activity in cells transduced with indicated lentivirus compared to cells transduced with shControl.

RNA replication in DDX3-depleted shCD81 cells is almost certainly the reason for subsequent reductions in infectious virus production levels, indicating that the absence of CD81 is not responsible for the unusual phenotype observed in Huh7L-#4 cells.

3.2.5. Selection of a DDX3-independent Mutant Virus.

In order to gain insight into the exact role of DDX3 in the lifecycle, I attempted to select JFH1 variants that could replicate efficiently in a DDX3-depleted background. The adapted mutations observed in such a virus could potentially be used to study how DDX3 influences viral RNA replication and virus production. I began by serially passaging DDX3-depleted Huh-7 cells that had been infected with $JFH1_{DSG}$ virus. $JFH1_{DSG}$ virus was used in place of $JFH1_{WT}$ in this experiment because the mutant virus can spread far more quickly in culture than $JFH1_{WT}$, potentially promoting the selection of variants resistant to DDX3 knockdown much more quickly.

Supernatant virus was collected after three passages and used to infect a fresh stock of DDX3-deficient Huh-7 cells. After repeating this cycle of transduction, infection and passaging four times (Fig 3.39A and B), the viral infectivity of transduced cells was compared between $JFH1_{DSG}$ and the serially-passaged $JFH1_{DSG}$ mutant virus by SEAP assay. Unfortunately, instead of the emergence of a DDX3-depleted viral variant, the $JFH1_{DSG}$ mutant virus was observed to impair HCV replication to an even greater extent than $JFH1_{DSG}$ virus, with a reduction of almost 90 % found between DDX3-depleted cells and shControl-transduced cells infected with $JFH1_{DSG}$ mutant virus (Fig 3.39C and D).

3.2.6. Discussion

DDX3 knockdown caused a two-fold reduction to infectious HCV production in Huh-7 cells. This drop was potentially due to the effect of reduced RNA replication in DDX3-depleted cells as observed in the reductions in luciferase activity in DDX3-depleted Huh-7 cells at 48 h post-N17 SGR/$JFH1_{WT}$ RNA electroporation, which would subsequently reduce viral titres. However, the possibility of direct viral cell-to-cell spread in Huh-7 cells carried the risk of inaccurate titres and could perhaps mask the

A

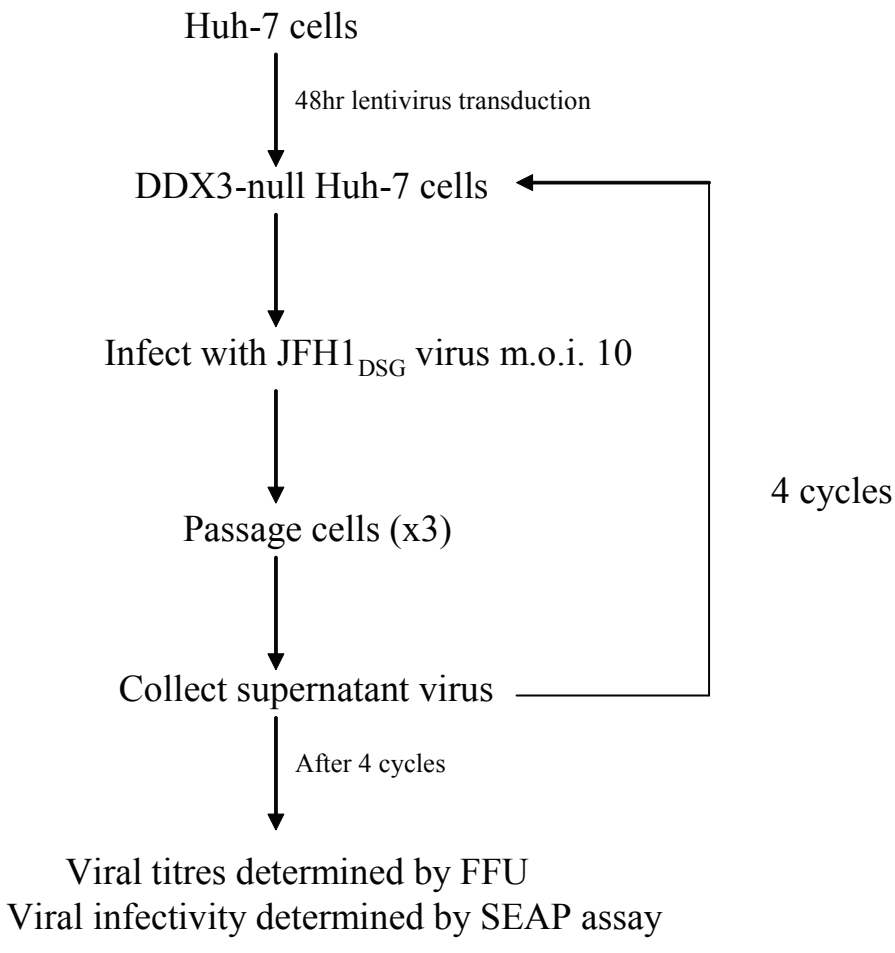
Huh-7 cells
48hr lentivirus transduction
DDX3-null Huh-7 cells
Infect with JFH1DSG virus m.o.i. 10
Passage cells (x3)
Collect supernatant virus
4 cycles
After 4 cycles
Viral titres determined by FFU
Viral infectivity determined by SEAP assay

B

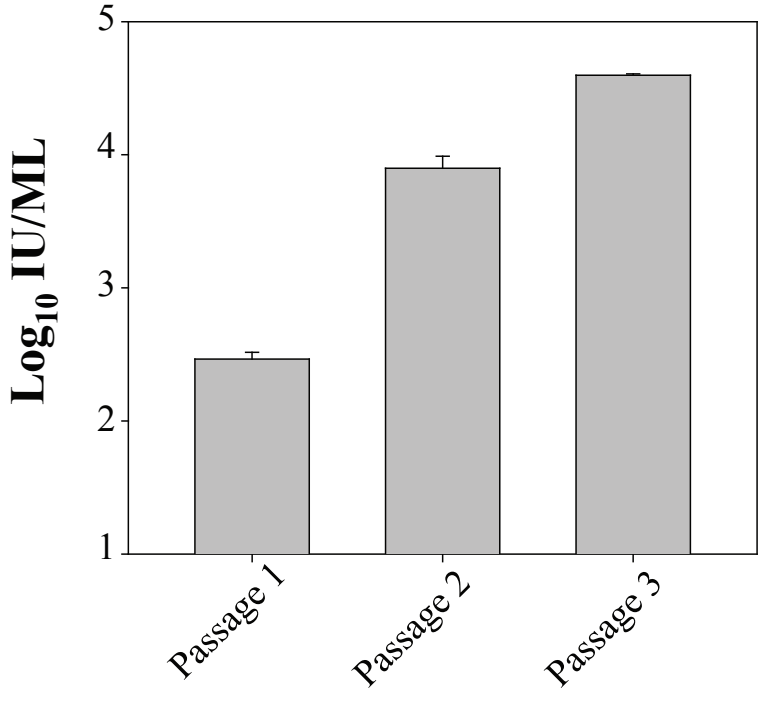
Log10 IU/ML
5
4
3
2
1
Passage 1
Passage 2
Passage 3

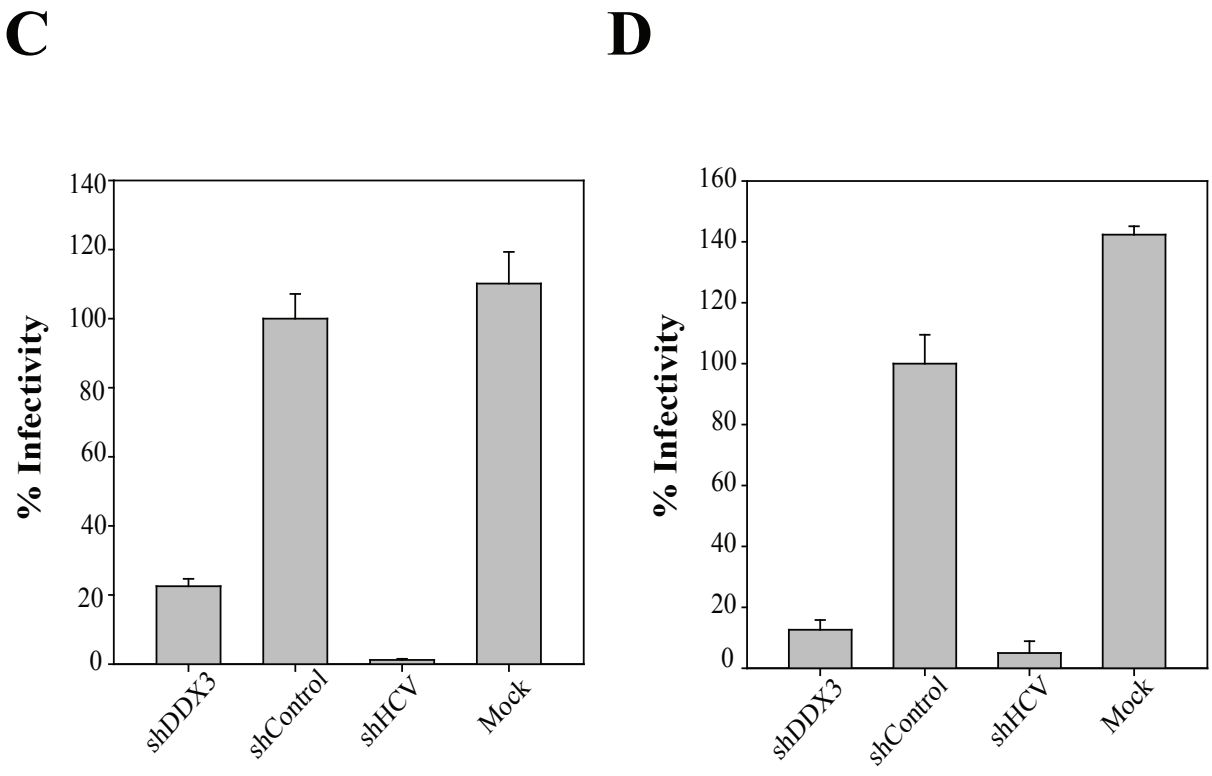

Figure 3.39. Attempted generation of a mutant virus that replicates independently of DDX3 function.

(A) Schematic diagram of the method used to select and amplify a mutant virus that replicates independent of DDX3 function. **(B)** Increase of $JFH1_{DSG}$ titres during cell passages. Virus titres were determined by FFU assay for the indicated cell passages during the 4^{th} cycle of infection. Mean values and standard deviations represent a single experiment performed with three technical repeats. **(C and D)** Comparison of infection kinetics in transduced cell lines infected with $JFH1_{DSG}$ virus **(C)** or with $JFH1_{DSG}$ mutant virus **(D).** Mean values and standard deviations represent single experiments, each performed with three technical repeats.

true effects of DDX3 knockdown on infectious virus production. Therefore, I employed a single cycle production assay using Huh7L-#4 cells to remove this complication. On doing this, I discovered that DDX3-depleted Huh7L-#4 cells produced markedly fewer infectious virus particles compared to shControl-transduced Huh7L-#4 cells (> 20-fold fewer particles). However, I also discovered that DDX3 knockdown does not impair N17 SGR/JFH1$_{WT}$ luciferase activity in a Huh7L-#4 background, suggesting that the drop in virus production in DDX3-depleted Huh7L-#4 cells is not due to reduced viral replication, unlike the negative control shHCV-transduced Huh7L-#4 cells. For some as yet unknown reason, the absence of DDX3 in this particular cell-line prevents the efficient assembly of HCV particles. Similar to the effect on viral replication in Huh-7 cells, DDX3 depletion only reduced infectious virus production if performed prior to the introduction of viral RNA into Huh7L-#4 cells.

I initially believed that the unusual phenotype observed in Huh7L-#4 cells may be related to the absence of CD81, a theory buoyed by the fact that replicon replication kinetics were very similar in Huh7L-#4 and shCD81 cells, and quite distinct from replicon replication levels in Huh-7 cells. However, while viral replication was unaltered between DDX3-deficient and control Huh7L-#4 cells, it was almost abrogated in DDX3-depleted shCD81 cells compared to control shCD81 cells. While this finding is in line with results published by Zhang *et al*. (2010), which detail the importance of CD81 in HCV genome replication as well as viral entry, this result also confirms that the absence of CD81 is not responsible for the phenotype observed in Huh7L-#4 cells. A recent study by Sainz *et al*. (2009) noted the differences in permissiveness and replication between phenotypically distinct Huh-7 cells and highlighted the potential of phenotypic drift in these cells. Thus, while Huh7L-#4 cells may be defined by their absence of CD81, these cells may have a mutated or depleted form of another crucial cellular factor(s) which explains the interesting phenotype I observe in them. Overall, this section has uncovered a potential role for DDX3 in infectious virus production unrelated to its other possible role in an aspect of viral RNA replication, suggesting that there are two distinct responsibilities for the protein in the HCV lifecycle.

4. Conclusions

4.1. Summary

A number of interesting results have emerged from this study regarding the role of DDX3 in the HCV life cycle. The findings in this study are recapitulated below, followed by a discussion section explaining some possible theories relating to the major findings of the work.

1. DDX3 knockdown from Huh-7 cells impaired the replication of $JFH1_{WT}$ following infection.

2. DDX3 acts at a post-translation stage of the HCV lifecycle in Huh-7 cells, impeding some as yet undefined element of HCV RNA replication.

3. DDX3-depleted cells transiently transfected with SGR RNA have greatly reduced viral replication compared to control cells, yet such an effect is not observed when DDX3 is depleted in cells stably replicating SGR RNA, highlighting the possibility that DDX3 influences the HCV replication complex (RC) machinery during HCV RNA replication.

4. DDX3 knockdown greatly alters infectious HCV production in Huh7L-#4 cells, with a ten-fold greater drop observed in these cells compared to Huh-7 cells. However, DDX3 is not important for efficient HCV RNA replication in these cells, indicating a possible pleiotropic role for the cellular helicase in the HCV lifecycle.

5. Analysis of HCV RNA replication and infectious virus production in shCD81 cells confirm that the absence of CD81 is not responsible for the phenotype observed in Huh7L-#4 cells.

6. Detailed characterisation studies indicated that the core-DDX3 interaction plays no role in regulating HCV RNA replication or infectious virus production.

4.2. Requirement of DDX3 During the Early Stages of the HCV Lifecycle in Huh-7 Cells

My results have confirmed the important role of DDX3 in the HCV lifecycle and deduced that DDX3 acts at a post-translation stage of the HCV lifecycle in Huh-7 cells. My results indicated that DDX3 targets a transient event that is an important aspect of HCV RNA replication, but does not alter steady-state HCV RNA replication.

While Geissler *et al*. (2012) postulated that DDX3 was a functional determinant of IRES-mediated translation, I found no evidence for such a role in my work. Geissler *et al*. (2012) found a 60-80 % reduction in replication in DDX3-depleted Huh-7 cells transiently replicating HCV replicon RNA at 1 h post-RNA electroporation. My experiments showed no significant difference in luciferase activity between DDX3-depleted cells and shControl-transduced Huh-7 cells transiently replicating N17 SGR JFH1 RNA at the same time point post-electroporation. I found similar results using both a replication-competent (N17 SGR JFH1 RNA_{WT}) and replication-deficient (N17 SGR JFH1 RNA_{GND}) replicon construct. I also performed control experiments where I varied levels of input replicon RNA or lengthened times of lentiviral transduction and noted no change to my observed DDX3-deficient phenotypes confirming a clear disparity between my results and those of Geissler *et al*. (2012). The reason behind such dissimilarity may be due to differences in experimental conditions, particularly the use of shRNA technology (present study) instead of siRNA (Geissler *et al*., 2012). Although shRNA and siRNA can be applied to achieve similar functional outcomes, they are intrinsically different molecules. The molecular mechanisms of action, the RNA interference pathways and the off-target effects of these systems have distinct variations between them. For instance, Dicer, an integral component of the RNA interference pathway, is known to promote mitotic localisation of DDX3 (Pek & Kai, 2011). It has been established that Dicer helps mediate the cleavage of shRNA to siRNA by forming part of the TRBP/PACT/Dicer complex (Murchison *et al*., 2005). Dicer-depleted mammalian cells can effectively load processed siRNAs onto the RNA-induced silencing complex (RISC) to allow RNA interference to begin, but shRNAs cannot be effectively processed and loaded onto RISC in Dicer's absence (Kok *et al*., 2007). Not only do these findings emphasise the different efficiencies in RNAi processing that may

account for the differences observed between this work and that of Geissler *et al*. (2012), they also suggest possible changes in cell-cycle regulation between DDX3-depleted cells treated with shRNA or siRNA. On the other hand, while siRNA can be loaded onto RISC without interacting with Dicer, TRBP or PACT, the loading process is ten times less efficient than shRNA, as shRNA can assimilate into the endogenous miRNA pathway. Concentrations of siRNAs needed for effective knockdown are often much higher than those required for shRNA and are introduced into cells by methods such as lipofection or electroporation which are more likely to trigger IFN induction in target cells compared to shRNA transduction. It has also been noted that siRNAs synthesised using a phage RNA polymerase system can trigger IFN induction in a variety of cell-lines due to the presence of 5'-triphosphates on such transcripts (Hornung *et al*., 2005; Hornung *et al*., 2006; Kim *et al*., 2004; Pichlmair *et al*., 2006). Another important point to note when considering conflicting results obtained by siRNA and shRNA is that shRNAs can be continuously synthesised by the host cell, ensuring a more durable knockdown effect compared to siRNAs, which undergo high levels of turnover and degradation after introduction into target cells.

My results also suggested that DDX3 influences the HCV replication complex machinery in enacting its important role in an aspect of RNA replication. This concept is supported by my findings which highlight diminished viral replication in DDX3-depleted cells transiently transfected with SGR RNA compared to control cells, in contrast to the minimal reductions observed in DDX3-deficient cells stably replicating SGR RNA. Not only are these results in line with findings published by Ariumi *et al*. (2007) and Randall *et al*. (2007), Geissler *et al*. (2012) also independently reported similar results at the same time I was undertaking these experiments. However, I was unable to state definitively whether DDX3 is incorporated into RC during viral replication or whether the cellular helicase influences the RC machinery via an indirect mechanism. Although I could not find evidence for DDX3's presence in RCs by IF analysis, it is possible that the protein may function in these structures at a level undetectable by this assay. If directly incorporated into the RC, I speculate that the presence of DDX3 in these structures prior to shRNA targeting may allow viral RNA replication to be sustained even in the face of nascent DDX3 depletion due to the low turnover rate of these complexes. The cellular autophagy machinery has recently been shown to be vital for the translation of incoming HCV genomes but unnecessary for

translation of progeny genomes (Dreux *et al*., 2009b). This observation and the results presented herein suggest that the cellular and viral factors required to initiate viral replication are different from those required to maintain it once RCs have formed, with DDX3 perhaps a crucial element of HCV replication initiation only. Another possible interpretation of my results may derive from the fact that expression of HCV proteins causes the reorganisation of cellular membranous compartments, which promotes the formation of RCs in modified cellular membranes. Thus, it is possible that the role of DDX3 could be to promote membrane alterations that are to harbour RCs, as has been suggested for cellular proteins such as ANXA2 (Saxena *et al*., 2012), known to directly interact with viral replicase factors such as NS5A and GBF1 (Goueslain *et al*., 2010), which is believed to influence RC activity despite being undetectable in the HCV RC by IF analysis.

Another interesting point to note from my results is that my colony forming assays indicate that DDX3-depleted replicon cells cannot be maintained in culture. This is unsurprising given the large number of cellular and viral processes in which the protein has been implicated (reviewed in Schröder, 2010), most notably apoptosis, where DDX3 has been found to be a component of an anti-apoptotic death receptor complex (Sun *et al*., 2008). Therefore, studies of the HCV lifecycle are limited to transient assays on early time points after infection in order to avoid disrupting additional host factors necessary for efficient cellular function. While cell viability is known to be unchanged up to 96 h post-DDX3 silencing (Ishaq *et al*., 2008; Angus *et al*., 2010; Ariumi *et al*., 2007; Randall *et al*., 2007), the results of Geissler *et al*. (2012) state that general translation is impaired in Huh-7 cells three days after addition of DDX3 siRNAs. Thus, it is possible that an altered translation pattern occurs in DDX3-depleted Huh-7 cells after lentivirus transduction, which may modify the replication kinetics of HCV genomes subsequently introduced into these cells. There are a number of studies which assert that DDX3 facilitates cellular translation initiation through association with initiation factors, ranging from eIF4F (Soto-Rifo *et al*., 2012), eIF4A, eIF2α, PABP (Lai *et al*., 2008) to eIF3 (Lee *et al*., 2008). eIF3 was also found to interact with DDX3 by Geissler *et al*. (2012). However, there have been reports published which disagree with this theory, with studies which describe DDX3 as a repressor rather than a facilitator of cap-dependent translation while enhancing IRES-dependent viral translation (Shih *et al*., 2008). A recent study also published results where knockdown of the 40S ribosomal

subunit, found by Geissler *et al*. (2012) to interact with DDX3, can suppress translation activity controlled by an HCV IRES yet leave cellular translation unperturbed (Huang *et al*., 2012), which suggests DDX3 does not affect cellular translation. Nevertheless, despite the differences between my study and that of Geissler *et al*. (2012), my data clearly illustrates the importance of DDX3 at a post-translation stage of the HCV lifecycle in Huh-7 cells, possibly impeding some as yet undetermined element of HCV RNA replication. Further work is required to understand why the two studies gave such divergent results and determine which gives a more accurate representation of the role of DDX3 *in vivo*. Repeating experiments performed in this study with siRNAs from the Geissler *et al*. (2012) study and the development of a functional HCV minigenome system would help me to clarify the disparities. Analysis of positive- and negative-strand HCV RNA by Reverse Transcription-Quantitative PCR (RT-qPCR) in shDDX3- and shControl-transduced cells would be extremely valuable in determining the role (if any) DDX3 plays in HCV genome synthesis. Biochemical assays looking at the stoichiometry of DDX3 in RCs as well as EM analysis investigating possible membrane alterations and potential interactors would also be very beneficial in determining the exact role of the helicase in these structures and in the HCV lifecycle in general.

4.3. Role of DDX3 in Infectious HCV Production

While the data from this study has confirmed that DDX3 acts at an undetermined stage of HCV RNA replication in Huh-7 cells, I also wished to determine if DDX3 depletion had any specific effect on HCV infectious virus production. Single cycle infectious virus production assays using Huh7L-#4 cells were developed to separate the different stages of the lifecycle and to eliminate the inaccuracy that viral spread poses to assembly assays. DDX3-deficient phenotypes observed in these cells showed substantial decreases in infectious virus production without impairment to levels of viral RNA replication, indicating a specific role for DDX3 in assembly of HCV particles.

Host factor requirement and their mechanisms of action are poorly understood in the context of HCV assembly, but numerous cellular factors have been found to be essential for this process. siRNA studies have confirmed that cellular factors apolipoprotein E (apoE) (Chang *et al*., 2007; Jiang & Luo, 2009), Annexin A2 (ANXA2) (Backes *et al*.,

2010), heat shock cognate protein 70 (HSC70) (Parent *et al*., 2009), μ subunit of clathrin adapter protein complex AP2M1 (Neveu *et al*., 2012), diacylglycerol acyltransferase-1 (DGAT1) (Camus *et al*., 2013; Herker *et al*., 2010) and the late endosomal protein HRS (Tamai *et al*., 2012) are each vital for HCV assembly. While virus production levels are not reduced by DDX3 depletion if HCV infection has already been established in the host system, viral assembly was greatly diminished in HCV-infected cells subsequently transfected with apoE siRNA (Jiang *et al*., 2009) or HSC70 siRNA (Parent *et al*., 2009). This disparity points to the potential importance of DDX3 in influencing HCV RC function. Given that LDs are in close proximity to RCs (Targett-Adams *et al*., 2008a), DDX3 may play a direct role in virus assembly by transferring the viral genome to sites of assembly. A recent study adds weight to this argument, as another host protein does exactly this role while also maintaining a separate vital role in viral RNA replication, showing similar characteristics to DDX3. The cytosolic phospholipase A2 gamma (PLA2G4C), an enzyme involved in lipid metabolism, is believed to be essential in the formation of membranous webs (MWs) during the early stages of HCV infection and is an integral part of the HCV RC. After sufficient accumulation of viral proteins during replication, stimulation of PLA2G4C expression occurs, causing the protein to interact with LDs and initiating translocation of the RC to sites of virion assembly (Xu *et al*., 2012). PLA2G4C's role in RC transfer may bridge the steps of RNA replication and HCV assembly. Although it is as yet undetermined whether DDX3 is incorporated into RCs or not, the potential dual role of DDX3 in the HCV life cycle may be of similar aspect.

The interaction of HCV core with cellular proteins has been found to play numerous diverse roles in the viral assembly process. Abrogating the core-DGAT1 interaction leads to the accumulation of core on ER membranes, with traffic of the capsid protein subsequently impeded to LDs, suggesting a defect at an early stage of assembly (Herker et al., 2010). Disrupting core-AP2M1 binding, however, leads to the accumulation of core on LDs by altering AP2M1's recruitment to LDs, resulting in decreased core localisation with E2 and elements of the trans-golgi network, suggesting the core-AP2M1 interaction mediates a later stage of assembly post-accumulation of core on LDs but before envelopment at ER sites (Neveu *et al*., 2012). In my study, disruption to the core-DDX3 interaction caused no adverse effects to HCV assembly. This result is strengthened after analysis of a conserved glycine residue, G33, located very close to

the tyrosine residue on core (Y35) essential for the core-DDX3 interaction. This glycine, when mutated to alanine during alanine-scanning mutagenesis studies, has been found to be critical for HCV assembly (Angus *et al*., 2012). Despite being unable to decipher the level of interaction with DDX3 in this G33A mutant, findings from the study excluded changes to the core-DDX3 interaction as an explanation for the assembly phenotype observed (Angus, unpublished). Another study which shows the irrelevance of the DDX3-core interaction in HCV replication and assembly comes from Kang *et al*. (2012), who observed that adaptive core mutants generated in a JFH1 background which exhibit enhanced viral infectivity display greatly reduced affinity for DDX3 in tandem.

It must always be borne in mind that Huh7L-#4 cells represent an individual subclone species of Huh-7/Lunet cells, a "cured" replicon cell line with a bimodal level of CD81 expression (Witteveldt *et al*., 2009). The Huh7L-#4 subspecies with low endogenous CD81 levels were generated after subjecting these cured cells to FACS analysis and limiting dilution cloning. Therefore, this cell-line may have different characteristics to Huh-7 cells. While Huh7L-#4 cells may be defined by their absence of CD81, I quickly confirmed that a lack of CD81 was not responsible for the interesting assembly phenotype they possess. This suggests that host cell factors essential for HCV RNA replication or virus production are differentially expressed in Huh7L-#4 cells compared to Huh-7 cells. The identification of this novel DDX3 function in Huh7L-#4 cells indicates that DDX3 plays a pleiotropic role in the HCV lifecycle. My data suggests that DDX3 may also play a vital part in efficient infectious virus production unrelated to its well-defined role in viral RNA replication. A microarray investigating differences in gene expression between Huh-7 and Huh7L-#4 cells followed by detailed functional studies on cellular factors exhibiting significant differences in this microarray would provide us with vital information on the role of DDX3 in infectious virus production.

4.4. The Importance of DDX3's Interactions with Viral Proteins

The core-DDX3 interaction has been previously found to be dispensable for HCV replication (Angus *et al*., 2010). Using the *in-vitro* cell systems available to us, I confirmed that the DDX3-core interaction did not play any role at any stage of the HCV life cycle, either in Huh-7 cells, Huh7.5 cells or in Huh7L-#4 cells (although the presence of specific high molecular weight species was observed only in cells with a functional core-DDX3 interaction when cellular extracts were lysed in non-reducing sample buffer (NR-SB) and examined with the anti-DDX3 mAb AO196 – see appendix 5). Replicon experiments performed in a Y35A or Δcore background showed no difference to replication results obtained in a WT background, both in cells stably expressing SGR RNA or those transiently transfected with SGR RNA. Although these results seem conclusive, there are several considerations that must be taken into account when interpreting these results. Firstly, the limitations and peculiarities of both the HCVcc and SGR systems may not truly represent HCV replication *in vivo* and thus mask the functions exerted by the core-DDX3 interaction. The cell-lines used in this study, Huh-7 cells and their subclones, may limit the necessity of core binding to DDX3 if they lack efficient immune defences. My results showed no difference in HCV replication between Huh-7 cells and Huh-7.5 cells, a subclone of Huh-7 cells which have a defective IFN response caused by a mutation in the RIG-I gene, suggesting that the proviral role of DDX3 is not influenced by the T55I RIG-I mutation. However, Huh-7 cells may not have an efficient immune response either, even in the presence of an unaltered RIG-I gene, a theory which would help explain why Huh-7 cells are the only cell-line capable of supporting high levels of HCV RNA replication.

Indeed, there is ample evidence in recent reports to suggest that DDX3 does positively regulate IFN-induction. DDX3's interaction with kinases IKK-ε (Schröder *et al.*, 2008), TBK1 (Soulat *et al.*, 2008) and IPS-1 (Oshiumi *et al*., 2010b) have all been found to contribute to this process. Schröder *et al*. (2008) found that a direct interaction between the vaccinia virus K7 protein and DDX3 could inhibit IFN-induction. The hypothesis that core was employing a similar strategy to K7, interacting with DDX3 so as to limit the role of the helicase role in positively regulating IFN-induction, was given weight by results published by Oshiumi *et al*. (2010a). In this study, Oshiumi *et al*. (2010a)

indicated that core protein could abrogate DDX3's role in IPS-1-mediated IFN-β induction by blocking the interaction between the C-terminal region of DDX3 and the CARD-like region of IPS-1 through its own interaction with DDX3. It is important to note that the authors used HEK293T cells instead of Huh-7 cells to observe these effects, so it is possible that an efficient innate immune response in HEK-293T cells allow changes in IFN-regulation to be accurately observed. It is also vital to remember that the results obtained in this study were achieved after transfecting large quantities of expression plasmids encoding tagged versions of IPS-1 or DDX3 into target cells. Overexpressed exogenous proteins may not accurately represent how endogenous cellular factors behave *in vivo*. Kang *et al*. (2012) reported that the IFN-modulating activity of adapted core mutants was greater than WT core due to their decreased binding activity to DDX3 after transfecting Huh-7 and Huh-7.5 cells with plasmids expressing tagged core and DDX3 proteins. The discrepancy between the results of Oshiumi *et al*. (2010a) and Kang *et al*. (2012) could be due to the adverse effects to cellular function brought about by excess quantities of different exogenous proteins introduced into cells by transfection.

In spite of this possibility, one must recognise that Huh-7 cells may not be the most suitable cell-line for analysing viral IFN-induction because they are a hepatocyte-derived cellular carcinoma cell-line. Differential regulation of DDX3 has been reported in a number of tumour cell-lines, including HCC (Botlagunta *et al.*, 2008; Chang *et al.*, 2006; Chao *et al.*, 2006; Huang *et al.*, 2004). This not only suggests that there may be differences in how the core-DDX3 interaction functions in Huh-7 cells compared to how it functions *in vivo* because of the likely altered DDX3 levels in this carcinoma cell-line, it also implies that DDX3 and its interaction with core may be involved in HCV-associated pathogenesis (Chang *et al.*, 2006; Huang *et al.*, 2004). DDX3 has also been found to be upregulated during HIV-1 replication (Krishnan & Zeichner, 2004), during the immune response to lipopolysaccharide-induced inflammation (Saban *et al.*, 2006) and during interferon treatment (de Veer *et al.*, 2001). These results, placed alongside data from Oshiumi *et al*. (2010a), insinuates that during active viral replication, HCV can recruit DDX3 to evade host immune responses and contribute to viral pathogenesis (Rosner & Rinkevich, 2007).

On the other hand, there are other hypotheses that account for the dispensable nature of the core-DDX3 interaction. One of the best explored is the theory that abrogation of the interaction could be supplanted through the recruitment of another cellular factor(s) by HCV. In line with this, another DEAD-box protein, DDX1, is present on LDs alongside DDX3 in core expressing Hep39 cells (Sato *et al.*, 2006). DDX1, like DDX3, has been implicated in HIV-1 RNA nuclear export (Fang *et al.*, 2004; Yedavalli *et al.*, 2004). Another DEAD-box protein, DDX5, has also been reported to interact with core and NS5B (Goh *et al.*, 2004; Kang *et al.*, 2005). Such related cellular proteins may be functionally interchangeable with DDX3 during virus replication.

My data obtained in a $JFH1_{Y35A}$ background suggests that the important role(s) DDX3 plays in the HCV lifecycle may derive through interaction with another viral protein(s) other than core or because of indirect associations with viral elements. I attempted to generate a mutant virus that functions independently of DDX3 function by selecting JFH1 variants that were resistant to the antiviral effect of DDX3 knockdown. If successful, the adapted mutations observed in these variants would have been introduced into the relevant viral protein of $JFH1_{WT}$ from which they arose and used to determine whether they were crucial for viral RNA replication or infectious virus production. This experiment would also have helped determine other viral protein(s) that interacted with DDX3. A similar approach was used to uncover the target of an antiviral drug that inhibited initiation of HCV RNA replication at the onset on infection (Gastaminza *et al.*, 2011). Unfortunately, developing such a virus variant proved elusive. Despite this disappointment, there are numerous published reports detailing the range and importance of DDX3's association with viral proteins in other viruses which provide us with clues to its mechanism of action and potential HCV interactors. DDX3's interactions with these proteins have been shown to be both proviral -inhibiting interferon induction by binding the vaccinia virus K7 protein (Schröder *et al.*, 2008) or aiding HIV-1 replication by targeting incompletely spliced mRNAs to cellular nuclear export protein CRM1 for export from the nucleus through its direct interaction with the viral rev protein (Yedavalli *et al.*, 2004) - and antiviral in nature – DDX3 can be incorporated into HBV nucleocapsids through its direct association with the HBV polymerase protein, where it inhibits reverse transcription of the virus (Wang *et al.*, 2009a). These results clearly illustrate that DDX3 can bind to a whole range of different viral proteins, both structural and non-structural.

As DDX3's influence on the RC machinery may drive its important function in both HCV RNA replication and viral assembly, it is conceivable that DDX3 may interact with viral non-structural proteins vital to the integrity of these structures. The NS proteins encompassing NS3 to NS5B are all known to be implicated in these complexes (Quinkert *et al*., 2005). If DDX3 promotes membrane alterations that are to harbour RCs, an interaction with NS4B is a distinct possibility, as NS4B induces the formation of the MW, a series of membrane alterations that serve as a scaffold for HCV RC formation (Egger *et al*., 2002; Gosert *et al*., 2003). DDX3 depletion could disrupt the ability of NS4B to bind to ER membranes and lead to a loss of proteins at the MW, resulting in diminshed viral replication. While DDX3 was not found to co-localise with NS5A by IF analysis, it is interesting to note that NS5A, an essential element of the RC, has been shown to be a key mediator of both viral RNA replication and infectious virus production through distinct mechanisms (Appel *et al*., 2005; Tellinghuisen *et al*., 2008a; Tellinghuisen *et al*., 2008b), as is also hypothesised for DDX3. These findings were derived from analysis of NS5A's hyperphosphorylation status. Given that NS4A can influence NS5A hyperphosphorylation (Lindenbach et al., 2007), it could be the case that DDX3 regulates NS5A's vital roles in viral replication and assembly indirectly through NS4A or, alternatively, directly with NS5A but at minute levels undetectable by IF assay. NS3 has also been found to play distinct roles in RNA replication and infectious particle assembly in the HCV lifecycle (Lohmann *et al*., 2003; Ma *et al*., 2008; Phan *et al*., 2009; Yi *et al*., 2007). While DDX3's direct interaction with the HBV polymerase (Wang *et al*., 2009a) implies that a similar interaction is possible between DDX3 and the HCV RNA-dependent RNA polymerase NS5B, Ariumi *et al*. (2007) found no association between DDX3 and NS5B by immunoprecipitation during that study's investigation of DDX3's role in HCV replication. Ariumi *et al*. (2007) did not observe an interaction between DDX3 and NS5A either, in line with my findings.

Is is also possible that DDX3's potential roles in viral replication and infectious virus production may derive from interactions with non-structural proteins that are not directly involved in RCs. NS2, known to be essential for the production of infectious virus particles, has been found to be localised to sites adjacent to RCs. Here, it has been observed to interact with NS5A (and potentially other RC components), potentially facilitating the co-ordination of genome replication and virion assembly (Tedbury *et al*.,

2011). The subcellular location of NS2 suggests it may provide a mechanism for the exportation of nascent genomes from RCs. By positioning at an exit site of the RC, NS2 may mediate the interaction between the RC and the structural proteins. Alternatively, it may function in the release of RNA from the RC and allow its encapsidation into nascent HCV particles. A serine residue (S168) within NS2 and an ion channel-independent function of p7 have been found to be essential for the efficient localisation of NS2 adjacent to RCs (Tedbury *et al*., 2011). The effects of DDX3 depletion on the subcellular localisation of NS2 are worthy of investigation, particularly if a direct interaction is subsequently observed between DDX3 and p7 or NS2. One must also take into account the fact recent RNA-protein interaction studies have discovered that DDX3 can bind directly to norovirus RNA. This interaction may be vital for norovirus replication, given that RNAi mediated knockdown of DDX3 inhibits norovirus replication in cell culture (Vashist *et al*., 2012). A similar event may be responsible for DDX3's role in the HCV life cycle, as RNA-protein interaction studies have suggested that DDX3 interacts with the 3'UTR of the HCV RNA genome in an as yet unknown manner (Harris *et al*., 2006). Indeed, a recent publication by Li *et al*. (2013b) has highlighted that DDX3 interacts directly with the 3'UTR, resulting in activation of IKK-α, which subsequently translocates to the nucleus and induces a CBP/300-mediated transcriptional programme involving sterol regulatory element binding-proteins (SREBPs). The induction of this innate pathway induces lipogenic genes and enhances lipid droplet formation, facilitating viral assembly (Li et al., 2013b). Determining whether this 3'UTR-DDX3 interaction, confirmed by co-immunoprecipitation analysis by Li *et al*. (2013b), was responsible for the reduced infectious virus production observed in DDX3-knockdown Huh-7 and Huh7L-#4 cells in this study would be an interesting next step in my lab's investigations into the proviral role of DDX3.

While DDX3 has been postulated as an integral component of cellular stress granules (Shih *et al*., 2012) (section 1.12.2.9), it has also been found to be one of a subset of cellular proteins that colocalise in discrete cytoplasmic foci similar in nature to stress granules known as processing (P) bodies. P-bodies are distinct granular structures where untranslated mRNAs can be stored for later release or where mRNAs undergo decay and translation repression. HCV and other members of the *Flaviviridae* family such as West Nile virus (WNV) have been found to hijack numerous P-body components, including DDX3, and recruit them to viral replication sites (Ariumi *et al*., 2011; Chahar

et al., 2013). Another P-body component is the DEAD-box helicase DDX6, which is an mRNA effector and has been found to associate directly with DDX3. DDX6, like DDX3, has also been found to positively regulate HCV RNA replication and was found to co-localise with core protein (Ariumi *et al*., 2011), suggesting that DDX3 may co-modulate DDX6 function and that the core-DDX3 interaction may be pivotal to this process. The reason why so many components of P-bodies are recruited to HCV replication sites has yet to be determined, although it has been proposed that they might influence switching between RNA replication and viral assembly (Beckham & Parker, 2008). The presence of DDX3 in P-bodies and its interaction with constituent elements of these cytoplasmic structures may help explain how DDX3 performs its pleiotropic role in the HCV life cycle.

4.5 Finishing Statement

The aim of this project was to determine the role of DDX3 in the HCV lifecycle. To this end, I have shown the importance of DDX3 at a post-translation stage of the HCV lifecycle in Huh-7 cells, impeding an undetermined aspect of HCV RNA replication. I also discovered a possible dual role for DDX3 in the lifecycle, with my data suggesting that DDX3 plays a significant part in efficient infectious virus production in Huh7L-#4 cells unrelated to its role in HCV RNA replication. As well as fulfilling the major aim of the project, my data also suggests that DDX3 plays a important function in HCV replication complex activity, in which it may perform its pleiotropic role in the HCV lifecycle, although I have not determined whether DDX3 performs this duty through a direct incorporation into the RC or via an indirect mechanism. Furthermore, I confirmed the lack of correlation between virus replication and the level of core-DDX3 binding. My investigations in a number of *in vitro* cell systems found no role for the core-DDX3 interaction, confirming its dispensable nature in the viral lifecycle. Undoubtedly, the data and reagents generated in this project will be of great utility for future studies investigating the molecular mechanisms behind DDX3's multiple roles in the HCV lifecycle, particularly its exact role in the HCV replication complex (Fig 4.1).

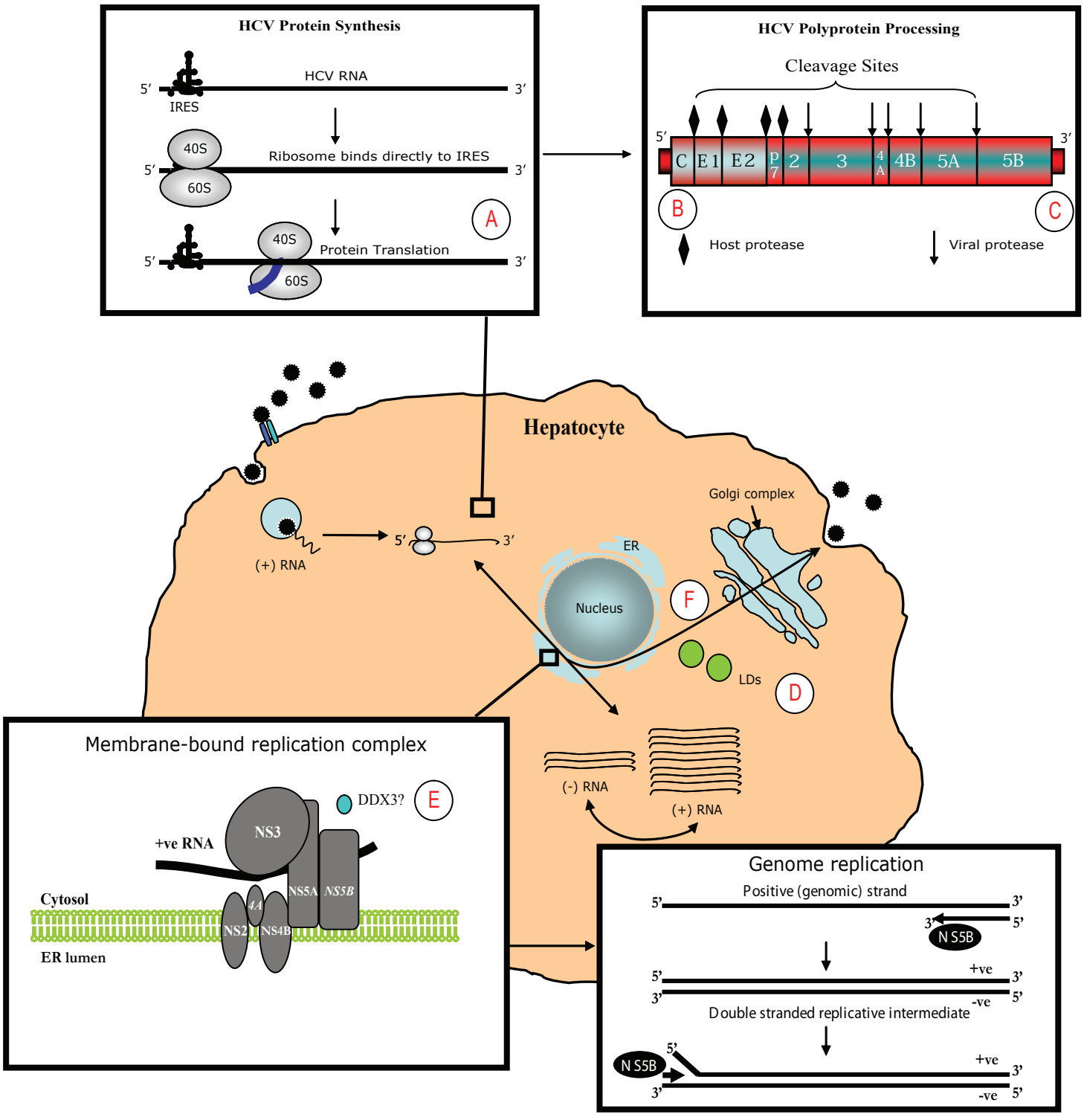
HCV Protein Synthesis
HCV RNA
5′
3′
IRES
40S
60S
Ribosome binds directly to IRES
A
Protein Translation
HCV Polyprotein Processing
Cleavage Sites
C
E1
E2
p7
2
3
4A
4B
5A
5B
B
C
Host protease
Viral protease
Hepatocyte
(+) RNA
Golgi complex
ER
Nucleus
F
LDs
D
(-) RNA
(+) RNA
Membrane-bound replication complex
DDX3?
E
+ve RNA
NS3
NS5A
NS5B
4A
NS2
NS4B
Cytosol
ER lumen
Genome replication
Positive (genomic) strand
NS5B
+ve
-ve
Double stranded replicative intermediate

Figure 4.1. Potential roles of DDX3 in the HCV lifecycle.

The potential importance of DDX3 at different stages of the HCV lifecycle is highlighted. (**A**) Geissler *et al*. (2012) state that DDX3 is a functional determinant of translation, both cap- and IRES-mediated. (**B**) Oshiumi *et al*. (2010a) postulate that core protein participates in suppression of DDX3-augmented IPS-1-mediated IFN-β induction through its association with DDX3. Angus et al. (2010) also unearthed a direct core-DDX3 interaction, abrogation of which had no effect on HCV RNA replication on infectious virus production.(**C, D**) DDX3 has been found to interact with the HCV 3'UTR (Harris *et al*., 2006, Li *et al*., 2013b). Li *et al*. (2013b) hypothesize that this interaction activates an innate pathway that induces lipogenic genes and enhances core-associated lipid droplet formation to facilitate viral assembly. (**E**) Data presented in this thesis suggests that DDX3 acts at a post-translation stage of the HCV lifecycle in Huh-7 cells, impeding some as yet undetermined element of HCV RNA replication. There is a possibility that DDX3 may be incorporated directly into HCV replication complexes to perform this potential role. (**F**) Another prominent finding in this thesis highlights how DDX3 knockdown alters infectious virus production in Huh7L-#4 cells despite having no effect of HCV RNA replication, indicating that DDX3 alters virus production in some as yet undetermined manner in this cell-line.

Appendices

Appendix 1: Primers used for core mutagenesis

Primer Name	Sequence (5' – 3')	Function
F130E sense	CACCCTAACGTGTGGCGAGGCCG ACCTCATGGGGT	Forward primer for site-directed mutagenesis of F130E in N17 SGR/JFH1$_{WT}$ plasmid
F130E antisense	ACCCCATGAGGTCGGCCTCGCCA CACGTTAGGGTG	Reverse primer for site-directed mutagenesis of F130E in N17 SGR/JFH1$_{WT}$ plasmid
Y35A sense	ATCGTTGGCGGAGTAGCCTTGTT GCCGCGCAGG	Forward primer for site-directed mutagenesis of Y35A in N17 SGR/JFH1$_{WT}$ plasmid
Y35A antisense	CCTGCGCGGCAACAAGGCTACTC CGCCAACGAT	Reverse primer for site-directed mutagenesis of Y35A in N17 SGR/JFH1$_{WT}$ plasmid

A

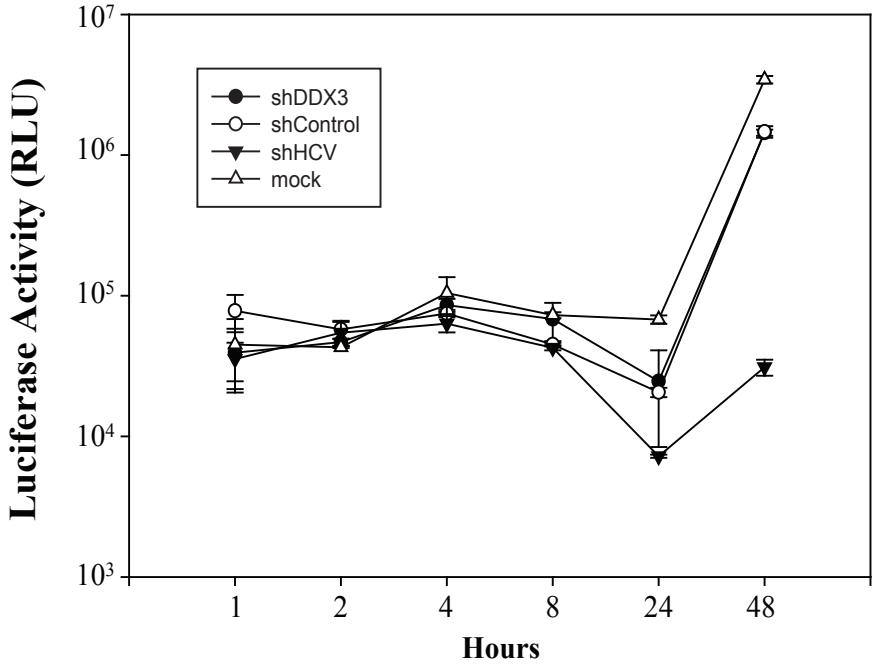

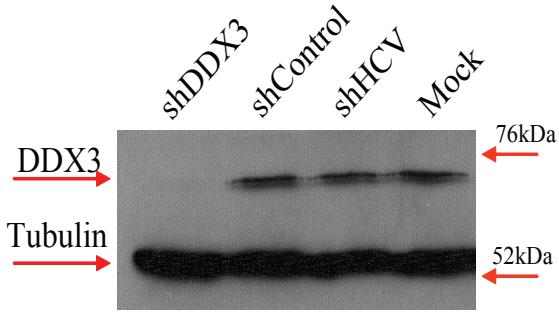

B

Fold change from shControl		
	24hrs	**48hrs**
shDDX3	+ 0.17	- 0.02
shHCV	- 2.85	- 47.28
mock	+ 3.29	+ 2.34

Appendix 2. Effect of DDX3 Knockdown in Huh7L-#4 cells transiently replicating B3P7$_{WT}$ replicon RNA at various timepoints.

(A) Huh7L-#4 cells were electroporated with 10 µg B3P7$_{WT}$ replicon RNA at 48 h post-transduction with indicated lentivirus. Cell lysates were assayed at the indicated time points post-electroporation for luciferase activity. Mean values and standard deviations represent a single experiment performed with three technical repeats. A portion of cells from each set of transduced cells were lysed in SB at 48 h post-transduction and probed with the anti-DDX3 mAb AO196. Anti-α-Tubulin mAb was used as a loading control. **(B)** Table showing the fold-changes in luciferase activity in cells transduced with indicated lentivirus compared to cells transduced with shControl.

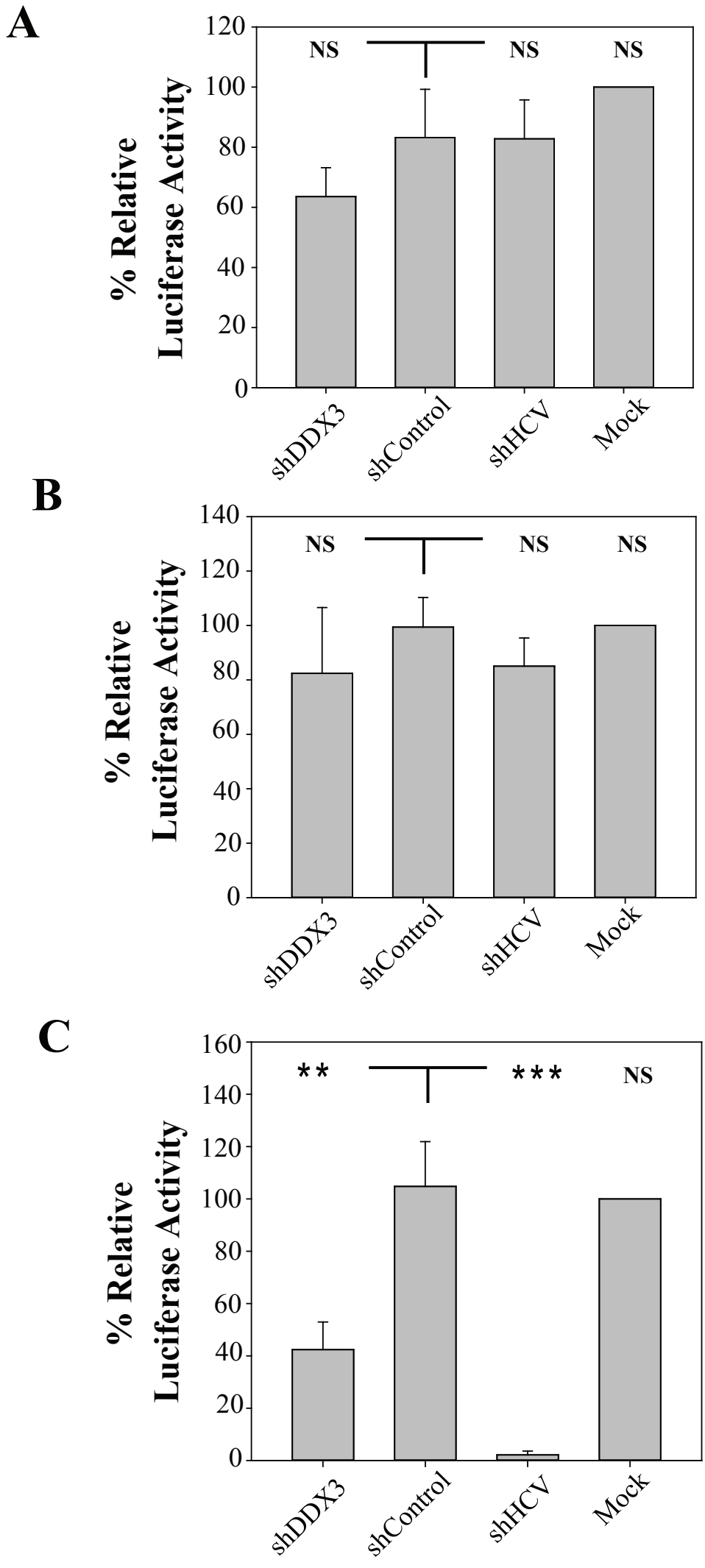
A
% Relative Luciferase Activity
120
100
80
60
40
20
0
NS
NS
NS
shDDX3
shControl
shHCV
Mock
B
% Relative Luciferase Activity
140
120
100
80
60
40
20
0
NS
NS
NS
shDDX3
shControl
shHCV
Mock
C
% Relative Luciferase Activity
160
140
120
100
80
60
40
20
0
**
***
NS
shDDX3
shControl
shHCV
Mock

D

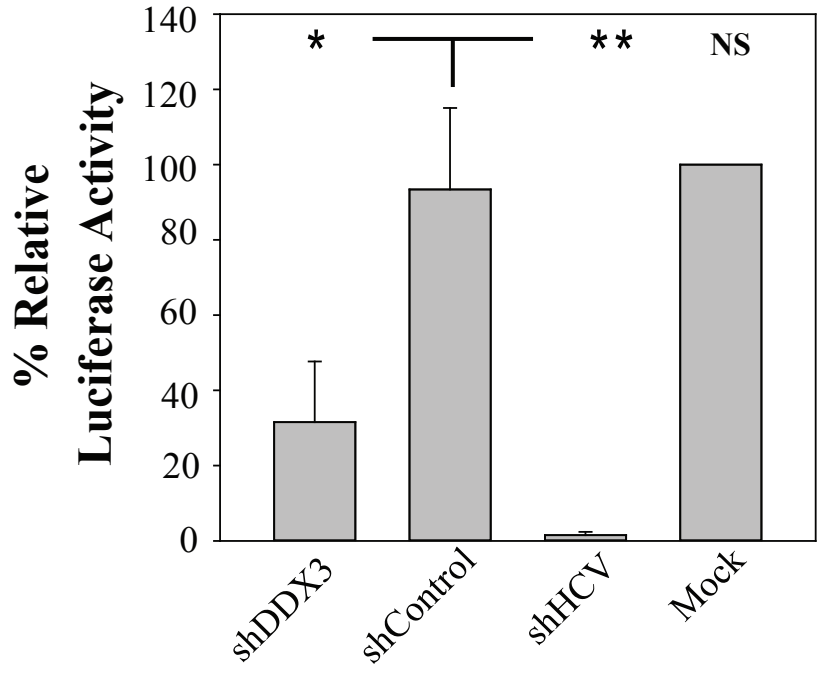

Appendix 3. Effect of DDX3 Knockdown in Huh-7 cells transiently replicating N17 SGR/JFH1$_{WT}$ replicon RNA at various timepoints.

Analysis of data presented in Fig 3.14 on a linear scale. Graphs plotted for individual time points of interest post-electroporation, 1 h (A) 2h (B) 24 h (C) and 48 h (D). Error bars indicate the standard deviation of the mean of three individual experiments. Student's t-test was performed to determine the P value. * $P < 0.05$, ** $P < 0.01$, *** $P < 0.001$, NS, not significant.

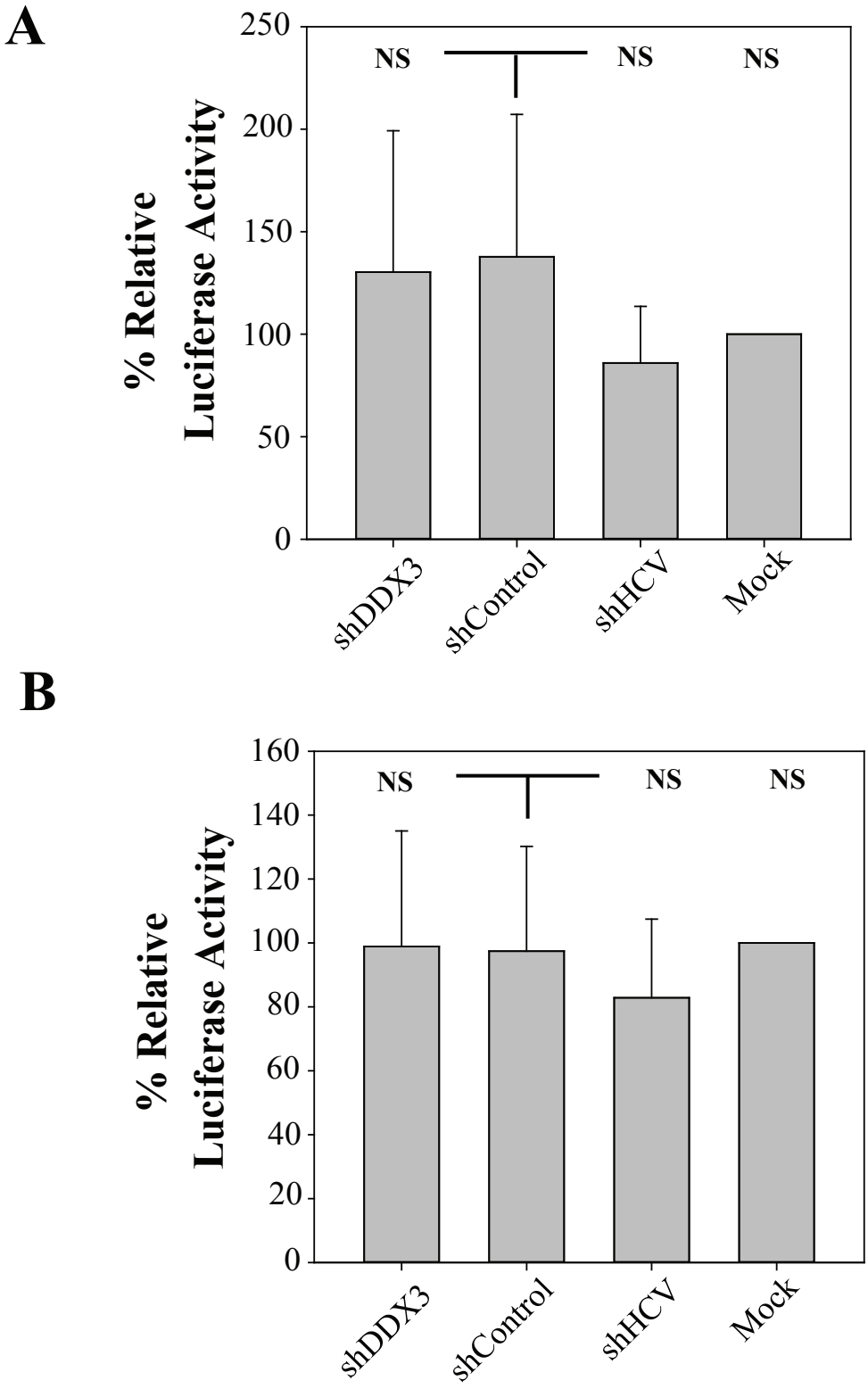

Appendix 4. Effect of DDX3 knockdown on HCV translation.

Analysis of data presented in Fig 3.20 on a linear scale. Graphs plotted for individual time points of interest post-electroporation, 1 h (A) and 2h (B). Error bars indicate the standard deviation of the mean of three individual experiments. Student's t-test was performed to determine the P value. * $P < 0.05$, ** $P < 0.01$, *** $P < 0.001$, NS, not significant.

Appendix 5. Investigating the Potential Role of the HCV Core-DDX3 Interaction in DDX3 Oligomerisation

5.1. Introduction

DDX3 has been shown to interact with, and be phosphorylated by, TBK1 and IKKε, kinases central to the induction of the cellular IFN response (Soulat *et al*., 2008). Indeed, results from Soulat *et al*. (2008) suggest that phosphorylation of DDX3 by TBK1 is vital for efficient IFN induction. Given that DDX3 depletion studies in HCVcc revealed that the requirement of DDX3 for HCV replication is unrelated to its interaction with viral core protein (Angus *et al*., 2010), the possibility of this interaction in phosphorylation of the helicase was investigated.

No difference in DDX3 species or intensity was seen at ~ 73 kDa between HEK-293T cells in the presence or absence of a functional core-DDX3 interaction. However, the presence of specific high molecular weight species was observed when HEK-293T cells with a functional core-DDX3 interaction were lysed in non-reducing sample buffer (NR-SB) and examined with the anti-DDX3 mAb AO196. These high molecular weight complexes were also observed in Huh-7 cells under similar conditions but were absent from both HEK-293T and Huh-7 extracts if samples were treated with reducing sample buffer (SB).

Analysis of these complexes in a modified 2-D gel system revealed the presence of DDX3 at high molecular weights in all cellular extracts, including those where a core-DDX3 interaction was not functional or where core was absent. Core was also detected in high molecular weight species under these conditions, but only in samples where an intact DDX3-core interaction could be observed, highlighting the possibility of a functional DDX3-core interaction being involved in core oligomerisation.

5.2. Results

Results from Soulat *et al*. (2008) highlighted the possibility that phosphorylation of DDX3 by TBK1 is vital for efficient IFN induction in HEK-293T cells. In this study, the authors observed two distinct species upon immunoblot analysis of HA-tagged derivatives of DDX3, one which the authors remarked was representive of a basal form of the protein, the other indicative of a phosphorylated species. In the present study, three predominant species were observed at ~ 73 kDa from lysates extracted from HEK-293T cells in non-reducing sample buffer (NR-SB) (composed of 30 mM Tris-HCl, pH 6.7; 1 % SDS; 5 % glycerol, 1 µg/ml bromophenol blue) and probed with the anti-DDX3 monoclonal mAb AO196. This difference in DDX3 species between my work (see appendix Fig 5.2A and B) and that of Soulat *et al*. (2008) may be explained by the fact that Soulat *et al*. (2008) detected overexpressed forms of DDX3, in contrast to the endogenous DDX3 detected in appendix Fig 5.2A. However, it was unclear whether any of the DDX3 species I observed represented a phosphoylated form of the protein (Transfection of tagged TBK1 or IKK-ε proteins into our cell-lines of interest, as Soulat *et al*. (2008) performed, could potentially be very useful in determining the phosphorylated status of each of the DDX3 species observed).

I wished to determine the effects the presence of a functional HCV core-DDX3 interaction had on endogenous DDX3 expression in these cells and whether I would observe changes to DDX3 species or intensity in cells where a core-DDX3 interaction was present compared to where it was absent. Thus, I transduced HEK-293T cells with a retroviral vector expressing the wild-type versions of the JFH1 structural proteins core, E1 and E2 (PQCXIP $CE1E2_{WT}$) (see materials and methods, section 2.2.9). Mutant versions of this construct were transduced in parallel, notably PQCXIP $CE1E2_{Y35A}$, which contains the core point mutation Y35A that abrogates the DDX3-core interaction, and PQCXIP $CE1E2_{F24Y,}$ which contains the core point mutation F24Y that is responsible for a greatly enhanced DDX3-core interaction (Angus, unpublished material, see also appendix Fig 5.1). I also transfected HEK-293T cells with MLV gag/pol HCV E1E2 (see materials and methods, section 2.2.4.2) in parallel as a negative control. At 24 h post-transduction, cells were extracted in in Lysis Buffer A (20mM Tris-HCl pH 7.4, 135 mM NaCl, 0.1 % Triton X-100, 50mM NaF, 5 mM Na_3VO_4, 1

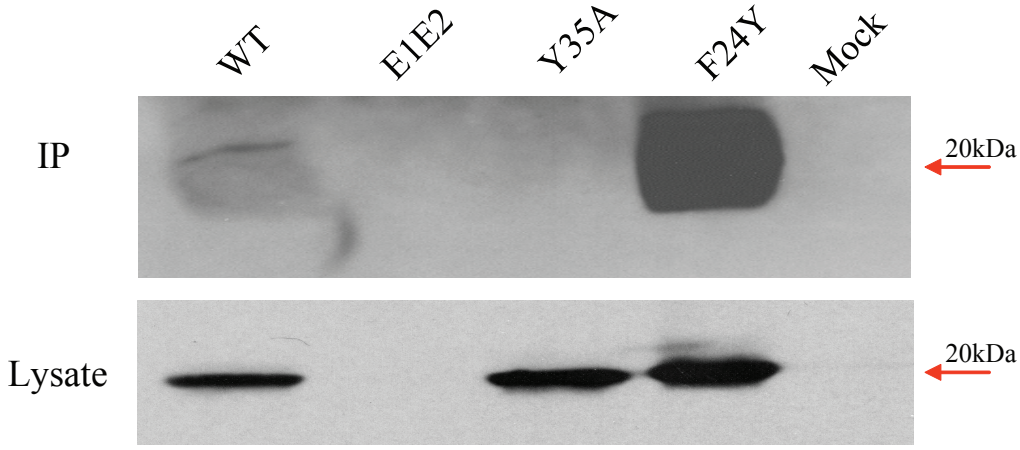

Appendix 5.1. The interaction of DDX3 with JFH1 core mutants.

HEK-293T cells were plated out at a density of 2 x 10^6 cells/dish onto 10-cm culture dishes. At 24 h post-seeding, cells were transfected with 30 µg of a PQCXIP expression vector (harbouring either $JFH1_{WT}$ core or a mutant derivatives of this protein, as indicated) using the calcium phosphate precipitation method. A plasmid encoding MLV gag-pol E1E2 was transfected in parallel as a negative control. At 24 h post-transfection, cells were lysed in 400 µl lysis buffer A. Each sample lysate was immunoprecipitated with the anti-DDX3 pAb R648. The resulting precipitates were examined by immunoblotting using anti-core mAb C7-50 (top panel). One twentieth of the cell lysate used in the co-immunoprecipitation assay was immunoblotted for core with mAb C7-50 as an input control (bottom panel).

mM PMSF), aliquots of which were subsequently treated with non-reducing sample buffer, loaded onto a 7.5% SDS-PAGE gel and examined via immunoblotting with the anti-DDX3 mAb AO196. I found no difference in endogenous DDX3 species or intensity at ~ 73 kDa between HEK-293T cells in the presence or absence of a functional core-DDX3 interaction. Furthermore, no such differences were observed in these cells in the presence or absence of core protein itself. However, I did observe the presence of specific high molecular weight species (appendix Fig 5.2A and B) in lysates from cells with a functional core-DDX3 interaction (appendix Fig 5.1) that had been probed with the anti-DDX3 mAb AO196. Two species were observed, one at ~ 150 kDa, one at ~ 220 kDa, which may represent dimers and trimers of DDX3, respectively. Interestingly, these complexes were absent from aliquots of the same cellular extracts that had been treated with a reducing sample buffer (SB) (composed of 200 mM Tris-HCl, pH 6.7; 0.5 % SDS; 5 % β-mercaptoethanol; 10 % glycerol, 1 µg/ml bromophenol blue) instead of non-reducing sample buffer (appendix Fig 5.3). These high molecular weight species were not observed in samples where the core-DDX3 interaction was abrogated or where core was absent, regardless of whether cellular lysates were loaded in reducing or non-reducing sample buffer.

A similar phenomenon was noted in Huh-7 cells replicating $JFH1_{WT}$ and $JFHI_{F24Y}$ viruses, with specific species observed after examination with AO196 at ~ 150 kDa and ~ 220 kDa (species also observed above 220 kDa, possibly representative of tetramers) in cellular extracts where a functional DDX3-core interaction was present that had been loaded onto SDS-PAGE gels with non-reducing sample buffer (appendix Fig 5.4A and B). Again, these high molecular weight species were absent from identical Huh-7 lysates that had been loaded onto SDS-PAGE gels with reducing sample buffer (appendix Fig 5.5). High-molecular weight species were not observed in $JFH1_{Y35A}$, $JFH1_{GND}$ and mock Huh-7 samples under either reducing or non-reducing buffer conditions.

To try and confirm whether these high molecular weight species were specific to cells with a functional core-DDX3 interaction, I analysed each of these complexes in a 2-D gel system, which I believed to be the most effective and accurate way of determining the protein composition of these complexes. Normally, 2-D electrophoresis involves using NativePAGE™ Gels (Invitrogen) in the first dimension followed by analysing

A

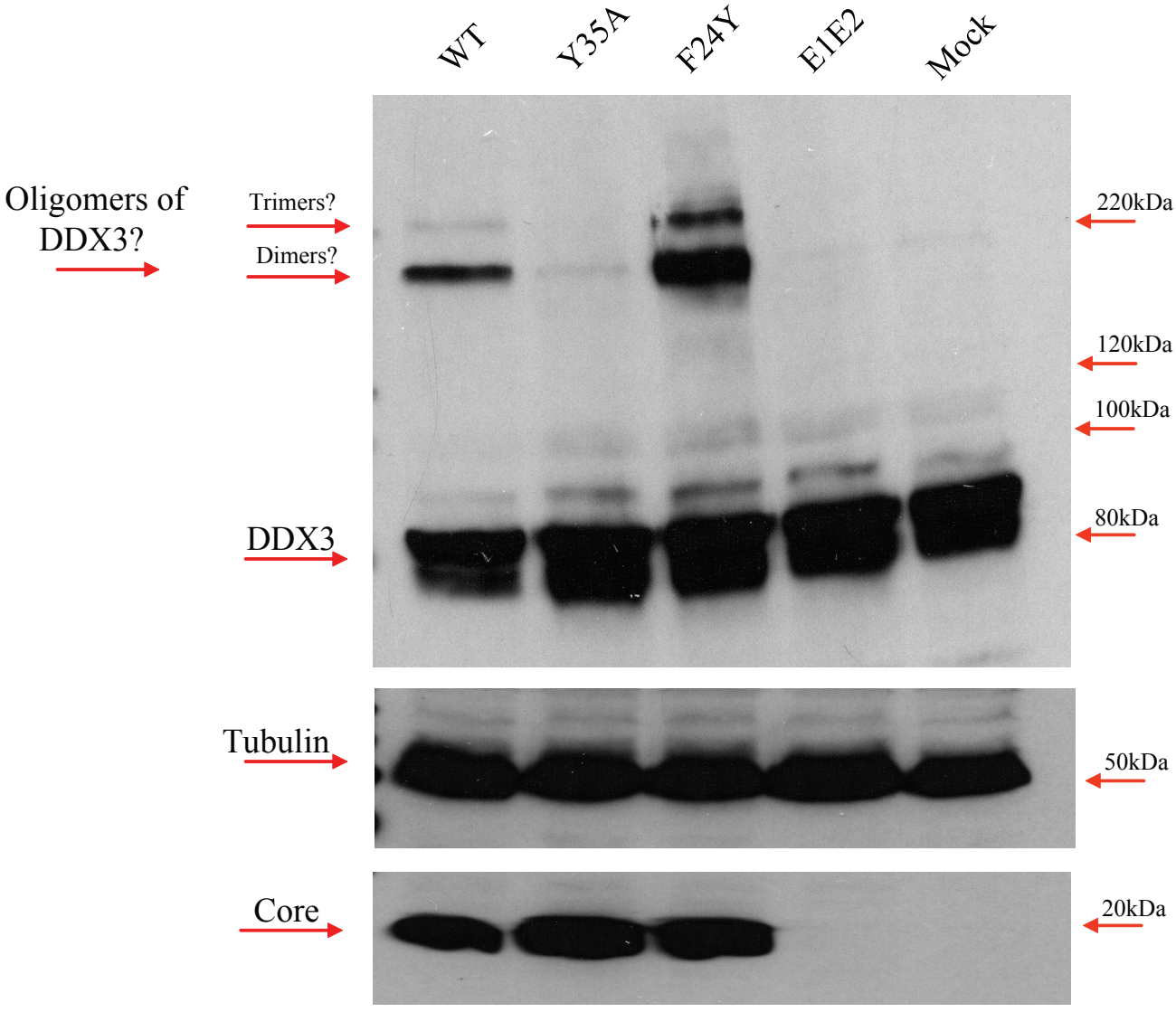
WT
Y35A
F24Y
E1E2
Mock
Oligomers of DDX3?
Trimers?
Dimers?
DDX3
Tubulin
Core
220kDa
120kDa
100kDa
80kDa
50kDa
20kDa

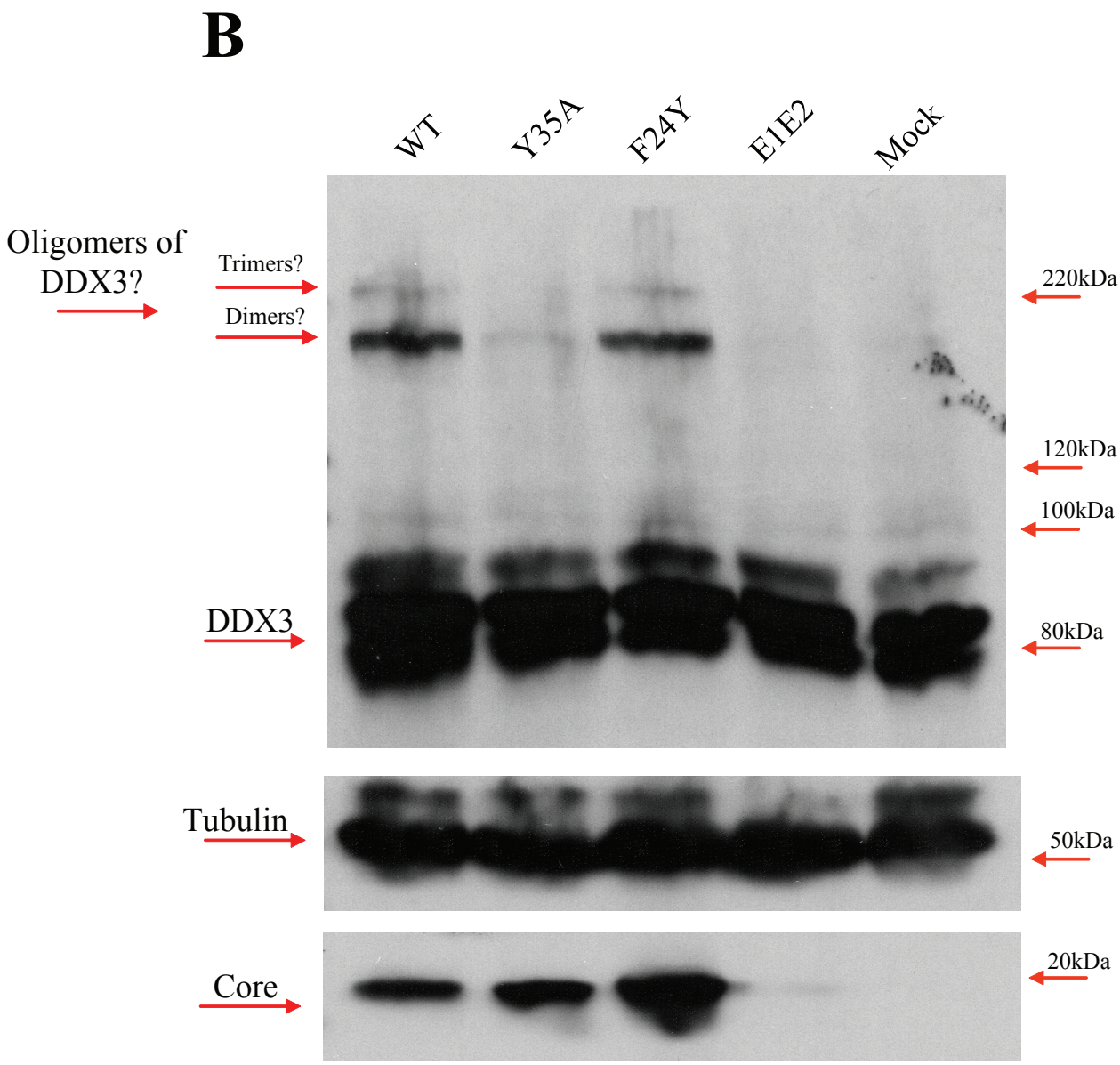

Appendix 5.2. Effect of overexpression of HCV Core and mutant variants on endogenous DDX3 protein in HEK-293T cells.

Two independent experiments represented by **A** and **B.** HEK-293T cells were plated out at a density of 2 x 10^6 cells/dish onto 10-cm culture dishes. At 24 h post-seeding, cells were transfected with 30 µg of a PQCXIP expression vector (harbouring either $JFH1_{WT}$ core or a mutant derivative of this protein, as indicated) using the calcium phosphate precipitation method. A plasmid encoding MLV gag-pol E1E2 was transfected in parallel as a negative control. At 24 h post-transfection, cells were lysed in 400 µl lysis buffer A. 20 µl of lysate from each sample was added to 6 µl non-reducing sample buffer (NR-SB) and analysed by immunoblotting for DDX3 and core expression using the mAbs AO196 and C7 -50, respectively. Anti-α-Tubulin mAb was used as a loading control.

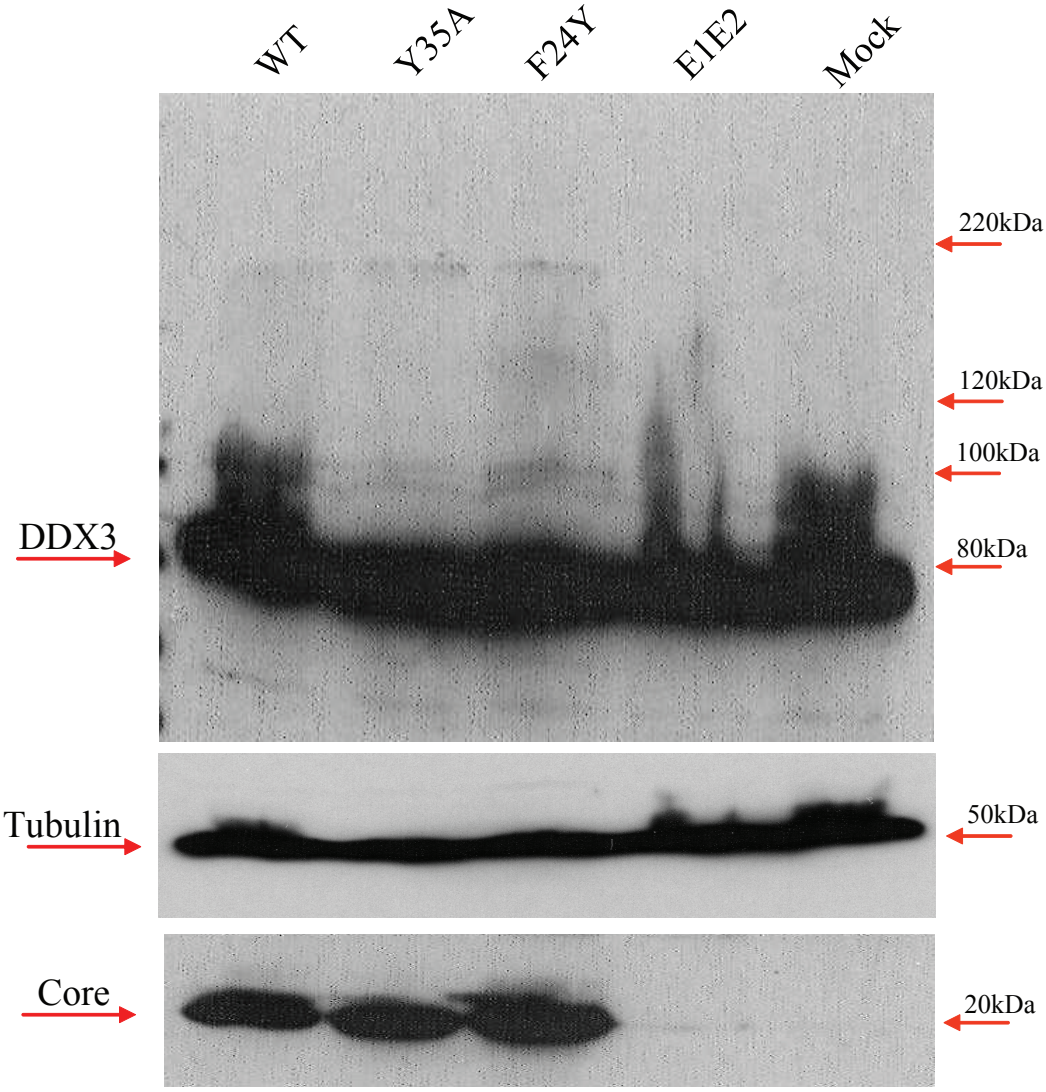

Appendix 5.3. Effect of overexpression of HCV core and mutant variants on endogenous DDX3 protein in HEK-293T cells.

In this instance, lysates derived from experiment Appendix 5.1A were treated with reducing sample buffer (SB) instead of non-reducing sample buffer (NR-SB) before immunoblotting. Immunoblot analysis of DDX3 and core expression was performed using the mAbs AO196 and C7-50, respectively. Anti-α-Tubulin mAb was used as a loading control.

A

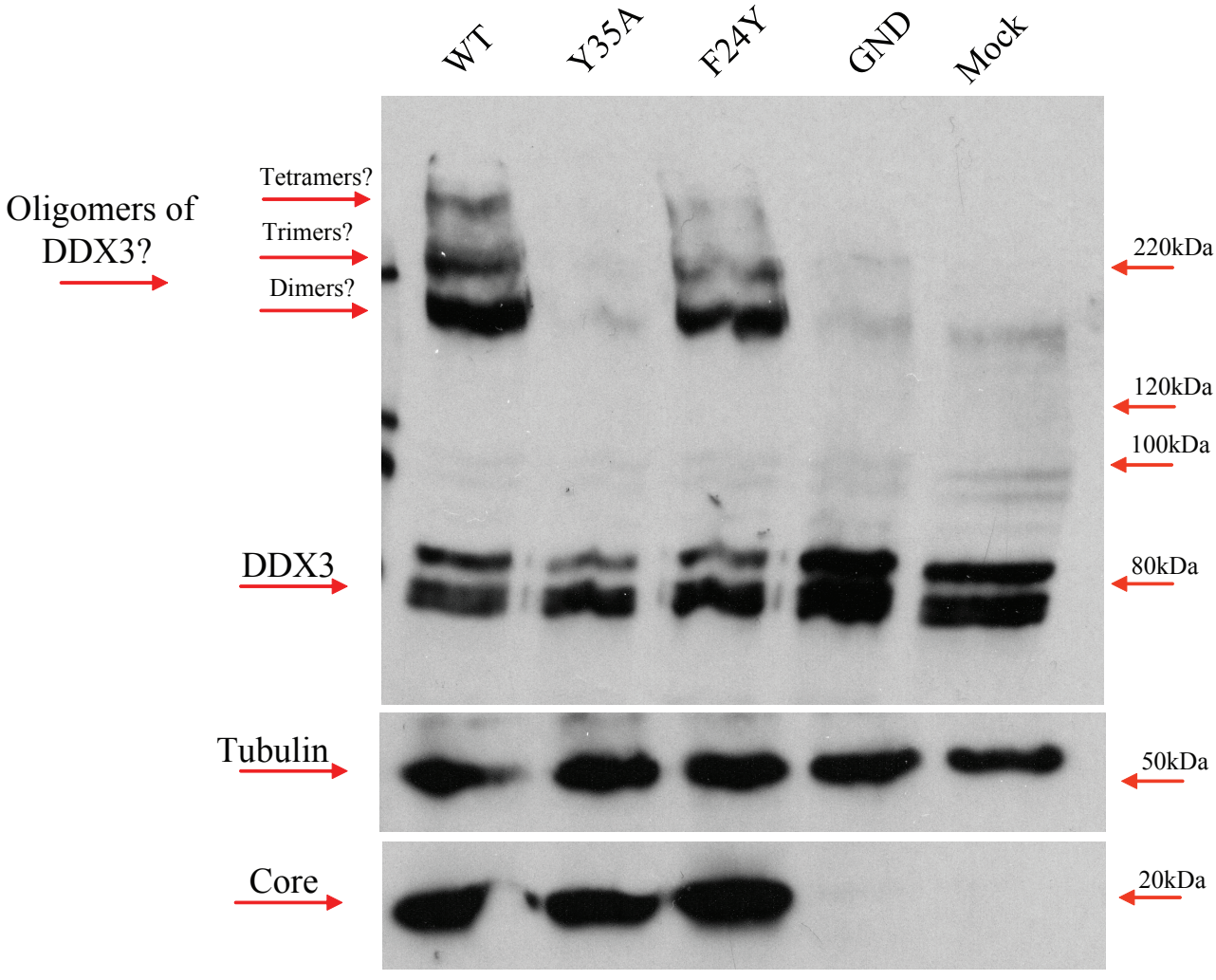
WT
Y35A
F24Y
GND
Mock
Oligomers of DDX3?
Tetramers?
Trimers?
Dimers?
DDX3
Tubulin
Core
220kDa
120kDa
100kDa
80kDa
50kDa
20kDa

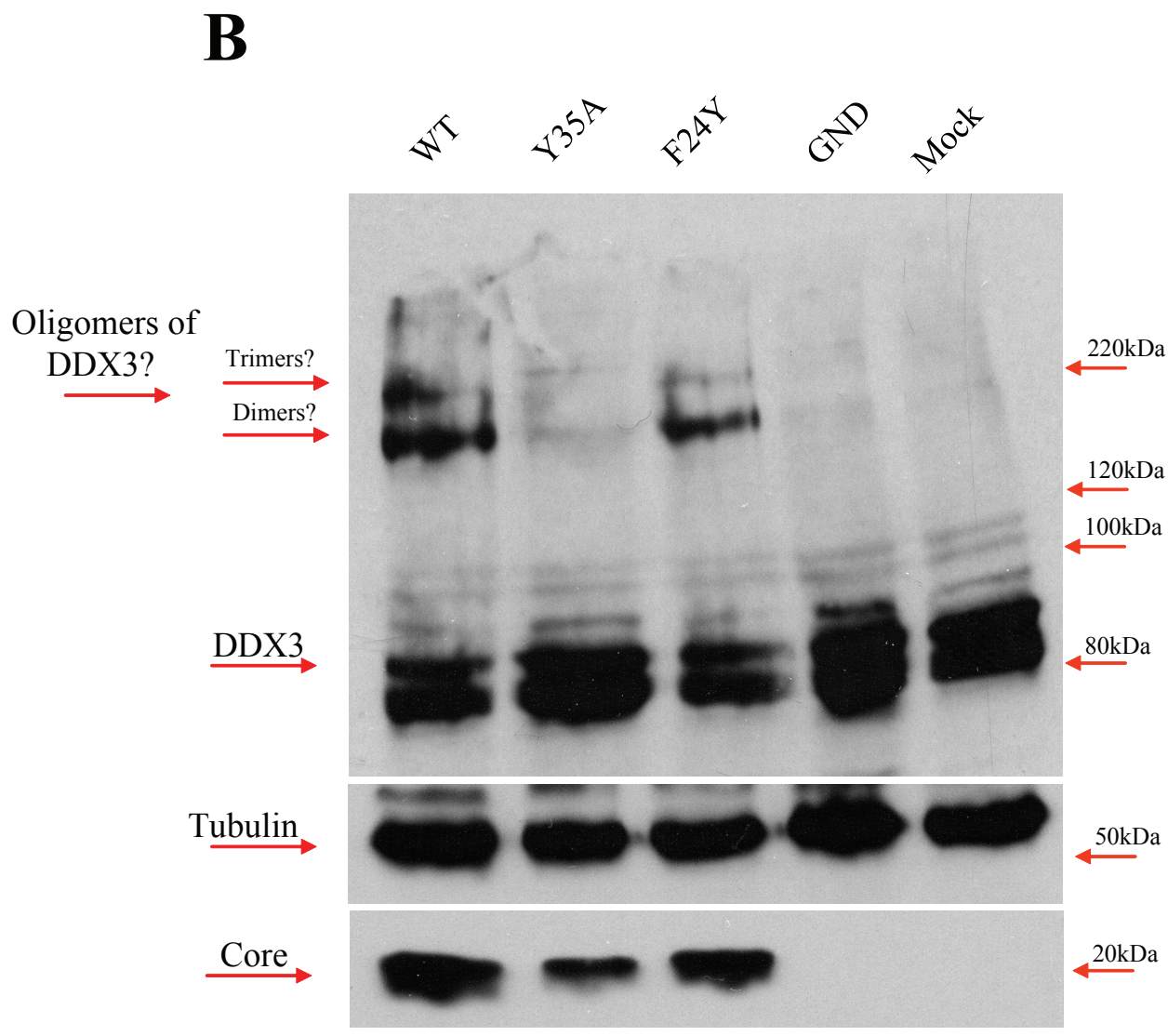

Appendix 5.4. Effect on endogenous DDX3 protein in Huh-7 cells transiently replicating $JFH1_{WT}$ and mutant variant RNA.

Two independent experiments represented by **A** and **B**. 10 µg of $JFH1_{WT}$ RNA (or mutant derivative, as indicated) was electroporated into 2 x 10^6 Huh-7 cells. At 48 h post-electroporation, each set of electroporated cells were lysed in 400 µl lysis buffer A. 20 µl of lysate from each sample was added to 6 µl non-reducing sample buffer (NR-SB) and analysed by immunoblotting for DDX3 and core expression using the mAbs AO196 and C7-50, respectively. Anti-α-Tubulin mAb was used as a loading control.

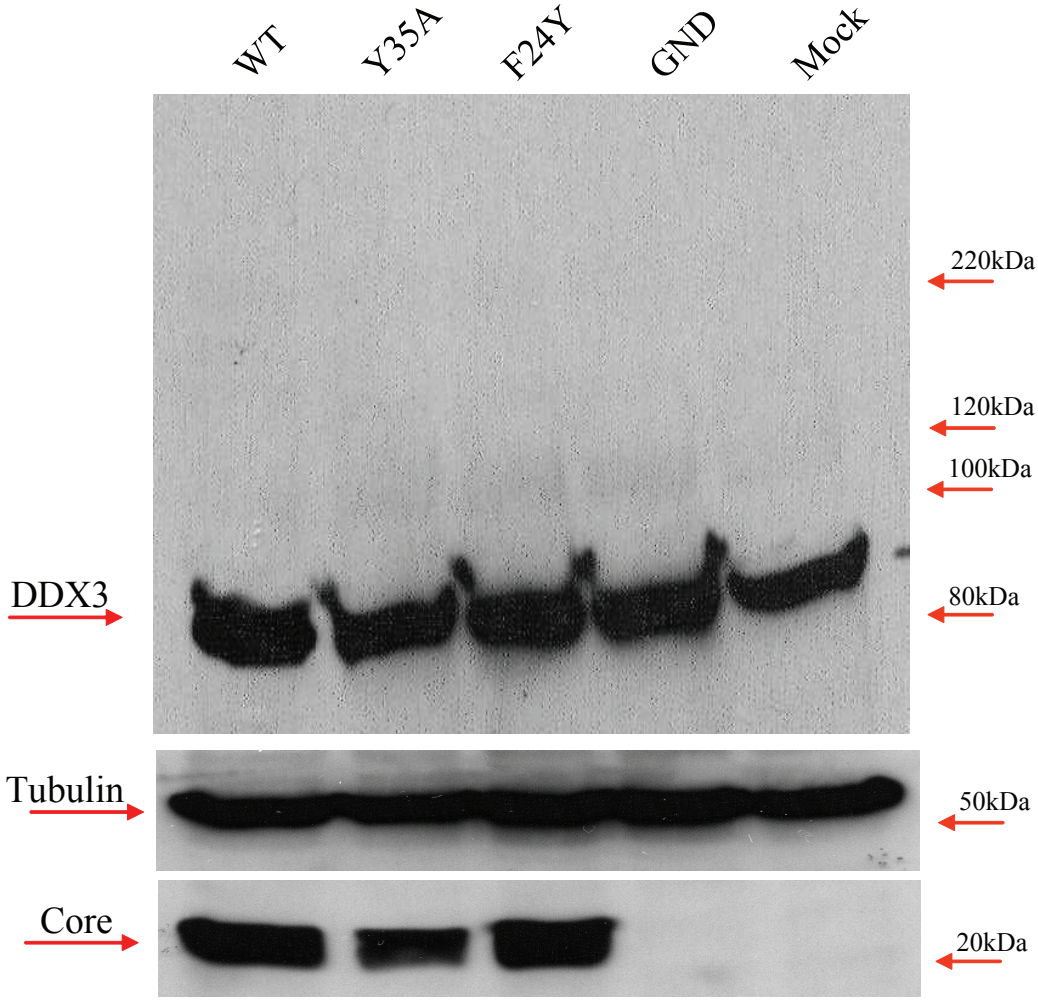

Appendix 5.5. Effect on endogenous DDX3 protein in Huh-7 cells transiently replicating $JFH1_{WT}$ and mutant variant RNA.

In this instance, lysates derived from experiment Appendix 5.4A were treated with reducing sample buffer (SB) instead of non-reducing sample buffer (NR-SB) before immunoblotting. Immunoblot analysis of DDX3 and core expression was performed using the mAbs AO196 and C7-50, respectively. Anti-α-Tubulin mAb was used as a loading control.

proteins (usually from one lane of the gel) using second dimension SDS-PAGE. Samples analysed in this way in my hands did not reveal anything after immonblotting with core and DDX3, nor did analysis of DDX3 in a 1-D NativePAGE environment show a specific protein after immunoblotting (data not shown). Thus, to investigate the properties of these putative high molecular weight complexes, I employed a modified form of 2-D gel electrophoresis. This involved running samples of interest in an SDS-PAGE environment in both dimensions. Cellular extracts of interest (Huh-7 cells replicating $JFH1_{WT}$ or related mutant virus that had been treated in non-reducing sample buffer) were run on a 7.5 % Bis-Tris SDS-PAGE Gel in the first dimension (as seen in appendix Fig 5.4). A gel strip containing the separated proteins of interest was excised from the first dimension gel before being equilibrated, reduced, and alkylated (see materials and methods, section 2.2.11) and loaded onto a second dimension NuPAGE® Novex® 4–12% Bis-Tris Gel (Invitrogen). This was then run and immunoblotted for DDX3 and core. Unlike in a 1-D setting, high molecular weight complexes of DDX3 were present in all samples (appendix Fig 5.6). However, core was also detected at high molecular weights under these conditions, but was only observed in $JFH1_{WT}$ and $JFH1_{F24Y}$ cells (appendix Fig 5.6A and C), where an intact DDX3-core interaction could be found. Core was not seen at these high molecular weights in extracts from $JFH1_{Y35A}$ and mock Huh-7 cells (appendix Fig 5.6B and D).

5.2. Discussion

This appendix chapter highlights an interesting phenomenon that can be seen under specific conditions in cells where a functional DDX3-core interaction is present. In both HEK-293T and Huh-7 cells transiently expressing HCV core protein, high molecular weight species were observed at ~150 kDa and ~ 220 kDa when cellular extracts were treated with non-reducing sample buffer (NR-SB) and examined with the anti-DDX3 mAb AO196 unless the core-DDX3 interaction had been abrogated or HCV core was absent. These species, which may represent oligomerised forms of DDX3 given the specificity of AO196, were not observed under any other conditions. The anti-DDX3 mAb AO166 and pAb R648 did not recognize these species, or even endogenous DDX3, after non-reducing sample buffer treatment in my hands (data not shown), and the high molecular weight species were absent after AO196 analysis of cellular extracts

A

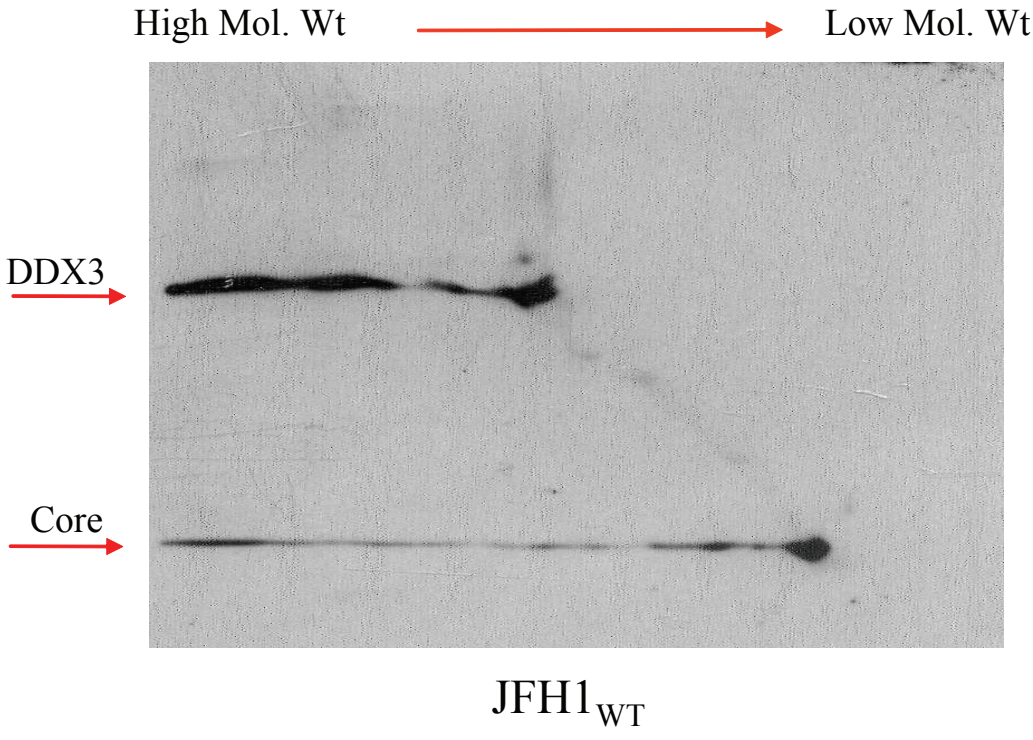

$JFH1_{WT}$

B

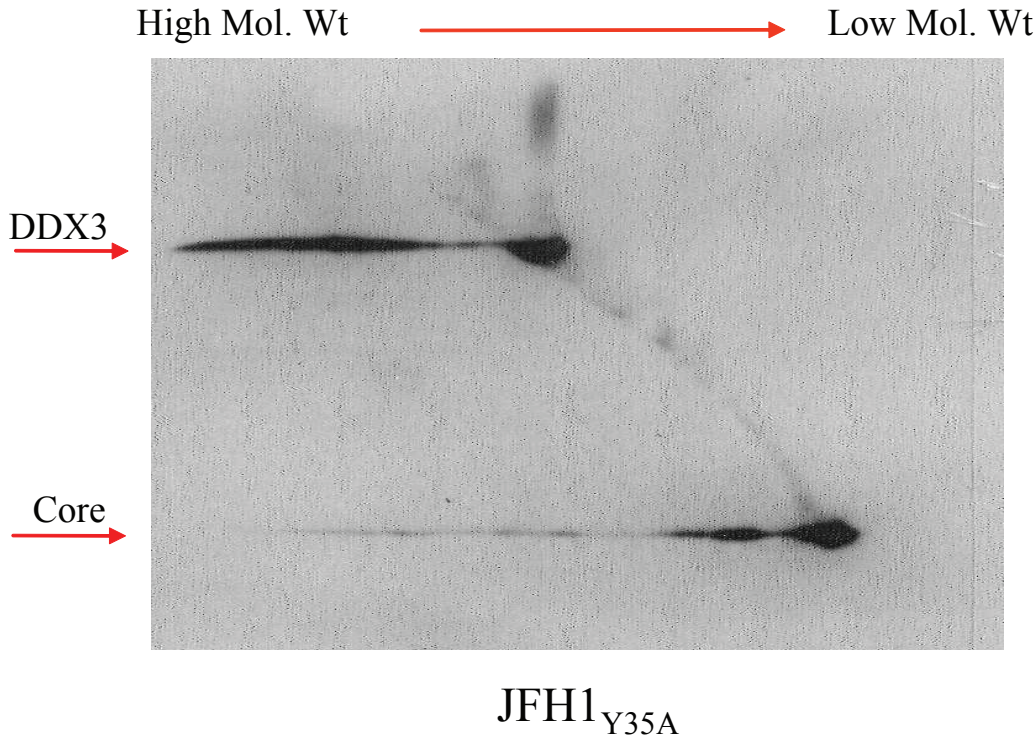

$JFH1_{Y35A}$

C

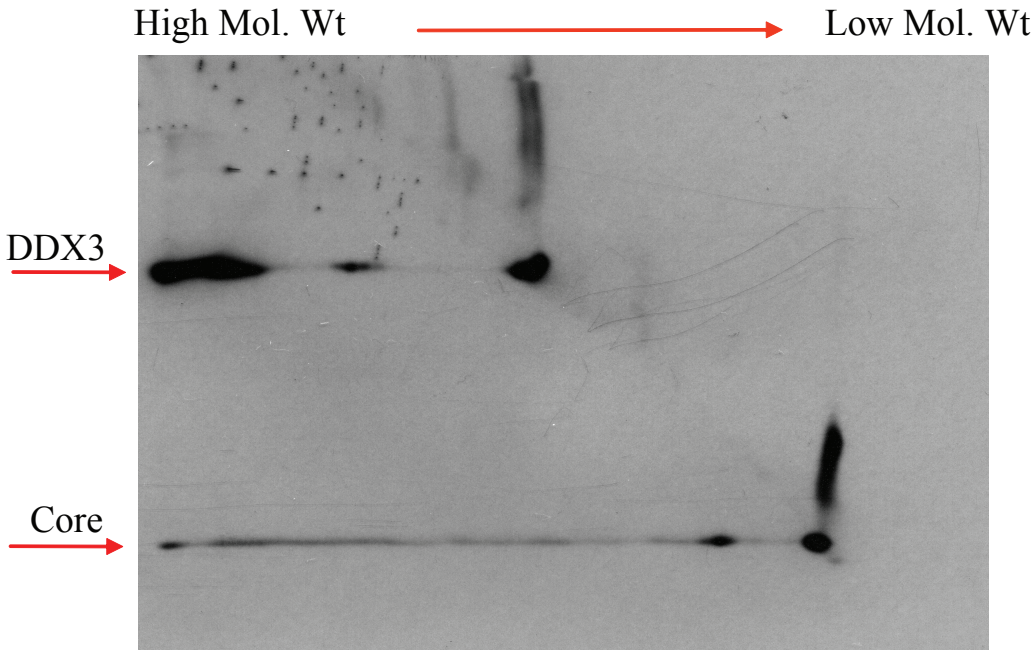

$JFH1_{F24Y}$

D

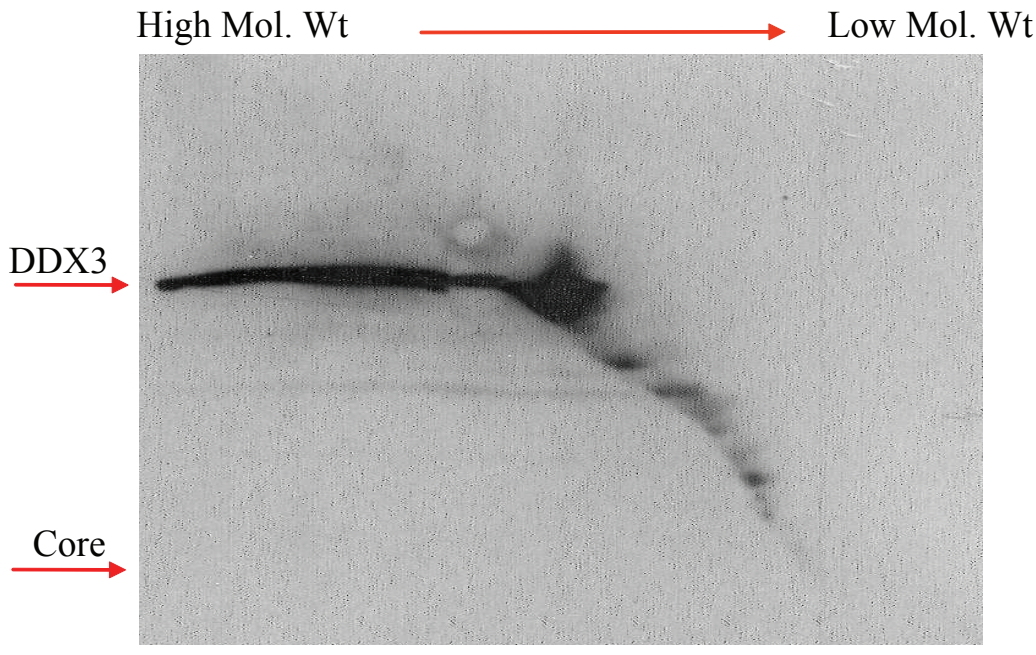

Mock Huh-7

Appendix 5.6. Analysis of high molecular weight species by 2-D SDS-PAGE gel electrophoresis.

Huh-7 lysates used in appendix fig 5.4 were also used in this experiment. Samples (A: $JFH1_{WT}$, B: $JFH1_{Y35A}$, C: $JFH1_{F24Y}$, D: mock Huh-7 cells) were run on a 7.5 % Bis-Tris SDS-PAGE gel in the first dimension. The lane containing the sample of interest was excised from the first dimension gel before being treated with reducing buffers and loaded onto a second dimension 4–12% Bis-Tris SDS-PAGE gel and analysed by immunoblotting for DDX3 and core expression using the mAbs AO196 and C7-50, respectively.

treated with reducing sample buffer (SB) instead of non-reducing sample buffer. The presence of β-mercaptoethanol in the reducing buffer cleaves any disulfide bonds present, denaturing the cellular proteins. This likely change in conformation may prevent the identification of these high molecular weight species by AO196.

While these high molecular weight species are observed only in the presence of a functional core-DDX3 interaction, I tried to determine whether this phenomenon was specifically caused by the viral-host association or merely due to a change in antibody reactivity because of conformational changes enacted by the Y35A core mutation. Analysis of these high molecular weight complexes through 2-D gel electrophoresis (albeit a modified form of the technique) helped provide more information towards the composition of these species. Immunoblot analysis of Huh-7 cells expressing $JFH1_{WT}$ or mutant derivatives examined after 2-D gel electrophoresis revealed DDX3 was present at high molecular weights in all cell-lines examined, including $JFH1_{Y35A}$ cells where the core-DDX3 interaction is abrogated and even in mock Huh-7 cells. While it can be argued that DDX3 is far more concentrated at high molecular weights in $JFH1_{F24Y}$ extracts compared to $JFH1_{Y35A}$ extracts, the DDX3 immunoblot profile is almost identical between $JFH1_{WT}$ and mock Huh-7 cells after 2-D gel electrophoresis.

While this observation suggested that the high molecular weight species observed in the presence of a DDX3-core interaction may be a non-specific phenomenon caused by antibody reactivity, the results observed after immunoblotting with anti-core mAb contradicted this theory. Core was found at high molecular weights after 2-D gel electrophoresis in $JFH1_{WT}$ and $JFH1_{F24Y}$ samples, but not in $JFH1_{Y35A}$ extracts. This finding suggests that a functional core-DDX3 interaction may be required for core oligomerisation or alternatively, that oligomerised core may need a functional core-DDX3 interaction to interact with oligomerised DDX3. Such hypotheses are in line with data presented by Mousseau *et al*. (2011), who state that the helicase region of the HCV protein NS3 physically interacts with the oligomerised HCV core protein, an interaction that requires the first 106 residues from core but is enhanced in the presence of a full-length core protein. The interaction can be inhibited by the small molecule SL201, a disruptor of core dimerization and of infectious HCV production (Mousseau *et al*., 2011). The absence of core in high molecular weight complexes from $JFH1_{Y35A}$ extracts suggest a similar role for the core-DDX3 interaction is possible.

However, while considering these prospects, it must be borne in mind that HCV RNA replication and infectious virus production are unimpeded in $JFH1_{Y35A}$ compared to $JFH1_{WT,}$ at least in the *in vitro* HCVcc system (Angus *et al*., 2010). One must also note that high molecular weight species indicative of core oligomerisation could not be observed under any circumstances when immunoblotting with an anti-core antibody and that DDX3 oligomerisation seemed unchanged in the presence or absence of a DDX3-core interaction after 2-D gel electrophoresis. The observation that the high molecular weight species evident after AO196 immunoblotting display substantial variation in both species and intensity during my limited investigations must also be taken into account when analysing these results. As I did not follow up these preliminary studies or repeat the experiments shown in this appendix chapter, the importance of these findings towards understanding the functional role (if any) of the core-DDX3 interaction are as yet inconclusive. However, they do form a basis upon which to begin new investigations into the interaction.

References

Abe, K., Ikeda, M., Ariumi, Y., Dansako, H., Wakita, T. & Kato, N. (2009). HCV genotype 1b chimeric replicon with NS5B of JFH-1 exhibited resistance to cyclosporine A. *Arch Virol* **154**, 1671-1677.

Abe, K., Ikeda, M., Dansako, H., Naka, K. & Kato, N. (2007). Cell culture-adaptive NS3 mutations required for the robust replication of genome-length hepatitis C virus RNA. *Virus Res* **125**, 88-97.

Agnello, V., Abel, G., Elfahal, M., Knight, G. B. & Zhang, Q. X. (1999). Hepatitis C virus and other flaviviridae viruses enter cells via low density lipoprotein receptor. *Proc Natl Acad Sci U S A* **96**, 12766-12771.

Ago, H., Adachi, T., Yoshida, A., Yamamoto, M., Habuka, N., Yatsunami, K. & Miyano, M. (1999). Crystal structure of the RNA-dependent RNA polymerase of hepatitis C virus. *Structure* **7**, 1417-1426.

Akazawa, D., Date, T., Morikawa, K., Murayama, A., Miyamoto, M., Kaga, M., Barth, H., Baumert, T. F., Dubuisson, J. & Wakita, T. (2007). CD81 expression is important for the permissiveness of Huh7 cell clones for heterogeneous hepatitis C virus infection. *J Virol* **81**, 5036-5045.

Albecka, A., Belouzard, S., Op de Beeck, A., Descamps, V., Goueslain, L., Bertrand-Michel, J., Terce, F., Duverlie, G., Rouille, Y. & Dubuisson, J. (2012). Role of low-density lipoprotein receptor in the hepatitis C virus life cycle. *Hepatology* **55**, 998-1007.

Ali, N. & Siddiqui, A. (1995). Interaction of polypyrimidine tract-binding protein with the 5' noncoding region of the hepatitis C virus RNA genome and its functional requirement in internal initiation of translation. *J Virol* **69**, 6367-6375.

Ali, N. & Siddiqui, A. (1997). The La antigen binds 5' noncoding region of the hepatitis C virus RNA in the context of the initiator AUG codon and stimulates internal ribosome entry site-mediated translation. *Proc Natl Acad Sci U S A* **94**, 2249-2254.

Ali, S., Leveque, V., Le Pogam, S., Ma, H., Philipp, F., Inocencio, N., Smith, M., Alker, A., Kang, H., Najera, I., Klumpp, K., Symons, J., Cammack, N. & Jiang, W. R. (2008). Selected replicon variants with low-level in vitro resistance to the hepatitis C virus NS5B polymerase inhibitor PSI-6130 lack cross-resistance with R1479. *Antimicrob Agents Chemother* **52**, 4356-4369.

Alsaleh, K., Delavalle, P. Y., Pillez, A., Duverlie, G., Descamps, V., Rouille, Y., Dubuisson, J. & Wychowski, C. (2010). Identification of basic amino acids at the N-terminal end of the core protein that are crucial for hepatitis C virus infectivity. *J Virol* **84**, 12515-12528.

Alter, H. J., Purcell, R. H., Holland, P. V. & Popper, H. (1978). Transmissible agent in non-A, non-B hepatitis. *Lancet* **1**, 459-463.

Alter, M. J. (2007). Epidemiology of hepatitis C virus infection. *World J Gastroenterol* **13**, 2436-2441.

Andre, P., Komurian-Pradel, F., Deforges, S., Perret, M., Berland, J. L., Sodoyer, M., Pol, S., Brechot, C., Paranhos-Baccala, G. & Lotteau, V. (2002). Characterization of low- and very-low-density hepatitis C virus RNA-containing particles. *J Virol* **76**, 6919-6928.

Andrus, L., Marukian, S., Jones, C. T., Catanese, M. T., Sheahan, T. P., Schoggins, J. W., Barry, W. T., Dustin, L. B., Trehan, K., Ploss, A., Bhatia, S. N. & Rice, C. M. (2011). Expression of paramyxovirus V proteins promotes replication and spread of hepatitis C virus in cultures of primary human fetal liver cells. *Hepatology* **54**, 1901-1912.

Angus, A. G., Dalrymple, D., Boulant, S., McGivern, D. R., Clayton, R. F., Scott, M. J., Adair, R., Graham, S., Owsianka, A. M., Targett-Adams, P., Li, K., Wakita, T., McLauchlan, J., Lemon, S. M. & Patel, A. H. (2010). Requirement of cellular DDX3 for hepatitis C virus replication is unrelated to its interaction with the viral core protein. *J Gen Virol* **91**, 122-132.

Angus, A. G., Loquet, A., Stack, S. J., Dalrymple, D., Gatherer, D., Penin, F. & Patel, A. H. (2012). Conserved glycine 33 residue in flexible domain I of hepatitis C virus core protein is critical for virus infectivity. *J Virol* **86**, 679-690.

Appel, N., Pietschmann, T. & Bartenschlager, R. (2005). Mutational analysis of hepatitis C virus nonstructural protein 5A: potential role of differential phosphorylation in RNA replication and identification of a genetically flexible domain. *J Virol* **79**, 3187-3194.

Appel, N., Zayas, M., Miller, S., Krijnse-Locker, J., Schaller, T., Friebe, P., Kallis, S., Engel, U. & Bartenschlager, R. (2008). Essential role of domain III of nonstructural protein 5A for hepatitis C virus infectious particle assembly. *PLoS Pathog* **4**, e1000035.

Ariumi, Y., Kuroki, M., Abe, K., Dansako, H., Ikeda, M., Wakita, T. & Kato, N. (2007). DDX3 DEAD-box RNA helicase is required for hepatitis C virus RNA replication. *J Virol* **81**, 13922-13926.

Ariumi, Y., Kuroki, M., Kushima, Y., Osugi, K., Hijikata, M., Maki, M., Ikeda, M. & Kato, N. (2011). Hepatitis C virus hijacks P-body and stress granule components around lipid droplets. *J Virol* **85**, 6882-6892.

Backes, P., Quinkert, D., Reiss, S., Binder, M., Zayas, M., Rescher, U., Gerke, V., Bartenschlager, R. & Lohmann, V. (2010). Role of annexin A2 in the production of infectious hepatitis C virus particles. *J Virol* **84**, 5775-5789.

Banerjee, A., Mazumdar, B., Meyer, K., Di Bisceglie, A. M., Ray, R. B. & Ray, R. (2011). Transcriptional repression of C4 complement by hepatitis C virus proteins. *J Virol* **85**, 4157-4166.

Bankwitz, D., Steinmann, E., Bitzegeio, J., Ciesek, S., Friesland, M., Herrmann, E., Zeisel, M. B., Baumert, T. F., Keck, Z. Y., Foung, S. K., Pecheur, E. I. & Pietschmann, T. (2010). Hepatitis C virus hypervariable region 1 modulates receptor interactions, conceals the CD81 binding site, and protects conserved neutralizing epitopes. *J Virol* **84**, 5751-5763.

Banroques, J., Cordin, O., Doere, M., Linder, P. & Tanner, N. K. (2011). Analyses of the functional regions of DEAD-box RNA "helicases" with deletion and chimera constructs tested in vivo and in vitro. *J Mol Biol* **413**, 451-472.

Banroques, J., Cordin, O., Doere, M., Linder, P. & Tanner, N. K. (2008). A conserved phenylalanine of motif IV in superfamily 2 helicases is required for cooperative, ATP-dependent binding of RNA substrates in DEAD-box proteins. *Mol Cell Biol* **28**, 3359-3371.

Barrera, J. M., Bruguera, M., Ercilla, M. G., Gil, C., Celis, R., Gil, M. P., del Valle Onorato, M., Rodes, J. & Ordinas, A. (1995). Persistent hepatitis C viremia after acute self-limiting posttransfusion hepatitis C. *Hepatology* **21**, 639-644.

Bartenschlager, R., Ahlborn-Laake, L., Mous, J. & Jacobsen, H. (1993). Nonstructural protein 3 of the hepatitis C virus encodes a serine-type proteinase required for cleavage at the NS3/4 and NS4/5 junctions. *J Virol* **67**, 3835-3844.

Bartenschlager, R., Ahlborn-Laake, L., Mous, J. & Jacobsen, H. (1994). Kinetic and structural analyses of hepatitis C virus polyprotein processing. *J Virol* **68**, 5045-5055.

Bartenschlager, R., Frese, M. & Pietschmann, T. (2004). Novel insights into hepatitis C virus replication and persistence. *Adv Virus Res* **63**, 71-180.

Bartenschlager, R., Lohmann, V., Wilkinson, T. & Koch, J. O. (1995). Complex formation between the NS3 serine-type proteinase of the hepatitis C virus and NS4A and its importance for polyprotein maturation. *J Virol* **69**, 7519-7528.

Bartenschlager, R., Penin, F., Lohmann, V. & Andre, P. (2011). Assembly of infectious hepatitis C virus particles. *Trends Microbiol* **19**, 95-103.

Bartenschlager, R. & Sparacio, S. (2007). Hepatitis C virus molecular clones and their replication capacity in vivo and in cell culture. *Virus Res* **127**, 195-207.

Barth, H., Robinet, E., Liang, T. J. & Baumert, T. F. (2008). Mouse models for the study of HCV infection and virus-host interactions. *J Hepatol* **49**, 134-142.

Barth, H., Schafer, C., Adah, M. I., Zhang, F., Linhardt, R. J., Toyoda, H., Kinoshita-Toyoda, A., Toida, T., Van Kuppevelt, T. H., Depla, E., Von Weizsacker, F., Blum, H. E. & Baumert, T. F. (2003). Cellular binding of hepatitis C virus envelope glycoprotein E2 requires cell surface heparan sulfate. *J Biol Chem* **278**, 41003-41012.

Barth, H., Schnober, E. K., Zhang, F., Linhardt, R. J., Depla, E., Boson, B., Cosset, F. L., Patel, A. H., Blum, H. E. & Baumert, T. F. (2006). Viral and cellular determinants of the hepatitis C virus envelope-heparan sulfate interaction. *J Virol* **80**, 10579-10590.

Bartosch, B., Dubuisson, J. & Cosset, F. L. (2003). Infectious hepatitis C virus pseudo-particles containing functional E1-E2 envelope protein complexes. *J Exp Med* **197**, 633-642.

Bartosch, B., Verney, G., Dreux, M., Donot, P., Morice, Y., Penin, F., Pawlotsky, J. M., Lavillette, D. & Cosset, F. L. (2005). An interplay between hypervariable region 1 of the hepatitis C virus E2 glycoprotein, the scavenger receptor BI, and high-density lipoprotein promotes both enhancement of infection and protection against neutralizing antibodies. *J Virol* **79**, 8217-8229.

Basu, A., Kanda, T., Beyene, A., Saito, K., Meyer, K. & Ray, R. (2007). Sulfated homologues of heparin inhibit hepatitis C virus entry into mammalian cells. *J Virol* **81**, 3933-3941.

Beck, J. & Nassal, M. (2007). Hepatitis B virus replication. *World J Gastroenterol* **13**, 48-64.

Beckham, C. J. & Parker, R. (2008). P bodies, stress granules, and viral life cycles. *Cell Host Microbe* **3**, 206-212.

Bellentani, S. & Tiribelli, C. (2001). The spectrum of liver disease in the general population: lesson from the Dionysos study. *J Hepatol* **35**, 531-537.

Benedicto, I., Molina-Jimenez, F., Bartosch, B., Cosset, F. L., Lavillette, D., Prieto, J., Moreno-Otero, R., Valenzuela-Fernandez, A., Aldabe, R., Lopez-Cabrera, M. & Majano, P. L. (2009). The tight junction-associated protein occludin is required for a postbinding step in hepatitis C virus entry and infection. *J Virol* **83**, 8012-8020.

Benga, W. J., Krieger, S. E., Dimitrova, M., Zeisel, M. B., Parnot, M., Lupberger, J., Hildt, E., Luo, G., McLauchlan, J., Baumert, T. F. & Schuster, C. (2010).

Apolipoprotein E interacts with hepatitis C virus nonstructural protein 5A and determines assembly of infectious particles. *Hepatology* **51**, 43-53.

Benhamou, Y., Bochet, M., Di Martino, V., Charlotte, F., Azria, F., Coutellier, A., Vidaud, M., Bricaire, F., Opolon, P., Katlama, C. & Poynard, T. (1999). Liver fibrosis progression in human immunodeficiency virus and hepatitis C virus coinfected patients. The Multivirc Group. *Hepatology* **30**, 1054-1058.

Berenguer, M., Ferrell, L., Watson, J., Prieto, M., Kim, M., Rayon, M., Cordoba, J., Herola, A., Ascher, N., Mir, J., Berenguer, J. & Wright, T. L. (2000). HCV-related fibrosis progression following liver transplantation: increase in recent years. *J Hepatol* **32**, 673-684.

Bernfield, M., Gotte, M., Park, P. W., Reizes, O., Fitzgerald, M. L., Lincecum, J. & Zako, M. (1999). Functions of cell surface heparan sulfate proteoglycans. *Annu Rev Biochem* **68**, 729-777.

Binder, M., Quinkert, D., Bochkarova, O., Klein, R., Kezmic, N., Bartenschlager, R. & Lohmann, V. (2007). Identification of determinants involved in initiation of hepatitis C virus RNA synthesis by using intergenotypic replicase chimeras. *J Virol* **81**, 5270-5283.

Bissig, K.D., Le, T.T., Woods, N.B., Verma, I.M. (2007). Repopulation of adult and neonatal mice with human hepatocytes: A chimeric animal model. *Proc Natl Acad Sci U S A* **104,** 20507-20511.

Bissig, K. D., Wieland, S. F., Tran, P., Isogawa, M., Le, T. T., Chisari, F. V. & Verma, I. M. (2010). Human liver chimeric mice provide a model for hepatitis B and C virus infection and treatment. *J Clin Invest* **120**, 924-930.

Biswal, B. K., Cherney, M. M., Wang, M., Chan, L., Yannopoulos, C. G., Bilimoria, D., Nicolas, O., Bedard, J. & James, M. N. (2005). Crystal structures of the RNA-dependent RNA polymerase genotype 2a of hepatitis C virus reveal two conformations and suggest mechanisms of inhibition by non-nucleoside inhibitors. *J Biol Chem* **280**, 18202-18210.

Bjoro, K., Skaug, K., Haaland, T. & Froland, S. S. (1999). Long-term outcome of chronic hepatitis C virus infection in primary hypogammaglobulinaemia. *Qjm* **92**, 433-441.

Blanchard, E., Belouzard, S., Goueslain, L., Wakita, T., Dubuisson, J., Wychowski, C. & Rouille, Y. (2006). Hepatitis C virus entry depends on clathrin-mediated endocytosis. *J Virol* **80**, 6964-6972.

Blasiole, D. A., Davis, R. A. & Attie, A. D. (2007). The physiological and molecular regulation of lipoprotein assembly and secretion. *Mol Biosyst* **3**, 608-619.

Bleichert, F. & Baserga, S. J. (2007). The long unwinding road of RNA helicases. *Mol Cell* **27**, 339-352.

Blight, K. J. (2011). Charged residues in hepatitis C virus NS4B are critical for multiple NS4B functions in RNA replication. *J Virol* **85**, 8158-8171.

Blight, K. J. (2007). Allelic variation in the hepatitis C virus NS4B protein dramatically influences RNA replication. *J Virol* **81**, 5724-5736.

Blight, K. J., Kolykhalov, A. A. & Rice, C. M. (2000). Efficient initiation of HCV RNA replication in cell culture. *Science* **290**, 1972-1974.

Blight, K. J., McKeating, J. A. & Rice, C. M. (2002). Highly permissive cell lines for subgenomic and genomic hepatitis C virus RNA replication. *J Virol* **76**, 13001-13014.

Blight, K. J. & Rice, C. M. (1997). Secondary structure determination of the conserved 98-base sequence at the 3' terminus of hepatitis C virus genome RNA. *J Virol* **71**, 7345-7352.

Boo, I., teWierik, K., Douam, F., Lavillette, D., Poumbourios, P. & Drummer, H. E. (2012). Distinct roles in folding, CD81 receptor binding and viral entry for conserved histidine residues of hepatitis C virus glycoprotein E1 and E2. *Biochem J* **443**, 85-94.

Boonstra, A., van der Laan, L. J., Vanwolleghem, T. & Janssen, H. L. (2009). Experimental models for hepatitis C viral infection. *Hepatology* **50**, 1646-1655.

Boson, B., Granio, O., Bartenschlager, R. & Cosset, F. L. (2011). A concerted action of hepatitis C virus p7 and nonstructural protein 2 regulates core localization at the endoplasmic reticulum and virus assembly. *PLoS Pathog* **7**, e1002144.

Botlagunta, M., Krishnamachary, B., Vesuna, F., Winnard, P. T., Jr., Bol, G. M., Patel, A. H. & Raman, V. (2011). Expression of DDX3 is directly modulated by hypoxia inducible factor-1 alpha in breast epithelial cells. *PLoS One* **6**, e17563.

Botlagunta, M., Vesuna, F., Mironchik, Y., Raman, A., Lisok, A., Winnard, P., Jr., Mukadam, S., Van Diest, P., Chen, J. H., Farabaugh, P., Patel, A. H. & Raman, V. (2008). Oncogenic role of DDX3 in breast cancer biogenesis. *Oncogene* **27**, 3912-3922.

Boucheix, C. & Rubinstein, E. (2001). Tetraspanins. *Cell Mol Life Sci* **58**, 1189-1205.

Boulant, S., Douglas, M. W., Moody, L., Budkowska, A., Targett-Adams, P. & McLauchlan, J. (2008). Hepatitis C virus core protein induces lipid droplet redistribution in a microtubule- and dynein-dependent manner. *Traffic* **9**, 1268-1282.

Boulant, S., Montserret, R., Hope, R. G., Ratinier, M., Targett-Adams, P., Lavergne, J. P., Penin, F. & McLauchlan, J. (2006). Structural determinants that target the hepatitis C virus core protein to lipid droplets. *J Biol Chem* **281**, 22236-22247.

Boulant, S., Targett-Adams, P. & McLauchlan, J. (2007). Disrupting the association of hepatitis C virus core protein with lipid droplets correlates with a loss in production of infectious virus. *J Gen Virol* **88**, 2204-2213.

Bradley, D. W., McCaustland, K. A., Cook, E. H., Schable, C. A., Ebert, J. W. & Maynard, J. E. (1985). Posttransfusion non-A, non-B hepatitis in chimpanzees. Physicochemical evidence that the tubule-forming agent is a small, enveloped virus. *Gastroenterology* **88**, 773-779.

Bradrick, S. S., Walters, R. W. & Gromeier, M. (2006). The hepatitis C virus 3'-untranslated region or a poly(A) tract promote efficient translation subsequent to the initiation phase. *Nucleic Acids Res* **34**, 1293-1303.

Brass, V., Bieck, E., Montserret, R., Wolk, B., Hellings, J. A., Blum, H. E., Penin, F. & Moradpour, D. (2002). An amino-terminal amphipathic alpha-helix mediates membrane association of the hepatitis C virus nonstructural protein 5A. *J Biol Chem* **277**, 8130-8139.

Brazzoli, M., Bianchi, A., Filippini, S., Weiner, A., Zhu, Q., Pizza, M. & Crotta, S. (2008). CD81 is a central regulator of cellular events required for hepatitis C virus infection of human hepatocytes. *J Virol* **82**, 8316-8329.

Bressanelli, S., Tomei, L., Rey, F. A. & De Francesco, R. (2002). Structural analysis of the hepatitis C virus RNA polymerase in complex with ribonucleotides. *J Virol* **76**, 3482-3492.

Brillanti, S., Foli, M., Gaiani, S., Masci, C., Miglioli, M. & Barbara, L. (1993). Persistent hepatitis C viraemia without liver disease. *Lancet* **341**, 464-465.

Brimacombe, C. L., Grove, J., Meredith, L. W., Hu, K., Syder, A. J., Flores, M. V., Timpe, J. M., Krieger, S. E., Baumert, T. F., Tellinghuisen, T. L., Wong-

Staal, F., Balfe, P. & McKeating, J. A. (2011). Neutralizing antibody-resistant hepatitis C virus cell-to-cell transmission. *J Virol* **85**, 596-605.

Brocard, M., Paulous, S., Komarova, A. V., Deveaux, V. & Kean, K. M. (2007). Evidence that PTB does not stimulate HCV IRES-driven translation. *Virus Genes* **35**, 5-15.

Brohm, C., Steinmann, E., Friesland, M., Lorenz, I. C., Patel, A., Penin, F., Bartenschlager, R. & Pietschmann, T. (2009). Characterization of determinants important for hepatitis C virus p7 function in morphogenesis by using trans-complementation. *J Virol* **83**, 11682-11693.

Brown, E. A., Zhang, H., Ping, L. H. & Lemon, S. M. (1992). Secondary structure of the 5' nontranslated regions of hepatitis C virus and pestivirus genomic RNAs. *Nucleic Acids Res* **20**, 5041-5045.

Bukh, J. (2012). Animal models for the study of hepatitis C virus infection and related liver disease. *Gastroenterology* **142**, 1279-1287 e1273.

Bukh, J., Purcell, R. H. & Miller, R. H. (1992). Sequence analysis of the 5' noncoding region of hepatitis C virus. *Proc Natl Acad Sci U S A* **89**, 4942-4946.

Bukh, J., Purcell, R. H. & Miller, R. H. (1994). Sequence analysis of the core gene of 14 hepatitis C virus genotypes. *Proc Natl Acad Sci U S A* **91**, 8239-8243.

Burbelo, P. D., Dubovi, E. J., Simmonds, P., Medina, J. L., Henriquez, J. A., Mishra, N., Wagner, J., Tokarz, R., Cullen, J. M., Iadarola, M. J., Rice, C. M., Lipkin, W. I. & Kapoor, A. (2012). Serology-enabled discovery of genetically diverse hepaciviruses in a new host. *J Virol* **86**, 6171-6178.

Burckin, T., Nagel, R., Mandel-Gutfreund, Y., Shiue, L., Clark, T. A., Chong, J. L., Chang, T. H., Squazzo, S., Hartzog, G. & Ares, M., Jr. (2005). Exploring functional relationships between components of the gene expression machinery. *Nat Struct Mol Biol* **12**, 175-182.

Cai, Z., Cai, L., Jiang, J., Chang, K. S., van der Westhuyzen, D. R. & Luo, G. (2007). Human serum amyloid A protein inhibits hepatitis C virus entry into cells. *J Virol* **81**, 6128-6133.

Callens, N., Ciczora, Y., Bartosch, B., Vu-Dac, N., Cosset, F. L., Pawlotsky, J. M., Penin, F. & Dubuisson, J. (2005). Basic residues in hypervariable region 1 of hepatitis C virus envelope glycoprotein e2 contribute to virus entry. *J Virol* **79**, 15331-15341.

Camus, G., Herker, E., Modi, A. A., Haas, J. T., Ramage, H. R., Farese, R. V., Jr. & Ott, M. (2013). Diacylglycerol glycerol acyltransferase-1 localizes hepatitis C virus NS5A protein to lipid droplets and enhances NS5A interaction with the viral capsid core. *J Biol Chem*.

Carrere-Kremer, S., Montpellier-Pala, C., Cocquerel, L., Wychowski, C., Penin, F. & Dubuisson, J. (2002). Subcellular localization and topology of the p7 polypeptide of hepatitis C virus. *J Virol* **76**, 3720-3730.

Castera, L., Chouteau, P., Hezode, C., Zafrani, E. S., Dhumeaux, D. & Pawlotsky, J. M. (2005). Hepatitis C virus-induced hepatocellular steatosis. *Am J Gastroenterol* **100**, 711-715.

Catanese, M. T., Ansuini, H., Graziani, R., Huby, T., Moreau, M., Ball, J. K., Paonessa, G., Rice, C. M., Cortese, R., Vitelli, A. & Nicosia, A. (2010). Role of scavenger receptor class B type I in hepatitis C virus entry: kinetics and molecular determinants. *J Virol* **84**, 34-43.

Catanese, M. T., Graziani, R., von Hahn, T., Moreau, M., Huby, T., Paonessa, G., Santini, C., Luzzago, A., Rice, C. M., Cortese, R., Vitelli, A. & Nicosia, A. (2007). High-avidity monoclonal antibodies against the human scavenger class

B type I receptor efficiently block hepatitis C virus infection in the presence of high-density lipoprotein. *J Virol* **81**, 8063-8071.

Chahar, H. S., Chen, S. & Manjunath, N. (2013). P-body components LSM1, GW182, DDX3, DDX6 and XRN1 are recruited to WNV replication sites and positively regulate viral replication. *Virology* **436**, 1-7.

Chandler, D. E., Penin, F., Schulten, K. & Chipot, C. (2012). The p7 protein of hepatitis C virus forms structurally plastic, minimalist ion channels. *PLoS Comput Biol* **8**, e1002702.

Chang, K. S., Jiang, J., Cai, Z. & Luo, G. (2007). Human apolipoprotein e is required for infectivity and production of hepatitis C virus in cell culture. *J Virol* **81**, 13783-13793.

Chang, P. C., Chi, C. W., Chau, G. Y., Li, F. Y., Tsai, Y. H., Wu, J. C. & Wu Lee, Y. H. (2006). DDX3, a DEAD box RNA helicase, is deregulated in hepatitis virus-associated hepatocellular carcinoma and is involved in cell growth control. *Oncogene* **25**, 1991-2003.

Chao, C. H., Chen, C. M., Cheng, P. L., Shih, J. W., Tsou, A. P. & Lee, Y. H. (2006). DDX3, a DEAD box RNA helicase with tumor growth-suppressive property and transcriptional regulation activity of the p21waf1/cip1 promoter, is a candidate tumor suppressor. *Cancer Res* **66**, 6579-6588.

Charrin, S., Le Naour, F., Labas, V., Billard, M., Le Caer, J. P., Emile, J. F., Petit, M. A., Boucheix, C. & Rubinstein, E. (2003). EWI-2 is a new component of the tetraspanin web in hepatocytes and lymphoid cells. *Biochem J* **373**, 409-421.

Chatterji, U., Bobardt, M., Selvarajah, S., Yang, F., Tang, H., Sakamoto, N., Vuagniaux, G., Parkinson, T., Gallay, P. (2009). The isomerase active site of cyclophilin A is critical for hepatitis C virus replication. *J Biol Chem* **284,** 16998- 17005.

Chatterji, U., Lim, P., Bobardt, M. D., Wieland, S., Cordek, D. G., Vuagniaux, G., Chisari, F., Cameron, C. E., Targett-Adams, P., Parkinson, T. & Gallay, P. A. (2010). HCV resistance to cyclosporin A does not correlate with a resistance of the NS5A-cyclophilin A interaction to cyclophilin inhibitors. *J Hepatol* **53**, 50-56.

Chevaliez, S. & Pawlotsky, J. M. (2007). Hepatitis C virus: virology, diagnosis and management of antiviral therapy. *World J Gastroenterol* **13**, 2461-2466.

Chevaliez, S. & Pawlotsky, J. M. (2009). Virological techniques for the diagnosis and monitoring of hepatitis B and C. *Annals of hepatology* **8**, 7-12.

Chevaliez, S., Rodriguez, C. & Pawlotsky, J. M. (2012). New virologic tools for management of chronic hepatitis B and C. *Gastroenterology* **142**, 1303-1313 e1301.

Chew, C. F., Vijayan, R., Chang, J., Zitzmann, N. & Biggin, P. C. (2009). Determination of pore-lining residues in the hepatitis C virus p7 protein. *Biophys J* **96**, L10-12.

Choi, Y. J. & Lee, S. G. (2012). The DEAD-box RNA helicase DDX3 interacts with DDX5, co-localizes with it in the cytoplasm during the G2/M phase of the cycle, and affects its shuttling during mRNP export. *J Cell Biochem* **113**, 985-996.

Choo, Q. L., Kuo, G., Ralston, R., Weiner, A., Chien, D., Van Nest, G., Han, J., Berger, K., Thudium, K., Kuo, C. & et al. (1994). Vaccination of chimpanzees against infection by the hepatitis C virus. *Proc Natl Acad Sci U S A* **91**, 1294-1298.

Choo, Q. L., Kuo, G., Weiner, A. J., Overby, L. R., Bradley, D. W. & Houghton, M. (1989). Isolation of a cDNA clone derived from a blood-borne non-A, non-B viral hepatitis genome. *Science* **244**, 359-362.

Choo, Q. L., Richman, K. H., Han, J. H., Berger, K., Lee, C., Dong, C., Gallegos, C., Coit, D., Medina-Selby, R., Barr, P. J. & et al. (1991). Genetic organization and diversity of the hepatitis C virus. *Proc Natl Acad Sci U S A* **88**, 2451-2455.

Choo, S. H., So, H. S., Cho, J. M. & Ryu, W. S. (1995). Association of hepatitis C virus particles with immunoglobulin: a mechanism for persistent infection. *J Gen Virol* **76 (Pt 9)**, 2337-2341.

Christie, J. M., Healey, C. J., Watson, J., Wong, V. S., Duddridge, M., Snowden, N., Rosenberg, W. M., Fleming, K. A., Chapel, H. & Chapman, R. W. (1997). Clinical outcome of hypogammaglobulinaemic patients following outbreak of acute hepatitis C: 2 year follow up. *Clin Exp Immunol* **110**, 4-8.

Chuang, R. Y., Weaver, P. L., Liu, Z. & Chang, T. H. (1997). Requirement of the DEAD-Box protein ded1p for messenger RNA translation. *Science* **275**, 1468-1471.

Ciczora, Y., Callens, N., Penin, F., Pecheur, E. I. & Dubuisson, J. (2007). Transmembrane domains of hepatitis C virus envelope glycoproteins: residues involved in E1E2 heterodimerization and involvement of these domains in virus entry. *J Virol* **81**, 2372-2381.

Clarke, B. (1997). Molecular virology of hepatitis C virus. *J Gen Virol* **78 (Pt 10)**, 2397-2410.

Clarke, D., Griffin, S., Beales, L., Gelais, C. S., Burgess, S., Harris, M. & Rowlands, D. (2006). Evidence for the formation of a heptameric ion channel complex by the hepatitis C virus p7 protein in vitro. *J Biol Chem* **281**, 37057-37068.

Coller, K. E., Berger, K. L., Heaton, N. S., Cooper, J. D., Yoon, R. & Randall, G. (2009). RNA interference and single particle tracking analysis of hepatitis C virus endocytosis. *PLoS Pathog* **5**, e1000702.

Coller, K. E., Heaton, N. S., Berger, K. L., Cooper, J. D., Saunders, J. L. & Randall, G. (2012). Molecular determinants and dynamics of hepatitis C virus secretion. *PLoS Pathog* **8**, e1002466.

Cordin, O., Banroques, J., Tanner, N. K. & Linder, P. (2006). The DEAD-box protein family of RNA helicases. *Gene* **367**, 17-37.

Cormier, E. G., Durso, R. J., Tsamis, F., Boussemart, L., Manix, C., Olson, W. C., Gardner, J. P. & Dragic, T. (2004a). L-SIGN (CD209L) and DC-SIGN (CD209) mediate transinfection of liver cells by hepatitis C virus. *Proc Natl Acad Sci U S A* **101**, 14067-14072.

Cormier, E. G., Tsamis, F., Kajumo, F., Durso, R. J., Gardner, J. P. & Dragic, T. (2004b). CD81 is an entry coreceptor for hepatitis C virus. *Proc Natl Acad Sci U S A* **101**, 7270-7274.

Counihan, N. A., Rawlinson, S. M. & Lindenbach, B. D. (2011). Trafficking of hepatitis C virus core protein during virus particle assembly. *PLoS Pathog* **7**, e1002302.

Crotty, S., Cameron, C. E. & Andino, R. (2001). RNA virus error catastrophe: direct molecular test by using ribavirin. *Proc Natl Acad Sci U S A* **98**, 6895-6900.

Cruciat, C. M., Dolde, C., de Groot, R. E., Ohkawara, B., Reinhard, C., Korswagen, H. C. & Niehrs, C. (2013). RNA Helicase DDX3 Is a Regulatory Subunit of Casein Kinase 1 in Wnt/beta-Catenin Signaling. *Science*.

Cua, I. H., Hui, J. M., Kench, J. G. & George, J. (2008). Genotype-specific interactions of insulin resistance, steatosis, and fibrosis in chronic hepatitis C. *Hepatology* **48**, 723-731.

Cukierman, L., Meertens, L., Bertaux, C., Kajumo, F. & Dragic, T. (2009). Residues in a highly conserved claudin-1 motif are required for hepatitis C virus entry and mediate the formation of cell-cell contacts. *J Virol* **83**, 5477-5484.

Cun, W., Jiang, J. & Luo, G. (2010). The C-terminal alpha-helix domain of apolipoprotein E is required for interaction with nonstructural protein 5A and assembly of hepatitis C virus. *J Virol* **84**, 11532-11541.

Da Costa, D., Turek, M., Felmlee, D. J., Girardi, E., Pfeffer, S., Long, G., Bartenschlager, R., Zeisel, M. B. & Baumert, T. F. (2012). Reconstitution of the entire hepatitis C virus life cycle in nonhepatic cells. *J Virol* **86**, 11919-11925.

Dao Thi, V. L., Granier, C., Zeisel, M. B., Guerin, M., Mancip, J., Granio, O., Penin, F., Lavillette, D., Bartenschlager, R., Baumert, T. F., Cosset, F. L. & Dreux, M. (2012). Characterization of hepatitis C virus particle subpopulations reveals multiple usage of the scavenger receptor BI for entry steps. *J Biol Chem* **287**, 31242-31257.

Davis, C., Harris, H. J., Hu, K., Drummer, H. E., McKeating, J. A., Mullins, J. G. & Balfe, P. (2012). In silico directed mutagenesis identifies the CD81/claudin-1 hepatitis C virus receptor interface. *Cell Microbiol* **14**, 1892-1903.

de la Fuente, C., Goodman, Z. & Rice, C. M. (2013). Genetic and functional characterization of the N-terminal region of the hepatitis C virus NS2 protein. *J Virol*.

de Lucas, S., Bartolome, J. & Carreno, V. (2005). Hepatitis C virus core protein down-regulates transcription of interferon-induced antiviral genes. *J Infect Dis* **191**, 93-99.

de Veer, M. J., Holko, M., Frevel, M., Walker, E., Der, S., Paranjape, J. M., Silverman, R. H. & Williams, B. R. (2001). Functional classification of interferon-stimulated genes identified using microarrays. *J Leukoc Biol* **69**, 912-920.

Deckert, J., Hartmuth, K., Boehringer, D., Behzadnia, N., Will, C. L., Kastner, B., Stark, H., Urlaub, H. & Luhrmann, R. (2006). Protein composition and electron microscopy structure of affinity-purified human spliceosomal B complexes isolated under physiological conditions. *Mol Cell Biol* **26**, 5528-5543.

Deleersnyder, V., Pillez, A., Wychowski, C., Blight, K., Xu, J., Hahn, Y. S., Rice, C. M. & Dubuisson, J. (1997). Formation of native hepatitis C virus glycoprotein complexes. *J Virol* **71**, 697-704.

Dentzer, T. G., Lorenz, I. C., Evans, M. J. & Rice, C. M. (2009). Determinants of the hepatitis C virus nonstructural protein 2 protease domain required for production of infectious virus. *J Virol* **83**, 12702-12713.

Dhillon, S., Witteveldt, J., Gatherer, D., Owsianka, A. M., Zeisel, M. B., Zahid, M. N., Rychlowska, M., Foung, S. K., Baumert, T. F., Angus, A. G. & Patel, A. H. (2010). Mutations within a conserved region of the hepatitis C virus E2 glycoprotein that influence virus-receptor interactions and sensitivity to neutralizing antibodies. *J Virol* **84**, 5494-5507.

Di Bisceglie, A. M. & Hoofnagle, J. H. (2002). Optimal therapy of hepatitis C. *Hepatology* **36**, S121-127.

Di Bisceglie, A. M., Shindo, M., Fong, T. L., Fried, M. W., Swain, M. G., Bergasa, N. V., Axiotis, C. A., Waggoner, J. G., Park, Y. & Hoofnagle, J. H. (1992). A pilot study of ribavirin therapy for chronic hepatitis C. *Hepatology* **16**, 649-654.

Diao, J., Pantua, H., Ngu, H., Komuves, L., Diehl, L., Schaefer, G. & Kapadia, S. B. (2012). Hepatitis C virus induces epidermal growth factor receptor activation via CD81 binding for viral internalization and entry. *J Virol* **86**, 10935-10949.

Diepolder, H. M., Gerlach, J. T., Zachoval, R., Hoffmann, R. M., Jung, M. C., Wierenga, E. A., Scholz, S., Santantonio, T., Houghton, M., Southwood, S., Sette, A. & Pape, G. R. (1997). Immunodominant CD4+ T-cell epitope within nonstructural protein 3 in acute hepatitis C virus infection. *J Virol* **71**, 6011-6019.

Diepolder, H. M., Zachoval, R., Hoffmann, R. M., Jung, M. C., Gerlach, T. & Pape, G. R. (1996). The role of hepatitis C virus specific CD4+ T lymphocytes in acute and chronic hepatitis C. *J Mol Med (Berl)* **74**, 583-588.

Domingo, E., Escarmis, C., Sevilla, N., Moya, A., Elena, S. F., Quer, J., Novella, I. S. & Holland, J. J. (1996). Basic concepts in RNA virus evolution. *Faseb J* **10**, 859-864.

Dorner, M., Horwitz, J. A., Robbins, J. B., Barry, W. T., Feng, Q., Mu, K., Jones, C. T., Schoggins, J. W., Catanese, M. T., Burton, D. R., Law, M., Rice, C. M. & Ploss, A. (2011). A genetically humanized mouse model for hepatitis C virus infection. *Nature* **474**, 208-211.

Douglas, M. W. & George, J. (2009). Molecular mechanisms of insulin resistance in chronic hepatitis C. *World J Gastroenterol* **15**, 4356-4364.

Dreux, M., Dao Thi, V. L., Fresquet, J., Guerin, M., Julia, Z., Verney, G., Durantel, D., Zoulim, F., Lavillette, D., Cosset, F. L. & Bartosch, B. (2009a). Receptor complementation and mutagenesis reveal SR-BI as an essential HCV entry factor and functionally imply its intra- and extra-cellular domains. *PLoS pathogens* **5**, e1000310.

Dreux, M., Gastaminza, P., Wieland, S. F. & Chisari, F. V. (2009b). The autophagy machinery is required to initiate hepatitis C virus replication. *Proc Natl Acad Sci U S A* **106**, 14046-14051.

Drummer, H. E., Boo, I., Maerz, A. L. & Poumbourios, P. (2006). A conserved Gly436-Trp-Leu-Ala-Gly-Leu-Phe-Tyr motif in hepatitis C virus glycoprotein E2 is a determinant of CD81 binding and viral entry. *J Virol* **80**, 7844-7853.

Drummer, H. E., Maerz, A. & Poumbourios, P. (2003). Cell surface expression of functional hepatitis C virus E1 and E2 glycoproteins. *FEBS Lett* **546**, 385-390.

Drummer, H. E., Wilson, K. A. & Poumbourios, P. (2002). Identification of the hepatitis C virus E2 glycoprotein binding site on the large extracellular loop of CD81. *J Virol* **76**, 11143-11147.

Drummer, H. E., Wilson, K. A. & Poumbourios, P. (2005). Determinants of CD81 dimerization and interaction with hepatitis C virus glycoprotein E2. *Biochem Biophys Res Commun* **328**, 251-257.

Dubuisson, J. & Rice, C. M. (1996). Hepatitis C virus glycoprotein folding: disulfide bond formation and association with calnexin. *J Virol* **70**, 778-786.

Duseja, A., Dhiman, R. K., Chawla, Y., Thumburu, K. K., Kumar, A., Das, A., Bhadada, S. & Bhansali, A. (2009). Insulin resistance is common in patients with predominantly genotype 3 chronic hepatitis C. *Dig Dis Sci* **54**, 1778-1782.

Dutartre, H., Boretto, J., Guillemot, J. C. & Canard, B. (2005). A relaxed discrimination of 2'-O-methyl-GTP relative to GTP between de novo and Elongative RNA synthesis by the hepatitis C RNA-dependent RNA polymerase NS5B. *J Biol Chem* **280**, 6359-6368.

Edwards, V. C., Tarr, A. W., Urbanowicz, R. A. & Ball, J. K. (2012). The role of neutralizing antibodies in hepatitis C virus infection. *J Gen Virol* **93**, 1-19.

Egger, D., Wolk, B., Gosert, R., Bianchi, L., Blum, H. E., Moradpour, D. & Bienz, K. (2002). Expression of hepatitis C virus proteins induces distinct membrane alterations including a candidate viral replication complex. *J Virol* **76**, 5974-5984.

Einav, S. & Koziel, M. J. (2002). Immunopathogenesis of hepatitis C virus in the immunosuppressed host. *Transpl Infect Dis* **4**, 85-92.

Elazar, M., Cheong, K. H., Liu, P., Greenberg, H. B., Rice, C. M. & Glenn, J. S. (2003). Amphipathic helix-dependent localization of NS5A mediates hepatitis C virus RNA replication. *J Virol* **77**, 6055-6061.

Elazar, M., Liu, P., Rice, C. M. & Glenn, J. S. (2004). An N-terminal amphipathic helix in hepatitis C virus (HCV) NS4B mediates membrane association, correct localization of replication complex proteins, and HCV RNA replication. *J Virol* **78**, 11393-11400.

Engering, A., Geijtenbeek, T. B., van Vliet, S. J., Wijers, M., van Liempt, E., Demaurex, N., Lanzavecchia, A., Fransen, J., Figdor, C. G., Piguet, V. & van Kooyk, Y. (2002). The dendritic cell-specific adhesion receptor DC-SIGN internalizes antigen for presentation to T cells. *J Immunol* **168**, 2118-2126.

Evans, M. J., Rice, C. M. & Goff, S. P. (2004). Phosphorylation of hepatitis C virus nonstructural protein 5A modulates its protein interactions and viral RNA replication. *Proc Natl Acad Sci U S A* **101**, 13038-13043.

Evans, M. J., von Hahn, T., Tscherne, D. M., Syder, A. J., Panis, M., Wolk, B., Hatziioannou, T., McKeating, J. A., Bieniasz, P. D. & Rice, C. M. (2007). Claudin-1 is a hepatitis C virus co-receptor required for a late step in entry. *Nature* **446**, 801-805.

Fairman-Williams, M. E., Guenther, U. P. & Jankowsky, E. (2010). SF1 and SF2 helicases: family matters. *Curr Opin Struct Biol* **20**, 313-324.

Fang, J., Kubota, S., Yang, B., Zhou, N., Zhang, H., Godbout, R. & Pomerantz, R. J. (2004). A DEAD box protein facilitates HIV-1 replication as a cellular co-factor of Rev. *Virology* **330**, 471-480.

Farci, P., Alter, H. J., Shimoda, A., Govindarajan, S., Cheung, L. C., Melpolder, J. C., Sacher, R. A., Shih, J. W. & Purcell, R. H. (1996). Hepatitis C virus-associated fulminant hepatic failure. *N Engl J Med* **335**, 631-634.

Farci, P., Alter, H. J., Wong, D., Miller, R. H., Shih, J. W., Jett, B. & Purcell, R. H. (1991). A long-term study of hepatitis C virus replication in non-A, non-B hepatitis. *N Engl J Med* **325**, 98-104.

Farci, P., Alter, H. J., Wong, D. C., Miller, R. H., Govindarajan, S., Engle, R., Shapiro, M. & Purcell, R. H. (1994). Prevention of hepatitis C virus infection in chimpanzees after antibody-mediated in vitro neutralization. *Proc Natl Acad Sci U S A* **91**, 7792-7796.

Farquhar, M. J., Hu, K., Harris, H. J., Davis, C., Brimacombe, C. L., Fletcher, S. J., Baumert, T. F., Rappoport, J. Z., Balfe, P. & McKeating, J. A. (2012). Hepatitis C virus induces CD81 and claudin-1 endocytosis. *J Virol* **86**, 4305-4316.

Feinstone, S. M., Kapikian, A. Z., Purcell, R. H., Alter, H. J. & Holland, P. V. (1975). Transfusion-associated hepatitis not due to viral hepatitis type A or B. *N Engl J Med* **292**, 767-770.

Feinstone, S. M., Mihalik, K. B., Kamimura, T., Alter, H. J., London, W. T. & Purcell, R. H. (1983). Inactivation of hepatitis B virus and non-A, non-B hepatitis by chloroform. *Infect Immun* **41**, 816-821.

Feld, J. J. & Hoofnagle, J. H. (2005). Mechanism of action of interferon and ribavirin in treatment of hepatitis C. *Nature* **436**, 967-972.

Fernandes, F., Poole, D.S., Hoover, S., Middleton, R., Andrei, A.C., Gerstner, J., Striker, R. (2007). Sensitivity of hepatitis C virus to cyclosporine A depends on non- structural proteins NS5A and NS5B. *Hepatology* **46,** 1026–1033.

Ferrari, E., He, Z., Palermo, R. E. & Huang, H. C. (2008). Hepatitis C virus NS5B polymerase exhibits distinct nucleotide requirements for initiation and elongation. *J Biol Chem* **283**, 33893-33901.

Ferraris, P., Blanchard, E. & Roingeard, P. (2010). Ultrastructural and biochemical analyses of hepatitis C virus-associated host cell membranes. *J Gen Virol* **91**, 2230-2237.

Flint, M. & McKeating, J. A. (1999). The C-terminal region of the hepatitis C virus E1 glycoprotein confers localization within the endoplasmic reticulum. *J Gen Virol* **80 (Pt 8)**, 1943-1947.

Flint, M., von Hahn, T., Zhang, J., Farquhar, M., Jones, C. T., Balfe, P., Rice, C. M. & McKeating, J. A. (2006). Diverse CD81 proteins support hepatitis C virus infection. *J Virol* **80**, 11331-11342.

Fofana, I., Krieger, S. E., Grunert, F., Glauben, S., Xiao, F., Fafi-Kremer, S., Soulier, E., Royer, C., Thumann, C., Mee, C. J., McKeating, J. A., Dragic, T., Pessaux, P., Stoll-Keller, F., Schuster, C., Thompson, J. & Baumert, T. F. (2010). Monoclonal anti-claudin 1 antibodies prevent hepatitis C virus infection of primary human hepatocytes. *Gastroenterology* **139**, 953-964, 964 e951-954.

Forns, X., Thimme, R., Govindarajan, S., Emerson, S. U., Purcell, R. H., Chisari, F. V. & Bukh, J. (2000). Hepatitis C virus lacking the hypervariable region 1 of the second envelope protein is infectious and causes acute resolving or persistent infection in chimpanzees. *Proc Natl Acad Sci U S A* **97**, 13318-13323.

Foy, E., Li, K., Sumpter, R., Jr., Loo, Y. M., Johnson, C. L., Wang, C., Fish, P. M., Yoneyama, M., Fujita, T., Lemon, S. M. & Gale, M., Jr. (2005). Control of antiviral defenses through hepatitis C virus disruption of retinoic acid-inducible gene-I signaling. *Proc Natl Acad Sci U S A* **102**, 2986-2991.

Franca, R., Belfiore, A., Spadari, S. & Maga, G. (2007). Human DEAD-box ATPase DDX3 shows a relaxed nucleoside substrate specificity. *Proteins* **67**, 1128-1137.

Frank, C., Mohamed, M. K., Strickland, G. T., Lavanchy, D., Arthur, R. R., Magder, L. S., El Khoby, T., Abdel-Wahab, Y., Aly Ohn, E. S., Anwar, W. & Sallam, I. (2000). The role of parenteral antischistosomal therapy in the spread of hepatitis C virus in Egypt. *Lancet* **355**, 887-891.

Fraser, J., Boo, I., Poumbourios, P. & Drummer, H. E. (2011). Hepatitis C virus (HCV) envelope glycoproteins E1 and E2 contain reduced cysteine residues essential for virus entry. *J Biol Chem* **286**, 31984-31992.

Friebe, P. & Bartenschlager, R. (2002). Genetic analysis of sequences in the 3' nontranslated region of hepatitis C virus that are important for RNA replication. *J Virol* **76**, 5326-5338.

Friebe, P., Lohmann, V., Krieger, N. & Bartenschlager, R. (2001). Sequences in the 5' nontranslated region of hepatitis C virus required for RNA replication. *J Virol* **75**, 12047-12057.

Fried, M. W. (2002). Side effects of therapy of hepatitis C and their management. *Hepatology* **36**, S237-244.

Fukushi, S., Okada, M., Kageyama, T., Hoshino, F. B., Nagai, K. & Katayama, K. (2001). Interaction of poly(rC)-binding protein 2 with the 5'-terminal stem loop of the hepatitis C-virus genome. *Virus Res* **73**, 67-79.

Furuse, M., Hirase, T., Itoh, M., Nagafuchi, A., Yonemura, S., Tsukita, S. & Tsukita, S. (1993). Occludin: a novel integral membrane protein localizing at tight junctions. *J Cell Biol* **123**, 1777-1788.

Furuse, M. & Tsukita, S. (2006). Claudins in occluding junctions of humans and flies. *Trends Cell Biol* **16**, 181-188.

Gale, M., Jr. & Foy, E. M. (2005). Evasion of intracellular host defence by hepatitis C virus. *Nature* **436**, 939-945.

Gale, M. J., Jr., Korth, M. J., Tang, N. M., Tan, S. L., Hopkins, D. A., Dever, T. E., Polyak, S. J., Gretch, D. R. & Katze, M. G. (1997). Evidence that hepatitis C virus resistance to interferon is mediated through repression of the PKR protein kinase by the nonstructural 5A protein. *Virology* **230**, 217-227.

Gane, E. (2012). Future perspectives: towards interferon-free regimens for HCV. *Antivir Ther* **17**, 1201-1210.

Gao, L., Aizaki, H., He, J. W. & Lai, M. M. (2004). Interactions between viral nonstructural proteins and host protein hVAP-33 mediate the formation of hepatitis C virus RNA replication complex on lipid raft. *J Virol* **78**, 3480-3488.

Gao, M., Nettles, R. E., Belema, M., Snyder, L. B., Nguyen, V. N., Fridell, R. A., Serrano-Wu, M. H., Langley, D. R., Sun, J. H., O'Boyle, D. R., 2nd, Lemm, J. A., Wang, C., Knipe, J. O., Chien, C., Colonno, R. J., Grasela, D. M., Meanwell, N. A. & Hamann, L. G. (2010). Chemical genetics strategy identifies an HCV NS5A inhibitor with a potent clinical effect. *Nature* **465**, 96-100.

Garbelli, A., Beermann, S., Di Cicco, G., Dietrich, U. & Maga, G. (2011). A motif unique to the human DEAD-box protein DDX3 is important for nucleic acid binding, ATP hydrolysis, RNA/DNA unwinding and HIV-1 replication. *PLoS One* **6**, e19810.

Gardner, J. P., Durso, R. J., Arrigale, R. R., Donovan, G. P., Maddon, P. J., Dragic, T. & Olson, W. C. (2003). L-SIGN (CD 209L) is a liver-specific capture receptor for hepatitis C virus. *Proc Natl Acad Sci U S A* **100**, 4498-4503.

Garry, R. F. & Dash, S. (2003). Proteomics computational analyses suggest that hepatitis C virus E1 and pestivirus E2 envelope glycoproteins are truncated class II fusion proteins. *Virology* **307**, 255-265.

Gastaminza, P., Cheng, G., Wieland, S., Zhong, J., Liao, W. & Chisari, F. V. (2008). Cellular determinants of hepatitis C virus assembly, maturation, degradation, and secretion. *J Virol* **82**, 2120-2129.

Gastaminza, P., Dryden, K. A., Boyd, B., Wood, M. R., Law, M., Yeager, M. & Chisari, F. V. (2010). Ultrastructural and biophysical characterization of hepatitis C virus particles produced in cell culture. *J Virol* **84**, 10999-11009.

Gastaminza, P., Kapadia, S. B. & Chisari, F. V. (2006). Differential biophysical properties of infectious intracellular and secreted hepatitis C virus particles. *J Virol* **80**, 11074-11081.

Gastaminza, P., Pitram, S. M., Dreux, M., Krasnova, L. B., Whitten-Bauer, C., Dong, J., Chung, J., Fokin, V. V., Sharpless, K. B. & Chisari, F. V. (2011). Antiviral stilbene 1,2-diamines prevent initiation of hepatitis C virus RNA replication at the outset of infection. *J Virol* **85**, 5513-5523.

Geissler, R., Golbik, R. P. & Behrens, S. E. (2012). The DEAD-box helicase DDX3 supports the assembly of functional 80S ribosomes. *Nucleic Acids Res* **40**, 4998-5011.

Germi, R., Crance, J. M., Garin, D., Guimet, J., Lortat-Jacob, H., Ruigrok, R. W., Zarski, J. P. & Drouet, E. (2002). Cellular glycosaminoglycans and low density lipoprotein receptor are involved in hepatitis C virus adsorption. *J Med Virol* **68**, 206-215.

Giannini, C. & Brechot, C. (2003). Hepatitis C virus biology. *Cell Death Differ* **10 Suppl 1**, S27-38.

Glue, P., Rouzier-Panis, R., Raffanel, C., Sabo, R., Gupta, S. K., Salfi, M., Jacobs, S. & Clement, R. P. (2000). A dose-ranging study of pegylated interferon alfa-2b and ribavirin in chronic hepatitis C. The Hepatitis C Intervention Therapy Group. *Hepatology* **32**, 647-653.

Goffard, A., Callens, N., Bartosch, B., Wychowski, C., Cosset, F. L., Montpellier, C. & Dubuisson, J. (2005). Role of N-linked glycans in the functions of hepatitis C virus envelope glycoproteins. *J Virol* **79**, 8400-8409.

Goh, P. Y., Tan, Y. J., Lim, S. P., Tan, Y. H., Lim, S. G., Fuller-Pace, F. & Hong, W. (2004). Cellular RNA helicase p68 relocalization and interaction with the hepatitis C virus (HCV) NS5B protein and the potential role of p68 in HCV RNA replication. *J Virol* **78**, 5288-5298.

Gomez, J., Martell, M., Quer, J., Cabot, B. & Esteban, J. I. (1999). Hepatitis C viral quasispecies. *J Viral Hepat* **6**, 3-16.

Gonzalez, M. E. & Carrasco, L. (2003). Viroporins. *FEBS Lett* **552**, 28-34.

Gorzin, A. A., Ramsland, P. A., Tachedjian, G. & Gowans, E. J. (2012). Identification of residues involved in NS2 homodimerization and elucidation of their impact on the HCV life cycle. *J Viral Hepat* **19**, 189-198.

Gosert, R., Egger, D., Lohmann, V., Bartenschlager, R., Blum, H. E., Bienz, K. & Moradpour, D. (2003). Identification of the hepatitis C virus RNA replication complex in Huh-7 cells harboring subgenomic replicons. *J Virol* **77**, 5487-5492.

Gottwein, J. M., Scheel, T. K., Jensen, T. B., Lademann, J. B., Prentoe, J. C., Knudsen, M. L., Hoegh, A. M. & Bukh, J. (2009). Development and characterization of hepatitis C virus genotype 1-7 cell culture systems: role of CD81 and scavenger receptor class B type I and effect of antiviral drugs. *Hepatology* **49**, 364-377.

Goueslain, L., Alsaleh, K., Horellou, P., Roingeard, P., Descamps, V., Duverlie, G., Ciczora, Y., Wychowski, C., Dubuisson, J. & Rouille, Y. (2010). Identification of GBF1 as a cellular factor required for hepatitis C virus RNA replication. *J Virol* **84**, 773-787.

Gouttenoire, J., Castet, V., Montserret, R., Arora, N., Raussens, V., Ruysschaert, J. M., Diesis, E., Blum, H. E., Penin, F. & Moradpour, D. (2009a). Identification of a novel determinant for membrane association in hepatitis C virus nonstructural protein 4B. *J Virol* **83**, 6257-6268.

Gouttenoire, J., Montserret, R., Kennel, A., Penin, F. & Moradpour, D. (2009b). An amphipathic alpha-helix at the C terminus of hepatitis C virus nonstructural protein 4B mediates membrane association. *J Virol* **83**, 11378-11384.

Gouttenoire, J., Moradpour, D. & Penin, F. (2006). Surprises from the crystal structure of the hepatitis C virus NS2-3 protease. *Hepatology* **44**, 1690-1693.

Grakoui, A., McCourt, D. W., Wychowski, C., Feinstone, S. M. & Rice, C. M. (1993). Characterization of the hepatitis C virus-encoded serine proteinase:

determination of proteinase-dependent polyprotein cleavage sites. *J Virol* **67**, 2832-2843.

Grakoui, A., Shoukry, N. H., Woollard, D. J., Han, J. H., Hanson, H. L., Ghrayeb, J., Murthy, K. K., Rice, C. M. & Walker, C. M. (2003). HCV persistence and immune evasion in the absence of memory T cell help. *Science* **302**, 659-662.

Grallert, B., Kearsey, S. E., Lenhard, M., Carlson, C. R., Nurse, P., Boye, E. & Labib, K. (2000). A fission yeast general translation factor reveals links between protein synthesis and cell cycle controls. *J Cell Sci* **113 (Pt 8)**, 1447-1458.

Gretton, S. N., Taylor, A. I. & McLauchlan, J. (2005). Mobility of the hepatitis C virus NS4B protein on the endoplasmic reticulum membrane and membrane-associated foci. *J Gen Virol* **86**, 1415-1421.

Griffin, S. D., Beales, L. P., Clarke, D. S., Worsfold, O., Evans, S. D., Jaeger, J., Harris, M. P. & Rowlands, D. J. (2003). The p7 protein of hepatitis C virus forms an ion channel that is blocked by the antiviral drug, Amantadine. *FEBS Lett* **535**, 34-38.

Griffin, S. D., Harvey, R., Clarke, D. S., Barclay, W. S., Harris, M. & Rowlands, D. J. (2004). A conserved basic loop in hepatitis C virus p7 protein is required for amantadine-sensitive ion channel activity in mammalian cells but is dispensable for localization to mitochondria. *J Gen Virol* **85**, 451-461.

Grobler, J. A., Markel, E. J., Fay, J. F., Graham, D. J., Simcoe, A. L., Ludmerer, S. W., Murray, E. M., Migliaccio, G. & Flores, O. A. (2003). Identification of a key determinant of hepatitis C virus cell culture adaptation in domain II of NS3 helicase. *J Biol Chem* **278**, 16741-16746.

Gu, L., Fullam, A., Brennan, R. & Schroder, M. (2013). The human DEAD-box helicase 3 couples IKK-epsilon to IRF3 activation. *Molecular and cellular biology*.

Guan, M., Wang, W., Liu, X., Tong, Y., Liu, Y., Ren, H., Zhu, S., Dubuisson, J., Baumert, T. F., Zhu, Y., Peng, H., Aurelian, L., Zhao, P. & Qi, Z. (2012). Three different functional microdomains in the hepatitis C virus hypervariable region 1 (HVR1) mediate entry and immune evasion. *J Biol Chem* **287**, 35631-35645.

Guidotti, L. G. & Chisari, F. V. (2001). Noncytolytic control of viral infections by the innate and adaptive immune response. *Annu Rev Immunol* **19**, 65-91.

Gururajan, R., Perry-O'Keefe, H., Melton, D. A. & Weeks, D. L. (1991). The Xenopus localized messenger RNA An3 may encode an ATP-dependent RNA helicase. *Nature* **349**, 717-719.

Haberstroh, A., Schnober, E. K., Zeisel, M. B., Carolla, P., Barth, H., Blum, H. E., Cosset, F. L., Koutsoudakis, G., Bartenschlager, R., Union, A., Depla, E., Owsianka, A., Patel, A. H., Schuster, C., Stoll-Keller, F., Doffoel, M., Dreux, M. & Baumert, T. F. (2008). Neutralizing host responses in hepatitis C virus infection target viral entry at postbinding steps and membrane fusion. *Gastroenterology* **135**, 1719-1728 e1711.

Hamamoto, I., Nishimura, Y., Okamoto, T., Aizaki, H., Liu, M., Mori, Y., Abe, T., Suzuki, T., Lai, M. M., Miyamura, T., Moriishi, K. & Matsuura, Y. (2005). Human VAP-B is involved in hepatitis C virus replication through interaction with NS5A and NS5B. *J Virol* **79**, 13473-13482.

Hanoulle, X., Badillo, A., Verdegem, D., Penin, F. & Lippens, G. (2010). The domain 2 of the HCV NS5A protein is intrinsically unstructured. *Protein Pept Lett* **17**, 1012-1018.

Hanoulle, X., Verdegem, D., Badillo, A., Wieruszeski, J. M., Penin, F. & Lippens, G. (2009). Domain 3 of non-structural protein 5A from hepatitis C virus is natively unfolded. *Biochem Biophys Res Commun* **381**, 634-638.

Hara, H., Aizaki, H., Matsuda, M., Shinkai-Ouchi, F., Inoue, Y., Murakami, K., Shoji, I., Kawakami, H., Matsuura, Y., Lai, M. M., Miyamura, T., Wakita, T. & Suzuki, T. (2009). Involvement of creatine kinase B in hepatitis C virus genome replication through interaction with the viral NS4A protein. *J Virol* **83**, 5137-5147.

Harris, D., Zhang, Z., Chaubey, B. & Pandey, V. N. (2006). Identification of cellular factors associated with the 3'-nontranslated region of the hepatitis C virus genome. *Mol Cell Proteomics* **5**, 1006-1018.

Harris, H. J., Davis, C., Mullins, J. G., Hu, K., Goodall, M., Farquhar, M. J., Mee, C. J., McCaffrey, K., Young, S., Drummer, H., Balfe, P. & McKeating, J. A. (2010). Claudin association with CD81 defines hepatitis C virus entry. *J Biol Chem* **285**, 21092-21102.

Harris, H. J., Farquhar, M. J., Mee, C. J., Davis, C., Reynolds, G. M., Jennings, A., Hu, K., Yuan, F., Deng, H., Hubscher, S. G., Han, J. H., Balfe, P. & McKeating, J. A. (2008). CD81 and claudin 1 coreceptor association: role in hepatitis C virus entry. *J Virol* **82**, 5007-5020.

Harrison, S. C. (2008). Viral membrane fusion. *Nat Struct Mol Biol* **15**, 690-698.

Harrus, D., Ahmed-El-Sayed, N., Simister, P. C., Miller, S., Triconnet, M., Hagedorn, C. H., Mahias, K., Rey, F. A., Astier-Gin, T. & Bressanelli, S. (2010). Further insights into the roles of GTP and the C terminus of the hepatitis C virus polymerase in the initiation of RNA synthesis. *J Biol Chem* **285**, 32906-32918.

He, L. F., Alling, D., Popkin, T., Shapiro, M., Alter, H. J. & Purcell, R. H. (1987). Determining the size of non-A, non-B hepatitis virus by filtration. *J Infect Dis* **156**, 636-640.

Heckel, J. L., Sandgren, E. P., Degen, J. L., Palmiter, R. D. & Brinster, R. L. (1990). Neonatal bleeding in transgenic mice expressing urokinase-type plasminogen activator. *Cell* **62**, 447-456.

Helle, F., Vieyres, G., Elkrief, L., Popescu, C. I., Wychowski, C., Descamps, V., Castelain, S., Roingeard, P., Duverlie, G. & Dubuisson, J. (2010). Role of N-linked glycans in the functions of hepatitis C virus envelope proteins incorporated into infectious virions. *J Virol* **84**, 11905-11915.

Henke, J. I., Goergen, D., Zheng, J., Song, Y., Schuttler, C. G., Fehr, C., Junemann, C. & Niepmann, M. (2008). microRNA-122 stimulates translation of hepatitis C virus RNA. *Embo J* **27**, 3300-3310.

Herker, E., Harris, C., Hernandez, C., Carpentier, A., Kaehlcke, K., Rosenberg, A. R., Farese, R. V., Jr. & Ott, M. (2010). Efficient hepatitis C virus particle formation requires diacylglycerol acyltransferase-1. *Nat Med* **16**, 1295-1298.

Higginbottom, A., Quinn, E. R., Kuo, C. C., Flint, M., Wilson, L. H., Bianchi, E., Nicosia, A., Monk, P. N., McKeating, J. A. & Levy, S. (2000). Identification of amino acid residues in CD81 critical for interaction with hepatitis C virus envelope glycoprotein E2. *J Virol* **74**, 3642-3649.

Hijikata, M., Mizushima, H., Akagi, T., Mori, S., Kakiuchi, N., Kato, N., Tanaka, T., Kimura, K. & Shimotohno, K. (1993a). Two distinct proteinase activities

required for the processing of a putative nonstructural precursor protein of hepatitis C virus. *J Virol* **67**, 4665-4675.

Hijikata, M., Shimizu, Y. K., Kato, H., Iwamoto, A., Shih, J. W., Alter, H. J., Purcell, R. H. & Yoshikura, H. (1993b). Equilibrium centrifugation studies of hepatitis C virus: evidence for circulating immune complexes. *J Virol* **67**, 1953-1958.

Hilgard, P. & Stockert, R. (2000). Heparan sulfate proteoglycans initiate dengue virus infection of hepatocytes. *Hepatology* **32**, 1069-1077.

Hishiki, T., Shimizu, Y., Tobita, R., Sugiyama, K., Ogawa, K., Funami, K., Ohsaki, Y., Fujimoto, T., Takaku, H., Wakita, T., Baumert, T. F., Miyanari, Y. & Shimotohno, K. (2010). Infectivity of hepatitis C virus is influenced by association with apolipoprotein E isoforms. *J Virol* **84**, 12048-12057.

Hoffmann, R. M., Diepolder, H. M., Zachoval, R., Zwiebel, F. M., Jung, M. C., Scholz, S., Nitschko, H., Riethmuller, G. & Pape, G. R. (1995). Mapping of immunodominant CD4+ T lymphocyte epitopes of hepatitis C virus antigens and their relevance during the course of chronic infection. *Hepatology* **21**, 632-638.

Hogbom, M., Collins, R., van den Berg, S., Jenvert, R. M., Karlberg, T., Kotenyova, T., Flores, A., Karlsson Hedestam, G. B. & Schiavone, L. H. (2007). Crystal structure of conserved domains 1 and 2 of the human DEAD-box helicase DDX3X in complex with the mononucleotide AMP. *J Mol Biol* **372**, 150-159.

Holland, J. J., De La Torre, J. C. & Steinhauer, D. A. (1992). RNA virus populations as quasispecies. *Curr Top Microbiol Immunol* **176**, 1-20.

Hollinger, F. B., Gitnick, G. L., Aach, R. D., Szmuness, W., Mosley, J. W., Stevens, C. E., Peters, R. L., Weiner, J. M., Werch, J. B. & Lander, J. J. (1978). Non-A, non-B hepatitis transmission in chimpanzees: a project of the transfusion-transmitted viruses study group. *Intervirology* **10**, 60-68.

Honda, M., Brown, E. A. & Lemon, S. M. (1996a). Stability of a stem-loop involving the initiator AUG controls the efficiency of internal initiation of translation on hepatitis C virus RNA. *Rna* **2**, 955-968.

Honda, M., Ping, L. H., Rijnbrand, R. C., Amphlett, E., Clarke, B., Rowlands, D. & Lemon, S. M. (1996b). Structural requirements for initiation of translation by internal ribosome entry within genome-length hepatitis C virus RNA. *Virology* **222**, 31-42.

Honda, M., Rijnbrand, R., Abell, G., Kim, D. & Lemon, S. M. (1999). Natural variation in translational activities of the 5' nontranslated RNAs of hepatitis C virus genotypes 1a and 1b: evidence for a long-range RNA-RNA interaction outside of the internal ribosomal entry site. *J Virol* **73**, 4941-4951.

Hoofnagle, J. H. (1997). Hepatitis C: the clinical spectrum of disease. *Hepatology* **26**, 15S-20S.

Hoofnagle, J. H. (2002). Course and outcome of hepatitis C. *Hepatology* **36**, S21-29.

Hope, R. G. & McLauchlan, J. (2000). Sequence motifs required for lipid droplet association and protein stability are unique to the hepatitis C virus core protein. *J Gen Virol* **81**, 1913-1925.

Horner, S. M. & Gale, M., Jr. (2009). Intracellular innate immune cascades and interferon defenses that control hepatitis C virus. *J Interferon Cytokine Res* **29**, 489-498.

Hornung, V., Ellegast, J., Kim, S., Brzozka, K., Jung, A., Kato, H., Poeck, H., Akira, S., Conzelmann, K. K., Schlee, M., Endres, S. & Hartmann, G. (2006). 5'-Triphosphate RNA is the ligand for RIG-I. *Science* **314**, 994-997.

Hornung, V., Guenthner-Biller, M., Bourquin, C., Ablasser, A., Schlee, M., Uematsu, S., Noronha, A., Manoharan, M., Akira, S., de Fougerolles, A., Endres, S. & Hartmann, G. (2005). Sequence-specific potent induction of IFN-alpha by short interfering RNA in plasmacytoid dendritic cells through TLR7. *Nat Med* **11**, 263-270.

Hsu, M., Zhang, J., Flint, M., Logvinoff, C., Cheng-Mayer, C., Rice, C. M. & McKeating, J. A. (2003). Hepatitis C virus glycoproteins mediate pH-dependent cell entry of pseudotyped retroviral particles. *Proc Natl Acad Sci U S A* **100**, 7271-7276.

Huang, H., Sun, F., Owen, D. M., Li, W., Chen, Y., Gale, M., Jr. & Ye, J. (2007). Hepatitis C virus production by human hepatocytes dependent on assembly and secretion of very low-density lipoproteins. *Proc Natl Acad Sci U S A* **104**, 5848-5853.

Huang, J. S., Chao, C. C., Su, T. L., Yeh, S. H., Chen, D. S., Chen, C. T., Chen, P. J. & Jou, Y. S. (2004). Diverse cellular transformation capability of overexpressed genes in human hepatocellular carcinoma. *Biochem Biophys Res Commun* **315**, 950-958.

Huang, J. Y., Su, W. C., Jeng, K. S., Chang, T. H. & Lai, M. M. (2012). Attenuation of 40S ribosomal subunit abundance differentially affects host and HCV translation and suppresses HCV replication. *PLoS Pathog* **8**, e1002766.

Huang, L., Hwang, J., Sharma, S. D., Hargittai, M. R., Chen, Y., Arnold, J. J., Raney, K. D. & Cameron, C. E. (2005). Hepatitis C virus nonstructural protein 5A (NS5A) is an RNA-binding protein. *J Biol Chem* **280**, 36417-36428.

Huber, K. R., Sebesta, C. & Bauer, K. (1996). Detection of common hepatitis C virus subtypes with a third-generation enzyme immunoassay. *Hepatology* **24**, 471-473.

Hughes, M., Griffin, S. & Harris, M. (2009). Domain III of NS5A contributes to both RNA replication and assembly of hepatitis C virus particles. *J Gen Virol* **90**, 1329-1334.

Hugle, T., Fehrmann, F., Bieck, E., Kohara, M., Krausslich, H. G., Rice, C. M., Blum, H. E. & Moradpour, D. (2001). The hepatitis C virus nonstructural protein 4B is an integral endoplasmic reticulum membrane protein. *Virology* **284**, 70-81.

Hussy, P., Langen, H., Mous, J. & Jacobsen, H. (1996). Hepatitis C virus core protein: carboxy-terminal boundaries of two processed species suggest cleavage by a signal peptide peptidase. *Virology* **224**, 93-104.

Iacob, R. E., Perdivara, I., Przybylski, M. & Tomer, K. B. (2008). Mass spectrometric characterization of glycosylation of hepatitis C virus E2 envelope glycoprotein reveals extended microheterogeneity of N-glycans. *J Am Soc Mass Spectrom* **19**, 428-444.

Icard, V., Diaz, O., Scholtes, C., Perrin-Cocon, L., Ramiere, C., Bartenschlager, R., Penin, F., Lotteau, V. & Andre, P. (2009). Secretion of hepatitis C virus envelope glycoproteins depends on assembly of apolipoprotein B positive lipoproteins. *PLoS One* **4**, e4233.

Ikeda, M., Abe, K., Dansako, H., Nakamura, T., Naka, K. & Kato, N. (2005). Efficient replication of a full-length hepatitis C virus genome, strain O, in cell culture, and development of a luciferase reporter system. *Biochem Biophys Res Commun* **329**, 1350-1359.

Ikeda, M., Yi, M., Li, K. & Lemon, S. M. (2002). Selectable subgenomic and genome-length dicistronic RNAs derived from an infectious molecular clone of

the HCV-N strain of hepatitis C virus replicate efficiently in cultured Huh7 cells. *J Virol* **76**, 2997-3006.

Iro, M., Witteveldt, J., Angus, A. G., Woerz, I., Kaul, A., Bartenschlager, R. & Patel, A. H. (2009). A reporter cell line for rapid and sensitive evaluation of hepatitis C virus infectivity and replication. *Antiviral Res* **83**, 148-155.

Ishaq, M., Hu, J., Wu, X., Fu, Q., Yang, Y., Liu, Q. & Guo, D. (2008). Knockdown of cellular RNA helicase DDX3 by short hairpin RNAs suppresses HIV-1 viral replication without inducing apoptosis. *Mol Biotechnol* **39**, 231-238.

Ito, T. & Lai, M. M. (1997). Determination of the secondary structure of and cellular protein binding to the 3'-untranslated region of the hepatitis C virus RNA genome. *J Virol* **71**, 8698-8706.

Ito, T., Tahara, S. M. & Lai, M. M. (1998). The 3'-untranslated region of hepatitis C virus RNA enhances translation from an internal ribosomal entry site. *J Virol* **72**, 8789-8796.

Ivashkina, N., Wolk, B., Lohmann, V., Bartenschlager, R., Blum, H. E., Penin, F. & Moradpour, D. (2002). The hepatitis C virus RNA-dependent RNA polymerase membrane insertion sequence is a transmembrane segment. *J Virol* **76**, 13088-13093.

Jackson, R. J., Hellen, C. U. & Pestova, T. V. (2010). The mechanism of eukaryotic translation initiation and principles of its regulation. *Nat Rev Mol Cell Biol* **11**, 113-127.

Jacobson, I. M., Pawlotsky, J. M., Afdhal, N. H., Dusheiko, G. M., Forns, X., Jensen, D. M., Poordad, F. & Schulz, J. (2012). A practical guide for the use of boceprevir and telaprevir for the treatment of hepatitis C. *J Viral Hepat* **19 Suppl 2**, 1-26.

Jamieson, D. J. & Beggs, J. D. (1991). A suppressor of yeast spp81/ded1 mutations encodes a very similar putative ATP-dependent RNA helicase. *Mol Microbiol* **5**, 805-812.

Jangra, R. K., Yi, M. & Lemon, S. M. (2010). Regulation of hepatitis C virus translation and infectious virus production by the microRNA miR-122. *J Virol* **84**, 6615-6625.

Jazwinski, A. B. & Muir, A. J. (2011). Emerging therapies in hepatitis C: dawn of the era of the direct-acting antivirals. *Gastroenterol Clin North Am* **40**, 481-494.

Ji, H., Fraser, C. S., Yu, Y., Leary, J. & Doudna, J. A. (2004). Coordinated assembly of human translation initiation complexes by the hepatitis C virus internal ribosome entry site RNA. *Proc Natl Acad Sci U S A* **101**, 16990-16995.

Jiang, J., Cun, W., Wu, X., Shi, Q., Tang, H. & Luo, G. (2012). Hepatitis C virus attachment mediated by apolipoprotein E binding to cell surface heparan sulfate. *J Virol* **86**, 7256-7267.

Jiang, J. & Luo, G. (2012). Cell culture-adaptive mutations promote viral protein-protein interactions and morphogenesis of infectious hepatitis C virus. *J Virol* **86**, 8987-8997.

Jiang, J. & Luo, G. (2009). Apolipoprotein E but not B is required for the formation of infectious hepatitis C virus particles. *J Virol* **83**, 12680-12691.

Jirasko, V., Montserret, R., Appel, N., Janvier, A., Eustachi, L., Brohm, C., Steinmann, E., Pietschmann, T., Penin, F. & Bartenschlager, R. (2008). Structural and functional characterization of nonstructural protein 2 for its role in hepatitis C virus assembly. *J Biol Chem* **283**, 28546-28562.

Jirasko, V., Montserret, R., Lee, J. Y., Gouttenoire, J., Moradpour, D., Penin, F. & Bartenschlager, R. (2010). Structural and functional studies of nonstructural

protein 2 of the hepatitis C virus reveal its key role as organizer of virion assembly. *PLoS Pathog* **6**, e1001233.

Jones, C. T., Murray, C. L., Eastman, D. K., Tassello, J. & Rice, C. M. (2007). Hepatitis C virus p7 and NS2 proteins are essential for production of infectious virus. *J Virol* **81**, 8374-8383.

Jones, D. M., Domingues, P., Targett-Adams, P. & McLauchlan, J. (2010). Comparison of U2OS and Huh-7 cells for identifying host factors that affect hepatitis C virus RNA replication. *The Journal of general virology* **91**, 2238-2248.

Jones, D. M., Patel, A. H., Targett-Adams, P. & McLauchlan, J. (2009). The hepatitis C virus NS4B protein can trans-complement viral RNA replication and modulates production of infectious virus. *J Virol* **83**, 2163-2177.

Jopling, C. L., Schutz, S. & Sarnow, P. (2008). Position-dependent function for a tandem microRNA miR-122-binding site located in the hepatitis C virus RNA genome. *Cell Host Microbe* **4**, 77-85.

Jopling, C. L., Yi, M., Lancaster, A. M., Lemon, S. M. & Sarnow, P. (2005). Modulation of hepatitis C virus RNA abundance by a liver-specific MicroRNA. *Science* **309**, 1577-1581.

Kaito, M., Watanabe, S., Tsukiyama-Kohara, K., Yamaguchi, K., Kobayashi, Y., Konishi, M., Yokoi, M., Ishida, S., Suzuki, S. & Kohara, M. (1994). Hepatitis C virus particle detected by immunoelectron microscopic study. *J Gen Virol* **75 (Pt 7)**, 1755-1760.

Kalverda, A. P., Thompson, G. S., Vogel, A., Schroder, M., Bowie, A. G., Khan, A. R. & Homans, S. W. (2009). Poxvirus K7 protein adopts a Bcl-2 fold: biochemical mapping of its interactions with human DEAD box RNA helicase DDX3. *J Mol Biol* **385**, 843-853.

Kanai, Y., Dohmae, N. & Hirokawa, N. (2004). Kinesin transports RNA: isolation and characterization of an RNA-transporting granule. *Neuron* **43**, 513-525.

Kang, J. I., Kwon, Y. C. & Ahn, B. Y. (2012). Modulation of the type I interferon pathways by culture-adaptive hepatitis C virus core mutants. *FEBS Lett* **586**, 1272-1278.

Kang, S. M., Shin, M. J., Kim, J. H. & Oh, J. W. (2005). Proteomic profiling of cellular proteins interacting with the hepatitis C virus core protein. *Proteomics* **5**, 2227-2237.

Kapadia, S. B., Barth, H., Baumert, T., McKeating, J. A. & Chisari, F. V. (2007). Initiation of hepatitis C virus infection is dependent on cholesterol and cooperativity between CD81 and scavenger receptor B type I. *J Virol* **81**, 374-383.

Kaplan, D. E., Sugimoto, K., Newton, K., Valiga, M. E., Ikeda, F., Aytaman, A., Nunes, F. A., Lucey, M. R., Vance, B. A., Vonderheide, R. H., Reddy, K. R., McKeating, J. A. & Chang, K. M. (2007). Discordant role of CD4 T-cell response relative to neutralizing antibody and CD8 T-cell responses in acute hepatitis C. *Gastroenterology* **132**, 654-666.

Kapoor, A., Simmonds, P., Gerold, G., Qaisar, N., Jain, K., Henriquez, J. A., Firth, C., Hirschberg, D. L., Rice, C. M., Shields, S. & Lipkin, W. I. (2011). Characterization of a canine homolog of hepatitis C virus. *Proc Natl Acad Sci U S A* **108**, 11608-11613.

Karlberg, T., Hammarstrom, M., Schutz, P., Svensson, L. & Schuler, H. (2010). Crystal structure of the catalytic domain of human PARP2 in complex with PARP inhibitor ABT-888. *Biochemistry* **49**, 1056-1058.

Kato, J., Kato, N., Yoshida, H., Ono-Nita, S. K., Shiratori, Y. & Omata, M. (2002). Hepatitis C virus NS4A and NS4B proteins suppress translation in vivo. *J Med Virol* **66**, 187-199.

Kato, N., Sekiya, H., Ootsuyama, Y., Nakazawa, T., Hijikata, M., Ohkoshi, S. & Shimotohno, K. (1993). Humoral immune response to hypervariable region 1 of the putative envelope glycoprotein (gp70) of hepatitis C virus. *J Virol* **67**, 3923-3930.

Kato, T., Date, T., Miyamoto, M., Furusaka, A., Tokushige, K., Mizokami, M. & Wakita, T. (2003). Efficient replication of the genotype 2a hepatitis C virus subgenomic replicon. *Gastroenterology* **125**, 1808-1817.

Kato, T., Furusaka, A., Miyamoto, M., Date, T., Yasui, K., Hiramoto, J., Nagayama, K., Tanaka, T. & Wakita, T. (2001). Sequence analysis of hepatitis C virus isolated from a fulminant hepatitis patient. *J Med Virol* **64**, 334-339.

Katze, M. G., Kwieciszewski, B., Goodlett, D. R., Blakely, C. M., Neddermann, P., Tan, S. L. & Aebersold, R. (2000). Ser(2194) is a highly conserved major phosphorylation site of the hepatitis C virus nonstructural protein NS5A. *Virology* **278**, 501-513.

Kaul, A., Stauffer, S., Berger, C., Pertel, T., Schmitt, J., Kallis, S., Zayas, M., Lohmann, V., Luban, J. & Bartenschlager, R. (2009). Essential role of cyclophilin A for hepatitis C virus replication and virus production and possible link to polyprotein cleavage kinetics. *PLoS Pathog* **5**, e1000546.

Kawaguchi, T., Taniguchi, E., Itou, M., Sakata, M., Sumie, S. & Sata, M. (2011). Insulin resistance and chronic liver disease. *World J Hepatol* **3**, 99-107.

Keck, Z., Wang, W., Wang, Y., Lau, P., Carlsen, T. H., Prentoe, J., Xia, J., Patel, A. H., Bukh, J. & Foung, S. K. (2013). Cooperativity in virus neutralization by human monoclonal antibodies to two adjacent regions located at the amino terminus of hepatitis C virus E2 glycoprotein. *Journal of virology* **87**, 37-51.

Kellner-Weibel, G., de La Llera-Moya, M., Connelly, M. A., Stoudt, G., Christian, A. E., Haynes, M. P., Williams, D. L. & Rothblat, G. H. (2000). Expression of scavenger receptor BI in COS-7 cells alters cholesterol content and distribution. *Biochemistry* **39**, 221-229.

Kelly, C., Klenerman, P. & Barnes, E. (2011). Interferon lambdas: the next cytokine storm. *Gut* **60**, 1284-1293.

Kenny-Walsh, E. (1999). Clinical outcomes after hepatitis C infection from contaminated anti-D immune globulin. Irish Hepatology Research Group. *N Engl J Med* **340**, 1228-1233.

Khoo, U. S., Chan, K. Y., Chan, V. S. & Lin, C. L. (2008). DC-SIGN and L-SIGN: the SIGNs for infection. *J Mol Med (Berl)* **86**, 861-874.

Kielian, M. & Rey, F. A. (2006). Virus membrane-fusion proteins: more than one way to make a hairpin. *Nat Rev Microbiol* **4**, 67-76.

Kim, D. H., Longo, M., Han, Y., Lundberg, P., Cantin, E. & Rossi, J. J. (2004). Interferon induction by siRNAs and ssRNAs synthesized by phage polymerase. *Nat Biotechnol* **22**, 321-325.

Kim, J. L., Morgenstern, K. A., Griffith, J. P., Dwyer, M. D., Thomson, J. A., Murcko, M. A., Lin, C. & Caron, P. R. (1998). Hepatitis C virus NS3 RNA helicase domain with a bound oligonucleotide: the crystal structure provides insights into the mode of unwinding. *Structure* **6**, 89-100.

Kim, J. L., Morgenstern, K. A., Lin, C., Fox, T., Dwyer, M. D., Landro, J. A., Chambers, S. P., Markland, W., Lepre, C. A., O'Malley, E. T., Harbeson, S.

L., Rice, C. M., Murcko, M. A., Caron, P. R. & Thomson, J. A. (1996). Crystal structure of the hepatitis C virus NS3 protease domain complexed with a synthetic NS4A cofactor peptide. *Cell* **87**, 343-355.

Kim, Y. K., Kim, C. S., Lee, S. H. & Jang, S. K. (2002). Domains I and II in the 5' nontranslated region of the HCV genome are required for RNA replication. *Biochem Biophys Res Commun* **290**, 105-112.

Kim, Y. S., Lee, S. G., Park, S. H. & Song, K. (2001). Gene structure of the human DDX3 and chromosome mapping of its related sequences. *Mol Cells* **12**, 209-214.

Kitadokoro, K., Bordo, D., Galli, G., Petracca, R., Falugi, F., Abrignani, S., Grandi, G. & Bolognesi, M. (2001). CD81 extracellular domain 3D structure: insight into the tetraspanin superfamily structural motifs. *Embo J* **20**, 12-18.

Klenerman, P. & Thimme, R. (2012). T cell responses in hepatitis C: the good, the bad and the unconventional. *Gut* **61**, 1226-1234.

Kok, K. H., Ng, M. H., Ching, Y. P. & Jin, D. Y. (2007). Human TRBP and PACT directly interact with each other and associate with dicer to facilitate the production of small interfering RNA. *J Biol Chem* **282**, 17649-17657.

Kolykhalov, A. A., Agapov, E. V., Blight, K. J., Mihalik, K., Feinstone, S. M. & Rice, C. M. (1997). Transmission of hepatitis C by intrahepatic inoculation with transcribed RNA. *Science* **277**, 570-574.

Kolykhalov, A. A., Feinstone, S. M. & Rice, C. M. (1996). Identification of a highly conserved sequence element at the 3' terminus of hepatitis C virus genome RNA. *J Virol* **70**, 3363-3371.

Koppel, E. A., van Gisbergen, K. P., Geijtenbeek, T. B. & van Kooyk, Y. (2005). Distinct functions of DC-SIGN and its homologues L-SIGN (DC-SIGNR) and mSIGNR1 in pathogen recognition and immune regulation. *Cell Microbiol* **7**, 157-165.

Kou, Y. H., Chou, S. M., Wang, Y. M., Chang, Y. T., Huang, S. Y., Jung, M. Y., Huang, Y. H., Chen, M. R., Chang, M. F. & Chang, S. C. (2006). Hepatitis C virus NS4A inhibits cap-dependent and the viral IRES-mediated translation through interacting with eukaryotic elongation factor 1A. *J Biomed Sci* **13**, 861-874.

Koutsoudakis, G., Herrmann, E., Kallis, S., Bartenschlager, R. & Pietschmann, T. (2007). The level of CD81 cell surface expression is a key determinant for productive entry of hepatitis C virus into host cells. *J Virol* **81**, 588-598.

Kovalev, N., Pogany, J. & Nagy, P. D. (2012). A Co-Opted DEAD-Box RNA helicase enhances tombusvirus plus-strand synthesis. *PLoS Pathog* **8**, e1002537.

Koziel, M. J. (1997). The role of immune responses in the pathogenesis of hepatitis C virus infection. *J Viral Hepat* **4 Suppl 2**, 31-41.

Kremsdorf, D. & Brezillon, N. (2007). New animal models for hepatitis C viral infection and pathogenesis studies. *World J Gastroenterol* **13**, 2427-2435.

Krey, T., d'Alayer, J., Kikuti, C. M., Saulnier, A., Damier-Piolle, L., Petitpas, I., Johansson, D. X., Tawar, R. G., Baron, B., Robert, B., England, P., Persson, M. A., Martin, A. & Rey, F. A. (2010). The disulfide bonds in glycoprotein E2 of hepatitis C virus reveal the tertiary organization of the molecule. *PLoS Pathog* **6**, e1000762.

Krieger, M. (2001). Scavenger receptor class B type I is a multiligand HDL receptor that influences diverse physiologic systems. *J Clin Invest* **108**, 793-797.

Krieger, N., Lohmann, V. & Bartenschlager, R. (2001). Enhancement of hepatitis C virus RNA replication by cell culture-adaptive mutations. *J Virol* **75**, 4614-4624.

Krieger, S. E., Zeisel, M. B., Davis, C., Thumann, C., Harris, H. J., Schnober, E. K., Mee, C., Soulier, E., Royer, C., Lambotin, M., Grunert, F., Dao Thi, V. L., Dreux, M., Cosset, F. L., McKeating, J. A., Schuster, C. & Baumert, T. F. (2010). Inhibition of hepatitis C virus infection by anti-claudin-1 antibodies is mediated by neutralization of E2-CD81-claudin-1 associations. *Hepatology* **51**, 1144-1157.

Krishnan, V. & Zeichner, S. L. (2004). Alterations in the expression of DEAD-box and other RNA binding proteins during HIV-1 replication. *Retrovirology* **1**, 42.

Kuiken, C. & Simmonds, P. (2009). Nomenclature and numbering of the hepatitis C virus. *Methods Mol Biol* **510**, 33-53.

Kuo, G., Choo, Q. L., Alter, H. J., Gitnick, G. L., Redeker, A. G., Purcell, R. H., Miyamura, T., Dienstag, J. L., Alter, M. J., Stevens, C. E. & et al. (1989). An assay for circulating antibodies to a major etiologic virus of human non-A, non-B hepatitis. *Science* **244**, 362-364.

Kushima, Y., Wakita, T. & Hijikata, M. (2010). A disulfide-bonded dimer of the core protein of hepatitis C virus is important for virus-like particle production. *J Virol* **84**, 9118-9127.

Lackmann, M. & Boyd, A. W. (2008). Eph, a protein family coming of age: more confusion, insight, or complexity? *Sci Signal* **1**, re2.

Lahn, B. T. & Page, D. C. (1997). Functional coherence of the human Y chromosome. *Science* **278**, 675-680.

Lai, M. C., Chang, W. C., Shieh, S. Y. & Tarn, W. Y. (2010). DDX3 regulates cell growth through translational control of cyclin E1. *Mol Cell Biol* **30**, 5444-5453.

Lai, M. C., Lee, Y. H. & Tarn, W. Y. (2008). The DEAD-box RNA helicase DDX3 associates with export messenger ribonucleoproteins as well as tip-associated protein and participates in translational control. *Mol Biol Cell* **19**, 3847-3858.

Lai, W. K., Sun, P. J., Zhang, J., Jennings, A., Lalor, P. F., Hubscher, S., McKeating, J. A. & Adams, D. H. (2006). Expression of DC-SIGN and DC-SIGNR on human sinusoidal endothelium: a role for capturing hepatitis C virus particles. *Am J Pathol* **169**, 200-208.

Lau, J. Y., Tam, R. C., Liang, T. J. & Hong, Z. (2002). Mechanism of action of ribavirin in the combination treatment of chronic HCV infection. *Hepatology* **35**, 1002-1009.

Lavanchy, D. (1999). Hepatitis C: public health strategies. *J Hepatol* **31 Suppl 1**, 146-151.

Lavie, M., Goffard, A. & Dubuisson, J. (2007). Assembly of a functional HCV glycoprotein heterodimer. *Curr Issues Mol Biol* **9**, 71-86.

Lavie, M., Voisset, C., Vu-Dac, N., Zurawski, V., Duverlie, G., Wychowski, C. & Dubuisson, J. (2006). Serum amyloid A has antiviral activity against hepatitis C virus by inhibiting virus entry in a cell culture system. *Hepatology* **44**, 1626-1634.

Lavillette, D., Bartosch, B., Nourrisson, D., Verney, G., Cosset, F. L., Penin, F. & Pecheur, E. I. (2006). Hepatitis C virus glycoproteins mediate low pH-dependent membrane fusion with liposomes. *J Biol Chem* **281**, 3909-3917.

Lavillette, D., Tarr, A. W., Voisset, C., Donot, P., Bartosch, B., Bain, C., Patel, A. H., Dubuisson, J., Ball, J. K. & Cosset, F. L. (2005). Characterization of host-range and cell entry properties of the major genotypes and subtypes of hepatitis C virus. *Hepatology* **41**, 265-274.

Lee, C. S., Dias, A. P., Jedrychowski, M., Patel, A. H., Hsu, J. L. & Reed, R. (2008). Human DDX3 functions in translation and interacts with the translation initiation factor eIF3. *Nucleic Acids Res* **36**, 4708-4718.

Lemay, K. L., Treadaway, J., Angulo, I. & Tellinghuisen, T. L. (2013). A hepatitis C virus NS5A phosphorylation site that regulates RNA replication. *J Virol* **87**, 1255-1260.

Leroy, P., Alzari, P., Sassoon, D., Wolgemuth, D. & Fellous, M. (1989). The protein encoded by a murine male germ cell-specific transcript is a putative ATP-dependent RNA helicase. *Cell* **57**, 549-559.

Lesburg, C. A., Cable, M. B., Ferrari, E., Hong, Z., Mannarino, A. F. & Weber, P. C. (1999). Crystal structure of the RNA-dependent RNA polymerase from hepatitis C virus reveals a fully encircled active site. *Nat Struct Biol* **6**, 937-943.

Levy, S. & Shoham, T. (2005). The tetraspanin web modulates immune-signalling complexes. *Nat Rev Immunol* **5**, 136-148.

Li, K., Foy, E., Ferreon, J. C., Nakamura, M., Ferreon, A. C., Ikeda, M., Ray, S. C., Gale, M., Jr. & Lemon, S. M. (2005). Immune evasion by hepatitis C virus NS3/4A protease-mediated cleavage of the Toll-like receptor 3 adaptor protein TRIF. *Proc Natl Acad Sci U S A* **102**, 2992-2997.

Li, Y., Masaki, T., Yamane, D., McGivern, D. R. & Lemon, S. M. (2013a). Competing and noncompeting activities of miR-122 and the 5' exonuclease Xrn1 in regulation of hepatitis C virus replication. *Proc Natl Acad Sci U S A* **110**, 1881-1886.

Li, Q., Pène, V., Krishnamurthy, S., Cha. H., Liang, T.J. (2013b). Hepatitis C virus infection activates an innate pathway involving IKK-α in lipogenesis and viral assembly. *Nat Med* **19,** 722-729.

Li, Y. P., Ramirez, S., Gottwein, J. M., Scheel, T. K., Mikkelsen, L., Purcell, R. H. & Bukh, J. (2012a). Robust full-length hepatitis C virus genotype 2a and 2b infectious cultures using mutations identified by a systematic approach applicable to patient strains. *Proc Natl Acad Sci U S A* **109**, E1101-1110.

Li, Y. P., Ramirez, S., Jensen, S. B., Purcell, R. H., Gottwein, J. M. & Bukh, J. (2012b). Highly efficient full-length hepatitis C virus genotype 1 (strain TN) infectious culture system. *Proc Natl Acad Sci U S A* **109**, 19757-19762.

Liang, Y., Ye, H., Kang, C. B. & Yoon, H. S. (2007). Domain 2 of nonstructural protein 5A (NS5A) of hepatitis C virus is natively unfolded. *Biochemistry* **46**, 11550-11558.

Lim, P. J., Chatterji, U., Cordek, D., Sharma, S. D., Garcia-Rivera, J. A., Cameron, C. E., Lin, K., Targett-Adams, P. & Gallay, P. A. (2012). Correlation between NS5A dimerization and hepatitis C virus replication. *J Biol Chem* **287**, 30861-30873.

Lin, C., Lindenbach, B. D., Pragai, B. M., McCourt, D. W. & Rice, C. M. (1994a). Processing in the hepatitis C virus E2-NS2 region: identification of p7 and two distinct E2-specific products with different C termini. *J Virol* **68**, 5063-5073.

Lin, C., Pragai, B. M., Grakoui, A., Xu, J. & Rice, C. M. (1994b). Hepatitis C virus NS3 serine proteinase: trans-cleavage requirements and processing kinetics. *J Virol* **68**, 8147-8157.

Lin, C., Thomson, J. A. & Rice, C. M. (1995). A central region in the hepatitis C virus NS4A protein allows formation of an active NS3-NS4A serine proteinase complex in vivo and in vitro. *J Virol* **69**, 4373-4380.

Lindenbach, B. D., Evans, M. J., Syder, A. J., Wolk, B., Tellinghuisen, T. L., Liu, C. C., Maruyama, T., Hynes, R. O., Burton, D. R., McKeating, J. A. & Rice,

C. M. (2005). Complete replication of hepatitis C virus in cell culture. *Science* **309**, 623-626.

Lindenbach, B. D., Meuleman, P., Ploss, A., Vanwolleghem, T., Syder, A. J., McKeating, J. A., Lanford, R. E., Feinstone, S. M., Major, M. E., Leroux-Roels, G. & Rice, C. M. (2006). Cell culture-grown hepatitis C virus is infectious in vivo and can be recultured in vitro. *Proc Natl Acad Sci U S A* **103**, 3805-3809.

Lindenbach, B. D., Pragai, B. M., Montserret, R., Beran, R. K., Pyle, A. M., Penin, F. & Rice, C. M. (2007). The C terminus of hepatitis C virus NS4A encodes an electrostatic switch that regulates NS5A hyperphosphorylation and viral replication. *J Virol* **81**, 8905-8918.

Linder, P. & Jankowsky, E. (2011). From unwinding to clamping - the DEAD box RNA helicase family. *Nat Rev Mol Cell Biol* **12**, 505-516.

Lindstrom, H., Lundin, M., Haggstrom, S. & Persson, M. A. (2006). Mutations of the Hepatitis C virus protein NS4B on either side of the ER membrane affect the efficiency of subgenomic replicons. *Virus Res* **121**, 169-178.

Linnen, J., Wages, J., Jr., Zhang-Keck, Z. Y., Fry, K. E., Krawczynski, K. Z., Alter, H., Koonin, E., Gallagher, M., Alter, M., Hadziyannis, S., Karayiannis, P., Fung, K., Nakatsuji, Y., Shih, J. W., Young, L., Piatak, M., Jr., Hoover, C., Fernandez, J., Chen, S., Zou, J. C., Morris, T., Hyams, K. C., Ismay, S., Lifson, J. D., Hess, G., Foung, S. K., Thomas, H., Bradley, D., Margolis, H. & Kim, J. P. (1996). Molecular cloning and disease association of hepatitis G virus: a transfusion-transmissible agent. *Science* **271**, 505-508.

Liu, J., Henao-Mejia, J., Liu, H., Zhao, Y. & He, J. J. (2011). Translational regulation of HIV-1 replication by HIV-1 Rev cellular cofactors Sam68, eIF5A, hRIP, and DDX3. *J Neuroimmune Pharmacol* **6**, 308-321.

Liu, S., Yang, W., Shen, L., Turner, J. R., Coyne, C. B. & Wang, T. (2009). Tight junction proteins claudin-1 and occludin control hepatitis C virus entry and are downregulated during infection to prevent superinfection. *J Virol* **83**, 2011-2014.

Lohmann, V., Hoffmann, S., Herian, U., Penin, F. & Bartenschlager, R. (2003). Viral and cellular determinants of hepatitis C virus RNA replication in cell culture. *J Virol* **77**, 3007-3019.

Lohmann, V., Korner, F., Dobierzewska, A. & Bartenschlager, R. (2001). Mutations in hepatitis C virus RNAs conferring cell culture adaptation. *J Virol* **75**, 1437-1449.

Lohmann, V., Korner, F., Koch, J., Herian, U., Theilmann, L. & Bartenschlager, R. (1999). Replication of subgenomic hepatitis C virus RNAs in a hepatoma cell line. *Science* **285**, 110-113.

Lorenz, I. C. (2010). The Hepatitis C Virus Nonstructural Protein 2 (NS2): An Up-and-Coming Antiviral Drug Target. *Viruses* **2**, 1635-1646.

Lorenz, I. C., Marcotrigiano, J., Dentzer, T. G. & Rice, C. M. (2006). Structure of the catalytic domain of the hepatitis C virus NS2-3 protease. *Nature* **442**, 831-835.

Love, R. A., Brodsky, O., Hickey, M. J., Wells, P. A. & Cronin, C. N. (2009). Crystal structure of a novel dimeric form of NS5A domain I protein from hepatitis C virus. *J Virol* **83**, 4395-4403.

Lozach, P. Y., Amara, A., Bartosch, B., Virelizier, J. L., Arenzana-Seisdedos, F., Cosset, F. L. & Altmeyer, R. (2004). C-type lectins L-SIGN and DC-SIGN

capture and transmit infectious hepatitis C virus pseudotype particles. *J Biol Chem* **279**, 32035-32045.

Lozach, P. Y., Lortat-Jacob, H., de Lacroix de Lavalette, A., Staropoli, I., Foung, S., Amara, A., Houles, C., Fieschi, F., Schwartz, O., Virelizier, J. L., Arenzana-Seisdedos, F. & Altmeyer, R. (2003). DC-SIGN and L-SIGN are high affinity binding receptors for hepatitis C virus glycoprotein E2. *J Biol Chem* **278**, 20358-20366.

Ludwig, I. S., Lekkerkerker, A. N., Depla, E., Bosman, F., Musters, R. J., Depraetere, S., van Kooyk, Y. & Geijtenbeek, T. B. (2004). Hepatitis C virus targets DC-SIGN and L-SIGN to escape lysosomal degradation. *J Virol* **78**, 8322-8332.

Luik, P., Chew, C., Aittoniemi, J., Chang, J., Wentworth, P., Jr., Dwek, R. A., Biggin, P. C., Venien-Bryan, C. & Zitzmann, N. (2009). The 3-dimensional structure of a hepatitis C virus p7 ion channel by electron microscopy. *Proc Natl Acad Sci U S A* **106**, 12712-12716.

Lundin, M., Lindstrom, H., Gronwall, C. & Persson, M. A. (2006). Dual topology of the processed hepatitis C virus protein NS4B is influenced by the NS5A protein. *J Gen Virol* **87**, 3263-3272.

Lundin, M., Monne, M., Widell, A., Von Heijne, G. & Persson, M. A. (2003). Topology of the membrane-associated hepatitis C virus protein NS4B. *J Virol* **77**, 5428-5438.

Lupberger, J., Zeisel, M. B., Xiao, F., Thumann, C., Fofana, I., Zona, L., Davis, C., Mee, C. J., Turek, M., Gorke, S., Royer, C., Fischer, B., Zahid, M. N., Lavillette, D., Fresquet, J., Cosset, F. L., Rothenberg, S. M., Pietschmann, T., Patel, A. H., Pessaux, P., Doffoel, M., Raffelsberger, W., Poch, O., McKeating, J. A., Brino, L. & Baumert, T. F. (2011). EGFR and EphA2 are host factors for hepatitis C virus entry and possible targets for antiviral therapy. *Nat Med* **17**, 589-595.

Ma, Y., Anantpadma, M., Timpe, J. M., Shanmugam, S., Singh, S. M., Lemon, S. M. & Yi, M. (2011). Hepatitis C virus NS2 protein serves as a scaffold for virus assembly by interacting with both structural and nonstructural proteins. *J Virol* **85**, 86-97.

Ma, Y., Yates, J., Liang, Y., Lemon, S. M. & Yi, M. (2008). NS3 helicase domains involved in infectious intracellular hepatitis C virus particle assembly. *J Virol* **82**, 7624-7639.

Maag, D., Castro, C., Hong, Z. & Cameron, C. E. (2001). Hepatitis C virus RNA-dependent RNA polymerase (NS5B) as a mediator of the antiviral activity of ribavirin. *J Biol Chem* **276**, 46094-46098.

Macdonald, A., Chan, J. K. & Harris, M. (2005). Perturbation of epidermal growth factor receptor complex formation and Ras signalling in cells harbouring the hepatitis C virus subgenomic replicon. *J Gen Virol* **86**, 1027-1033.

Macdonald, A., Crowder, K., Street, A., McCormick, C., Saksela, K. & Harris, M. (2003). The hepatitis C virus non-structural NS5A protein inhibits activating protein-1 function by perturbing ras-ERK pathway signaling. *J Biol Chem* **278**, 17775-17784.

Macdonald, A. & Harris, M. (2004). Hepatitis C virus NS5A: tales of a promiscuous protein. *J Gen Virol* **85**, 2485-2502.

Machlin, E. S., Sarnow, P. & Sagan, S. M. (2012). Combating hepatitis C virus by targeting microRNA-122 using locked nucleic acids. *Curr Gene Ther* **12**, 301-306.

Maga, G., Falchi, F., Garbelli, A., Belfiore, A., Witvrouw, M., Manetti, F. & Botta, M. (2008). Pharmacophore modeling and molecular docking led to the discovery of inhibitors of human immunodeficiency virus-1 replication targeting the human cellular aspartic acid-glutamic acid-alanine-aspartic acid box polypeptide 3. *J Med Chem* **51**, 6635-6638.

Maillard, P., Huby, T., Andreo, U., Moreau, M., Chapman, J. & Budkowska, A. (2006). The interaction of natural hepatitis C virus with human scavenger receptor SR-BI/Cla1 is mediated by ApoB-containing lipoproteins. *Faseb J* **20**, 735-737.

Malathi, K., Dong, B., Gale, M. Jr, Silverman, R.H. (2007). Small self-RNA generated by RNase L amplifies antiviral innate immunity. *Nature* **448,** 816-819.

Mamiya, N. & Worman, H. J. (1999). Hepatitis C virus core protein binds to a DEAD box RNA helicase. *J Biol Chem* **274**, 15751-15756.

Mandl, C. W., Kroschewski, H., Allison, S. L., Kofler, R., Holzmann, H., Meixner, T. & Heinz, F. X. (2001). Adaptation of tick-borne encephalitis virus to BHK-21 cells results in the formation of multiple heparan sulfate binding sites in the envelope protein and attenuation in vivo. *J Virol* **75**, 5627-5637.

Martell, M., Esteban, J. I., Quer, J., Genesca, J., Weiner, A., Esteban, R., Guardia, J. & Gomez, J. (1992). Hepatitis C virus (HCV) circulates as a population of different but closely related genomes: quasispecies nature of HCV genome distribution. *J Virol* **66**, 3225-3229.

Martinez-Sierra, C., Arizcorreta, A., Diaz, F., Roldan, R., Martin-Herrera, L., Perez-Guzman, E. & Giron-Gonzalez, J. A. (2003). Progression of chronic hepatitis C to liver fibrosis and cirrhosis in patients coinfected with hepatitis C virus and human immunodeficiency virus. *Clin Infect Dis* **36**, 491-498.

Marukian, S., Andrus, L., Sheahan, T. P., Jones, C. T., Charles, E. D., Ploss, A., Rice, C. M. & Dustin, L. B. (2011). Hepatitis C virus induces interferon-lambda and interferon-stimulated genes in primary liver cultures. *Hepatology* **54**, 1913-1923.

Masaki, T., Suzuki, R., Murakami, K., Aizaki, H., Ishii, K., Murayama, A., Date, T., Matsuura, Y., Miyamura, T., Wakita, T. & Suzuki, T. (2008). Interaction of hepatitis C virus nonstructural protein 5A with core protein is critical for the production of infectious virus particles. *J Virol* **82**, 7964-7976.

Matsumoto, M., Hwang, S. B., Jeng, K. S., Zhu, N. & Lai, M. M. (1996). Homotypic interaction and multimerization of hepatitis C virus core protein. *Virology* **218**, 43-51.

McCaffrey, K., Boo, I., Tewierek, K., Edmunds, M. L., Poumbourios, P. & Drummer, H. E. (2012). Role of conserved cysteine residues in hepatitis C virus glycoprotein e2 folding and function. *J Virol* **86**, 3961-3974.

McCaffrey, K., Gouklani, H., Boo, I., Poumbourios, P. & Drummer, H. E. (2011). The variable regions of hepatitis C virus glycoprotein E2 have an essential structural role in glycoprotein assembly and virion infectivity. *J Gen Virol* **92**, 112-121.

McGuinness, P. H., Bishop, G. A., Painter, D. M., Chan, R. & McCaughan, G. W. (1996). Intrahepatic hepatitis C RNA levels do not correlate with degree of liver injury in patients with chronic hepatitis C. *Hepatology* **23**, 676-687.

McLauchlan, J. (2000). Properties of the hepatitis C virus core protein: a structural protein that modulates cellular processes. *J Viral Hepat* **7**, 2-14.

McLauchlan, J. (2009). Hepatitis C virus: viral proteins on the move. *Biochem Soc Trans* **37**, 986-990.

McLauchlan, J., Lemberg, M. K., Hope, G. & Martoglio, B. (2002). Intramembrane proteolysis promotes trafficking of hepatitis C virus core protein to lipid droplets. *Embo J* **21**, 3980-3988.

McManus, M. T. & Sharp, P. A. (2002). Gene silencing in mammals by small interfering RNAs. *Nature reviews* **3**, 737-747.

McMullan, L. K., Grakoui, A., Evans, M. J., Mihalik, K., Puig, M., Branch, A. D., Feinstone, S. M. & Rice, C. M. (2007). Evidence for a functional RNA element in the hepatitis C virus core gene. *Proc Natl Acad Sci U S A* **104**, 2879-2884.

Meertens, L., Bertaux, C., Cukierman, L., Cormier, E., Lavillette, D., Cosset, F. L. & Dragic, T. (2008). The tight junction proteins claudin-1, -6, and -9 are entry cofactors for hepatitis C virus. *J Virol* **82**, 3555-3560.

Mehta, S. H., Cox, A., Hoover, D. R., Wang, X. H., Mao, Q., Ray, S., Strathdee, S. A., Vlahov, D. & Thomas, D. L. (2002). Protection against persistence of hepatitis C. *Lancet* **359**, 1478-1483.

Meister, G. & Tuschl, T. (2004). Mechanisms of gene silencing by double-stranded RNA. *Nature* **431**, 343-349.

Melen, K., Fagerlund, R., Nyqvist, M., Keskinen, P. & Julkunen, I. (2004). Expression of hepatitis C virus core protein inhibits interferon-induced nuclear import of STATs. *J Med Virol* **73**, 536-547.

Mercer, D. F., Schiller, D. E., Elliott, J. F., Douglas, D. N., Hao, C., Rinfret, A., Addison, W. R., Fischer, K. P., Churchill, T. A., Lakey, J. R., Tyrrell, D. L. & Kneteman, N. M. (2001). Hepatitis C virus replication in mice with chimeric human livers. *Nat Med* **7**, 927-933.

Meredith, L. W., Wilson, G. K., Fletcher, N. F. & McKeating, J. A. (2012). Hepatitis C virus entry: beyond receptors. *Rev Med Virol* **22**, 182-193.

Merz, A., Long, G., Hiet, M. S., Brugger, B., Chlanda, P., Andre, P., Wieland, F., Krijnse-Locker, J. & Bartenschlager, R. (2011). Biochemical and morphological properties of hepatitis C virus particles and determination of their lipidome. *J Biol Chem* **286**, 3018-3032.

Merz, C., Urlaub, H., Will, C. L. & Luhrmann, R. (2007). Protein composition of human mRNPs spliced in vitro and differential requirements for mRNP protein recruitment. *Rna* **13**, 116-128.

Meuleman, P. & Leroux-Roels, G. (2008). The human liver-uPA-SCID mouse: a model for the evaluation of antiviral compounds against HBV and HCV. *Antiviral Res* **80**, 231-238.

Meuleman, P., Libbrecht, L., De Vos, R., de Hemptinne, B., Gevaert, K., Vandekerckhove, J., Roskams, T. & Leroux-Roels, G. (2005). Morphological and biochemical characterization of a human liver in a uPA-SCID mouse chimera. *Hepatology* **41**, 847-856.

Meunier, J. C., Russell, R. S., Engle, R. E., Faulk, K. N., Purcell, R. H. & Emerson, S. U. (2008a). Apolipoprotein c1 association with hepatitis C virus. *J Virol* **82**, 9647-9656.

Meunier, J. C., Russell, R. S., Goossens, V., Priem, S., Walter, H., Depla, E., Union, A., Faulk, K. N., Bukh, J., Emerson, S. U. & Purcell, R. H. (2008b). Isolation and characterization of broadly neutralizing human monoclonal antibodies to the e1 glycoprotein of hepatitis C virus. *J Virol* **82**, 966-973.

Meylan, E., Curran, J., Hofmann, K., Moradpour, D., Binder, M., Bartenschlager, R. & Tschopp, J. (2005). Cardif is an adaptor protein in the RIG-I antiviral pathway and is targeted by hepatitis C virus. *Nature* **437**, 1167-1172.

Miao, X., Yang, Z. L., Xiong, L., Zou, Q., Yuan, Y., Li, J., Liang, L., Chen, M. & Chen, S. (2013). Nectin-2 and DDX3 are biomarkers for metastasis and poor prognosis of squamous cell/adenosquamous carcinomas and adenocarcinoma of gallbladder. *Int J Clin Exp Pathol* **6**, 179-190.

Michalak, J. P., Wychowski, C., Choukhi, A., Meunier, J. C., Ung, S., Rice, C. M. & Dubuisson, J. (1997). Characterization of truncated forms of hepatitis C virus glycoproteins. *J Gen Virol* **78 (Pt 9)**, 2299-2306.

Miller, R. H. & Purcell, R. H. (1990). Hepatitis C virus shares amino acid sequence similarity with pestiviruses and flaviviruses as well as members of two plant virus supergroups. *Proc Natl Acad Sci U S A* **87**, 2057-2061.

Miyamura, T. & Matsuura, Y. (1993). Structural proteins of hepatitis C virus. *Trends Microbiol* **1**, 229-231.

Miyanari, Y., Atsuzawa, K., Usuda, N., Watashi, K., Hishiki, T., Zayas, M., Bartenschlager, R., Wakita, T., Hijikata, M. & Shimotohno, K. (2007). The lipid droplet is an important organelle for hepatitis C virus production. *Nat Cell Biol* **9**, 1089-1097.

Molina, S., Castet, V., Fournier-Wirth, C., Pichard-Garcia, L., Avner, R., Harats, D., Roitelman, J., Barbaras, R., Graber, P., Ghersa, P., Smolarsky, M., Funaro, A., Malavasi, F., Larrey, D., Coste, J., Fabre, J. M., Sa-Cunha, A. & Maurel, P. (2007). The low-density lipoprotein receptor plays a role in the infection of primary human hepatocytes by hepatitis C virus. *J Hepatol* **46**, 411-419.

Mondelli, M. U., Cerino, A., Meola, A. & Nicosia, A. (2003). Variability or conservation of hepatitis C virus hypervariable region 1? Implications for immune responses. *J Biosci* **28**, 305-310.

Montserret, R., Saint, N., Vanbelle, C., Salvay, A. G., Simorre, J. P., Ebel, C., Sapay, N., Renisio, J. G., Bockmann, A., Steinmann, E., Pietschmann, T., Dubuisson, J., Chipot, C. & Penin, F. (2010). NMR structure and ion channel activity of the p7 protein from hepatitis C virus. *J Biol Chem* **285**, 31446-31461.

Moradpour, D., Brass, V., Bieck, E., Friebe, P., Gosert, R., Blum, H. E., Bartenschlager, R., Penin, F. & Lohmann, V. (2004). Membrane association of the RNA-dependent RNA polymerase is essential for hepatitis C virus RNA replication. *J Virol* **78**, 13278-13284.

Moradpour, D., Englert, C., Wakita, T. & Wands, J. R. (1996). Characterization of cell lines allowing tightly regulated expression of hepatitis C virus core protein. *Virology* **222**, 51-63.

Mori, K., Abe, K., Dansako, H., Ariumi, Y., Ikeda, M. & Kato, N. (2008). New efficient replication system with hepatitis C virus genome derived from a patient with acute hepatitis C. *Biochem Biophys Res Commun* **371**, 104-109.

Morikawa, K., Zhao, Z., Date, T., Miyamoto, M., Murayama, A., Akazawa, D., Tanabe, J., Sone, S. & Wakita, T. (2007). The roles of CD81 and glycosaminoglycans in the adsorption and uptake of infectious HCV particles. *J Med Virol* **79**, 714-723.

Moriya, K., Yotsuyanagi, H., Shintani, Y., Fujie, H., Ishibashi, K., Matsuura, Y., Miyamura, T. & Koike, K. (1997). Hepatitis C virus core protein induces hepatic steatosis in transgenic mice. *J Gen Virol* **78 (Pt 7)**, 1527-1531.

Mosley, R. T., Edwards, T. E., Murakami, E., Lam, A. M., Grice, R. L., Du, J., Sofia, M. J., Furman, P. A. & Otto, M. J. (2012). Structure of hepatitis C virus polymerase in complex with primer-template RNA. *J Virol* **86**, 6503-6511.

Moucari, R., Asselah, T., Cazals-Hatem, D., Voitot, H., Boyer, N., Ripault, M. P., Sobesky, R., Martinot-Peignoux, M., Maylin, S., Nicolas-Chanoine, M. H., Paradis, V., Vidaud, M., Valla, D., Bedossa, P. & Marcellin, P. (2008). Insulin resistance in chronic hepatitis C: association with genotypes 1 and 4, serum HCV RNA level, and liver fibrosis. *Gastroenterology* **134**, 416-423.

Mousseau, G., Kota, S., Takahashi, V., Frick, D.N., Strosberg, A.D. (2011). Dimerization-driven interaction of hepatitis C virus core protein with NS3 helicase. *J Gen Virol* **92,** 101-111.

Murchison, E. P., Partridge, J. F., Tam, O. H., Cheloufi, S. & Hannon, G. J. (2005). Characterization of Dicer-deficient murine embryonic stem cells. *Proc Natl Acad Sci U S A* **102**, 12135-12140.

Murray, C. L., Jones, C. T. & Rice, C. M. (2008). Architects of assembly: roles of Flaviviridae non-structural proteins in virion morphogenesis. *Nat Rev Microbiol* **6**, 699-708.

Murray, C. L., Jones, C. T., Tassello, J. & Rice, C. M. (2007). Alanine scanning of the hepatitis C virus core protein reveals numerous residues essential for production of infectious virus. *J Virol* **81**, 10220-10231.

Murray, C. L. & Rice, C. M. (2011). Turning hepatitis C into a real virus. *Annu Rev Microbiol* **65**, 307-327.

Namba, K., Naka, K., Dansako, H., Nozaki, A., Ikeda, M., Shiratori, Y., Shimotohno, K. & Kato, N. (2004). Establishment of hepatitis C virus replicon cell lines possessing interferon-resistant phenotype. *Biochem Biophys Res Commun* **323**, 299-309.

Narbus, C. M., Israelow, B., Sourisseau, M., Michta, M. L., Hopcraft, S. E., Zeiner, G. M. & Evans, M. J. (2011). HepG2 cells expressing microRNA miR-122 support the entire hepatitis C virus life cycle. *J Virol* **85**, 12087-12092.

Neddermann, P., Quintavalle, M., Di Pietro, C., Clementi, A., Cerretani, M., Altamura, S., Bartholomew, L. & De Francesco, R. (2004). Reduction of hepatitis C virus NS5A hyperphosphorylation by selective inhibition of cellular kinases activates viral RNA replication in cell culture. *J Virol* **78**, 13306-13314.

Neumann-Haefelin, C., Blum, H. E., Chisari, F. V. & Thimme, R. (2005). T cell response in hepatitis C virus infection. *J Clin Virol* **32**, 75-85.

Neumann, A. U., Lam, N. P., Dahari, H., Gretch, D. R., Wiley, T. E., Layden, T. J. & Perelson, A. S. (1998). Hepatitis C viral dynamics in vivo and the antiviral efficacy of interferon-alpha therapy. *Science* **282**, 103-107.

Neveu, G., Barouch-Bentov, R., Ziv-Av, A., Gerber, D., Jacob, Y. & Einav, S. (2012). Identification and targeting of an interaction between a tyrosine motif within hepatitis C virus core protein and AP2M1 essential for viral assembly. *PLoS Pathog* **8**, e1002845.

Nguyen, M. H. & Keeffe, E. B. (2005). Prevalence and treatment of hepatitis C virus genotypes 4, 5, and 6. *Clin Gastroenterol Hepatol* **3**, S97-S101.

Nielsen, S. U., Bassendine, M. F., Burt, A. D., Martin, C., Pumeechockchai, W. & Toms, G. L. (2006). Association between hepatitis C virus and very-low-density lipoprotein (VLDL)/LDL analyzed in iodixanol density gradients. *J Virol* **80**, 2418-2428.

Novak, J. E. & Kirkegaard, K. (1994). Coupling between genome translation and replication in an RNA virus. *Genes Dev* **8**, 1726-1737.

Oda, S., Schroder, M. & Khan, A. R. (2009). Structural basis for targeting of human RNA helicase DDX3 by poxvirus protein K7. *Structure* **17**, 1528-1537.

Okamoto, T., Nishimura, Y., Ichimura, T., Suzuki, K., Miyamura, T., Suzuki, T., Moriishi, K. & Matsuura, Y. (2006). Hepatitis C virus RNA replication is regulated by FKBP8 and Hsp90. *Embo J* **25**, 5015-5025.

Op De Beeck, A., Cocquerel, L. & Dubuisson, J. (2001). Biogenesis of hepatitis C virus envelope glycoproteins. *J Gen Virol* **82**, 2589-2595.

Op De Beeck, A., Voisset, C., Bartosch, B., Ciczora, Y., Cocquerel, L., Keck, Z., Foung, S., Cosset, F. L. & Dubuisson, J. (2004). Characterization of functional hepatitis C virus envelope glycoproteins. *J Virol* **78**, 2994-3002.

Oshiumi, H., Ikeda, M., Matsumoto, M., Watanabe, A., Takeuchi, O., Akira, S., Kato, N., Shimotohno, K. & Seya, T. (2010a). Hepatitis C virus core protein abrogates the DDX3 function that enhances IPS-1-mediated IFN-beta induction. *PLoS One* **5**, e14258.

Oshiumi, H., Sakai, K., Matsumoto, M. & Seya, T. (2010b). DEAD/H BOX 3 (DDX3) helicase binds the RIG-I adaptor IPS-1 to up-regulate IFN-beta-inducing potential. *Eur J Immunol* **40**, 940-948.

Osterlund, P. I., Pietila, T. E., Veckman, V., Kotenko, S. V. & Julkunen, I. (2007). IFN regulatory factor family members differentially regulate the expression of type III IFN (IFN-lambda) genes. *J Immunol* **179**, 3434-3442.

Owen, D. M., Huang, H., Ye, J. & Gale, M., Jr. (2009). Apolipoprotein E on hepatitis C virion facilitates infection through interaction with low-density lipoprotein receptor. *Virology* **394**, 99-108.

Owsianka, A., Tarr, A. W., Juttla, V. S., Lavillette, D., Bartosch, B., Cosset, F. L., Ball, J. K. & Patel, A. H. (2005). Monoclonal antibody AP33 defines a broadly neutralizing epitope on the hepatitis C virus E2 envelope glycoprotein. *J Virol* **79**, 11095-11104.

Owsianka, A. M. & Patel, A. H. (1999). Hepatitis C virus core protein interacts with a human DEAD box protein DDX3. *Virology* **257**, 330-340.

Owsianka, A. M., Timms, J. M., Tarr, A. W., Brown, R. J., Hickling, T. P., Szwejk, A., Bienkowska-Szewczyk, K., Thomson, B. J., Patel, A. H. & Ball, J. K. (2006). Identification of conserved residues in the E2 envelope glycoprotein of the hepatitis C virus that are critical for CD81 binding. *J Virol* **80**, 8695-8704.

Parathath, S., Connelly, M. A., Rieger, R. A., Klein, S. M., Abumrad, N. A., De La Llera-Moya, M., Iden, C. R., Rothblat, G. H. & Williams, D. L. (2004). Changes in plasma membrane properties and phosphatidylcholine subspecies of insect Sf9 cells due to expression of scavenger receptor class B, type I, and CD36. *J Biol Chem* **279**, 41310-41318.

Parent, R., Qu, X., Petit, M. A. & Beretta, L. (2009). The heat shock cognate protein 70 is associated with hepatitis C virus particles and modulates virus infectivity. *Hepatology* **49**, 1798-1809.

Paul, D., Romero-Brey, I., Gouttenoire, J., Stoitsova, S., Krijnse-Locker, J., Moradpour, D. & Bartenschlager, R. (2011). NS4B self-interaction through conserved C-terminal elements is required for the establishment of functional hepatitis C virus replication complexes. *J Virol* **85**, 6963-6976.

Pavio, N. & Lai, M. M. (2003). The hepatitis C virus persistence: how to evade the immune system? *J Biosci* **28**, 287-304.

Pawlotsky, J. M. (2012). Is hepatitis virus resistance to antiviral drugs a threat? *Gastroenterology* **142**, 1369-1372.

Pawlotsky, J. M. (2011). Treatment failure and resistance with direct-acting antiviral drugs against hepatitis C virus. *Hepatology* **53**, 1742-1751.

Pawlotsky, J. M. (1998). Hepatitis C virus infection: virus/host interactions. *J Viral Hepat* **5 Suppl 1**, 3-8.
Pawlotsky, J. M. (1999). Hepatitis C virus (HCV) NS5A protein: role in HCV replication and resistance to interferon-alpha. *J Viral Hepat* **6 Suppl 1**, 47-48.
Pawlotsky, J. M. (2002). Use and interpretation of virological tests for hepatitis C. *Hepatology* **36**, S65-73.
Pawlotsky, J. M. (2004). Pathophysiology of hepatitis C virus infection and related liver disease. *Trends Microbiol* **12**, 96-102.
Pek, J. W. & Kai, T. (2011). DEAD-box RNA helicase Belle/DDX3 and the RNA interference pathway promote mitotic chromosome segregation. *Proc Natl Acad Sci U S A* **108**, 12007-12012.
Pene, V., Hernandez, C., Vauloup-Fellous, C., Garaud-Aunis, J. & Rosenberg, A. R. (2009). Sequential processing of hepatitis C virus core protein by host cell signal peptidase and signal peptide peptidase: a reassessment. *J Viral Hepat* **16**, 705-715.
Peng, B., Yu, M., Xu, S., Lee, Y. J., Tian, Y., Yang, H., Chan, K., Mo, H., McHutchison, J., Delaney, W. t. & Cheng, G. (2013). Development of robust hepatitis C virus genotype 4 subgenomic replicons. *Gastroenterology* **144**, 59-61 e56.
Penin, F., Combet, C., Germanidis, G., Frainais, P. O., Deleage, G. & Pawlotsky, J. M. (2001). Conservation of the conformation and positive charges of hepatitis C virus E2 envelope glycoprotein hypervariable region 1 points to a role in cell attachment. *J Virol* **75**, 5703-5710.
Penin, F., Dubuisson, J., Rey, F. A., Moradpour, D. & Pawlotsky, J. M. (2004). Structural biology of hepatitis C virus. *Hepatology* **39**, 5-19.
Perotti, M., Mancini, N., Diotti, R. A., Tarr, A. W., Ball, J. K., Owsianka, A., Adair, R., Patel, A. H., Clementi, M. & Burioni, R. (2008). Identification of a broadly cross-reacting and neutralizing human monoclonal antibody directed against the hepatitis C virus E2 protein. *J Virol* **82**, 1047-1052.
Pestova, T. V., de Breyne, S., Pisarev, A. V., Abaeva, I. S. & Hellen, C. U. (2008). eIF2-dependent and eIF2-independent modes of initiation on the CSFV IRES: a common role of domain II. *Embo J* **27**, 1060-1072.
Phan, T., Beran, R. K., Peters, C., Lorenz, I. C. & Lindenbach, B. D. (2009). Hepatitis C virus NS2 protein contributes to virus particle assembly via opposing epistatic interactions with the E1-E2 glycoprotein and NS3-NS4A enzyme complexes. *J Virol* **83**, 8379-8395.
Phan, T., Kohlway, A., Dimberu, P., Pyle, A. M. & Lindenbach, B. D. (2011). The acidic domain of hepatitis C virus NS4A contributes to RNA replication and virus particle assembly. *J Virol* **85**, 1193-1204.
Piccininni, S., Varaklioti, A., Nardelli, M., Dave, B., Raney, K. D. & McCarthy, J. E. (2002). Modulation of the hepatitis C virus RNA-dependent RNA polymerase activity by the non-structural (NS) 3 helicase and the NS4B membrane protein. *J Biol Chem* **277**, 45670-45679.
Pichlmair, A., Schulz, O., Tan, C. P., Naslund, T. I., Liljestrom, P., Weber, F. & Reis e Sousa, C. (2006). RIG-I-mediated antiviral responses to single-stranded RNA bearing 5'-phosphates. *Science* **314**, 997-1001.
Pietschmann, T., Kaul, A., Koutsoudakis, G., Shavinskaya, A., Kallis, S., Steinmann, E., Abid, K., Negro, F., Dreux, M., Cosset, F. L. & Bartenschlager, R. (2006). Construction and characterization of infectious

intragenotypic and intergenotypic hepatitis C virus chimeras. *Proc Natl Acad Sci U S A* **103**, 7408-7413.

Pietschmann, T., Zayas, M., Meuleman, P., Long, G., Appel, N., Koutsoudakis, G., Kallis, S., Leroux-Roels, G., Lohmann, V. & Bartenschlager, R. (2009). Production of infectious genotype 1b virus particles in cell culture and impairment by replication enhancing mutations. *PLoS Pathog* **5**, e1000475.

Pileri, P., Uematsu, Y., Campagnoli, S., Galli, G., Falugi, F., Petracca, R., Weiner, A. J., Houghton, M., Rosa, D., Grandi, G. & Abrignani, S. (1998). Binding of hepatitis C virus to CD81. *Science* **282**, 938-941.

Ploss, A., Evans, M. J., Gaysinskaya, V. A., Panis, M., You, H., de Jong, Y. P. & Rice, C. M. (2009). Human occludin is a hepatitis C virus entry factor required for infection of mouse cells. *Nature* **457**, 882-886.

Pohlmann, S., Zhang, J., Baribaud, F., Chen, Z., Leslie, G. J., Lin, G., Granelli-Piperno, A., Doms, R. W., Rice, C. M. & McKeating, J. A. (2003). Hepatitis C virus glycoproteins interact with DC-SIGN and DC-SIGNR. *J Virol* **77**, 4070-4080.

Pokrovskii, M. V., Bush, C. O., Beran, R. K., Robinson, M. F., Cheng, G., Tirunagari, N., Fenaux, M., Greenstein, A. E., Zhong, W., Delaney, W. E. t. & Paulson, M. S. (2011). Novel mutations in a tissue culture-adapted hepatitis C virus strain improve infectious-virus stability and markedly enhance infection kinetics. *J Virol* **85**, 3978-3985.

Popescu, C. I., Callens, N., Trinel, D., Roingeard, P., Moradpour, D., Descamps, V., Duverlie, G., Penin, F., Heliot, L., Rouille, Y. & Dubuisson, J. (2011a). NS2 protein of hepatitis C virus interacts with structural and non-structural proteins towards virus assembly. *PLoS Pathog* **7**, e1001278.

Popescu, C. I. & Dubuisson, J. (2009). Role of lipid metabolism in hepatitis C virus assembly and entry. *Biol Cell* **102**, 63-74.

Popescu, C. I., Rouille, Y. & Dubuisson, J. (2011b). Hepatitis C virus assembly imaging. *Viruses* **3**, 2238-2254.

Potel, J., Rassam, P., Montpellier, C., Kaestner, L., Werkmeister, E., Tews, B. A., Couturier, C., Popescu, C. I., Baumert, T. F., Rubinstein, E., Dubuisson, J., Milhiet, P. E. & Cocquerel, L. (2013). EWI-2wint promotes CD81 clustering that abrogates Hepatitis C Virus entry. *Cell Microbiol*.

Poynard, T., Bedossa, P. & Opolon, P. (1997). Natural history of liver fibrosis progression in patients with chronic hepatitis C. The OBSVIRC, METAVIR, CLINIVIR, and DOSVIRC groups. *Lancet* **349**, 825-832.

Price, D. A., Bassendine, M. F., Norris, S. M., Golding, C., Toms, G. L., Schmid, M. L., Morris, C. M., Burt, A. D. & Donaldson, P. T. (2006). Apolipoprotein epsilon3 allele is associated with persistent hepatitis C virus infection. *Gut* **55**, 715-718.

Prince, A. M., Brotman, B., Grady, G. F., Kuhns, W. J., Hazzi, C., Levine, R. W. & Millian, S. J. (1974). Long-incubation post-transfusion hepatitis without serological evidence of exposure to hepatitis-B virus. *Lancet* **2**, 241-246.

Quinkert, D., Bartenschlager, R. & Lohmann, V. (2005). Quantitative analysis of the hepatitis C virus replication complex. *J Virol* **79**, 13594-13605.

Radi, M., Falchi, F., Garbelli, A., Samuele, A., Bernardo, V., Paolucci, S., Baldanti, F., Schenone, S., Manetti, F., Maga, G. & Botta, M. (2012). Discovery of the first small molecule inhibitor of human DDX3 specifically designed to target the RNA binding site: towards the next generation HIV-1 inhibitors. *Bioorg Med Chem Lett* **22**, 2094-2098.

Randall, G., Panis, M., Cooper, J. D., Tellinghuisen, T. L., Sukhodolets, K. E., Pfeffer, S., Landthaler, M., Landgraf, P., Kan, S., Lindenbach, B. D., Chien, M., Weir, D. B., Russo, J. J., Ju, J., Brownstein, M. J., Sheridan, R., Sander, C., Zavolan, M., Tuschl, T. & Rice, C. M. (2007). Cellular cofactors affecting hepatitis C virus infection and replication. *Proc Natl Acad Sci U S A* **104**, 12884-12889.

Ray, R. B. & Ray, R. (2001). Hepatitis C virus core protein: intriguing properties and functional relevance. *FEMS Microbiol Lett* **202**, 149-156.

Ray, S. C., Wang, Y. M., Laeyendecker, O., Ticehurst, J. R., Villano, S. A. & Thomas, D. L. (1999). Acute hepatitis C virus structural gene sequences as predictors of persistent viremia: hypervariable region 1 as a decoy. *J Virol* **73**, 2938-2946.

Reed, K. E. & Rice, C. M. (1999). Identification of the major phosphorylation site of the hepatitis C virus H strain NS5A protein as serine 2321. *J Biol Chem* **274**, 28011-28018.

Reed, K. E. & Rice, C. M. (2000). Overview of hepatitis C virus genome structure, polyprotein processing, and protein properties. *Curr Top Microbiol Immunol* **242**, 55-84.

Rehermann, B. (2009). Hepatitis C virus versus innate and adaptive immune responses: a tale of coevolution and coexistence. *J Clin Invest* **119**, 1745-1754.

Reynolds, J. E., Kaminski, A., Carroll, A. R., Clarke, B. E., Rowlands, D. J. & Jackson, R. J. (1996). Internal initiation of translation of hepatitis C virus RNA: the ribosome entry site is at the authentic initiation codon. *Rna* **2**, 867-878.

Rhainds, D. & Brissette, L. (2004). The role of scavenger receptor class B type I (SR-BI) in lipid trafficking. defining the rules for lipid traders. *Int J Biochem Cell Biol* **36**, 39-77.

Rigotti, A., Miettinen, H. E. & Krieger, M. (2003). The role of the high-density lipoprotein receptor SR-BI in the lipid metabolism of endocrine and other tissues. *Endocr Rev* **24**, 357-387.

Robertson, B., Myers, G., Howard, C., Brettin, T., Bukh, J., Gaschen, B., Gojobori, T., Maertens, G., Mizokami, M., Nainan, O., Netesov, S., Nishioka, K., Shin i, T., Simmonds, P., Smith, D., Stuyver, L. & Weiner, A. (1998). Classification, nomenclature, and database development for hepatitis C virus (HCV) and related viruses: proposals for standardization. International Committee on Virus Taxonomy. *Arch Virol* **143**, 2493-2503.

Robida, J.M., Nelson, H.B., Liu, Z., Tang, H. (2007). Characterization of hepatitis C virus subgenomic replicon resistance to cyclosporine in vitro. *J. Virol* **81,** 5829–5840.

Rocha-Perugini, V., Montpellier, C., Delgrange, D., Wychowski, C., Helle, F., Pillez, A., Drobecq, H., Le Naour, F., Charrin, S., Levy, S., Rubinstein, E., Dubuisson, J. & Cocquerel, L. (2008). The CD81 partner EWI-2wint inhibits hepatitis C virus entry. *PLoS One* **3**, e1866.

Roingeard, P. & Hourioux, C. (2008). Hepatitis C virus core protein, lipid droplets and steatosis. *J Viral Hepat* **15**, 157-164.

Romero-Brey, I., Merz, A., Chiramel, A., Lee, J. Y., Chlanda, P., Haselman, U., Santarella-Mellwig, R., Habermann, A., Hoppe, S., Kallis, S., Walther, P., Antony, C., Krijnse-Locker, J. & Bartenschlager, R. (2012). Three-dimensional architecture and biogenesis of membrane structures associated with hepatitis C virus replication. *PLoS Pathog* **8**, e1003056.

Romero-Lopez, C., Barroso-Deljesus, A., Garcia-Sacristan, A., Briones, C. & Berzal-Herranz, A. (2012). The folding of the hepatitis C virus internal ribosome entry site depends on the 3'-end of the viral genome. *Nucleic Acids Res* **40**, 11697-11713.

Rosen, H. R. (2011). Clinical practice. Chronic hepatitis C infection. *N Engl J Med* **364**, 2429-2438.

Rosenberg, P. M., Farrell, J. J., Abraczinskas, D. R., Graeme-Cook, F. M., Dienstag, J. L. & Chung, R. T. (2002). Rapidly progressive fibrosing cholestatic hepatitis--hepatitis C virus in HIV coinfection. *Am J Gastroenterol* **97**, 478-483.

Rosner, A. & Rinkevich, B. (2007). The DDX3 subfamily of the DEAD box helicases: divergent roles as unveiled by studying different organisms and in vitro assays. *Curr Med Chem* **14**, 2517-2525.

Rosnoblet, C., Fritzinger, B., Legrand, D., Launay, H., Wieruszeski, J. M., Lippens, G. & Hanoulle, X. (2012). Hepatitis C virus NS5B and host cyclophilin A share a common binding site on NS5A. *J Biol Chem* **287**, 44249-44260.

Russell, R. S., Meunier, J. C., Takikawa, S., Faulk, K., Engle, R. E., Bukh, J., Purcell, R. H. & Emerson, S. U. (2008). Advantages of a single-cycle production assay to study cell culture-adaptive mutations of hepatitis C virus. *Proc Natl Acad Sci U S A* **105**, 4370-4375.

Saban, M. R., Hellmich, H. L., Turner, M., Nguyen, N. B., Vadigepalli, R., Dyer, D. W., Hurst, R. E., Centola, M. & Saban, R. (2006). The inflammatory and normal transcriptome of mouse bladder detrusor and mucosa. *BMC Physiol* **6**, 1.

Saeed, M., Gondeau, C., Hmwe, S., Yokokawa, H., Date, T., Suzuki, T., Kato, T., Maurel, P. & Wakita, T. (2013). Replication of hepatitis C virus genotype 3a in cultured cells. *Gastroenterology* **144**, 56-58 e57.

Saeed, M., Scheel, T. K., Gottwein, J. M., Marukian, S., Dustin, L. B., Bukh, J. & Rice, C. M. (2012). Efficient replication of genotype 3a and 4a hepatitis C virus replicons in human hepatoma cells. *Antimicrob Agents Chemother* **56**, 5365-5373.

Sainz, B., Jr., Barretto, N., Martin, D. N., Hiraga, N., Imamura, M., Hussain, S., Marsh, K. A., Yu, X., Chayama, K., Alrefai, W. A. & Uprichard, S. L. (2012). Identification of the Niemann-Pick C1-like 1 cholesterol absorption receptor as a new hepatitis C virus entry factor. *Nat Med* **18**, 281-285.

Sainz, B., Jr., Barretto, N. & Uprichard, S. L. (2009). Hepatitis C virus infection in phenotypically distinct Huh7 cell lines. *PLoS One* **4**, e6561.

Saito, T., Owen, D. M., Jiang, F., Marcotrigiano, J. & Gale, M., Jr. (2008). Innate immunity induced by composition-dependent RIG-I recognition of hepatitis C virus RNA. *Nature* **454**, 523-527.

Sakai, A., Claire, M. S., Faulk, K., Govindarajan, S., Emerson, S. U., Purcell, R. H. & Bukh, J. (2003). The p7 polypeptide of hepatitis C virus is critical for infectivity and contains functionally important genotype-specific sequences. *Proc Natl Acad Sci U S A* **100**, 11646-11651.

Santolini, E., Migliaccio, G. & La Monica, N. (1994). Biosynthesis and biochemical properties of the hepatitis C virus core protein. *J Virol* **68**, 3631-3641.

Sato, S., Fukasawa, M., Yamakawa, Y., Natsume, T., Suzuki, T., Shoji, I., Aizaki, H., Miyamura, T. & Nishijima, M. (2006). Proteomic profiling of lipid droplet proteins in hepatoma cell lines expressing hepatitis C virus core protein. *J Biochem* **139**, 921-930.

Saunier, B., Triyatni, M., Ulianich, L., Maruvada, P., Yen, P. & Kohn, L. D. (2003). Role of the asialoglycoprotein receptor in binding and entry of hepatitis C virus structural proteins in cultured human hepatocytes. *J Virol* **77**, 546-559.

Saxena, V., Lai, C. K., Chao, T. C., Jeng, K. S. & Lai, M. M. (2012). Annexin A2 is involved in the formation of hepatitis C virus replication complex on the lipid raft. *J Virol* **86**, 4139-4150.

Scarselli, E., Ansuini, H., Cerino, R., Roccasecca, R. M., Acali, S., Filocamo, G., Traboni, C., Nicosia, A., Cortese, R. & Vitelli, A. (2002). The human scavenger receptor class B type I is a novel candidate receptor for the hepatitis C virus. *Embo J* **21**, 5017-5025.

Schaller, T., Appel, N., Koutsoudakis, G., Kallis, S., Lohmann, V., Pietschmann, T. & Bartenschlager, R. (2007). Analysis of hepatitis C virus superinfection exclusion by using novel fluorochrome gene-tagged viral genomes. *J Virol* **81**, 4591-4603.

Schmidt-Mende, J., Bieck, E., Hugle, T., Penin, F., Rice, C. M., Blum, H. E. & Moradpour, D. (2001). Determinants for membrane association of the hepatitis C virus RNA-dependent RNA polymerase. *J Biol Chem* **276**, 44052-44063.

Schneider, M. R. & Wolf, E. (2009). The epidermal growth factor receptor ligands at a glance. *J Cell Physiol* **218**, 460-466.

Schnell, G., Loo, Y. M., Marcotrigiano, J. & Gale, M., Jr. (2012). Uridine composition of the poly-U/UC tract of HCV RNA defines non-self recognition by RIG-I. *PLoS Pathog* **8**, e1002839.

Schroder, M. (2010). Human DEAD-box protein 3 has multiple functions in gene regulation and cell cycle control and is a prime target for viral manipulation. *Biochem Pharmacol* **79**, 297-306.

Schroder, M. (2011). Viruses and the human DEAD-box helicase DDX3: inhibition or exploitation? *Biochem Soc Trans* **39**, 679-683.

Schroder, M., Baran, M. & Bowie, A. G. (2008). Viral targeting of DEAD box protein 3 reveals its role in TBK1/IKKepsilon-mediated IRF activation. *Embo J* **27**, 2147-2157.

Schutz, P., Karlberg, T., van den Berg, S., Collins, R., Lehtio, L., Hogbom, M., Holmberg-Schiavone, L., Tempel, W., Park, H. W., Hammarstrom, M., Moche, M., Thorsell, A. G. & Schuler, H. (2010). Comparative structural analysis of human DEAD-box RNA helicases. *PLoS One* **5**.

Scrima, N., Caillet-Saguy, C., Ventura, M., Harrus, D., Astier-Gin, T. & Bressanelli, S. (2012). Two crucial early steps in RNA synthesis by the hepatitis C virus polymerase involve a dual role of residue 405. *J Virol* **86**, 7107-7117.

Sekiguchi, T., Kurihara, Y. & Fukumura, J. (2007). Phosphorylation of threonine 204 of DEAD-box RNA helicase DDX3 by cyclin B/cdc2 in vitro. *Biochem Biophys Res Commun* **356**, 668-673.

Sen, G. C. (2001). Viruses and interferons. *Annu Rev Microbiol* **55**, 255-281.

Serebrov, V. & Pyle, A. M. (2004). Periodic cycles of RNA unwinding and pausing by hepatitis C virus NS3 helicase. *Nature* **430**, 476-480.

Sharma, N. R., Mateu, G., Dreux, M., Grakoui, A., Cosset, F. L. & Melikyan, G. B. (2011). Hepatitis C virus is primed by CD81 protein for low pH-dependent fusion. *J Biol Chem* **286**, 30361-30376.

Shavinskaya, A., Boulant, S., Penin, F., McLauchlan, J. & Bartenschlager, R. (2007). The lipid droplet binding domain of hepatitis C virus core protein is a major determinant for efficient virus assembly. *J Biol Chem* **282**, 37158-37169.

Shepard, C. W., Finelli, L. & Alter, M. J. (2005). Global epidemiology of hepatitis C virus infection. *Lancet Infect Dis* **5**, 558-567.

Shih, J. W., Tsai, T. Y., Chao, C. H. & Wu Lee, Y. H. (2008). Candidate tumor suppressor DDX3 RNA helicase specifically represses cap-dependent translation by acting as an eIF4E inhibitory protein. *Oncogene* **27**, 700-714.

Shih, J. W., Wang, W. T., Tsai, T. Y., Kuo, C. Y., Li, H. K. & Wu Lee, Y. H. (2012). Critical roles of RNA helicase DDX3 and its interactions with eIF4E/PABP1 in stress granule assembly and stress response. *Biochem J* **441**, 119-129.

Shimakami, T., Hijikata, M., Luo, H., Ma, Y. Y., Kaneko, S., Shimotohno, K. & Murakami, S. (2004). Effect of interaction between hepatitis C virus NS5A and NS5B on hepatitis C virus RNA replication with the hepatitis C virus replicon. *J Virol* **78**, 2738-2748.

Shimakami, T., Honda, M., Kusakawa, T., Murata, T., Shimotohno, K., Kaneko, S. & Murakami, S. (2006). Effect of hepatitis C virus (HCV) NS5B-nucleolin interaction on HCV replication with HCV subgenomic replicon. *J Virol* **80**, 3332-3340.

Shin, K., Fogg, V. C. & Margolis, B. (2006). Tight junctions and cell polarity. *Annu Rev Cell Dev Biol* **22**, 207-235.

Shirota, Y., Luo, H., Qin, W., Kaneko, S., Yamashita, T., Kobayashi, K. & Murakami, S. (2002). Hepatitis C virus (HCV) NS5A binds RNA-dependent RNA polymerase (RdRP) NS5B and modulates RNA-dependent RNA polymerase activity. *J Biol Chem* **277**, 11149-11155.

Shoukry, N. H., Grakoui, A., Houghton, M., Chien, D. Y., Ghrayeb, J., Reimann, K. A. & Walker, C. M. (2003). Memory CD8+ T cells are required for protection from persistent hepatitis C virus infection. *J Exp Med* **197**, 1645-1655.

Simister, P., Schmitt, M., Geitmann, M., Wicht, O., Danielson, U. H., Klein, R., Bressanelli, S. & Lohmann, V. (2009). Structural and functional analysis of hepatitis C virus strain JFH1 polymerase. *J Virol* **83**, 11926-11939.

Simmonds, P. (2004). Genetic diversity and evolution of hepatitis C virus--15 years on. *J Gen Virol* **85**, 3173-3188.

Simmonds, P., Bukh, J., Combet, C., Deleage, G., Enomoto, N., Feinstone, S., Halfon, P., Inchauspe, G., Kuiken, C., Maertens, G., Mizokami, M., Murphy, D. G., Okamoto, H., Pawlotsky, J. M., Penin, F., Sablon, E., Shin, I. T., Stuyver, L. J., Thiel, H. J., Viazov, S., Weiner, A. J. & Widell, A. (2005). Consensus proposals for a unified system of nomenclature of hepatitis C virus genotypes. *Hepatology* **42**, 962-973.

Song, Y., Friebe, P., Tzima, E., Junemann, C., Bartenschlager, R. & Niepmann, M. (2006). The hepatitis C virus RNA 3'-untranslated region strongly enhances translation directed by the internal ribosome entry site. *J Virol* **80**, 11579-11588.

Soriano, V., Peters, M. G. & Zeuzem, S. (2009). New therapies for hepatitis C virus infection. *Clin Infect Dis* **48**, 313-320.

Soto-Rifo, R., Rubilar, P. S., Limousin, T., de Breyne, S., Decimo, D. & Ohlmann, T. (2012). DEAD-box protein DDX3 associates with eIF4F to promote translation of selected mRNAs. *Embo J* **31**, 3745-3756.

Soulat, D., Burckstummer, T., Westermayer, S., Goncalves, A., Bauch, A., Stefanovic, A., Hantschel, O., Bennett, K. L., Decker, T. & Superti-Furga, G. (2008). The DEAD-box helicase DDX3X is a critical component of the

TANK-binding kinase 1-dependent innate immune response. *Embo J* **27**, 2135-2146.

Spangberg, K., Goobar-Larsson, L., Wahren-Herlenius, M. & Schwartz, S. (1999). The La protein from human liver cells interacts specifically with the U-rich region in the hepatitis C virus 3' untranslated region. *J Hum Virol* **2**, 296-307.

Spillmann, D. (2001). Heparan sulfate: anchor for viral intruders? *Biochimie* **83**, 811-817.

Stamataki, Z., Shannon-Lowe, C., Shaw, J., Mutimer, D., Rickinson, A. B., Gordon, J., Adams, D. H., Balfe, P. & McKeating, J. A. (2009). Hepatitis C virus association with peripheral blood B lymphocytes potentiates viral infection of liver-derived hepatoma cells. *Blood* **113**, 585-593.

Stapleford, K. A. & Lindenbach, B. D. (2011). Hepatitis C virus NS2 coordinates virus particle assembly through physical interactions with the E1-E2 glycoprotein and NS3-NS4A enzyme complexes. *J Virol* **85**, 1706-1717.

Stapleton, J. T., Foung, S., Muerhoff, A. S., Bukh, J. & Simmonds, P. (2011). The GB viruses: a review and proposed classification of GBV-A, GBV-C (HGV), and GBV-D in genus Pegivirus within the family Flaviviridae. *The Journal of general virology* **92**, 233-246.

Stegen, C., Yakova, Y., Henaff, D., Nadjar, J., Duron, J. & Lippe, R. (2013). Analysis of virion-incorporated host proteins required for herpes simplex virus type 1 infection through a RNA interference screen. *PLoS One* **8**, e53276.

Steinmann, E., Penin, F., Kallis, S., Patel, A. H., Bartenschlager, R. & Pietschmann, T. (2007). Hepatitis C virus p7 protein is crucial for assembly and release of infectious virions. *PLoS Pathog* **3**, e103.

Steinmann, E. & Pietschmann, T. (2010). Hepatitis C virus p7-a viroporin crucial for virus assembly and an emerging target for antiviral therapy. *Viruses* **2**, 2078-2095.

Stevens, S. W., Ryan, D. E., Ge, H. Y., Moore, R. E., Young, M. K., Lee, T. D. & Abelson, J. (2002). Composition and functional characterization of the yeast spliceosomal penta-snRNP. *Mol Cell* **9**, 31-44.

StGelais, C., Foster, T. L., Verow, M., Atkins, E., Fishwick, C. W., Rowlands, D., Harris, M. & Griffin, S. (2009). Determinants of hepatitis C virus p7 ion channel function and drug sensitivity identified in vitro. *J Virol* **83**, 7970-7981.

Sugimoto, K., Kaplan, D. E., Ikeda, F., Ding, J., Schwartz, J., Nunes, F. A., Alter, H. J. & Chang, K. M. (2005). Strain-specific T-cell suppression and protective immunity in patients with chronic hepatitis C virus infection. *J Virol* **79**, 6976-6983.

Sumpter, R., Jr., Loo, Y. M., Foy, E., Li, K., Yoneyama, M., Fujita, T., Lemon, S. M. & Gale, M., Jr. (2005). Regulating intracellular antiviral defense and permissiveness to hepatitis C virus RNA replication through a cellular RNA helicase, RIG-I. *J Virol* **79**, 2689-2699.

Sumpter, R., Jr., Wang, C., Foy, E., Loo, Y. M. & Gale, M., Jr. (2004). Viral evolution and interferon resistance of hepatitis C virus RNA replication in a cell culture model. *J Virol* **78**, 11591-11604.

Sun, C., Pager, C. T., Luo, G., Sarnow, P. & Cate, J. H. (2010). Hepatitis C virus core-derived peptides inhibit genotype 1b viral genome replication via interaction with DDX3X. *PLoS One* **5**.

Sun, M., Song, L., Li, Y., Zhou, T. & Jope, R. S. (2008). Identification of an antiapoptotic protein complex at death receptors. *Cell Death Differ* **15**, 1887-1900.

Sun, M., Song, L., Zhou, T., Gillespie, G. Y. & Jope, R. S. (2011). The role of DDX3 in regulating Snail. *Biochim Biophys Acta* **1813**, 438-447.

Tabor, E., Gerety, R. J., Drucker, J. A., Seeff, L. B., Hoofnagle, J. H., Jackson, D. R., April, M., Barker, L. F. & Pineda-Tamondong, G. (1978). Transmission of non-A, non-B hepatitis from man to chimpanzee. *Lancet* **1**, 463-466.

Tai, C. L., Chi, W. K., Chen, D. S. & Hwang, L. H. (1996). The helicase activity associated with hepatitis C virus nonstructural protein 3 (NS3). *J Virol* **70**, 8477-8484.

Takamizawa, A., Mori, C., Fuke, I., Manabe, S., Murakami, S., Fujita, J., Onishi, E., Andoh, T., Yoshida, I. & Okayama, H. (1991). Structure and organization of the hepatitis C virus genome isolated from human carriers. *J Virol* **65**, 1105-1113.

Tamai, K., Shiina, M., Tanaka, N., Nakano, T., Yamamoto, A., Kondo, Y., Kakazu, E., Inoue, J., Fukushima, K., Sano, K., Ueno, Y., Shimosegawa, T. & Sugamura, K. (2012). Regulation of hepatitis C virus secretion by the Hrs-dependent exosomal pathway. *Virology* **422**, 377-385.

Tan, S. L. & Katze, M. G. (2001). How hepatitis C virus counteracts the interferon response: the jury is still out on NS5A. *Virology* **284**, 1-12.

Tanaka, T., Kato, N., Cho, M. J., Sugiyama, K. & Shimotohno, K. (1996). Structure of the 3' terminus of the hepatitis C virus genome. *J Virol* **70**, 3307-3312.

Tanji, Y., Kaneko, T., Satoh, S. & Shimotohno, K. (1995). Phosphorylation of hepatitis C virus-encoded nonstructural protein NS5A. *J Virol* **69**, 3980-3986.

Tao, W., Xu, C., Ding, Q., Li, R., Xiang, Y., Chung, J. & Zhong, J. (2009). A single point mutation in E2 enhances hepatitis C virus infectivity and alters lipoprotein association of viral particles. *Virology* **395**, 67-76.

Targett-Adams, P., Boulant, S. & McLauchlan, J. (2008a). Visualization of double-stranded RNA in cells supporting hepatitis C virus RNA replication. *J Virol* **82**, 2182-2195.

Targett-Adams, P., Hope, G., Boulant, S. & McLauchlan, J. (2008b). Maturation of hepatitis C virus core protein by signal peptide peptidase is required for virus production. *J Biol Chem* **283**, 16850-16859.

Tarr, A. W., Owsianka, A. M., Jayaraj, D., Brown, R. J., Hickling, T. P., Irving, W. L., Patel, A. H. & Ball, J. K. (2007). Determination of the human antibody response to the epitope defined by the hepatitis C virus-neutralizing monoclonal antibody AP33. *J Gen Virol* **88**, 2991-3001.

Tarr, A. W., Owsianka, A. M., Timms, J. M., McClure, C. P., Brown, R. J., Hickling, T. P., Pietschmann, T., Bartenschlager, R., Patel, A. H. & Ball, J. K. (2006). Characterization of the hepatitis C virus E2 epitope defined by the broadly neutralizing monoclonal antibody AP33. *Hepatology* **43**, 592-601.

Tarr, A. W., Urbanowicz, R. A. & Ball, J. K. (2012). The role of humoral innate immunity in hepatitis C virus infection. *Viruses* **4**, 1-27.

Taylor, D.R., Puig, M., Darnell, M.E., Mihalik, K., Feinstone, S.M. (2005). New antiviral pathway that mediates hepatitis C virus replicon interferon sensitivity through ADAR1

Taylor, D. R., Shi, S. T., Romano, P. R., Barber, G. N. & Lai, M. M. (1999). Inhibition of the interferon-inducible protein kinase PKR by HCV E2 protein. *Science* **285**, 107-110. *J Virol* **79,** 6291-6298.

Tedbury, P., Welbourn, S., Pause, A., King, B., Griffin, S. & Harris, M. (2011). The subcellular localization of the hepatitis C virus non-structural protein NS2 is

regulated by an ion channel-independent function of the p7 protein. *J Gen Virol* **92**, 819-830.

Tellinghuisen, T. L., Evans, M. J., von Hahn, T., You, S. & Rice, C. M. (2007). Studying hepatitis C virus: making the best of a bad virus. *J Virol* **81**, 8853-8867.

Tellinghuisen, T. L., Foss, K. L. & Treadaway, J. (2008a). Regulation of hepatitis C virion production via phosphorylation of the NS5A protein. *PLoS Pathog* **4**, e1000032.

Tellinghuisen, T. L., Foss, K. L., Treadaway, J. C. & Rice, C. M. (2008b). Identification of residues required for RNA replication in domains II and III of the hepatitis C virus NS5A protein. *J Virol* **82**, 1073-1083.

Tellinghuisen, T. L., Marcotrigiano, J., Gorbalenya, A. E. & Rice, C. M. (2004). The NS5A protein of hepatitis C virus is a zinc metalloprotein. *J Biol Chem* **279**, 48576-48587.

Tellinghuisen, T. L., Marcotrigiano, J. & Rice, C. M. (2005). Structure of the zinc-binding domain of an essential component of the hepatitis C virus replicase. *Nature* **435**, 374-379.

Terenin, I. M., Dmitriev, S. E., Andreev, D. E. & Shatsky, I. N. (2008). Eukaryotic translation initiation machinery can operate in a bacterial-like mode without eIF2. *Nat Struct Mol Biol* **15**, 836-841.

Terrault, N. A. & Berenguer, M. (2006). Treating hepatitis C infection in liver transplant recipients. *Liver Transpl* **12**, 1192-1204.

Thibault, P. A., Huys, A., Dhillon, P. & Wilson, J. A. (2013). MicroRNA-122-dependent and -independent replication of Hepatitis C Virus in Hep3B human hepatoma cells. *Virology* **436**, 179-190.

Thimme, R., Oldach, D., Chang, K. M., Steiger, C., Ray, S. C. & Chisari, F. V. (2001). Determinants of viral clearance and persistence during acute hepatitis C virus infection. *J Exp Med* **194**, 1395-1406.

Thomson, B. J. (2009). Hepatitis C virus: the growing challenge. *Br Med Bull* **89**, 153-167.

Thomssen, R., Bonk, S., Propfe, C., Heermann, K. H., Kochel, H. G. & Uy, A. (1992). Association of hepatitis C virus in human sera with beta-lipoprotein. *Med Microbiol Immunol* **181**, 293-300.

Thomssen, R., Bonk, S. & Thiele, A. (1993). Density heterogeneities of hepatitis C virus in human sera due to the binding of beta-lipoproteins and immunoglobulins. *Med Microbiol Immunol* **182**, 329-334.

Timpe, J. M., Stamataki, Z., Jennings, A., Hu, K., Farquhar, M. J., Harris, H. J., Schwarz, A., Desombere, I., Roels, G. L., Balfe, P. & McKeating, J. A. (2008). Hepatitis C virus cell-cell transmission in hepatoma cells in the presence of neutralizing antibodies. *Hepatology* **47**, 17-24.

Tomei, L., Failla, C., Santolini, E., De Francesco, R. & La Monica, N. (1993). NS3 is a serine protease required for processing of hepatitis C virus polyprotein. *J Virol* **67**, 4017-4026.

Troesch, M., Meunier, I., Lapierre, P., Lapointe, N., Alvarez, F., Boucher, M. & Soudeyns, H. (2006). Study of a novel hypervariable region in hepatitis C virus (HCV) E2 envelope glycoprotein. *Virology* **352**, 357-367.

Tscherne, D. M., Jones, C. T., Evans, M. J., Lindenbach, B. D., McKeating, J. A. & Rice, C. M. (2006). Time- and temperature-dependent activation of hepatitis C virus for low-pH-triggered entry. *J Virol* **80**, 1734-1741.

Tsubota, A., Fujise, K., Namiki, Y. & Tada, N. (2011). Peginterferon and ribavirin treatment for hepatitis C virus infection. *World J Gastroenterol* **17**, 419-432.

Van Itallie, C. M. & Anderson, J. M. (2004). The molecular physiology of tight junction pores. *Physiology (Bethesda)* **19**, 331-338.

Vanwolleghem, T., Libbrecht, L., Hansen, B. E., Desombere, I., Roskams, T., Meuleman, P. & Leroux-Roels, G. (2010). Factors determining successful engraftment of hepatocytes and susceptibility to hepatitis B and C virus infection in uPA-SCID mice. *J Hepatol* **53**, 468-476.

Varnum, S. M., Streblow, D. N., Monroe, M. E., Smith, P., Auberry, K. J., Pasa-Tolic, L., Wang, D., Camp, D. G., 2nd, Rodland, K., Wiley, S., Britt, W., Shenk, T., Smith, R. D. & Nelson, J. A. (2004). Identification of proteins in human cytomegalovirus (HCMV) particles: the HCMV proteome. *J Virol* **78**, 10960-10966.

Vashist, S., Urena, L., Chaudhry, Y. & Goodfellow, I. (2012). Identification of RNA-protein interaction networks involved in the norovirus life cycle. *J Virol* **86**, 11977-11990.

Vassilaki, N., Friebe, P., Meuleman, P., Kallis, S., Kaul, A., Paranhos-Baccala, G., Leroux-Roels, G., Mavromara, P. & Bartenschlager, R. (2008). Role of the hepatitis C virus core+1 open reading frame and core cis-acting RNA elements in viral RNA translation and replication. *J Virol* **82**, 11503-11515.

Vieyres, G., Brohm, C., Friesland, M., Gentzsch, J., Wolk, B., Roingeard, P., Steinmann, E. & Pietschmann, T. (2013). Subcellular localization and function of an epitope-tagged p7 viroporin in hepatitis C virus-producing cells. *J Virol* **87**, 1664-1678.

Vieyres, G., Dubuisson, J. & Patel, A. H. (2011). Characterization of antibody-mediated neutralization directed against the hypervariable region 1 of hepatitis C virus E2 glycoprotein. *J Gen Virol* **92**, 494-506.

Vieyres, G., Thomas, X., Descamps, V., Duverlie, G., Patel, A. H. & Dubuisson, J. (2010). Characterization of the envelope glycoproteins associated with infectious hepatitis C virus. *J Virol* **84**, 10159-10168.

Villano, S. A., Vlahov, D., Nelson, K. E., Cohn, S. & Thomas, D. L. (1999). Persistence of viremia and the importance of long-term follow-up after acute hepatitis C infection. *Hepatology* **29**, 908-914.

Voisset, C., Callens, N., Blanchard, E., Op De Beeck, A., Dubuisson, J. & Vu-Dac, N. (2005). High density lipoproteins facilitate hepatitis C virus entry through the scavenger receptor class B type I. *J Biol Chem* **280**, 7793-7799.

Wahid, A., Helle, F., Descamps, V., Duverlie, G., Penin, F. & Dubuisson, J. (2013). Disulfide bonds in hepatitis C virus glycoprotein E1 control the assembly and entry functions of E2 glycoprotein. *J Virol* **87**, 1605-1617.

Wakita, T., Pietschmann, T., Kato, T., Date, T., Miyamoto, M., Zhao, Z., Murthy, K., Habermann, A., Krausslich, H. G., Mizokami, M., Bartenschlager, R. & Liang, T. J. (2005). Production of infectious hepatitis C virus in tissue culture from a cloned viral genome. *Nat Med* **11**, 791-796.

Waller, H., Chatterji, U., Gallay, P., Parkinson, T. & Targett-Adams, P. (2010). The use of AlphaLISA technology to detect interaction between hepatitis C virus-encoded NS5A and cyclophilin A. *J Virol Methods* **165**, 202-210.

Wang, C., Gale, M., Jr., Keller, B. C., Huang, H., Brown, M. S., Goldstein, J. L. & Ye, J. (2005). Identification of FBL2 as a geranylgeranylated cellular protein required for hepatitis C virus RNA replication. *Mol Cell* **18**, 425-434.

Wang, H., Kim, S. & Ryu, W. S. (2009a). DDX3 DEAD-Box RNA helicase inhibits hepatitis B virus reverse transcription by incorporation into nucleocapsids. *J Virol* **83**, 5815-5824.

Wang, H. & Ryu, W. S. (2010). Hepatitis B virus polymerase blocks pattern recognition receptor signaling via interaction with DDX3: implications for immune evasion. *PLoS Pathog* **6**, e1000986.

Wang, N., Liang, Y., Devaraj, S., Wang, J., Lemon, S. M. & Li, K. (2009b). Toll-like receptor 3 mediates establishment of an antiviral state against hepatitis C virus in hepatoma cells. *J Virol* **83**, 9824-9834.

Waris, G., Sarker, S. & Siddiqui, A. (2004). Two-step affinity purification of the hepatitis C virus ribonucleoprotein complex. *Rna* **10**, 321-329.

Washburn, M. L., Bility, M. T., Zhang, L., Kovalev, G. I., Buntzman, A., Frelinger, J. A., Barry, W., Ploss, A., Rice, C. M. & Su, L. (2011). A humanized mouse model to study hepatitis C virus infection, immune response, and liver disease. *Gastroenterology* **140**, 1334-1344.

Weiner, A. J., Geysen, H. M., Christopherson, C., Hall, J. E., Mason, T. J., Saracco, G., Bonino, F., Crawford, K., Marion, C. D., Crawford, K. A. & et al. (1992). Evidence for immune selection of hepatitis C virus (HCV) putative envelope glycoprotein variants: potential role in chronic HCV infections. *Proc Natl Acad Sci U S A* **89**, 3468-3472.

Weinlich, S., Huttelmaier, S., Schierhorn, A., Behrens, S. E., Ostareck-Lederer, A. & Ostareck, D. H. (2009). IGF2BP1 enhances HCV IRES-mediated translation initiation via the 3'UTR. *Rna* **15**, 1528-1542.

Williams, B. R. (1999). PKR; a sentinel kinase for cellular stress. *Oncogene* **18**, 6112-6120.

Witteveldt, J., Evans, M. J., Bitzegeio, J., Koutsoudakis, G., Owsianka, A. M., Angus, A. G., Keck, Z. Y., Foung, S. K., Pietschmann, T., Rice, C. M. & Patel, A. H. (2009). CD81 is dispensable for hepatitis C virus cell-to-cell transmission in hepatoma cells. *J Gen Virol* **90**, 48-58.

Wolk, B., Sansonno, D., Krausslich, H. G., Dammacco, F., Rice, C. M., Blum, H. E. & Moradpour, D. (2000). Subcellular localization, stability, and trans-cleavage competence of the hepatitis C virus NS3-NS4A complex expressed in tetracycline-regulated cell lines. *J Virol* **74**, 2293-2304.

Wood, J., Frederickson, R. M., Fields, S. & Patel, A. H. (2001). Hepatitis C virus 3'X region interacts with human ribosomal proteins. *J Virol* **75**, 1348-1358.

Wozniak, A. L., Griffin, S., Rowlands, D., Harris, M., Yi, M., Lemon, S. M. & Weinman, S. A. (2010). Intracellular proton conductance of the hepatitis C virus p7 protein and its contribution to infectious virus production. *PLoS Pathog* **6**, e1001087.

Wu, X., Robotham, J. M., Lee, E., Dalton, S., Kneteman, N. M., Gilbert, D. M. & Tang, H. (2012). Productive hepatitis C virus infection of stem cell-derived hepatocytes reveals a critical transition to viral permissiveness during differentiation. *PLoS Pathog* **8**, e1002617.

Xu, S., Pei, R., Guo, M., Han, Q., Lai, J., Wang, Y., Wu, C., Zhou, Y., Lu, M. & Chen, X. (2012). Cytosolic phospholipase A2 gamma is involved in hepatitis C virus replication and assembly. *J Virol* **86**, 13025-13037.

Xu, Z., Choi, J., Yen, T. S., Lu, W., Strohecker, A., Govindarajan, S., Chien, D., Selby, M. J. & Ou, J. (2001). Synthesis of a novel hepatitis C virus protein by ribosomal frameshift. *Embo J* **20**, 3840-3848.

Yamamoto, M., Aizaki, H., Fukasawa, M., Teraoka, T., Miyamura, T., Wakita, T. & Suzuki, T. (2011). Structural requirements of virion-associated cholesterol for infectivity, buoyant density and apolipoprotein association of hepatitis C virus. *The Journal of general virology* **92**, 2082-2087.

Yanagi, M., Purcell, R. H., Emerson, S. U. & Bukh, J. (1997). Transcripts from a single full-length cDNA clone of hepatitis C virus are infectious when directly transfected into the liver of a chimpanzee. *Proc Natl Acad Sci U S A* **94**, 8738-8743.

Yanagi, M., St Claire, M., Emerson, S. U., Purcell, R. H. & Bukh, J. (1999). In vivo analysis of the 3' untranslated region of the hepatitis C virus after in vitro mutagenesis of an infectious cDNA clone. *Proc Natl Acad Sci U S A* **96**, 2291-2295.

Yang, J., Lei, Y. F., An, Q. X., Yin, W., Lu, X., Ye, L., Wei, S. H., Jia, Z. & Xu, Z. K. (2010). Properties of hepatitis C virus minigenome containing mutated 5'UTR region and luciferase transgene. *Acta Virol* **54**, 105-112.

Yano, M., Kumada, H., Kage, M., Ikeda, K., Shimamatsu, K., Inoue, O., Hashimoto, E., Lefkowitch, J. H., Ludwig, J. & Okuda, K. (1996). The long-term pathological evolution of chronic hepatitis C. *Hepatology* **23**, 1334-1340.

Yao, N., Hesson, T., Cable, M., Hong, Z., Kwong, A. D., Le, H. V. & Weber, P. C. (1997). Structure of the hepatitis C virus RNA helicase domain. *Nat Struct Biol* **4**, 463-467.

Yasui, K., Wakita, T., Tsukiyama-Kohara, K., Funahashi, S. I., Ichikawa, M., Kajita, T., Moradpour, D., Wands, J. R. & Kohara, M. (1998). The native form and maturation process of hepatitis C virus core protein. *J Virol* **72**, 6048-6055.

Yedavalli, V. S., Neuveut, C., Chi, Y. H., Kleiman, L. & Jeang, K. T. (2004). Requirement of DDX3 DEAD box RNA helicase for HIV-1 Rev-RRE export function. *Cell* **119**, 381-392.

Yedavalli, V. S., Zhang, N., Cai, H., Zhang, P., Starost, M. F., Hosmane, R. S. & Jeang, K. T. (2008). Ring expanded nucleoside analogues inhibit RNA helicase and intracellular human immunodeficiency virus type 1 replication. *J Med Chem* **51**, 5043-5051.

Yi, M. & Lemon, S. M. (2003). Structure-function analysis of the 3' stem-loop of hepatitis C virus genomic RNA and its role in viral RNA replication. *Rna* **9**, 331-345.

Yi, M. & Lemon, S. M. (2004). Adaptive mutations producing efficient replication of genotype 1a hepatitis C virus RNA in normal Huh7 cells. *J Virol* **78**, 7904-7915.

Yi, M., Ma, Y., Yates, J. & Lemon, S. M. (2007). Compensatory mutations in E1, p7, NS2, and NS3 enhance yields of cell culture-infectious intergenotypic chimeric hepatitis C virus. *J Virol* **81**, 629-638.

Yi, M., Villanueva, R. A., Thomas, D. L., Wakita, T. & Lemon, S. M. (2006). Production of infectious genotype 1a hepatitis C virus (Hutchinson strain) in cultured human hepatoma cells. *Proc Natl Acad Sci U S A* **103**, 2310-2315.

You, L. R., Chen, C. M., Yeh, T. S., Tsai, T. Y., Mai, R. T., Lin, C. H. & Lee, Y. H. (1999). Hepatitis C virus core protein interacts with cellular putative RNA helicase. *J Virol* **73**, 2841-2853.

You, S. & Rice, C. M. (2008). 3' RNA elements in hepatitis C virus replication: kissing partners and long poly(U). *J Virol* **82**, 184-195.

Yu, G. Y., Lee, K. J., Gao, L. & Lai, M. M. (2006). Palmitoylation and polymerization of hepatitis C virus NS4B protein. *J Virol* **80**, 6013-6023.

Yu, S., Chen, J., Wu, M., Chen, H., Kato, N. & Yuan, Z. (2010). Hepatitis B virus polymerase inhibits RIG-I- and Toll-like receptor 3-mediated beta interferon induction in human hepatocytes through interference with interferon regulatory factor 3 activation and dampening of the interaction between TBK1/IKKepsilon and DDX3. *J Gen Virol* **91**, 2080-2090.

Zahid, M. N., Turek, M., Xiao, F., Dao Thi, V. L., Guerin, M., Fofana, I., Bachellier, P., Thompson, J., Delang, L., Neyts, J., Bankwitz, D., Pietschmann, T., Dreux, M., Cosset, F. L., Grunert, F., Baumert, T. F. & Zeisel, M. B. (2013). The postbinding activity of scavenger receptor class B type I mediates initiation of hepatitis C virus infection and viral dissemination. *Hepatology* **57**, 492-504.

Zebedee, S.L., Lamb, R.A. (1988). Influenza A virus M2 protein: monoclonal antibody restriction of virus growth and detection of M2 in virions. *J Virol* **62,** 2762-2772.

Zeisel, M. B., Koutsoudakis, G., Schnober, E. K., Haberstroh, A., Blum, H. E., Cosset, F. L., Wakita, T., Jaeck, D., Doffoel, M., Royer, C., Soulier, E., Schvoerer, E., Schuster, C., Stoll-Keller, F., Bartenschlager, R., Pietschmann, T., Barth, H. & Baumert, T. F. (2007). Scavenger receptor class B type I is a key host factor for hepatitis C virus infection required for an entry step closely linked to CD81. *Hepatology* **46**, 1722-1731.

Zeuzem, S., Teuber, G., Naumann, U., Berg, T., Raedle, J., Hartmann, S. & Hopf, U. (2000). Randomized, double-blind, placebo-controlled trial of interferon alfa2a with and without amantadine as initial treatment for chronic hepatitis C. *Hepatology* **32**, 835-841.

Zhang, J., Randall, G., Higginbottom, A., Monk, P., Rice, C. M. & McKeating, J. A. (2004). CD81 is required for hepatitis C virus glycoprotein-mediated viral infection. *J Virol* **78**, 1448-1455.

Zhang, J., Yamada, O., Sakamoto, T., Yoshida, H., Araki, H. & Shimotohno, K. (2005). Exploiting cis-acting replication elements to direct hepatitis C virus-dependent transgene expression. *J Virol* **79**, 5923-5932.

Zhang, J., Yamada, O., Yoshida, H., Sakamoto, T., Araki, H. & Shimotohno, K. (2007a). Helper virus-independent trans-replication of hepatitis C virus-derived minigenome. *Biochem Biophys Res Commun* **352**, 170-176.

Zhang, P., Wu, C. G., Mihalik, K., Virata-Theimer, M. L., Yu, M. Y., Alter, H. J. & Feinstone, S. M. (2007b). Hepatitis C virus epitope-specific neutralizing antibodies in Igs prepared from human plasma. *Proc Natl Acad Sci U S A* **104**, 8449-8454.

Zhang, P., Zhong, L., Struble, E. B., Watanabe, H., Kachko, A., Mihalik, K., Virata-Theimer, M. L., Alter, H. J., Feinstone, S. & Major, M. (2009). Depletion of interfering antibodies in chronic hepatitis C patients and vaccinated chimpanzees reveals broad cross-genotype neutralizing activity. *Proc Natl Acad Sci U S A* **106**, 7537-7541.

Zhang, Y. Y., Zhang, B. H., Ishii, K. & Liang, T. J. (2010). Novel function of CD81 in controlling hepatitis C virus replication. *J Virol* **84**, 3396-3407.

Zheng, A., Yuan, F., Li, Y., Zhu, F., Hou, P., Li, J., Song, X., Ding, M. & Deng, H. (2007). Claudin-6 and claudin-9 function as additional coreceptors for hepatitis C virus. *J Virol* **81**, 12465-12471.

Zhong, J., Gastaminza, P., Cheng, G., Kapadia, S., Kato, T., Burton, D. R., Wieland, S. F., Uprichard, S. L., Wakita, T. & Chisari, F. V. (2005). Robust hepatitis C virus infection in vitro. *Proc Natl Acad Sci U S A* **102**, 9294-9299.

Zhou, Z., Licklider, L. J., Gygi, S. P. & Reed, R. (2002). Comprehensive proteomic analysis of the human spliceosome. *Nature* **419**, 182-185.
Zhu, F. X., Chong, J. M., Wu, L. & Yuan, Y. (2005). Virion proteins of Kaposi's sarcoma-associated herpesvirus. *J Virol* **79**, 800-811.